

**Vehicular Networks: A Value of Information driven
Distributed Resource Allocation Protocol
(VALINDRA)**

Von der Fakultät für Elektrotechnik und Informatik
der Gottfried Wilhelm Leibniz Universität Hannover
zur Erlangung des akademischen Grades

Doktor-Ingenieur (Dr.-Ing.)

genehmigte

Dissertation

von

M. Sc. Florian Alexander Schiegg
geboren am 12. Mai 1992
in Berlin

2022

1. Referent : Prof. Dr.-Ing. Markus Fidler
2. Referent : Prof. Dr. Chao Wang
Betreuer bei Bosch : Dr.-Ing. Ignacio Llatser

Tag der Promotion : 21. Dezember 2021

Florian Alexander Schiegg: *Vehicular Networks: A Value of Information driven Distributed Resource Allocation Protocol (VALINDRA)*, Dissertation, © 2021

ABSTRACT

Our modern society is in constant change. The significant technological advances of the past decades have led to unprecedented prosperity but have also come along with great new challenges. A high demand for mobility and the vast deployment of transportation systems have made traffic accidents the most likely cause of death for children and young adults worldwide. To counteract this, traffic authorities around the world place their hopes in the development of Connected Intelligent Transportation Systems (C-ITS). Vehicle-to-Everything (V2X) communication is currently being introduced to enable road users and infrastructure to exchange relevant information to provide the required basis for decision-making. The rapidly growing amount of data managed by V2X services, e.g., for improved satellite navigation, warning of critical traffic situations, sharing of sensor-detected objects, and maneuver coordination, however, pushes the resilience of the wireless communication channel to its limits. Current approaches allocating communication resources within the network are either channel-load agnostic or message-content agnostic, leading to relevant performance impairments. In the scope of this doctoral work, the underlying decentralized resource allocation problem is formalized, and a comprehensive solution is proposed with application examples for the cutting-edge V2X services Collective Perception, Collaborative Localization, and Maneuver Coordination: The VALue of INFORMATION driven Distributed Resource Allocation protocol VALINDRA. It allows to maximize the value of information effectively disseminated within the network. After a thorough analytical examination and a comparison with state-of-the-art V2X protocols, VALINDRA is investigated in simulation and with real-world data for urban and highway scenarios. Both the comparison with the prior art and the simulative investigation evidence considerable improvements in terms of V2X channel utilization, achieved localization and object-tracking accuracies, environmental perception, and traffic safety, among others.

Keywords: V2V, V2X, V2I, Vehicular Networks, Intelligent Transportation Systems, Communication, Value of Information, Decentralized Congestion Control, C-V2X, ITS-G5, 5G-V2X, LTE-V2X, IEEE 802.11p, Collective Perception, Maneuver Coordination, Collaborative Localization.

ZUSAMMENFASSUNG

Unsere Gesellschaft ist in ständigem Wandel. Insbesondere die zahlreichen technologischen Fortschritte der vergangenen Jahrzehnte führten zu niemals dagewesenem Wohlstand, sind aber auch mit neuen großen Herausforderungen verbunden. So ist die wahrscheinlichste Todesursache für Kinder und junge Erwachsene weltweit, aufgrund des massiven Ausbaus moderner Verkehrssysteme, mit großem Abstand ein Verkehrsunfall. Die größte Hoffnung etablierter Verkehrsbehörden weltweit sind die intelligente Vernetzung und die Automatisierung des Verkehrs. Mittels Fahrzeug-zu-Alles (V2X; engl. Vehicle-to-Everything) Kommunikation sollen Verkehrsteilnehmer und Infrastruktur relevante Informationen austauschen können, um eine solide Entscheidungsgrundlage zu schaffen. Die rasant wachsende Anzahl mittels V2X Diensten ausgetauschter Daten, u.A. zur verbesserten Satelliten-gestützten Navigation, Warnung vor kritischen Verkehrssituationen, dem Teilen von Sensor-detektierten Objekten und der Manöverabstimmung, bringt die Belastbarkeit des drahtlosen Kommunikationskanals jedoch an ihre Grenzen. Gegenwärtige Ansätze zum Zuweisen von Kommunikationsressourcen innerhalb der Fahrzeugnetzwerke sind entweder unabhängig von der Anzahl verfügbarer Ressourcen oder vom Wert der zu übermittelnden Informationen, was zu erheblichen Leistungsverlusten führt. Im Rahmen dieses Promotionsvorhabens wird das zugrundeliegende dezentrale Ressourcenallokationsproblem formalisiert und eine umfassende Lösung mit Anwendungsbeispielen für die wegweisenden V2X-Dienste Collective Perception, Collaborative Localization und Maneuver Coordination vorgeschlagen: VALINDRA (engl. „The VALue of INformation driven Distributed Resource Allocation protocol“). Nach einer gründlichen analytischen Untersuchung und einem Vergleich mit etablierten V2X-Protokollen wird VALINDRA simulativ und mit realen Daten in Stadt- und Autobahnumgebungen untersucht. Sowohl der Vergleich mit dem Stand der Technik als auch die simulative Untersuchung offenbaren deutliche Verbesserungen in Bezug auf die erreichte Kanalauslastung, Umgebungswahrnehmung, Navigations- und Objekttrackinggenauigkeiten, und Verkehrssicherheit unter anderem.

Schlüsselwörter: Fahrzeugkommunikation, Kooperative Manöverabstimmung, Kooperative Wahrnehmung, Kooperative Positionierung, Überlastkontrolle

摘要

我们的现代社会在不断变化。过去几十年的巨大技术进步带来了前所未有的繁荣，但也带来了巨大的新挑战。对流动性的高需求和交通系统的广泛部署使交通事故成为全球儿童和年轻人最可能的死亡原因。为了解决这个问题，世界各地的交通当局部门都寄希望于互联智能交通系统 (C-ITS) 的发展。目前正在被引入的车辆对一切 (V2X) 通信，以使道路使用者和基础设施能够交换相关信息，为决策提供所需的基础。然而，来自 V2X 服务的数据量迅速增长，例如用于改进卫星导航、危急交通情况警告、传感器检测对象的共享以及机动协调，将无线通信信道的弹性推到了极限。当前在网络内分配通信资源的方法要么与信道负载无关，要么与消息内容无关，从而导致相关的性能损失。在本博士工作的范围内，对底层的分散资源分配问题进行了形式化，并提出了一个综合解决方案，同时并提供了尖端 V2X 服务集体感知、协作定位和机动协调的应用示例：VALINDRA（英语 „The VALue of INformation driven Distributed Resource Allocation protocol”）。经过彻底的分析检查并与最先进的 V2X 协议进行比较后，使用在城市和高速公路场景中的模拟数据以及真实数据对 VALINDRA 在模拟和城市和高速公路场景的真实世界数据中进行了研究。与现有技术的比较和模拟研究调查都证明了其在 V2X 通道利用方面非常有希望的结果，提供了定位和对象跟踪的准确性、环境感知和交通安全等。V2X 通道的利用，提供的定位和物体追踪的准确性，环境感知和交通安全上有非常好的结果。

关键词: V2V、V2X、V2I、车载网络、智能交通系统、通信、信息价值、分散拥塞控制、C-V2X、ITS-G5、5G-V2X、LTE-V2X、IEEE 802.11p、集体感知、机动协调、协作本土化

CONTENT

ABSTRACT.....	III
ZUSAMMENFASSUNG	V
摘要.....	VII
CONTENT.....	IX
LIST OF FIGURES	XIII
LIST OF TABLES.....	XV
LIST OF ABBREVIATIONS	XVII
1. INTRODUCTION	1
1.1 Motivation	1
1.2. General Remarks	6
1.3. Structure	8
2. VEHICLE TO EVERYTHING COMMUNICATION	11
2.1. Connected Vehicles.....	11
2.1.1. Regulation and Standardization.....	12
2.1.2. V2X Market and Key Players.....	15
2.1.3. Network Architecture	17
2.1.4. System Architecture	18
2.1.5. Automation Levels	21
2.2. V2X Protocol Stack.....	23
2.2.1. Application Layer	24
2.2.1.1. Safety and Traffic Efficiency.....	24
2.2.1.2. Other Applications	26
2.2.2. Facility Layer.....	26
2.2.2.1. Cooperative Awareness.....	28
2.2.2.2. Decentralized Environmental Notification	30

2.2.2.3. Collective Perception	31
2.2.2.4. Collaborative Localization.....	32
2.2.2.5. Platooning	35
2.2.2.6. Maneuver Coordination	36
2.2.3. Networking and Transport Layer	38
2.2.3.1. Basic Transport Protocol.....	39
2.2.3.2. GeoNetworking Protocol	39
2.2.4. Access Technologies	40
2.2.4.1. IEEE 802.11p.....	40
2.2.4.2. IEEE 802.11bd.....	41
2.2.4.3. LTE-V2X	42
2.2.4.4. NR-V2X.....	44
2.2.5. Management and Security Layer	45
2.3. Congestion Control Mechanisms	46
2.3.1. Facility Layer DCC	47
2.3.2. Networking and Transport Layer DCC	48
2.3.3. Access Layer DCC for IEEE 802.11p/bd.....	49
2.3.3.1. Reactive Approach.....	49
2.3.3.2. Adaptive Approach	50
2.3.3.3. Other Approaches	51
2.3.4. Cross-Layer DCC	52
2.3.5. Congestion Control in C-V2X.....	53
2.4. Resource Allocation Optimization.....	54
2.4.1. Congestion-aware Approaches.....	55
2.4.2. Content-aware Approaches.....	56
2.4.3. Integrated Approaches	58
2.4.4. Research Gap Refinement	59

3. DECENTRALIZED VOI-MAXIMIZING RESOURCE ALLOCATION	61
3.1. Problem Formulation.....	61
3.2. Introducing VALINDRA	64
3.3. A Service-specific Example	69
3.4. The Value of Information.....	71
3.4.1. Collective Perception.....	72
3.4.2. Maneuver Coordination.....	75
3.4.3. Collaborative Localization	79
3.4.4. VoI Functions in the Literature	83
3.5. Analytical Evaluation.....	90
3.5.1. Requirement Fulfillment.....	90
3.5.2. System Stability.....	92
3.5.3. Comparison to other Protocols	97
3.5.4. Further Aspects.....	100
4. PERFORMANCE EVALUATION	103
4.1. Simulation Environment	103
4.1.1. Requirements and State-of-the-Art.....	104
4.1.2. Introducing TEPLITS	106
4.1.2.1. Traffic and Vehicle Dynamics	106
4.1.2.2. Vehicle Sensors and Communication	107
4.1.2.3. Vehicle Perception and Control.....	108
4.1.3. System Architecture	108
4.2. Collaborative Localization	112
4.2.1. Service Definition.....	113
4.2.1.1. Positioning Algorithms	113
4.2.1.2. Message Generation.....	114
4.2.2. Parameter Settings	115

4.2.3. Channel Sensitivity.....	118
4.2.4. VoI Definition.....	121
4.2.5. VALINDRA-based Resource Allocation	126
4.2.6. Conclusion	127
4.3. Collective Perception	128
4.3.1. Parameter Settings	128
4.3.2. Channel Demand	131
4.3.3. Environmental Perception	139
4.3.3.1. Environmental Awareness Ratio.....	139
4.3.3.2. Detected Object Redundancy and Update Period.....	143
4.3.3.3. Object Tracking Accuracy	146
4.3.4. Risk Awareness and Safety	150
4.3.4.1. Environmental Risk Awareness.....	150
4.3.4.2. Comprehensive Safety Metric.....	153
4.3.5. Conclusion	156
5. CONCLUSION AND OUTLOOK.....	159
PUBLICATIONS.....	163
REFERENCES	165
SCIENTIFIC CAREER	193

LIST OF FIGURES

Fig. 1: Main causes of death for children and young adults worldwide	2
Fig. 2: RF spectra allocated to ITS applications in various regions of the world.....	14
Fig. 3: Communication links between road users and infrastructure	17
Fig. 4: High-level system architecture of a connected vehicle	18
Fig. 5: Relation between manifestation levels of automated and cooperative driving.	22
Fig. 6: European protocol stack with references to some of its core standards	23
Fig. 7: V2X applications supporting cooperative driving.....	25
Fig. 8: Selection of V2X messages and their structure.....	27
Fig. 9: Example scenario for Cooperative Awareness.....	28
Fig. 10: Example scenario for Decentralized Environmental Notification.....	30
Fig. 11: Example scenario for Collective Perception.	31
Fig. 12: Example scenario for Collaborative Localization	33
Fig. 13: Example scenario for Platooning	36
Fig. 14: Example scenario for Maneuver Coordination	37
Fig. 15: C-V2X sidelink resource pool and its constituents.	42
Fig. 16: DCC Architecture developed by ETSI for ITS-G5	46
Fig. 17: Architecture and main data flows of VALINDRA.	64
Fig. 18: Working principle of VALINDRA with Collaborative Localization.....	70
Fig. 19: Dynamic state space of VALINDRA in the α - β domain.....	95
Fig. 20: System behavior of VALINDRA regarding (a) equilibrium channel load and (b) convergence to equilibrium after the occurrence of a system perturbation	96
Fig. 21: Network-size-dependent protocol performances in terms of (a) equilibrium CBR and average message frequency, and (b) convergence speed	98
Fig. 22: Components and functionalities of TEPLITS	105
Fig. 23: Simplified overview of the vehicle system architecture in TEPLITS.....	109
Fig. 24: Proposed content of a satellite measurement object transmitted in a CLM	114
Fig. 25: CarMaker view of the investigated city square in Frankfurt (Main).....	115
Fig. 26: Propagation modes of the GNSS signals in (a) a schematic representation and (b) the investigated Frankfurt city square	116
Fig. 27: Positioning accuracy as a function of the generation jitter	119
Fig. 28: (a) Number of received messages for different channel loads, and (b) effect of the channel load on the age of information of the received CLMs	120
Fig. 29: Effect of the channel load on the area spanned by the vehicles of which CLMs are received	120

Fig. 30: Performance of Collaborative Localization in dependance of the number of connected stations and the number of shared satellite measurements per CLM.....	124
Fig. 31: Local optimum of the average horizontal positioning accuracy as a function of the number of connected stations.....	125
Fig. 32: Global optimum of the average horizontal positioning accuracy as a function of the number of connected stations employing VALINDRA	126
Fig. 33: Traffic characterization in terms of: (a,b) vehicle density and (c,d) speed distribution for (a,c) the low and (b,d) the high traffic density scenario. Traffic speed and density have a high impact on the performance of Collective Perception	129
Fig. 34: High-density highway segment of scenario B: (a) Ground truth positions of the vehicles; (b) Visualization of the environmental perception of a vehicle.....	130
Fig. 35: Message generation for the low-density scenario: (a) Vehicles on a highway section; (b) corresponding generated messages over time.....	132
Fig. 36: PDF and CDF of the number of objects per CPM for (a) E-CPM, R-CPM, A-CPM or P-CPM and (b) V-CPM.....	134
Fig. 37: Equipment rate dependence of (a) message size and (b) frequency	135
Fig. 38: CBR resulting from the five CPM dissemination modes: (a) for varying V2X equipment rates and (b) as PDF for full V2X equipment.	137
Fig. 39: Environmental Awareness Ratio for (a) low and (b) high-density scenario.....	140
Fig. 40: Updates per second for (a) low and (b) the high-density scenario.....	145
Fig. 41: Object Tracking Accuracy for (a) low and (b) high traffic-density scenario.....	147
Fig. 42: Object Tracking Accuracy for (a) low and (b) high traffic-density scenario.....	149
Fig. 43: Environmental Risk Awareness for (a) low and (b) high-density scenario	152
Fig. 44: Schematic visualizing the computation of the Comprehensive Safety Metric....	154
Fig. 45: Comprehensive Safety Metric for (a) low and (b) high-density scenario.....	155

Note: Several of the street scenarios were constructed using the © C2C-CC toolkit.

LIST OF TABLES

Table 1: Parameters for the 5-state reactive approach of DCC_ACC.....	50
Table 2: Performance of VALINDRA for different parameter choices of α	97
Table 3: Performance comparison between VALINDRA and the two state-of-the-art V2X protocols LIMERIC and A-DCC.	99
Table 4: Simulation parameters for a city square in Frankfurt.....	116
Table 5: GNSS-, sensor-, and communication parameters.	117
Table 6: Investigated highway scenarios with low (A) and high (B) traffic density.	129

LIST OF ABBREVIATIONS

Abbreviation	Explanation
3GPP	3rd Generation Partnership Project, formed by different telecommunications SDOs around the world, incl. ETSI
3GPP Rel-X	3GPP Release X. Important releases for V2X communications are Rel-14, Rel-15, Rel-16, and the upcoming Rel-17 and Rel-18
(4G) LTE V2X	LTE-based V2X communication technology mainly specified in 3GPP Rel-14 and Rel-15
5GAA	5G Automotive Association, formed by automotive and other companies to drive the development of C-V2X
5G NR V2X	NR-based V2X communication technology mainly specified in 3GPP Rel-16 and Rel-17
A-DCC	Adaptive DCC approach
ABS	Anti-lock Braking System
AC	Access Category: defines EDCA queue of a V2X packet, derived from TC in ITS-G5
ACC	Adaptive Cruise Control
ADAS	Advanced Driver Assistance System
AEB	Autonomous Emergency Braking
AOI	Age Of Information
AV	Automated Vehicle
BCC	Binary Convolutional Coding
BPSK	Binary Phase Shift Keying
BSM	Basic Safety Message: introduced by SAE for the US. Its European analogue is the CAM
BSS	Basic Service Set
BSW	Blind Spot Warning
BTP	Basic Transport Protocol
C-ACC	Cooperative/Connected ACC
C-ITS	Cooperative/Connected ITS
C-SAE	China Society of Automotive Engineers

C-V2X	Cellular Vehicle to Everything, ambiguously referring to LTE-V2X or NR-V2X
C2C-CC	CAR to CAR Communication Consortium, formed by automotive companies to drive the development of V2X
CAM	Cooperative Awareness Message
CAN	Controller Area Network
CBR	Channel Busy Ratio
CCU	Connectivity Control Unit
CCSA	China Communications Standards Association
CDF	Cumulative Distribution Function
CDOP	Cooperative DOP
CSMA/CA	Carrier-Sense Multiple Access with Collision Avoidance
CEN	European Committee for Standardization (French: <i>Comité Européen de Normalisation</i>)
CEPT	European Conference of Postal and Telecommunications Administrations (French: <i>Conférence Européenne des Administrations des Postes et des Télécommunications</i>)
CLM	Collaborative Localization Message
CNR	Code-to-Noise Ratio
CPF	Cognitive Particle Filter
CPM	Collective Perception Message. In the scope of this thesis the implementation modes E-CPM, R-CPM, A-CPM, P-CPM, and V-CPM are introduced (see Subsection 4.3.1).
CR	Channel occupancy Ratio
CSM	Comprehensive Safety Metric
CV	Connected Vehicle
D2D	Device-to-Device: Cellular side-link enables short range direct communication between devices
Day 1 / 2 / 3+	Successive C-ITS deployment phases of use cases and technologies defined by the C2C-CC
DCC	Decentralized Congestion Control: mechanism that aims at reducing channel congestion in ITS-G5 based networks; features components across the layers of the ITS-G5 stack (DCC_ACC, DCC_NET, DCC_CROSS, and DCC_FAC)
DCM	Dual-Carrier Modulation

DENM	Decentralized Environmental Notification Message
DFT-s-OFDM	Discrete Fourier Transform spread OFDM
DOP	Dilution Of Precision
DOR	Detected Object Redundancy
DP	DCC Profile, defines DCC queue for V2X packets transmitted via ITS-G5
DSRC	Dedicated Short Range Communication based on IEEE 802.11p
EAR	Environmental Awareness Ratio
EC	European Commission
ECC	Electronic Communications Committee, subsidiary of the CEPT
EDCA	Enhanced Distributed Channel Access
EKF	Extended Kalman Filter
eNB	eNodeB or evolved Node B: 3GPP-compliant implementation of 4G LTE base station
ENU	East-North-Up; widely used local tangent plane coordinate system
ERA	Environmental Risk Awareness
ESC	Electronic Stability Control
ETSI	European Telecommunication Standards Institute
ETSI TC ITS	ETSI Technical Committee dealing with ITS
FCC	Federal Communications Commission
FCW	Forward Collision Warning
FOV	Field Of View
FuSa	Functional Safety as defined in ISO 26262, IEC 61508
Galileo	European Global Navigation Satellite System
GEM	Global Environmental Model, see also LEM and LDM
GDOP	Geometric DOP
GLOSA	Green Light Optimized Speed Advisory
GLONASS	Russian Global Navigation Satellite System
GN solver	Gauss-Newton solver
gNB	gNodeB or 5G Node B: 3GPP-compliant implementation of 5G NR base station

GNP	GeoNetworking Protocol
GNSS	Global Navigation Satellite System
GPS	U.S. Global Positioning System
HARQ	Hybrid Automatic Repeat reQuest
HMI	Human Machine Interface
ICRW	Intersection Collision Risk Warning
IEEE	Institute of Electrical and Electronics Engineers
IEEE 802.11p	Ad-hoc short-range WLAN communication designed for automotive application, also referred to as pWLAN or WLANp
IEEE 802.11bd	Enhanced IEEE 802.11p, also referred to as NGV
IMA	Intersection Movement Assist
IMAGinE	German publicly funded project, flagship for the development of cooperative connected driving (German: <i>Intelligente Manöver Automatisierung - kooperative Gefahrenvermeidung in Echtzeit</i>)
IMU	Inertial Motion Unit
IP	Internet Protocol
ISO	International Organization for Standardization
ITS	Intelligent Transport Systems
ITS-G5	Intelligent Transport System @5.9GHz: European implementation of WLANp or NGV
ITS-S	ITS Station (e.g., vehicle, RSU, or VRU)
ITU (-R)	International Telecommunications Union (Radiocommunication Sector)
LCRW	Longitudinal Collision Risk Warning
LDM	Local Dynamic Map: a representation of the perceived environment within an ITS-S. See also LEM and GEM
LDPC	Low-Density Parity-Check
LDW	Lane Departure Warning
LEM	Local Environmental Model, see also GEM and LDM
LIMERIC	LInear MESSage Rate Integrated Control
LKA	Lane Keep Assist
LOS	Line of Sight
LTA	Left Turn Assist

LTE	Long Term Evolution, cellular communication technology
MAC	Medium Access Control
MCM	Maneuver Coordination Message
MCO	Multi-Channel Operation
MCS	Modulation and Coding Scheme
MIB	Management Information Base
MIMO	Multiple-Input Multiple-Output
MP	MultiPath propagation mode of GNSS signals
MSCM	Maneuver Sharing and Coordinating Message; US analogue for the VAM
MTU	Maximum Transmission Unit
mmWave	Millimeter Wave
NCAP	New Car Assessment Program
NGV	Next Generation V2X: see IEEE 802.11bd
NLOS	Non-LOS propagation mode of GNSS signals
NHTSA	National Highway Traffic Safety Administration, a subsidiary agency of USDOT
NR	New Radio
NT	Networking and Transport
OCB	Out-of-Context of a BSS
OFDM	Orthogonal Frequency Division Multiplexing
OEM	Original Equipment Manufacturer
OSI	Open Systems Interconnection, model defining the layers of a protocol stack
OTA	Object Tracking Accuracy
PC5	Direct communication interface for ITS-S
PCM	Platoon Control Message
PDR	Packet Delivery Ratio
PDU	Protocol Data Unit
PHY	Physical Layer
PMM	Platoon Management Message
PRN	Pseudo Random Noise; characteristic to each GNSS satellite

PSM	Personal Safety Message: defined by SAE, for European analogue see VAM
QAM	Quadrature Amplitude Modulation
QoS	Quality of Service
QPSK	Quaternary Phase-Shift Keying
R-DCC	Reactive DCC approach
RB	Resource Block; smallest unit of resources that can be allocated to a UE in C-V2X
Rel-X	Release X, see 3GPP Rel-X
RF	Radio Frequency
RGP	Remote Garage Pilot
RHS / RHW	Road Hazard Signaling / Road Hazard Warning
RMS	Root-Mean-Square
ROS	Robot Operating System
RP	Resource Pool; logical abstraction for flexible management of resources in C-V2X
RPP	Remote Parking Pilot
RSSI	Received Signal Strength Indicator
RSU	Road Side Unit (ITS Station)
Rx	Receiver
SAE	Society of Automotive Engineers
SAE L1 to L5	SAE automation levels from manually to fully automated driving
SCI	Sidelink Control Information
SCS	Subcarrier Spacing
SDAP	Service Data Adaptation Protocol
SDSM	Sensor Data Sharing Message: defined by SAE, for European analogue see CPM
SDO	Standards Developing Organization
SEC	Security entity; cross layer component of the ITS protocol stack
SHB	Single Hop Broadcast
SINR	Signal-to-Interference-and-Noise Ratio
SLAM	Simultaneous Localization And Mapping

SNR	Signal-to-Noise Ratio
SOTIF	Safety Of The Intended Functionality as defined in ISO 21448
SPLOS	Single-Path LOS propagation mode of GNSS signals
SPS	Semi-Persistent Scheduling; used in LTE-V2X mode 4
TB	Transport Block; payload passed between MAC and PHY in C-V2X
TC	Traffic Class; defines a V2X packet's priority for ITS-G5 and C-V2X. Not to be confused with ETSI TC ITS, where TC stands for Technical Committee
TDC	Transmit Data-rate Control
TEPLITS	Development and TESt Platform for ITS
Tier 1 / 2 / 3	Automotive suppliers and engineering companies
TJP	Traffic Jam Pilot
ToC	Transition of Control; from vehicle to driver or vice versa
TPC	Transmit Power Control
TR	Technical Report
TRC	Transmit Rate Control
TS	Technical Specification

1. INTRODUCTION

In this chapter the reader is introduced into the broader scope of this doctoral work. Section 1.1 motivates and works out the challenges addressed, highlighting the relevance of the work. Section 1.2 then gives insights into the background of the work and points out important aspects for its understanding. Finally, Section 1.3 illustrates the structure of this thesis.

1.1 Motivation

Our modern society is experiencing profound structural changes. Globalization has enabled previously unthinkable economic opportunities, leading to unprecedented wealth and prosperity on one side, but also to an irreversible extinction of cultural- and biodiversity on the other [1]. In the 21st century globalization is expected to eradicate another 50-90% of contemporary languages [2, 3] (compared to 6% in the 20th century [4]) and around 2-10% of contemporary species [5, 6] (compared to the natural background extinction rate of 0.01-0.02% [5]). This development is especially worrying, as natural barriers such as mountain ranges, oceans, deserts and raging rivers, historically the main sources of cultural- and biodiversity, are easily overcome, substantially reducing the likelihood of new emerging cultures and species. On the other hand, the relativization of these barriers has also led to the emergence of large multinational companies and the rapid spread of new technologies. The accompanying increase in prosperity and life expectancy has led to an exponential increase in the world population. Almost 7% of all individuals who have ever lived in the 2 million years of human history are alive today [7, 8, 9] and have increasing demands on high living standards including access to adequate health care, education, housing, and a high degree of mobility. However, in contrast to the latter, all other mentioned factors have a positive effect on live expectancy. The observed urge for individual mobility poses significant challenges to future traffic safety, efficiency, and comfort. The number of worldwide vehicle registrations reached the 1 billion mark in 2010, currently roughly doubling every 25 years [10, 11, 12]. In its Global Status Report on Road Safety 2018 the World Health Organization (WHO) estimates the number of road traffic casualties to

already exceed 1.35 million each year [13], which amounts to almost 4,000 a day! To put this into perspective, road injury is by far the leading cause of death for children and young adults between 5 and 29 years according to the WHO [14, 15] as is illustrated in Fig. 1 (data based on [16]).

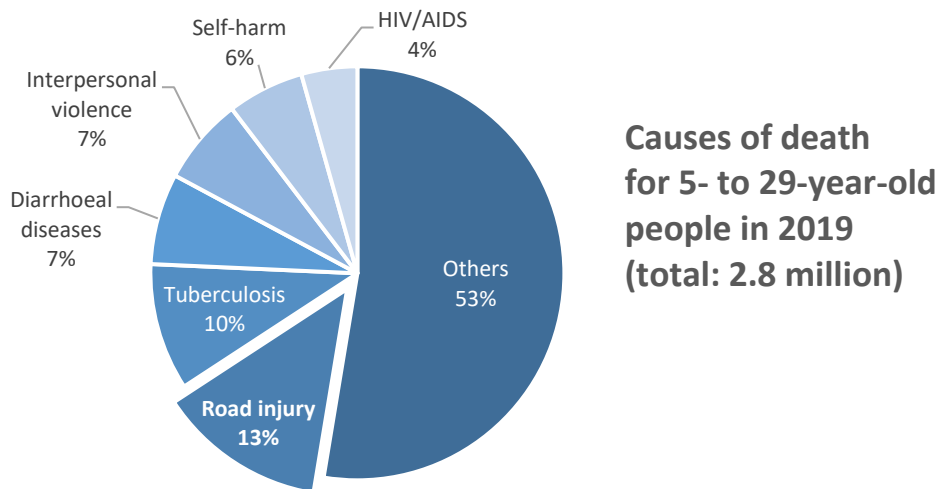


Fig. 1: Main causes of death for children and young adults worldwide, according to the databases maintained by the WHO.

Even though not comparable to the loss of human lives, the globally rising traffic density has come along with further major challenges. Considering the up to 50 million non-fatal traffic accidents [17], the annual global macroeconomic burden for the world economy is estimated to be surpassing the EUR 1.5 trillion mark¹ [18]. According to [18] this corresponds to a yearly loss of 0.12% of the global gross domestic product projected by the World Bank for the coming 10 years [19, 20] or 70 million disability-adjusted life-years² [21] worldwide.

Another relevant aspect is the time spent in traffic jams. Before the global Covid-19 pandemic it amounted to yearly 42h in the US [22] and to 31h in Europe [23] for an average driver, roughly equating a full working week per year. In bigger cities the average time lost in traffic jams is even four times higher [24]. Besides the time lost, traffic jams also contribute to the unnecessary generation of greenhouse gas exhausts. In the US, France, Germany, and the UK alone idle

¹ Based on the actual USD/EUR exchange rate of 0.85 EUR per USD (7th Aug 2021)

² Disability-adjusted life-years (DALY): measure of 'healthy' life lost due to disability, early death or other impediments and burdens.

engines waste around six billion liters of fuel yearly, corresponding to over 15 million tons of CO₂. With an annual absorption of 0.6 tons of CO₂ per hectare [25], 2.5 million hectares of tropical forests (comparable to the size of Belgium!) would be required only to bind the CO₂ produced by traffic jams in these four countries. Additionally, the fuel wasted in traffic jams costs the average household over EUR 1500³ annually with a strongly rising tendency forecasted until 2030 [26].

All these drawbacks of the rapidly growing global traffic density have led politics and industry to push the development of new technologies to increase traffic safety, efficiency, and comfort. 27 years after Karl Benz filed his famous patent *Fahrzeug mit Gasmotorenbetrieb* (German; “Gas powered vehicle”) in 1886 [27], Bosch introduced the Bosch light [28], which would quickly become standard in Europe, replacing the earlier used candle-based headlights. The first rear-view mirrors were mounted on passenger cars in 1914, e.g., on the Ford Model T. Less than 10 years later it would already become mandatory in some regions of the world [29]. In 1918 Malcolm Loughead engineered the first four-wheel hydraulic-brake system, which was first implemented in the Duesenberg 1918 and would experience a vast adoption in the automotive world in the following years [30]. The first electric three-color traffic light was developed and installed in Detroit, Michigan by police officer William Potts in 1920 [31]. The first crumple zones were developed and patented by Mercedes-Benz in 1952 and installed in the Mercedes-Benz 220 in 1959 [32]. Nils Bohlin introduced the first three-point seat belt, which was first sold in a Volvo PV544 that same year [33, 34]. In a large-scale crash study, he could show that while unbelted drivers risked fatal injuries for all tested speeds, none of the belted drivers were fatally injured at speeds below 60 mph [34]. Another 9 years later the first airbag was introduced after Allen K. Breed had invented a ball-in-tube crash detection sensor [35]. Though it wouldn’t be until 13 years later that, in 1981, Mercedes-Benz equipped its S-Class W126 with airbags, becoming the first commercial passenger cars with such equipment [36]. However, before the eventual introduction of the airbag, it was the time of another disruptive innovation developed in a tight cooperation between Bosch and Daimler: the anti-lock braking system (ABS). It was launched with the W116 Mercedes-Benz S-Class in 1978 [37]. The first

³ Based on the actual USD/EUR exchange rate of 0.85 EUR per USD (7th Aug 2021)

adaptive cruise control (ACC) system was introduced by Toyota on board of the Toyota Celsior in 1997 [38]. After this first lidar-based ACC Mercedes introduced the first radar-assisted ACC on the W220 Mercedes-Benz S-Class and the CL-Class in 1999 [39, 40]. That same year Subaru launched the first camera-assisted ACC on board of the Subaru Legacy Lancaster [41]. Only one year later the first lane departure warning (LDW) system, developed by Iteris, made its debut on a Mercedes Actros [42]. Another three years later, in 2003, the first lane keep assist (LKA) system was launched with the Honda Inspire [43]. Around 2007 the wireless local area network (WLAN)-based standard for inter-vehicle-communication IEEE 802.11p got stable, with the approved amendment being published in 2010 [44]. It builds the basis of Europe's intelligent transport systems operating in the 5 GHz frequency range (ITS-G5) communication standard [45], the American dedicated short-range communications (DSRC) [46], and the Japanese Association of Radio Industries and Businesses (ARIB) STD-T109 [47]. In 2013 Mercedes launched *distronic plus with steering assist and stop&go pilot*, the first autonomy level 2 system, available on the market [48]. It enables automated longitudinal and lateral control at once. Two years later, Toyota became the first automotive original equipment manufacturer (OEM) to launch vehicle-to-everything (V2X)-enabled vehicles [49]. The V2X-enabled models launched were Toyota Prius, Toyota Crown Majesta, Toyota Crown Royal, and Toyota Crown Athlete [50]. In summer 2017, Audi intended to launch the first autonomy level 3 series production vehicle with the fourth generation Audi A8 [51]. Level 3 autonomy already permits the driver to turn his attention away from driving until he is explicitly requested by the vehicle to take control again [48]. The system comprised an automation-level-3 capable Traffic Jam Pilot (TJP) and the Audi AI Remote Parking Pilot (RPP) as well as the Audi AI Remote Garage Pilot (RGP), the latter two being able to park the vehicle without the driver's engagement [51]. However, the introduction of the system was delayed [52] and finally cancelled entirely [53] due to the missing legal basis for such autonomy levels. That same year, in 2017, the 3rd Generation Partnership Project (3GPP) published the specifications for cellular V2X (C-V2X) in Release 14 as an alternative to the WLAN-based IEEE 802.11p communication standard [54]. C-V2X extends IEEE 802.11p's direct vehicle-to-vehicle (V2V) and vehicle-to-infrastructure (V2I) communication by adding mechanisms for wide

area cellular network communication, referred to as vehicle-to-network (V2N) communication.

In view of the fast technological progress, also legislation is catching up and in May 2021 the German Bundestag proposed the “Gesetz zum autonomen Fahren” (German; Autonomous Driving Act), clearing the way for level 4 automated driving [55]. Level 4, referred to as “high automation”, allows the driver to completely rely on their vehicle in predefined driving modes, thus assuming his responsibility even in critical fallback scenarios [48]. Only a few days after the proposal the Bundesrat, the German Federal Council, approved the legislative resolution of the Bundestag in a shortened period, making Germany the pioneer in bringing traffic automation to the streets [55]. At the same time, the number of connected vehicles is expected to be reaching the 2 million units mark [56]. In this context Euro NCAP (New Car Assessment Program) and the German General Automobile Club ADAC (German; Allgemeiner Deutscher Automobil-Club), the largest and most influential in Europe [57], have tested and recognized the tremendous potential of V2X communication for traffic safety, with Volkswagen’s ITS-G5-based communication system aboard the Golf 8 becoming the first innovative technology being rewarded by Euro NCAP in nearly six years [58], and passing the ADAC test [59].

Overall, these and numerous other of the latest developments strongly suggest a rapid introduction and spreading of the two technologies regarded as key for a safer future of road traffic: automated and connected driving. According to the American National Highway Traffic Safety Administration (NHTSA) alone the two V2V-enabled technologies intersection movement assist (IMA) and left turning assist (LTA) could help preventing 41-55% of intersection crashes and 36-62% of left turn crashes respectively and have a mitigating effect on the severity of unavoidable crashes [60]. Overall, the report states that up to 1,083 lives could yearly be saved in the US by IMA and LTA, representing a 3% of 2020’s traffic fatalities [61]. Further, NHTSA estimates that 270,000 injuries, amounting to 14% of the almost 2 million reported cases, could be prevented [62]. Expectably, the development of further automated and connected driving functions, such as sensor-data sharing, hazard warning, and maneuver coordination, will greatly contribute to enhance road safety. However, also road efficiency and comfort are expected to increase considerably with the help of connected and automated driving. According to studies, the time drivers waste

due to traffic congestion could be reduced by more than 30% [63]. Returning to the examples given above, this would imply average annual savings of almost two working days spent in traffic and EUR 500 in wasted fuels per individual. Moreover, the US, France, Germany, and the UK could reduce their yearly greenhouse emissions by 5 million tons of CO₂, corresponding to the absorption capacity of over 1 million soccer fields of tropical forests.

Nevertheless, while automated driving is generally regarded as an inherently scalable technology, even profiting from higher market penetration rates, the case of connected driving is clearly more complex. On one side, higher market penetration rates lead to more available data and thus a potentially better decision basis [A5]. On the other, the amount of shared data is expected to pose serious challenges to the communication technologies by saturating the wireless channel, deteriorating the systems performance [A4, A7]. For this reason, an essential condition for a successful deployment of connected driving is the orchestration of the increasing number of V2X services competing for the scarce channel resources [64]. Such a technology should be able to assess the value of all data available for transmission, such as the vehicle state, sensor data, planned or requested driving trajectories, live street maps or traffic light phases, to decide in a decentralized manner which data should be granted access to the wireless channel. This doctoral work faces the challenge and introduces VALINDRA (value of information based decentralized resource allocation), a cross-service communication protocol designed to maximize the value of information disseminated in vehicular networks of tomorrow.

1.2. General Remarks

In order to achieve the ambitious goal defined in the previous section, various preparatory tasks and studies were necessary in view of their high degree of innovation and the associated prevailing state-of-the-art at the beginning of this doctoral work. These preparatory tasks and studies are an essential part of this “doctoral work”, as without them this work would not have been possible. They are however not part of this document, the “doctoral thesis”, for two reasons: (i) to maintain the highest possible level of novelty throughout the thesis, and (ii) since they are required to develop the solution to the identified research gap but not essential part of the solution itself. The distinction between terms “doctoral work” and “doctoral thesis” is kept throughout this document.

Thus, while the remainder of this thesis focusses on the design and evaluation of VALINDRA, in the following a short overview of the other endeavors necessary for the completion of this doctoral work is provided. Many of these have resulted in publications (see appendix “Publications”) and are characterized by the notation [A{reference number}] in this thesis.

An extensive examination of the existing state-of-the-art unveiled the lack of a suitable **simulation framework** bringing together all required system components, such as inter-vehicle communication, traffic and single-vehicle dynamics, on-board sensors, and autonomous driving functions [A5]. For this reason, a framework meeting these requirements was set up comprising all until then identified relevant components and including a highway-merging assistant as well as both direct V2X communication technologies, IEEE 802.11p and C-V2X [A5]. This simulation environment, referred to as **TEPLITS (testing platform for intelligent transportation systems)**, was later extended by a Global Navigation Satellite System (GNSS) signal generator in [A8], after the high relevancy of an accurate GNSS positioning simulation was identified. TEPLITS was built on the Robot Operating System (ROS), allowing a rapid transfer from simulation into real test vehicles. In a cooperation with Stefan Jesenski (Robert Bosch GmbH) TEPLITS could be further enhanced by synthetically extending drone-recorded vehicle tracks with the help of Bayesian networks, opening new simulative investigation possibilities [A2].

In parallel three novel V2X services were chosen for the final investigation: (i) Collective Perception, enabling the exchange of detected object data within the vehicular network to enhance the environmental perception, (ii) Maneuver Coordination, enabling the exchange of driving trajectories for cooperative maneuvering, and (iii) Collaborative Localization, enabling the exchange of raw GNSS measurements to enhance the networks absolute and relative positioning. As these services have not been standardized yet, the definition of suitable generation rules and message formats was necessary for the later use with VALINDRA.

For **Collective Perception**, the most advanced of the three V2X services, the standardization process was monitored closely, including active participation at the responsible institutes, ETSI (European Telecommunications Standards Institute) and C2C-CC (Car-to-Car Communication Consortium) based on analytical [A3, A4, A7] and simulative studies [A5, A14, A15]. The latter were

part of a cooperation with Georg Volk (University of Tübingen) and Quentin Delooz (Hochschule Ingolstadt). In October 2021 the author was elected rapporteur of the WI “Collective Perception” at ETSI to lead the standardization of V2X-based sensor-data sharing in Europe.

The work on **Maneuver Coordination**, already featuring a work item at ETSI, however in a very early state, resulted in a fruitful cooperation with Daniel Bischoff (Opel GmbH) and later Johann Thunberg and Alexey Vinel (both Halmstad University, Sweden). Cooperative maneuvering was analyzed in simulation and analytically, quantifying its overall benefit and the impact of communication, and new data-aware generation rules were proposed [A6, A9, A13, A18, A19].

Finally, **Collaborative Localization**, for which no V2X service had been specified before, was developed and investigated analytically [A10] and in simulation [A8, A11, A12] based on key findings from previous field tests [A1]. With the developed message format and generation rules it was then first presented to the research community in [A16]. This work was carried out in collaboration with Simon Ollander, and Nikolay Mikhaylov (both Robert Bosch GmbH).

Many of these works were supported by Ignacio Llatser (Robert Bosch GmbH), great friend and mentor, who contributed with his vast experience in V2X technology and valuable ideas. Further, several of the mentioned publications were supported by or carried out in the scope of student internships or master theses. Master students contributing to this doctoral work were Tobias Frye, Johannes Frye, Johannes Krost, Yan Jiang, Shuo Li, Yichen Liu, and Edmir Xhoxhi.

1.3. Structure

The remainder of this thesis is structured as follows. Chapter 2 introduces all background information related to V2X communication relevant for the understanding of this thesis, giving insights into regulation and standardization history, the market and its key players, and the system architecture of connected vehicles and vehicular networks. It then presents the V2X protocol stack and the corresponding congestion control mechanisms with special remark on the facility layer. The latter is particularly relevant for the development of a data-aware dissemination mechanism like VALINDRA, as this layer administrates the

payload of V2X messages. Chapter 2 is concluded with a refinement of the goal of this thesis, only roughly defined in Section 1.1 and the research gap analysis carried out in the preceding subsections.

In Chapter 3 the identified resource allocation problem is formalized and VALINDRA is introduced as possible solution. In the scope of its definition, the Value of Information (VoI) is defined exemplarily for three distinct V2X services. Subsequently, VALINDRA is submitted to a thorough analytical evaluation, investigating its closeness to the optimal solution of the resource allocation problem, the system stability and convergence speed, and the extent to which it fulfils the previously identified requirements. VALINDRA is finally compared to existing protocols and relevant aspects such as compatibility with other congestion control mechanisms, integrability into the current V2X protocol stack, and optimizability are discussed.

The target of Chapter 4 is the investigation of VALINDRA in a full-fledged V2X environment. To this end, it first briefly introduces TEPLITS, the simulation and testing platform developed in the scope of this doctoral work, before detailing the implementation and tuning of VALINDRA on the example of Collaborative Localization, which is also introduced in this chapter. After an extensive discussion of different VoI definitions and their impact on VALINDRA, the chapter is concluded with a comparison of the developed protocol with state-of-the-art congestion control mechanisms on the example of Collective Perception.

Finally, Chapter 5 summarizes the key findings of this work, gives an outlook on eventual transfer scenarios for their adoption, and identifies possible future research directions.

2. VEHICLE TO EVERYTHING COMMUNICATION

This chapter is intended to provide the reader all necessary background information required for the understanding of this work. Section 2.1. introduces the concept of connected vehicles and gives insights into the related regulatory and standardization activities, the global V2X market and the system architecture. Section 2.2 discusses the V2X protocol stack, with special remark on the facility layer and the V2X services it hosts. Based on the V2X protocol stack Section 2.3 then reviews the standardized congestion control mechanisms designed to maintain the amount of data accessing the communication channel within acceptable limits. Finally, Section 2.4 analyzes the state-of-the-art resource allocation mechanisms and refines the research questions based on the previous research gap analysis.

2.1. Connected Vehicles

Vehicles are equipped with an increasing level of Advanced Driver Assistance Systems (ADAS) and Autonomous Driving (AD), aimed at supporting the driver's decision making (partly) relieving him from the vehicle control (see Subsections 2.1.4 and 2.1.5). Both systems rely on a real-time assessment of the vehicle's environment enabled by the vehicle's on-board sensors, such as radars, LIDARs, or video cameras. The gathered sensor data is fused into the so-called Local Environmental Model (LEM), which is a representation of the vehicle's environmental perception.

However, the vehicle's local perception faces relevant limitations, such as a limited field of view and perception range of the on-board sensors used for its generation. Their perception is further generally restricted to regions in Line of Sight (LOS), thus being unable to perceive occluded objects [A3]. Only partly visible objects may not be detected accurately or not be detected at all. Moreover, it is a known fact that today's sensor systems do not work reliably in adverse weather conditions [65]. Apart from these limitations regarding the real-time assessment of the vehicle's environment, also the prediction of other traffic participant's trajectories is an extremely challenging task. Let alone an efficient and reliable cooperative maneuver coordination and execution. Altogether, these limitations result in an inaccurate perception and interpretation of the current and predicted traffic situation, risking suboptimal [A5] or even erroneous [66, 67] output of the vehicle controller.

To overcome the identified limitations and enhance the vehicles' environmental perception, V2X communication enables vehicles to behave cooperatively by exchanging information with their environment [68]. Currently there are two technologies competing as enablers of V2X communications [69]: the WLAN-based IEEE 802.11p standard and 3GPP's cellular-based C-V2X. While IEEE 802.11p is a purely direct communication technology, C-V2X supports a network-controlled operation mode (also referred to as mode 3 in LTE-V2X and mode 1 in NR-V2X) in addition to the direct autonomous operation mode (also referred to as mode 4 in LTE-V2X and mode 2 in NR-V2X) over the PC5 interface [54]. A detailed discussion of the access layer technologies is provided in Subsection 2.2.4.

By making use of these technologies, Connected Vehicles (CVs) are able to warn each other of detected potential road hazards (e.g., animals, lost items, or frozen street segments), exchange data related to the traffic (e.g., their own states, detected traffic participants, road signs, or traffic light phases), and even to coordinate maneuvers by negotiating driving trajectories. CVs are thus expected to greatly enhance the functionality spectrum of ADAS and AD, significantly improving driving safety, efficiency, and comfort.

This section is aimed at providing the relevant background for the understanding of CVs, as well as an introduction to the underlying technologies. Subsection 2.1.1 elaborates on the regulation and standardization history of CVs. Subsection 2.1.2 then gives an overview of the V2X market and its key players. Subsections 2.1.3 and 2.1.4 introduce the vehicular network architecture and the CV's internal architecture, respectively. Subsection 2.1.5 finally introduces the levels of vehicular automation and makes the link to CVs.

2.1.1. Regulation and Standardization

Regulation and standardization are, especially in the field of wireless communication technology, essential to ensure interoperability between manufacturers, an orchestrated market introduction and penetration, and an adequate allocation of the limited frequency spectrum. These tasks are pursued by numerous international, national, and regional regulatory authorities, standard developing organizations (SDO), and industry associations.

CVs are intended to, among others, share traffic safety and efficiency related data. To guarantee high levels of reliability and compliance with the latency requirements of safety-critical applications (see, e.g., [A19]), a dedicated share of the Radio Frequency (RF) spectrum must be assigned to ITS applications.

Already in 1999, the American Federal Communications Commission (FCC) allocated 75 MHz in the 5.9 GHz band to ITS use cases based on DSRC [70]. In the following years several pre-deployment projects, such as the US Department of Transportation (USDOT)

Test Plan [71], the New York DOT Pilot [72, 73], the Wyoming DOT Pilot [74, 75], the Ann Arbor Connected Vehicle Test Environment [76, 77], and the Virginia Connected Corridor [78, 79], were carried out under the supervision of the USDOT, convincing its subsidiary NHTSA of the technology's maturity [80]. Thereupon, NHTSA published an advance notice of proposed rulemaking in the US Federal Register proposing the technology's mandatory introduction to foster a rapid rollout [81]. However, in December 2019 the FCC communicated its intention to reevaluate the spectrum allocation [82]. A year later FCC ruled the lower 45 MHz of the spectrum, previously designated to ITS safety purposes, to be redesignated to consumer WLAN, namely Wi-Fi 5 (WLAN 802.11ac [83]) and Wi-Fi 6 (WLAN 802.11ax [84]). The decision became effective in July 2021 [85], despite determined objections from USDOT [86] (cf. Fig. 2).

In Europe, the European Commission (EC) designated 30 MHz to ITS applications in 2008, nine years after the initial consideration of ITS spectra by the FCC [87]. The decision was based on an EU-wide harmonized ETSI standard for the operation of ITS-G5 [88] and adopted by the European Parliament and the European Council in 2010 [89]. Additionally, the European Electronic Communications Committee (ECC), a subsidiary organization of the European Conference of Postal and Telecommunications Administrations (CEPT), proposed to extend the ITS spectrum by 20 MHz on the upper frequency range and another 20 MHz for non-safety applications on the lower frequency range [90, 91]. The spectrum was originally foreseen entirely for the operation based on the ITS-G5 technology. However, in 2019 the European Council rejected the corresponding Delegated Act, currently leaving the door open for technology neutrality [92]. Numerous initiatives and testbeds have been launched for pre-deployment purposes in the EU, such as the C-Roads Platform [93], the C-ITS Corridor [94], SCOOP@F [95], the A2/M2 Connected Vehicle Corridor [96], Nordic Way [97], and Interoperable Corridors [98], among others. Contrary to the situation in the US, Europe strongly opposes the segregation of the ITS spectrum and mandates co-channel coexistence and backwards compatibility with ITS-G5 [99]. This view was ratified in the CEPT WG FM meeting during October 4-8th 2021, opposing the spectrum segregation proposal of 5GAA [100].

Similar developments have taken place in other regions of the world. Fig. 2 summarizes the corresponding RF spectra dedicated to ITS applications, differentiating between safety and non-safety channels, and highlighting the control channels reserved for critical safety applications. The spectra were allocated closely following the recommendation of the International Telecommunications Union Radiocommunication Sector (ITU-R), also depicted in Fig. 2 [101]. For a more comprehensive survey on spectrum regulation and ITS pre-deployment initiatives the interested reader is kindly referred to [102].

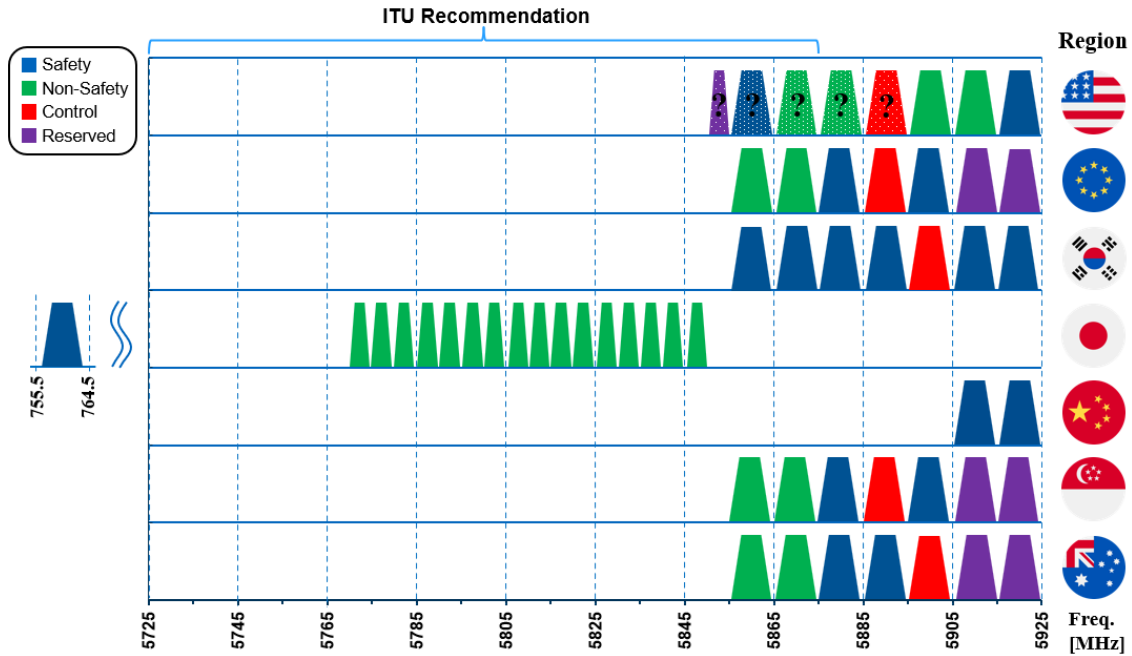


Fig. 2: RF spectra allocated to ITS applications in various regions of the world, adopted and extended from [85, 102, 103, 104].

Given the allocated share of the RF spectrum in the different regions of the world, the interoperability between equipment manufactured by distinct OEMs must be ensured. To this end numerous SDOs and industry alliances have developed and maintained automotive ITS standards. The most important interoperability standards are released in binding norms by the corresponding regulatory authorities. Due to its interdisciplinarity, connecting several formerly unrelated market segments such as automotive, big data, telecommunications, retail, and the internet of things, the number of SDOs and industry alliances active in standardization is accordingly vast (see Subsection 2.1.2). These institutions are generally active in well-defined parts of the ITS protocol stack (see Section 2.2). In the following only some of the most influential ones are mentioned. The most relevant related standards are provided in the indicated subsections.

The highest layers of the ITS protocol stack, known as application layer (Subsection 2.2.1) and facilities layer (Subsection 2.2.2), specify the use-cases of CVs and the enabling V2X services. The standardization activities on these layers are driven by SDOs such as ETSI (EU), US-SAE (American Society of Automotive Engineers; US), SAE-China (Chinese Society of Automotive Engineers; China), and CCSA (China Communications Standards Association; China). These SDOs are supported by industry alliances such as

the C2C-CC (EU), ITS America (US), CAICV (China Industry Innovation Alliance for Intelligent and Connected Vehicles; China), and 5GAA (5G Automotive Association; International).

On the transport and networking layers (Subsection 2.2.3) some of the active SDOs are ETSI (EU), US-SAE (US), SAE-China (China), and IEEE (International). They are supported by ISO (International Standards Organization) in the definition of security services on the cross-stack security layer (Subsection 2.2.5).

Finally, on the radio access layers (Subsection 2.2.4) IEEE is the main driver behind IEEE 802.11p and its successor IEEE 802.11bd, while 3GPP, a partnership between the SDOs ARIB, ATIS, CCSA, ETSI, TSDSI, TTA, and TTC, develops and specifies the C-V2X family, including LTE-V2X and NR-V2X up to now.

2.1.2. V2X Market and Key Players

The volume of the global market for connected vehicles was estimated to have amounted to around EUR 46 billion in 2020 as reported by the world's largest market research store MarketsandMarkets Research [105]. According to the same source by 2025 the connected vehicles market is expected to reach EUR 141 billion. Capgemini Invent reported 119 million connected cars sold until 2018 and expects this number to reach 353 million by 2023 [106]. Roughly one third of these vehicles were sold in the EU, another third in the US, a sixth in China. For 2023 this proportion is expected to shift slightly in favor of China at the expense of the US, with the EU keeping their market share.

As with most innovative technologies that must undergo extensive legislation, technology development, and standardization activities, the market introduction of direct V2X communication enabled vehicles requires an accordingly longer ramp-up time than that of V2N enabled vehicles. In 2020, the automotive V2X market was estimated to have amounted to comparably low EUR 584 million and it is forecasted to reach EUR 10,904 million by 2028 [107, 108]⁴. Overall, this corresponds to a Compound Annual Growth Rate (CAGR) of 44.2%. In terms of regional shares Europe is expected to be the leading V2X market for direct communication.

Some of the key players active in the connected car ecosystem, clustered according to industry segments, are chipset vendors (e.g., NXP Semiconductors, Autotalks Ltd., Qualcomm Technologies Inc., STMicroelectronics, Marvell⁵, Intel Corporation, Nvidia, Texas Instruments Inc., Infineon Technologies AG, and Fujitsu), wireless module vendors

⁴ Based on the actual USD/EUR exchange rate of 0.85 EUR per USD (7th Aug 2021)

⁵ Formerly Cavium.

(e.g., Huawei Technologies Co. Ltd., ublox, Harman International, Gemalto, Sierra Wireless, Ficoso Internacional S.A., Unex Technology Corp.), operating systems and software platforms (e.g., IBM, Google, Microsoft, QNX), middleware providers (e.g., AT&T, Cisco Systems Inc., Nuance), databases (e.g., IBM, MySQL, Oracle, Hitachi Data Systems), V2X software stack and services (e.g., Cohda Wireless, Commsignia Ltd., Infineon Technologies AG, Marben Products, Altran, Escrypt GmbH, Vector Informatik GmbH, Danlaw Inc.), tier 1 and tier 2 suppliers (e.g., Robert Bosch GmbH, Continental AG, Denso Corporation, Delphi Technologies, Aptiv, Magneti Marelli, Hella GmbH, Lear Corporation, Magna International), automotive OEMs (e.g., Volkswagen AG, Toyota Motor Corporation, General Motors, Ford Motor Company, BMW AG, Daimler AG, Audi AG, Stellantis, Groupe Renault, McLaren Group, Tata Motors, Hyundai Motor Company, Nissan Motor Corporation, Mitsubishi Corporation), and road side infrastructure (e.g., Kapsch Group, Commsignia Ltd., Robert Bosch GmbH, and Siemens AG). Additionally, the network-assisted connected driving ecosystem further includes mobile network operators (MNOs, e.g., AT&T, Verizon Communications, T-Mobile International, Sprint Corporation), telematics service providers (TSPs, e.g., WirelessCar AB, Aeris Communications, Airbiquity, Agero Inc., Hughes Telematics), cloud platform providers (e.g., Ericsson, BMW AG, Robert Bosch GmbH, CloudMade, Harman International, IBM), and app platforms (e.g., Android Auto, Apple CarPlay, OpenCar, CarForce, AppCarousel, Automatic). With the automotive V2X market still in the process of unfolding, and the RF access technology not ultimately defined it is still too early for clear forecasts regarding the distribution of the market's shares among the different stakeholders and industries.

The average total deployment cost of connected vehicle technology is expected to fall from EUR 295 in 2020 to EUR 189 in 2058 with full market penetration according to NHTSA [109]⁶. These costs arise from the vehicle equipment costs (falling from EUR 279 in 2020 to EUR 158-169 in 2058), the additional fuel consumption generated by the weight of the equipment (constant between EUR 7 and EUR 15), the security credential costs attributed to the required deployment of RSUs (estimated at EUR 2 per connected car), and security credential management system units to authenticate the received data (averaging a constant EUR 7). Additionally, the report stresses the impact of the utilized access technology on the total price. While the Wi-Fi-based IEEE 802.11p is free of charge, cellular technology is expected to almost double in costs per vehicle over the analyzed period. This increase is justified with the rising data requirements as the number of cooperating vehicles increases. Overall, the costs of connectivity thus lie well below the

⁶ All values based on the actual USD/EUR exchange rate of 0.85 EUR per USD (7th Aug 2021).

expected positive impact of the technology, reaching an economic break even in less than a year, while enabling relevant time savings, relieving the environment, and considerably reducing the crash rate (cf. Section 1.1 for numbers).

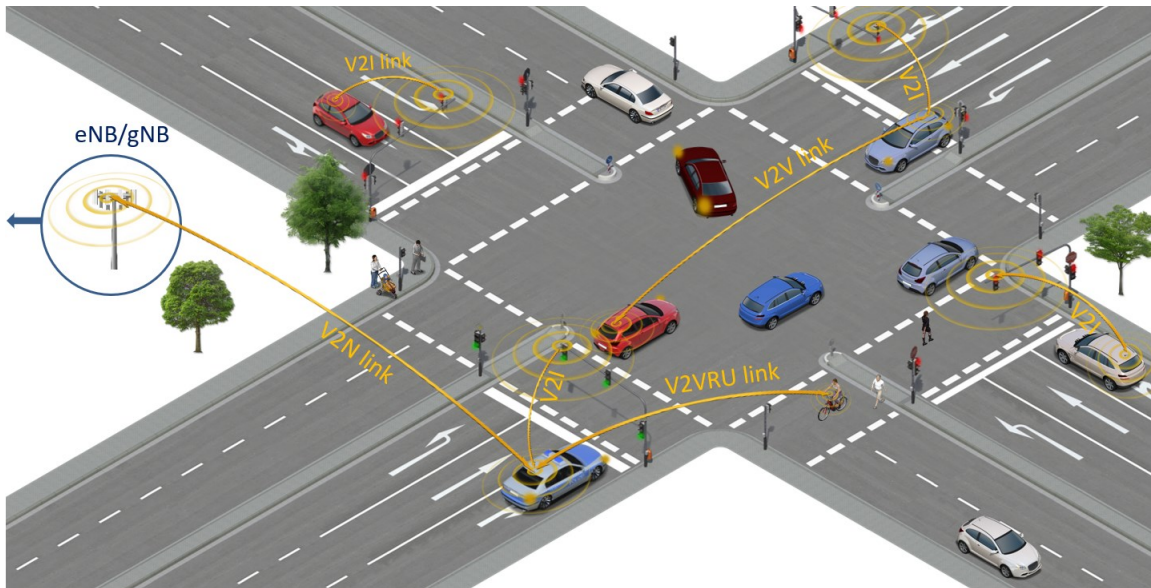


Fig. 3: Communication links between road users and infrastructure for a standard urban intersection scenario.

2.1.3. Network Architecture

Road traffic is complex. Numerous road users interact with each other, with road infrastructure, and the environment. The same applies to vehicular networks. Fig. 3 shows a standard intersection scenario with connected and legacy non-connected traffic participants, jointly referred to as mixed traffic. Four types of links are represented: (i) Vehicle-to-Vehicle (V2V), (ii) Vehicle-to-Vulnerable-Road-User (V2VRU) with the subcategory Vehicle-to-Pedestrian (V2P), (iii) Vehicle-to-Infrastructure (V2I), and (iv) Vehicle-to-Network (V2N). While the former three are most commonly implemented using broadcast communication, the latter is generally implemented in a unicast fashion. The broadcast nature of V2V, V2VRU, and V2I offers great potential for larger-scale data exchange and hence a more holistic understanding of the vehicle's environment, but also significantly increases the complexity of the network. Thus, for the sake of clarity, only some of the links between connected stations are shown in Fig. 3. As stated before, the V2N link, in the cellular community also referred to as Uu link, is purely realized over cellular 4G or 5G communication between a traffic participant and the corresponding

network. This connection mode is generally used for non-(traffic-)safety-critical data, such as infotainment services, due to its high latency compared to direct communication [110]. It is thus not the focus of this work. In the example, a police car exchanges data, such as navigation information and status reports, with a 4G or 5G node, more frequently referred to as evolved NodeB (eNB) or 5G NodeB (gNB), respectively.

The direct communication links may use the already introduced IEEE 802.11p or the C-V2X access technology. Also hybrid connectivity solutions are conceivable [A17]). While IEEE 802.11p relies on a Wi-Fi-based mechanism (see Subsection 2.2.4), C-V2X required the introduction of a PC5 interface to implement the so-called sidelink (in contrast to up- and down-link in the Uu interface). C-V2X supports a network-assisted and an autonomous mode, referred to as mode 3 and 4, respectively, in LTE-V2X and mode 1 and 2, respectively, in 5G NR-V2X. Due to its out-of-coverage availability, in contrast to the network-assisted mode, autonomous mode enables vehicles to coordinate the resource allocation in a distributed way (see Subsection 2.2.4), making it more robust against connectivity losses. This out-of-coverage availability is regarded as key for the safety of deployed connected vehicle systems. In the figure two vehicles are coordinating their respective left-turns within the intersection, three traffic lights are transmitting information about their phase, and a bicycle driver is warning an approaching police car of her presence.

2.1.4. System Architecture

A CV's system architecture is OEM specific and can thus only be generalized to a limited extend. Fig. 4 is an attempt to bring together the most relevant components and their interactions.

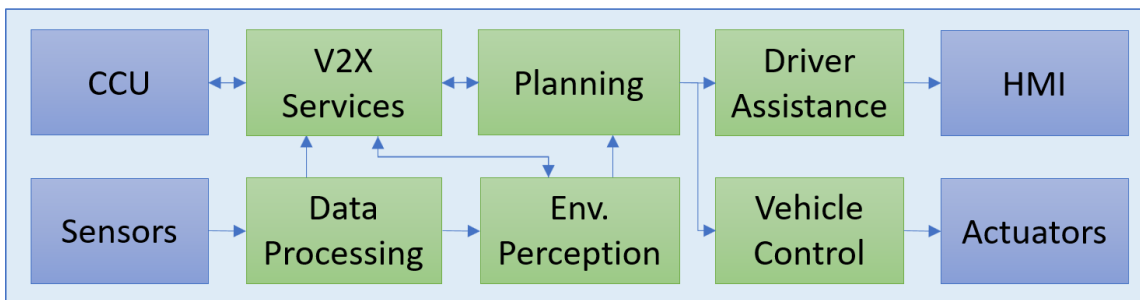


Fig. 4: High-level system architecture of a connected vehicle, differentiating between hardware (blue) and software (green) components.

Vehicles must perceive and monitor their environment for correct driver information and decision making. To this end, modern vehicles are equipped with over 100 sensors, and this number is expected to increase significantly with further vehicle automation in the

coming years [111]. Sensors are the primary source of information for vehicles to perceive their environment. As hinted by their number, there is a wide variety of parameters they monitor. In general, they can be grouped into sensors monitoring (i) the state of the vehicle components and its occupants, (ii) the vehicle's dynamics, and (iii) the vehicle's surroundings.

The first group of sensors, monitoring vehicle components and its passengers, is without question the most diverse. It includes all types of sensors measuring current, pressure, light exposure, temperature, and gas and fluid properties among others, to collect data, e.g., about tire pressure, fuel and battery level, ambient light, and exhaust gas composition. Vehicles can further be equipped with microphones, weight sensors, seatbelt tension sensors, and less frequently inward-facing cameras, infrared and capacitive contact sensors to monitor the driver's state.

The second group of sensors track the vehicle dynamics relative to the exterior static inertial frame. These include Inertial Motion Units (IMUs), steering angle sensors, odometers, and state-of-the-art absolute positioning Global Navigation Satellite System (GNSS) sensors such as the American NAVSTAR Global Positioning System (GPS), the Russian GLONASS, the European Galileo and the Chinese Beidou. The absolute position of a vehicle may further be computed with the help of cameras, radars, ultra-sonic sensors, and LIDARs to perform Simultaneous Localization and Mapping (SLAM) or using, e.g., the respective Road Signatures of Bosch [112]. Finally, also multi-angulation or -lateration techniques, e.g., using RF signals (Wi-Fi, Bluetooth, cellular, ...) are possible [113, 114].

The third group consists of sensors gathering information about the vehicle's exterior environment. It has a large overlap with the second group of sensors, also including radars, cameras, ultra-sonic sensors, and LIDARs. Sensors belonging to this group detect and track traffic participants in the environment, determine free space and potentially hazardous objects on the vehicle's route. In a wider sense, also the Communication Control Unit (CCU) can be seen as a sensor to obtain information about the vehicle's surroundings. The data shared over V2X communication is discussed in Section 2.2.

Data obtained by the vehicle's on-board sensors and received by the CCU is then processed in dedicated processing instances and the corresponding V2X services. While the latter must only be decoded, the data obtained from the sensor systems requires further extraction of meta-data, such as the generation of point-clouds and bounding-boxes.

Subsequently, the extracted metadata from the sensors is aggregated into the Local Environmental Model (LEM), one of the main constituents of a vehicle's environmental perception. It gathers all data relevant for describing the vehicle's environment, including the states of other vehicles and pedestrians, but also of buildings, lane markings and traffic

signs. The data is merged by making use of association algorithms such as the Joint Probabilistic Data Association (JPDA [115]) and subsequently filtered and fused, e.g., with Kalman filters [116], particle filters [117] or factor graphs [118]. Tracks are created when additional traffic participants or objects are detected, existing tracks are updated with every new measurement and outdated tracks are deleted after a certain time. V2X-data, provided by the V2X services, is not included into the LEM to avoid data incest and to maintain a fallback decision basis in case faulty or maliciously altered V2X-data is received. For these reasons a separate Global Environmental Model (GEM) is maintained by CVs in parallel to the LEM. LEM and GEM are often jointly referred to as Local Dynamical Map (LDM).

The vehicle's environmental perception, featuring, amongst others, LEM and V2X-enhanced GEM, is the basis for the situation analysis and planning module. The latter uses the environmental perception information to assess the current vehicle state and the traffic situation it is facing and take its decisions accordingly. It could for example determine that the vehicle just crossed an intersection and is approaching a slight turn to the right, that it is situated on the right-most lane of the street, and that there are no further vehicles in its direct vicinity. Moreover, it could infer the speed limit of the road segment from previously detected traffic signs or from the street type and its environment. The situation analysis may further incorporate data from local maps contained in the LEM. The consideration of information from the GEM can further improve the situation analysis. In the previous example, the vehicle may have received the signaling phase from the next intelligent traffic light and have gained knowledge about other CVs outside the field-of-view of its object tracking sensors and hence learn about a traffic jam ahead. Based on this information and knowing the status of its gasoline tank, it could plan to save fuel, decelerate as the traffic light is about to switch, and join the traffic jam only later without risking to be overtaken. For a more in-depth discussion of the system architecture with focus on maneuver planning and coordination the interested reader is kindly referred to [A6].

This information is then passed to the driver assistance module that controls the various HMIs, such as displays or voice advice. Additionally, depending on the automation level (see Subsection 2.1.5), the determined reaction to the environmental situation could be forwarded to the vehicle control module responsible to operate the various actuators, such as gear box, steering, acceleration, and brakes. For a more detailed description the reader is encouraged to refer to [A5].

V2X services, such as the Cooperative Awareness Basic Service informing about the transmitting station's state, the Decentralized Environmental Notification Basic Service informing about hazardous events on the road, the Collective Perception Service informing about tracked objects and free space, and the Collaborative Localization service

exchanging GNSS positioning information, are responsible for the dissemination the data within V2X messages. They most commonly obtain the required information from the data processing, environmental perception, and planning module. Examples are the Collaborative Localization service potentially requiring preprocessed sensor data or fused perception data, the Maneuver Coordination Service requiring planned trajectories generated by the planning module, and the Platoon Control service, requiring information regarding the fuel level, the status of the breaks, the CVs weight and dynamic properties, and the measured distance to the vehicle ahead must be communicated to the other platoon members among others.

Each V2X service has its own generation rules. These include the situation specific aggregation of the data to be transmitted and the message frequency, among others. Typical generation frequencies range between 1 Hz for the Collaborative Localization Message (CLM) to 25 Hz for the Platoon Control Message (PCM). Once a V2X message has been generated, it is handed over to the adjacent lower layer of the V2X protocol stack (see Section 2.2). It decides the routing of the message and the radio access technology to be used for the transmission in case both options are available and finally passes the message over to the CCU for transmission.

2.1.5. Automation Levels

The term “connected driving” is often used interchangeably with “automated driving”. A possible reason is that these represent the two most discussed disruptive technological advances for future traffic safety. Another reason is simply the strong link between both technologies. Fig. 5 shows the relation between different levels of automation as defined by SAE and the cooperation levels of CVs.

SAE defines six levels of automation [48]. The lowest level, “no automation”, leaves all driving tasks in the driver’s responsibility. The vehicle’s driver support is limited to inform the driver and provide momentary assistance, e.g., through features like AEB, Blind Spot Warning (BSW), and LDW. Level 1, “driver assistance”, includes some independent driver assistance features for steering or accelerating/braking. Examples are ACC or LKA. Level 2, “partial automation”, already provides combined steering, acceleration, and braking support. Joint ACC and LKA are an example of a level 2 system. With level 3, “conditional automation”, the responsibility of monitoring the driving environment passes to the vehicle. While features corresponding to level 3 are active, the feature is in full control of the vehicle. However, it may request the driver to take back control. Examples are TJP and basic VRU protection. With level 4, “high automation”, the system can carry out all driving functions for well-defined use cases, such as local driverless taxi, and fixed-

route shuttles. The driver has the option to take over control if wanted. Pedals and steering wheel are not necessarily installed. Finally, with level 5, “full autonomy”, vehicles are able to drive everywhere in all conditions. Steering wheel and pedals are most likely not to be installed and the space can be used for other purposes (cf. concept of “third living space” [119]).

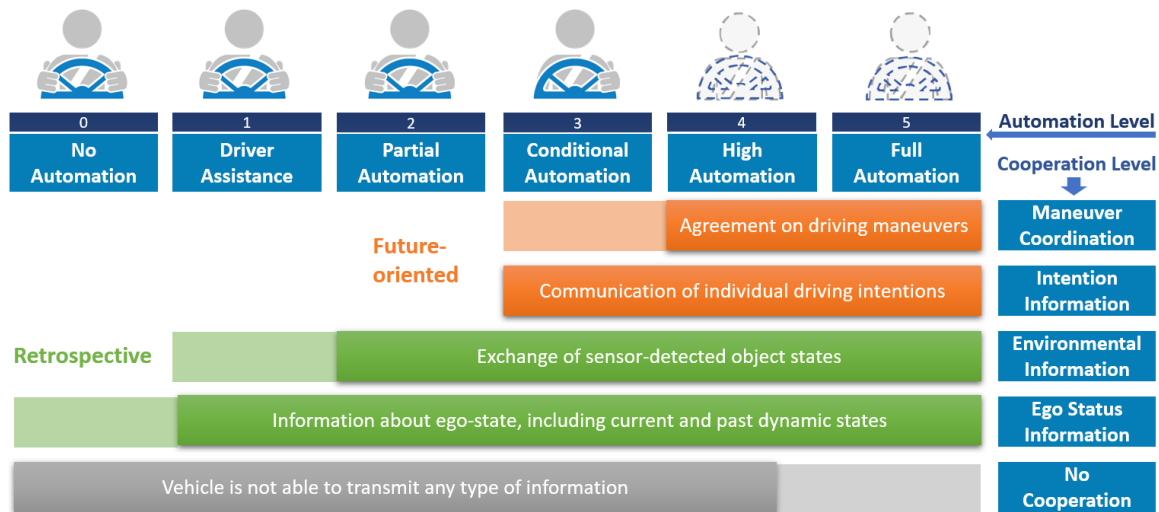


Fig. 5: Relation between manifestation levels of automated and cooperative driving.

On the other side, connected vehicles can be categorized according to their level of cooperativeness. In the lowest level, “no cooperation” they are not connected and hence not able to cooperate in any form. Non-connected vehicles can potentially be enabled with all levels of automation. It is however unclear to what extent high automation levels will be feasible, let alone efficient, without connectivity. Cooperation level 1, “ego-status information”, allows vehicles and other connected station to share status information (see Subsection 2.2.2.1). These so-called V2X “day 1” applications enable a basic level of safety. Typical use cases are traffic light information, emergency vehicle warning, and traffic-jam warning. Cooperation level 2, “environment information”, enables vehicles to share objects detected by their on-board sensors, greatly increasing the benefit of cooperation (see, e.g., Subsection 2.2.2.3). Such V2X “day 2” applications are currently being developed in the different regions of the world and deployment is expected in the near future. Examples of day 2 use cases are VRU protection, Cooperative ACC (C-ACC), and overtaking warning. Cooperation level 1 and 2 are both retrospective services intended to warn the driver or the vehicle of the last known traffic state. While cooperation level 1 is useful for an automation level 1 or higher, bringing partial benefit to non-automated

vehicles, cooperation level 2 supports systems of at least automation level 2, with partial benefit for driver assistance systems. This is especially the case, because cooperation level 2 requires a sufficiently capable sensor system, which is generally equipped on at least partly automated vehicles. Cooperation level 3, “intention information” allows vehicles to exchange driving intentions. For a correct assessment of the driving intention, the vehicle must be in driving control since the driver’s intention can only be predicted to some extent. Exemplary use cases are target driving area reservation, Green Light Optimal Speed Advisory (GLOSA), and Transition of Control (ToC) notification. Cooperation level 4, “Maneuver Coordination”, allows maneuver negotiation among connected stations. It requires the vehicle to act according to the agreed driving maneuver and is thus restricted to the highest levels of automation. Examples are cooperative overtaking, cooperative merging, and automated GLOSA with I2V negotiation. Automation level 3 and 4, both V2X “day 3+” applications, are future-oriented services, whose focus is the increase of traffic efficiency. For more use case examples categorized according to their level of automation and cooperation see Fig. 7 in Subsection 2.2.1.

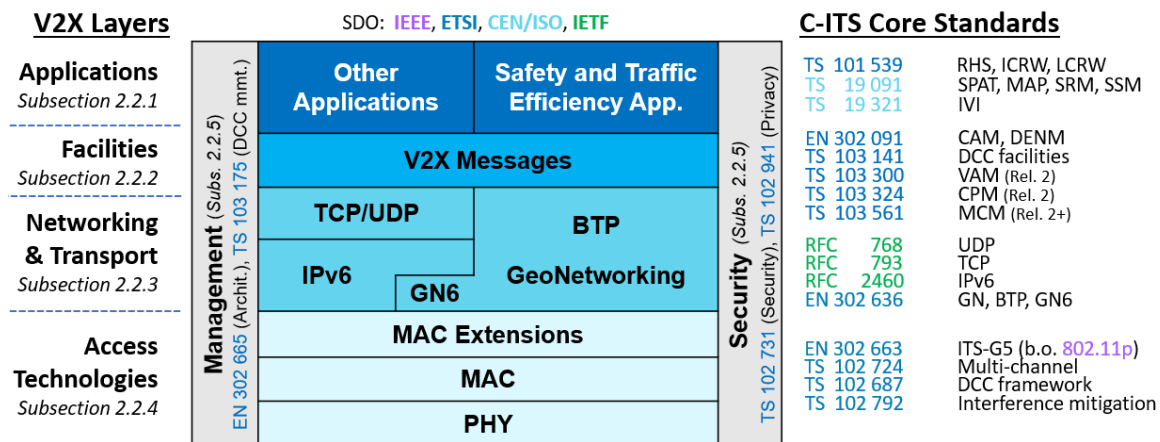


Fig. 6: European protocol stack with references to some of its core standards.

2.2. V2X Protocol Stack

In the following, the V2X protocol stack is discussed layer by layer on the example of the European connected ITS (C-ITS) protocol architecture presented in Fig. 6. Additionally, the main differences to the American protocol stack and the inclusion of the recently introduced C-V2X access technology are discussed.

The V2X protocol stack follows the Open Systems Interconnection (OSI) model standardized by ITU [120] and ISO [121]. On the highest layer, the application layer (OSI

layer 7, see Subsection 2.2.1), are the various V2X applications, such as Road Hazard Signaling (RHS [122]), Intersection Collision Risk Warning (ICRW [123]), and Longitudinal Collision Risk Warning (LCRW [124]). These applications rely on V2X services, such as the Cooperative Awareness Basic Service and the Collective Perception Service, located at the facilities layer (OSI layer 5 and 6, see Subsection 2.2.2) for the generation of V2X messages containing the data required by the corresponding applications, the preprocessing of receive message data, and the provisioning of the latter to the applications in a suitable form (e.g., the GEM, see Subsection 2.1.4). Generated messages are handed over to the networking and transport layer (OSI layer 3 and 4, see Subsection 2.2.3), which is responsible for the data multiplexing, segmentation, and routing amongst others. Finally, the access layers, comprising Medium Access Control (MAC, OSI layer 2) and physical layer (PHY, OSI layer 1), coordinate the medium access behavior of different network nodes and carry out the data transmission and reception over the physical medium. The proceeding subsections elaborate on these layers of the V2X protocol stack, as they are important for the understanding of this work, providing the relevant standards, literature, and research studies for the deeper understanding of the interested reader.

2.2.1. Application Layer

The number of V2X applications has been steadily growing over the past years. Depending on their goal, they can be classified into two classes: safety and traffic efficiency relevant applications (Subsection 2.2.1.1), and other applications (Subsection 2.2.1.2). The distinction is particularly relevant in view of the data transfer requirements for the lower protocol layers. Applications belonging to both groups are presented in the following.

2.2.1.1. *Safety and Traffic Efficiency*

Safety and traffic efficiency are central drivers of new technology developments in the automotive sector. Fig. 7 shows a range of connected driving applications categorized according to their automation and cooperation level (cf., Subsection 2.1.5) and the dominating communication link (cf., Subsection 2.1.3). From the simple Day 1 Electronic Emergency Brake Light (EEBL [125]) warning, intended to warn the driver of abruptly braking preceding vehicles, to the highly connected Automated Highway Systems (AHS) the spectrum of applications being developed and standardized is considerable. Some of these applications, such as Traffic Light Information (TLI [126]) and Green Light Optimized Speed Advisory (GLOSA [127]), require infrastructure support over I2V links.

Others, such as Transition of Control (ToC [128]) warning, Special Vehicle Prioritization (SVP [128]), and Cooperative Emergency Lane Change (CELC [129]) are typically of V2V nature. Also further links are possible, such as is the case for basic VRU protection that could be enabled over P2V, I2V, or V2V links. Besides the safety and traffic efficiency applications shown in Fig. 7, numerous other applications have been proposed, e.g., by ETSI (RHS [122], ICRW [123], and LCRW [124]) and CEN/ISO (SPaT, MAP, SSM, and SRM [130], and IVI [131]). For a more detailed discussion the interested reader is kindly forwarded to compilations of the USDOT [132], ETSI C-ITS Release 1 [133], the C2C-CC roadmap [128], and the 5GAA roadmap [134].

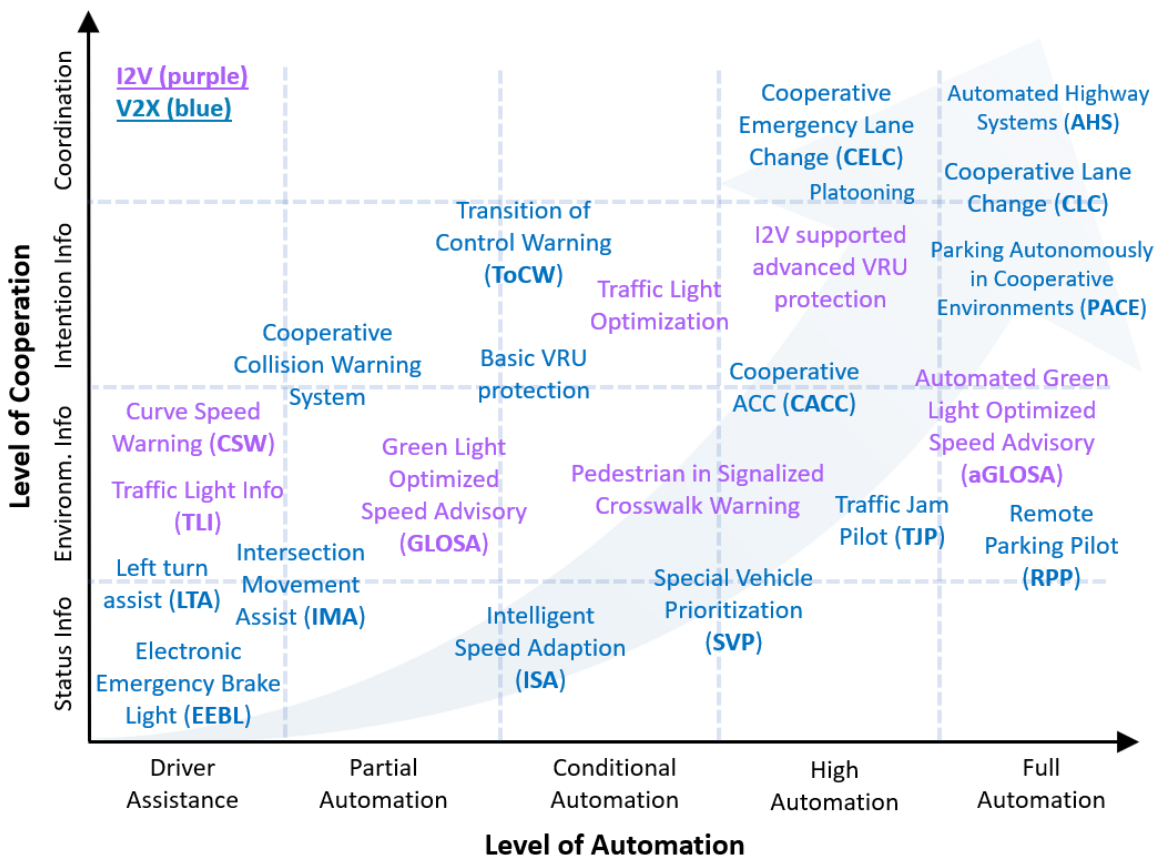


Fig. 7: V2X applications supporting cooperative driving by automation level, cooperation level, and communication link.

2.2.1.2. Other Applications

Other neither safety nor traffic efficiency related V2X applications exist targeting passenger comfort, system and environment monitoring and remote maintenance amongst others. These applications are not the focus of this thesis (cf. Section 1.1) and are thus only discussed briefly for the sake of completeness. Typical infotainment applications to enhance the passenger comfort are streaming services and entertainment apps. Connected monitoring applications make use of the vehicular networks, e.g., for probe-based pavement maintenance, probe-enabled traffic monitoring, vehicle classification-based traffic studies, and CV-enabled origin-destination studies [132]. Remote maintenance enables OEMs to carry out fleet-level or stand-alone system updates remotely, avoiding costly recall campaigns. Such applications do not have access to the safety-related channels of the ITS spectrum (cf. Subsection 2.1.1) and make use of other networking and transport protocols as well as channel access technologies (see Subsections 2.2.3 and 2.2.4).

2.2.2. Facility Layer

The facility layer comprises, among others, LEM and GEM corresponding to layer 6 of the OSI reference architecture and the V2X services on OSI layer 5. It serves as information basis for the previously introduced application layer lying on top of it. Most safety V2X services draw information from the GEM to generate V2X messages according to customized generation rules. They are further responsible for provisioning GEM and applications with data received from other connected stations. However, if the inclusion of data from the GEM could potentially lead to back coupling in connected stations this data is obtained from the LEM instead (cf. Subsection 2.1.4). It should be noted that due to the great diversity of V2X services, the number of data sources is not limited to GEM and LEM. Comfort and infotainment services, for example, tend to draw information from sensors directly. However, also safety and efficiency relevant services often construct their messages based on data originating, e.g., from single sensors or from the vehicle's planning module. Examples are unfused detected objects as part of the Collective Perception Message (CPM), the fuel-level dependent power-to-mass ratio carried in the Platoon Control Message (PCM), and trajectories and costs provided by the maneuver planner for the Maneuver Coordination Message (MCM). In the following, a selection of V2X services and their corresponding messages (see Fig. 8) is introduced to the extent in which each of them is relevant for this work. They can be categorized into two classes according to Fig. 5 in Subsection 2.1.5.: (i) retrospective perception-oriented safety services, and (ii) proactive planning-oriented traffic efficiency services. For a more comprehensive

treatment of the facility layer components and the featured V2X services with their corresponding messages, the interested reader is kindly referred to the following documents by ETSI [135], SAE [136], C-SAE [137], and the C2C-CC [128].

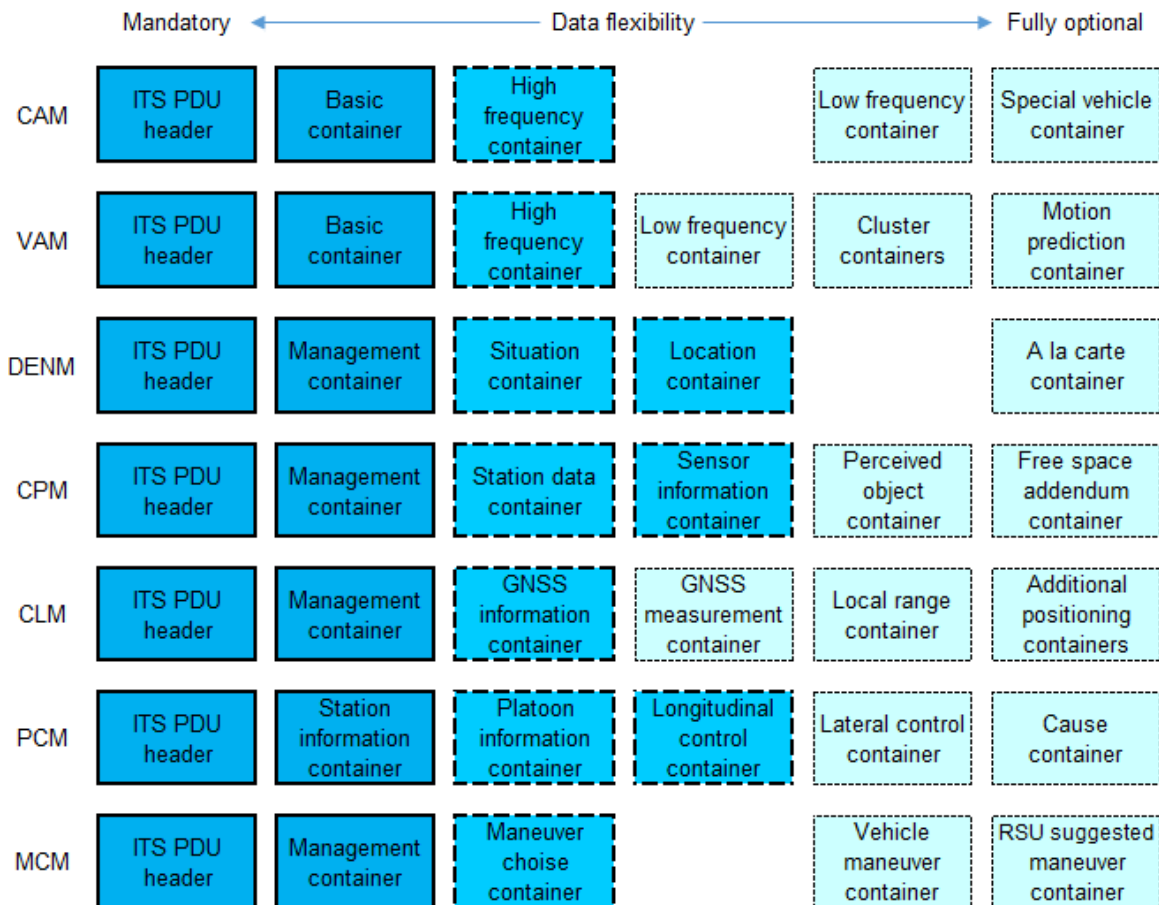


Fig. 8: Selection of V2X messages and their structure, classified in terms of the flexibility of the amount of included data.

Retrospective Perception-oriented Services:

During the past years several services have been proposed and standardized, whose main purpose is the enhancement of the traffic participant’s environmental perception. The Cooperative Awareness and the Decentralized Environmental Notification Basic Services have been among the first to be standardized and are already being deployed in modern passenger cars [138]. Other services are well advanced in standardization, such as the Collective Perception Service, and still others are currently being defined, such as it is the

case with the Collaborative Localization service. Their main purpose is the increase of traffic safety.

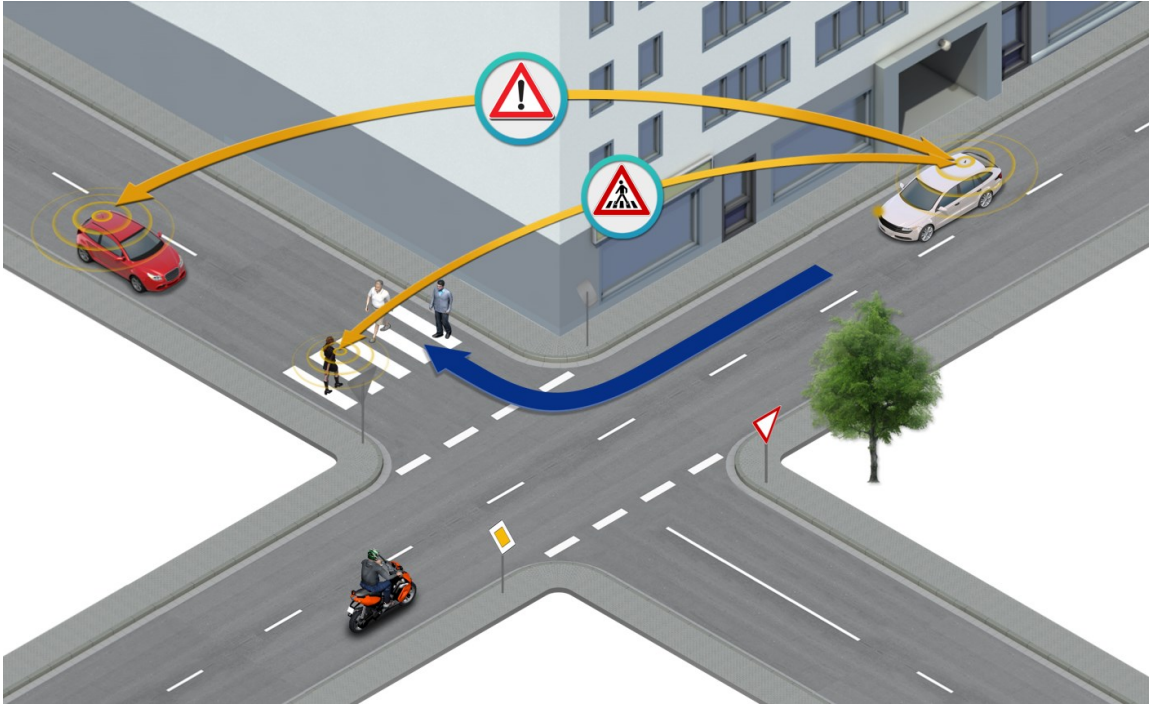


Fig. 9: Example scenario for Cooperative Awareness. The white vehicle is informed about the presence of the red vehicle and pedestrians walking on a zebra crossing, both outside of its sensor's line of sight, through their CAM and VPM messages, respectively. Adapted from [A16].

2.2.2.1. Cooperative Awareness

Cooperative Awareness enables vehicles to share information about their state, such as their current position, speed, and heading (see red and white vehicle in Fig. 9). Additionally, former states can be shared to facilitate the association and fusion of the data into the receivers' GEMs. The service has been standardized in different regions of the world and is based on the Cooperative Awareness Message (CAM [139]) in Europe and the Basic Safety Message (BSM [136]) in the US and China. The messages are generated quasi-periodically depending on the variation of the transmitting vehicle's dynamic state. The service periodically checks if at least one of the following criteria is met since the last transmission of a CAM:

- The vehicle's position changed by more than 4 m
- The vehicle's speed changed by more than 0.5 m/s
- The vehicle's heading changed by more than 4°
- At least one second has passed

The periodicity depends on the state of the communication channel (see Section 2.3.) and varies between 100 and 1000 ms. If at least one generation criterium is fulfilled, a new CAM is generated to inform the surrounding vehicles. The Cooperative Awareness Basic Service will thus lower the CAM generation frequency if the vehicle's state is constant or changing only slowly, leaving the channel resources to more dynamic vehicles. This way it searches to improve the value of the information shared within the vehicular network.

Fig. 8 shows the CAM's message format as specified in [139]. The CAM consists of an ITS Protocol Data Unit (PDU) header (containing the protocol version, message ID and station ID), the basic container (specifying the transmitting station's type, position, and confidence ellipse), and the high frequency container (carrying the stations heading, speed, acceleration, yaw rate, and dimensions among others). Optionally, two further containers can be added to the CAM. The low frequency container is appended every 500 ms and contains the station's role, its path history described by up to 40 path points, and the state of its exterior lights. Finally, the special vehicle container depends on the self-explaining sender roles *publicTransport*, *heavyTransport*, *dangerousGoods*, *roadwork*, *rescue*, *emergency*, and *safetyCar* [139]. In case the transmitting station has a special role, the special vehicle container is appended to the CAM every 500 ms.

Lately, the pendant of the CAM for VRUs, the so-called VRU Awareness Message (VAM) has been standardized [140] and is, in a broader sense, also part of Cooperative Awareness. It follows a similar approach, but includes some peculiarities for VRUs, such as a prediction of the VRU's future trajectory and the possibility to group VRUs into clusters (cf. message formats in Fig. 8). In contrast to the CAM, the consideration of predicted future trajectories makes the VAM a hybrid retrospective and future-oriented service (cf. Fig. 5 in Subsection 2.1.5). Its SAE analogue is the Personal Safety Messages (PSM) defined in [141]. Fig. 9 shows pedestrians crossing a crosswalk and transmitting VAMs with their mobile phones to warn potential right-turning vehicles whose sensors are occluded by the building.

2.2.2.2. Decentralized Environmental Notification

The main purpose of the DEN basic service [142] is to alert connected stations about eventually detected hazardous situations and events. It is typically used by the Cooperative Road Hazard Warning (RHW) application (see Subsection 2.2.1.). To date the RHW consists of thirteen use-cases, such as *wrong way driving warning*, *stationary vehicle – accident*, *signal violation warning*, *roadwork warning*, *collision risk warning*, *hazardous location*, *strong winds* and *reduced visibility* [143]. If one of the triggering conditions is fulfilled, the detecting ITS station immediately generates a DENM to inform potentially affected ITS-S inside a determined geographical area. Destination region and stations (see *GeoUnicast*, *GeoBroadcast*, and *GeoAnycast* in Subsection 2.2.3), number and frequency of retransmission, and expiration time depend on the type of the detected event. Similar functionalities as attributed to the DENM in Europe are assigned to, e.g., Traveler Information Message (TIM) and Road Safety Message (RSM) [144] in the US. Fig. 10 shows two DENM use-cases: (i) two vehicles involved in an accident, generate a DENM to alert following vehicles. The DENM is additionally relayed by the red vehicle to inform the vehicle in its rear. (ii) A damaged road-section is detected by the red vehicle and broadcasted in a separate DENM.

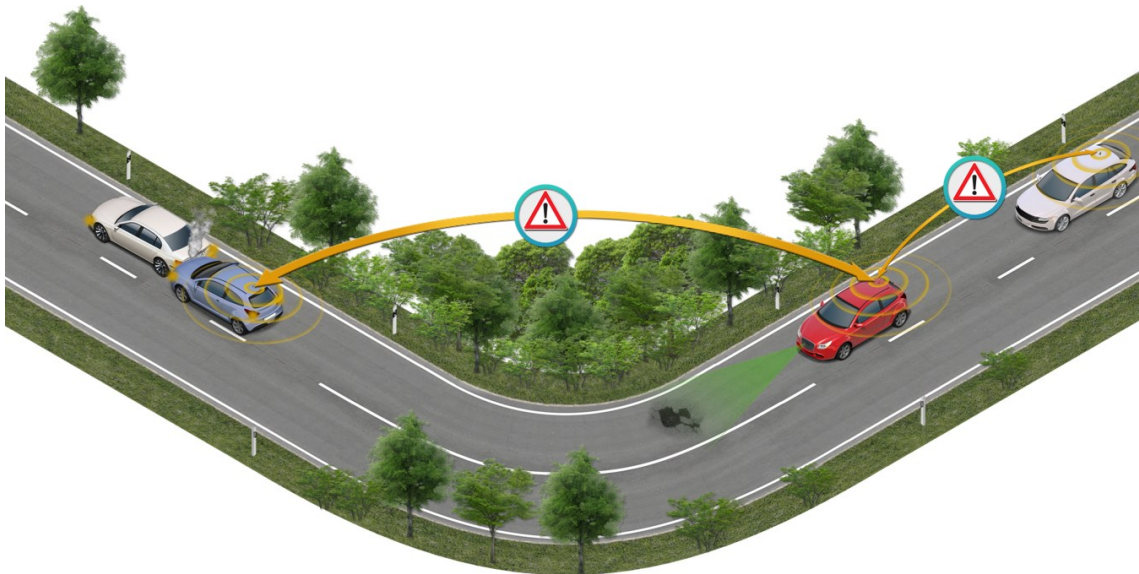


Fig. 10: Example scenario for Decentralized Environmental Notification. The red vehicle is informed about a crash after the curve by means of a DENM. Besides forwarding the message to vehicles behind it, it also transmits a DENM to warn about a street damage ahead of it. Adopted from [A16].

As shown in Fig. 8, the DENM consists of five data containers: (i) an ITS PDU header similar to the one of the CAM, (ii) a management container indicating the reliability level, the event evolution and the event termination among others, (iii) an optional situation container describing the perceived event and its potential implications for traffic safety and efficiency, (iv) an optional location container specifying event position, location referencing and relevance area, and (v) a special à la carte container carrying additional information required by the respectively served application.

2.2.2.3. Collective Perception

Collective Perception allows ITS-S to share data collected by their on-board object-tracking sensors. As the Technical Specifications (TS) of the service are still in an early phase at ETSI [145], the following discussion is mainly based on the Technical Report (TR) published by the end of 2019 [146]. It stipulates that the shared data may essentially include objects (such as pedestrians, obstacles, and other vehicles) and implicitly indicated free spaces (i.e., object- and infrastructure-free regions). Collective Perception not only increases the completeness of the GEM, but also its accuracy. Fig. 11 shows a child playing at a bus stop. The sensors' field of view of the approaching blue vehicle is occluded by the bus, hindering it from detecting the child. This potentially dangerous situation can be overcome by Collective Perception, where the V2X equipped bus detects the playing child and broadcasts its state together with other objects. The blue vehicle eventually receives the transmitted CPMs and includes the child into its GEM, allowing it to react accordingly.

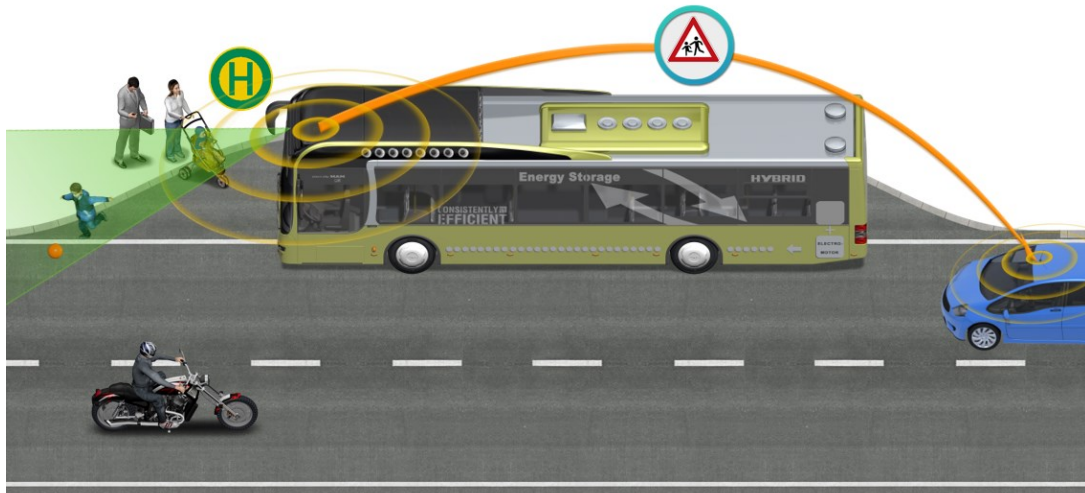


Fig. 11: Example scenario for Collective Perception. The blue vehicle is warned by the bus about a child, playing in front of it by means of a CPM. Adopted from [A16].

The message format of the CPM is depicted in Fig. 8. It consists of six containers: (i) the standard ITS PDU header, (ii) a management container including the station's type, position and confidence, (iii) the station data container indicating the station's heading, speed, acceleration and yaw rate among others, (iv) the sensor information container indicating the station's sensor specifications, (v) the perceived object container, carrying the detected objects including their dynamic state, confidence intervals, dimensions, estimated type and the detecting sensors, and (vi) the free-space addendum container providing the required data to compute empty regions within the sensors' field of views and their respective confidences. The CPM dissemination rules are strongly based on those of the CAM. As for the CAM, the periodicity of the CPM's generation cycle depends on the state of the communication channel, ranging between 100 and 1000 ms. Detected objects must pass a series of filters to be added to a new CPM depending on the object's (i) confidence level, (ii) relevance, and (iii) V2X detection redundancy. For the latter the TR introduces frequency-, dynamics-, confidence-, and entropy-based redundancy mitigation techniques aiming to discard objects detected by several other connected ITS-S. The remaining objects are then divided into two groups. Non-VRU objects are further filtered according to the CAM generation rules, while VRU objects are included every 500 ms. Objects of both groups detected for the first time are always included. A special case for the first group occurs when it is foreseeable that the object would be included in the next CPM cycle according to the stated rules, and at least one other object has been included. In this case, the object is already added in the current cycle. Consequently, the CPM is extended by a sensor information container if more than 1000 ms have passed since its last inclusion and additionally by a free space addendum container if the detected free space cannot be correctly assessed by a potential receiver based on the list of detected objects and the sensor specifications. Finally, should the size of the CPM exceed the Maximum Transmission Unit (MTU) only the candidate objects with the highest utility function are included until the size reaches the MTU. The utility function depends on the object confidence, the object dynamics, and the time passed since the object's last inclusion into a CPM. While the TS is expected to be finalized in 2022 laying the foundation for the rollout of day 2 applications, in the US SAE is working on two different sensor-sharing messages: the Sensor Data Sharing Message (SDSM [147]), and the "Surrogate BSM" (the latter allowing stations to transmit BSMs on behalf of detected non-V2X-equipped ITS-S).

2.2.2.4. Collaborative Localization

Despite the tremendous potential of V2X communication, the precision of the GEM is often insufficient for critical driving functions. While faulty and intentionally modified

measurements can be filtered out by comparison with the LEM and with the data provided by connected ITS-S, smaller, yet relevant errors may prevail. These errors have various sources. The most relevant ones are: (i) the error associated to the on-board object-detection sensor, (ii) the transformation from the transmitting ITS-S's relative coordinates to absolute coordinates and (iii) the back-transformation from absolute coordinates into the receiving ITS-S's relative coordinates for the incorporation of the detected object into the GEM. Both source (ii) and source (iii) depend on the accuracy of the respective ITS-S's absolute positioning. Hence, the accuracy of the state-of-the-art absolute positioning system GNSS receives special attention.

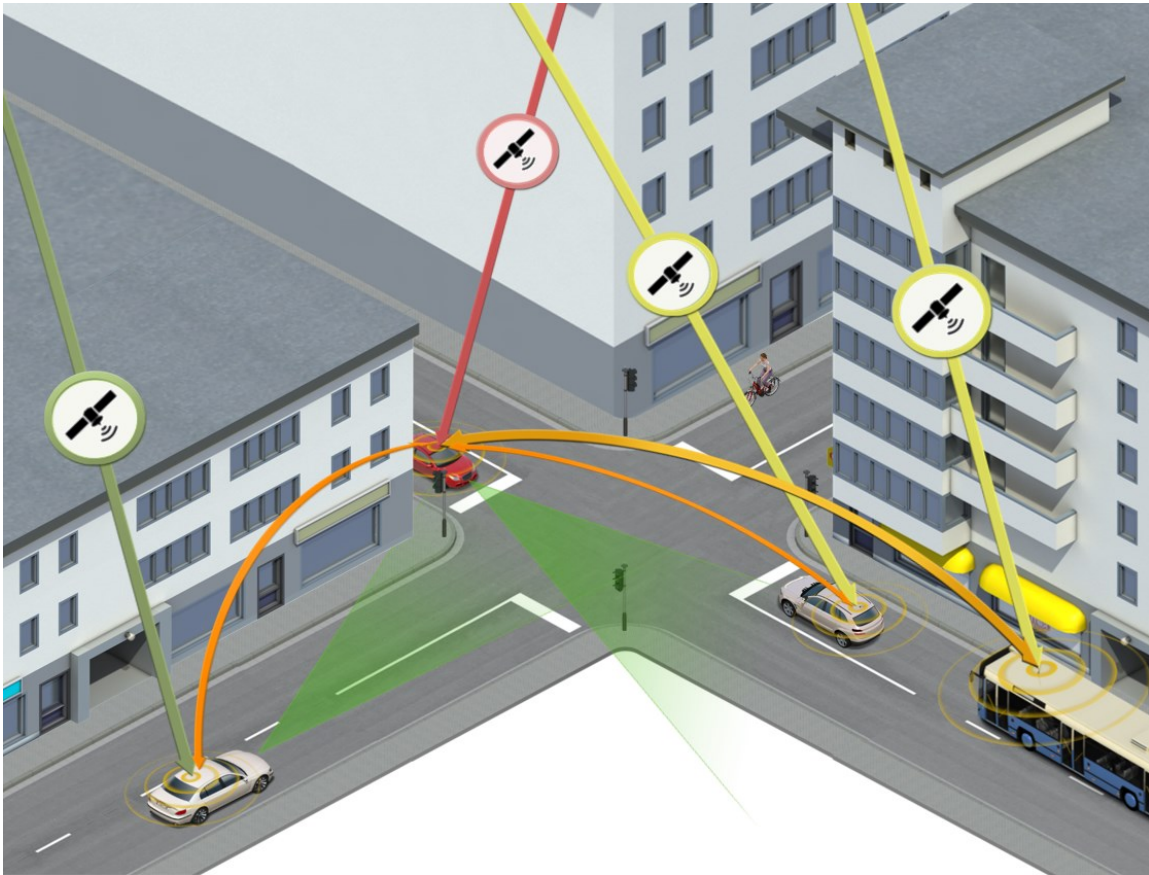


Fig. 12: Example scenario for Collaborative Localization. The red vehicle, previously not obtaining sufficient GNSS measurements for positioning, receives CLMs from neighboring stations, allowing it to compute its absolute position. Adapted from [A16].

However, especially in multipath-prone areas, the GNSS positioning may experience large errors [A1], with severe consequences for the ITS-Ss' environmental models. By

sharing raw GNSS measurements as shown in Fig. 12, and knowing the distance between receivers, also known as local ranges, traffic participants are able to enhance accuracy, integrity, and availability of the obtained absolute position. This process is commonly referred to as Collaborative Localization or Collaborative Positioning. While the red vehicle in Fig. 12 would not be able to obtain a stand-alone GNSS positioning as direct line-of-sight to at least 4 satellites is necessary, a positioning with Collaborative Localization is possible.

Despite great recent advances in the technology [148, 149, 150], a V2X service has not yet been standardized nor proposed due to its novelty. In the scope of this doctoral work, a first message format together with a set of generation rules are proposed.

The proposed format for the Collaborative Localization Message (CLM) is depicted in Fig. 8 and is closely related to the other sensor data sharing message, the CPM. It consists of six data containers: (i) the standard ITS PDU header, (ii) a management container including the station's type, position and confidence, (iii) the station data container indicating the station's heading, speed, acceleration and yaw rate among others, (iv) the GNSS information container indicating the station's GNSS receivers specifications and Pseudo-Random-Noise (PRNs) of the satellites whose ephemeris is known to the station, (v) the GNSS measurement container, carrying the satellite measurements and optionally the satellite positions, and (vi) the local range container carrying the measured local ranges, i.e., distances to cooperating stations. Other containers with relevant positioning information (e.g., point clouds for cooperative SLAM, landmarks, and others) may be included in the future.

The satellite measurements contain information about a single GNSS-channel that is to be included in (and transmitted with) the CLM. This information includes the space vehicle identifier, the GLONASS frequency, the channel/signal status, the Signal-to-Noise Ratio (SNR), the pseudorange, the range rate, and the integrated carrier phase contribution with their respective Root-Mean-Square (RMS) errors among others. Further, Collaborative Localization requires the states of all satellites (position, velocity, and acceleration) of which measurements are used. These can be computed from the satellites' ephemeris in Kepler format. The latter is updated every two hours. The consequence is that a satellite measurement of which Kepler is not known to the receiver can't be used by the latter. One approach to prevent this is to append the Kepler parameters to the corresponding satellite measurements. However, this implies a large amount of data. On the other side, the dynamic nature of vehicular ad hoc networks does not allow to transmit the Kepler parameters only every two hours. A solution is the computation of the satellite states already in the transmitter, considerably reducing the amount of necessary data for

transmission. Another solution is the broadcasting of the satellite PRNs known to each ITS-S instead of Kepler or the computed states. This allows connected stations to determine when satellite states or Kepler parameters are needed by a certain station and appending them only then, considerably relieving the communication channel. In this thesis, the PRNs of the satellites whose ephemeris is known to the station are included in the GNSS measurement container, while the actual satellite positions are appended to the respective satellite measurements when potentially required by a connected station.

Different from CAM and CPM, the measurements of all GNSS receivers are synchronized to the satellite system, leading to a CLM generation every GPS second. This simultaneous generation of CLMs by all CL-enabled stations represents a major challenge for the communication channel and is addressed in Section 4.2. together with the dynamic measurement inclusion rules.

Prospective Planning-oriented Services:

Prospective planning-oriented services go one step further than the just described perception-enhancing services. In addition to improving the environmental model, they allow traffic participants to coordinate their traffic behavior, improving traffic efficiency. Two prominent examples of such services are given below.

2.2.2.5. Platooning

The facility layer platooning protocol is currently being designed to support the platooning application introduced in the previous section. Unlike most other facility layer protocols, it comprises two services: platoon management and platoon control. Thus, it requires two BTP ports (cf. Subsection 2.2.3.1). One of the main drivers of service and application is the project ENSEMBLE co-founded by the European Commission [151]. In the scope of this project, a service discovery was proposed, consisting in the extension of the CAM by a special platooning container. This container allows platooning-enabled traffic participants to express their willingness to form a platoon. Potential interested ITS-S may then transmit a join request, which is answered by a join response (for further details see [152]). Once the platoon is formed, its members exchange status information through the Platoon Control Message (PCM). The basic structure of a PCM is shown in Fig. 8. It consists of the standard ITS PDU header and a platoon control container, which in turn consists of four message segments: a station information container, a platoon information container, and a longitudinal control container, as well as the optional lateral control container and the cause container. If a vehicle needs to leave the platoon, a special leave

request is sent to the cooperating platoon members with a Platoon Management Message (PMM) in order to jointly coordinate the maneuver. More complex maneuvers, such as temporally splitting the platoon to allow other traffic participants to cross (see red vehicle in Fig. 13), can also be effectuated. The safety requirements arising from the extremely reduced inter-vehicle distances demand higher dissemination frequencies than other services. Frequencies between 10 and 50 Hz have been investigated [153, 154, 155]. ETSI is currently carrying out a pre-standardization study on platooning in [156], with publication expected by the end of 2022.

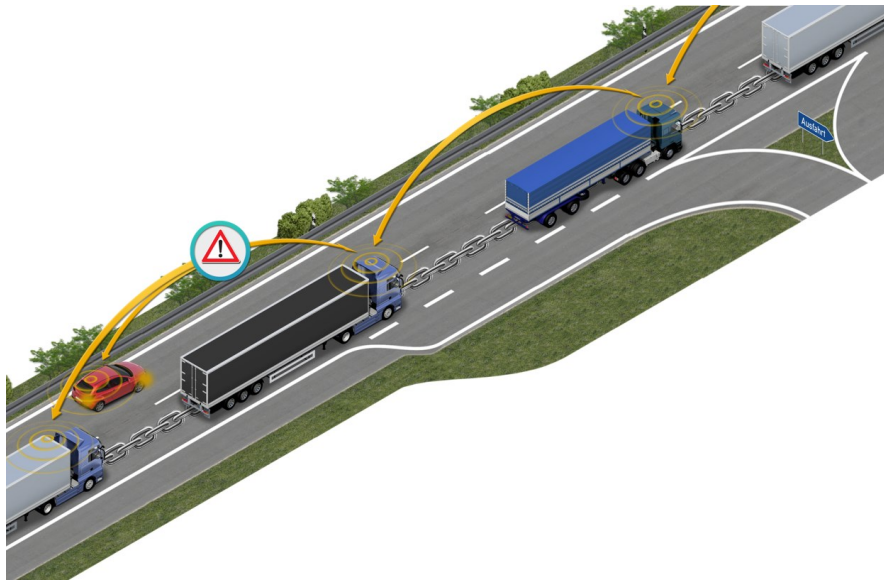


Fig. 13: Example scenario for Platooning. The trucks exchange precise driving information by means of PCMs, enabling a highly synchronized platoon operation. The extremely safety-critical low inter-vehicle distance requires highly reliable, low latency communication represented by chains connecting the platoon members. Joining requests, such as issued by the red vehicle, are communicated by means of PMMs.

2.2.2.6. *Maneuver Coordination*

A new service, referred to as Maneuver Coordination Service, is currently being developed to support applications such as cooperative left turning (see Fig. 14), highway merging, and overtaking on country roads. Some of the main drivers of this development are the V2I-based EU-funded project TransAID [157], the French PAC-V2X [158], and the V2V-based German project IMAGinE [159]. The service involves the exchange of possible future trajectories among ITS stations. Due to its early stage of development no generation

rules have yet been specified for the service by ETSI. Early test implementations make use of fixed generation frequencies, generally ranging between 1 and 10 Hz. Also, the message format is still subject of discussion. A message format proposed in the scope of TransAID is shown in Fig. 8 [160]. It consists of three containers: (i) an ITS PDU header, and (ii) a basic container, both similar to the ones specified for the CAM, as well as (iii) a maneuver choice container. The latter may contain (iii-a) a vehicle maneuver container or (iii-b) an RSU suggested maneuver container. While the vehicle maneuver container specifies the planned trajectory, up to one additional desired trajectory, the vehicle dynamics, the target automation level, timing information, and an advice response list to react to RSU suggestions, the RSU suggested maneuver container holds the target station ID and optionally a lane advice container, a speed and gap advice container and a transition of control advice container.

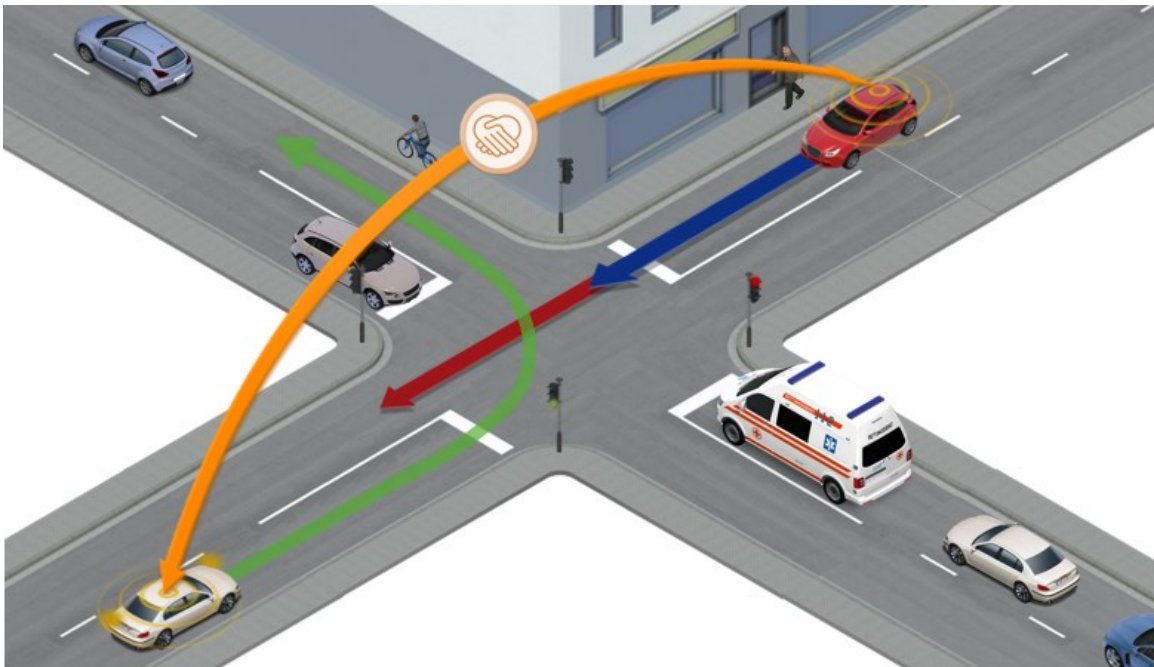


Fig. 14: Example scenario for Maneuver Coordination. The white vehicle, driving at a high speed, requests right of way permission from the slower red vehicle. After confirmation by the latter, only a small change in speed is required to perform the maneuver.

Within IMAGinE, the main approach is the assignation of costs to possible trajectories for the ego-vehicle, which represent how beneficial a trajectory is to the vehicle. Based on these costs, trajectories can be grouped in three categories:

1) Reference Trajectory:

The reference trajectory is the trajectory the vehicle is currently following. It must be collision free with the nearby vehicles' reference trajectories (potential collisions are solved according to traffic rules) and has cost C_0 .

2) Request Trajectories:

Request trajectories are trajectories that have lower costs than the reference trajectory $C_R < C_0$ and that may interfere with trajectories of other vehicles and require coordination with the latter. They represent cooperation requests. Once a request trajectory is accepted by the vehicles whose reference trajectories collided with it and these have been modified accordingly, the request trajectory becomes a reference trajectory and can be followed by the vehicle requesting it.

3) Alternative Trajectories:

Alternative trajectories are trajectories that have higher costs than the reference trajectory $C_A > C_0$ and that are transmitted as cooperation offers for other vehicles.

According to this IMAGinE approach, all vehicles will provide their reference trajectory and, whenever a need for cooperation is identified, at least one alternative or request trajectory. The number of alternative and request trajectories may vary in dependence of the cooperation willingness of the driver or external factors (car manufacturers, regulations, etc.).

The exchange of trajectories is common to most maneuver coordination approaches. However, they vary in their parametrization, such as the number of transmitted trajectories and the aggregation level of the data describing them. At ETSI the Maneuver Coordination Service is currently being developed and standardized in [161] and [162], respectively. Simultaneously, SAE is working on the definition of the Maneuver Sharing and Coordinating Message (MSCM [163]).

2.2.3. Networking and Transport Layer

The networking and transport layers are located at the layers 3 and 4 of the OSI- reference model respectively. They are responsible for the end-to-end transmission, and the routing and forwarding of the data packets.

While non-safety relevant applications generally rely on the well-known members of the internet protocol family, namely IPv6, TCP and UDP, safety relevant ITS applications make use of protocols especially designed for this purpose, namely the Basic Transport

Protocol (BTP) and the GeoNetworking Protocol (GNP⁷). They are briefly introduced below.

2.2.3.1. Basic Transport Protocol

As its name suggests, the BTP [164] is a light-weight transport protocol located at layer 4 of the OSI reference architecture. It is preferably used in conjunction with the GeoNetworking protocol introduced below and regulates the end-to-end transmission of the packets generated at the facility layer. Like UDP, it is a connection-less protocol, multiplexing data among V2X services from different connected stations. To this end, it makes use of two different header types: BTP-A and BTP-B. While the BTP-A header carries *source* and *destination port* of the corresponding facility layer protocol entities of the transmitting and receiving station respectively, the BTP-B header includes the *destination port*, but no *source port*. Instead, it may specify the *destination port info* coding the identified facility layer service. The specification of the *source port* may be of use if the port to which a reply to the BTP PDU should be addressed is of relevance for the destination ITS-S. The port numbers and related standards of the facility layer services available to date can be found in [165].

2.2.3.2. GeoNetworking Protocol

Once a packet obtained its BTP header, it is handed over to the networking layer (OSI layer 3) to make use of the services of the Geographical Networking protocol [166], often abbreviated as GeoNetworking protocol. GeoNetworking was introduced to cope with the requirements of highly dynamical ad hoc networks allowing point-to-point and point-to-multipoint transmissions. To this end, the GeoNetworking protocol features three forwarding modes specifying the destination region (*GeoUnicast*, *GeoBroadcast*, and *GeoAnycast*), and two location independent modes: *Topological Scope Broadcast (TSB)*, and *Single Hop Broadcast (SHB)*. Contrary to SHB, messages send in the TSB forwarding mode may be retransmitted by cooperating stations in a multi-hop fashion by setting the intended number of retransmissions by the corresponding retransmission counter. While CAMs, CPMs and MCMs rely on *SHB*, DENMs frequently make use of *TSB*.

The GeoNetworking protocol is separated into media-independent and media-dependent functionalities to allow the use of multiple ITS access technologies. While the

⁷ Usually abbreviated as GN. In this thesis GNP is used to differentiate it from the Gauss-Newton solver.

formers are common to all access technologies for ad hoc wireless communication, the latter extend the media-independent functionalities [166] for a specific ITS access technology, such as ITS-G5 [167] and LTE-V2X [168].

2.2.4. Access Technologies

The access layers, comprising Medium Access Control (MAC, OSI layer 2) and Physical (PHY, OSI layer 1) layer, are responsible for the transmission of packets received from the upper layers through the physical medium. The spectrum allocated to ITS applications in the different regions of the world was discussed in Subsection 2.1.1. In the following the two currently available access technologies, namely IEEE 802.11p (Subsection 2.2.4.1) and LTE-V2X (Subsection 2.2.4.3) are discussed. Additionally, an outlook on the respective evolution technologies IEEE 802.11bd (Subsection 2.2.4.2) and 5G NR-V2X (Subsection 2.2.4.4) is provided. For non-safety relevant V2N applications also access technologies such as 4G [169] and 5G [170] may be used. Interested readers are encouraged to refer to the provided references.

2.2.4.1. IEEE 802.11p

IEEE 802.11p, the basis for ITS-G5 in Europe and DSRC/WAVE in the US, was first released in 2010, as an amendment to IEEE 802.11a (Wi-Fi 2 [171]) addressing the highly dynamic environment of ad hoc vehicular networks [172]. On the MAC layer, corresponding to OSI layer 2, IEEE 802.11p is designed to work without the use of a Basic Service Set (BSS). This Out-of-Context of a BSS (OCB) operation mode can achieve lower latencies than BSS-based networks by renouncing to association and authentication before channel sensing. The MAC layer further makes use of Enhanced Distributed Channel Access (EDCA) first introduced in IEEE 802.11e [173] to coordinate the channel access by different applications and services. To this end, EDCA uses Carrier Sense Multiple Access with Collision Avoidance (CSMA/CA) and a mapping of data to so-called Access Categories (AC) enabling to prioritize data, e.g., from safety-relevant applications (cf. [A7]).

The PHY layer (OSI layer 1) of IEEE 802.11p is based on Orthogonal Frequency Division Multiplexing (OFDM) with a channel bandwidth of 10 MHz. This halving of the bandwidth with regard to IEEE 802.11a serves the purpose of a better transmission in a network with mobile, fast-moving nodes [69, 174]. IEEE 802.11p implements 64 sub-carriers with the corresponding 156.25 kHz sub-carrier spacing. 48 of these sub-carriers are used for data, 4 for pilots, and 12 for DC tone and guard bands. Further, IEEE 802.11p

offers eight combinations of Modulation and Coding Schemes (MCS) to address the network conditions, e.g., channel state, required Quality of Service (QoS), and intended communication range (cf. Table I in [175]). The standard uses Binary Convolutional Coding (BCC) and requires Signal-to-Interference-and-Noise Ratios (SINR) of 10 dB to 27 dB for the modulation and coding rates Binary Phase Shift Keying (BPSK) 1/2 and 64-Quadrature Amplitude Modulation (QAM) 3/4, respectively.

Overall, with IEEE 802.11p data rates of 3 to 27 Mbps [175], with a range of up to 500 m on the V2V link and 1000 m on the V2I link, and relative node speeds of 200 km/h can be achieved. The technology is well tested and mature for deployment [69], featuring already around one million ITS-G5 equipped vehicles in Europe. Studies showed that while the PHY layer of IEEE 802.11p was generally outperformed by LTE-V2X (Subsection 2.2.4.3), its MAC layer presented a better handling of high-density scenarios within the safety-critical range [176, 177]. The benefit of CSMA/CA was found to be even more pronounced with realistic network traffic consisting of aperiodic messages with variable sizes (see Subsection 2.2.2 and Fig. 35 in Subsection 4.3.2).

2.2.4.2. IEEE 802.11bd

IEEE 802.11bd, also referred to as Next Generation V2X (NGV), is currently being developed as evolution of IEEE 802.11p [178]. With the publication of the specifications expected for 2023, the following discussion of amendments with respect to IEEE 802.11p is based on the current draft version [179]. IEEE 802.11bd is based on IEEE 802.11ac (Wi-Fi 5 [83]), bringing some significant performance benefits with regard to the IEEE 802.11a based IEEE 802.11p. As in its predecessor, the MAC layer of IEEE 802.11bd is based on EDCA implementing CSMA/CA in an OCB operation mode. It enables retransmissions by transmitting OFDM symbols over two different sub-carriers and will further include a mechanism to reduce packet collisions by adapting the packet length based on the sensed congestion state of the wireless channel [180]. As IEEE 802.11p presented its main weaknesses on the PHY layer when compared to C-V2X, most amendments for IEEE 802.11bd are undertaken on this layer. Some of the major changes are an additional 20 MHz bandwidth operation mode, the extension of the MCS by two 256-QAM based profiles for enhanced data-rates and one BPSK profile with Dual-Carrier Modulation (DCM) to augment the communication range by splitting the bandwidth for redundant transmissions, the substitution of BCC by Low-Density Parity-Check (LDPC) codes for channel coding to enhance the reliability, the support of Multiple-Input Multiple-Output (MIMO) antennas for higher throughput and new RF-based positioning features, an optional support of millimeter Wave (mmWave) communication, and a Doppler recovery

method using midambles in-between OFDM symbols to estimate the channel variation and increase robustness and message integrity. The BPSK-based MCS profile implementing DCM, commonly referred to as IEEE 802.11bd^{DC}, is an extension of IEEE 802.11ax (Wi-Fi 6 [84]) and is mainly intended for extended safety-range scenarios, such as highway merging, characterized by high vehicle speeds and often very reduced visibility.

Overall, IEEE 802.11bd is expected to yield twice the performance of its predecessor IEEE 802.11p in terms of throughput, enabled relative velocities, and communication ranges, while assuring backward compatibility and interoperability with IEEE 802.11p [181, 182].

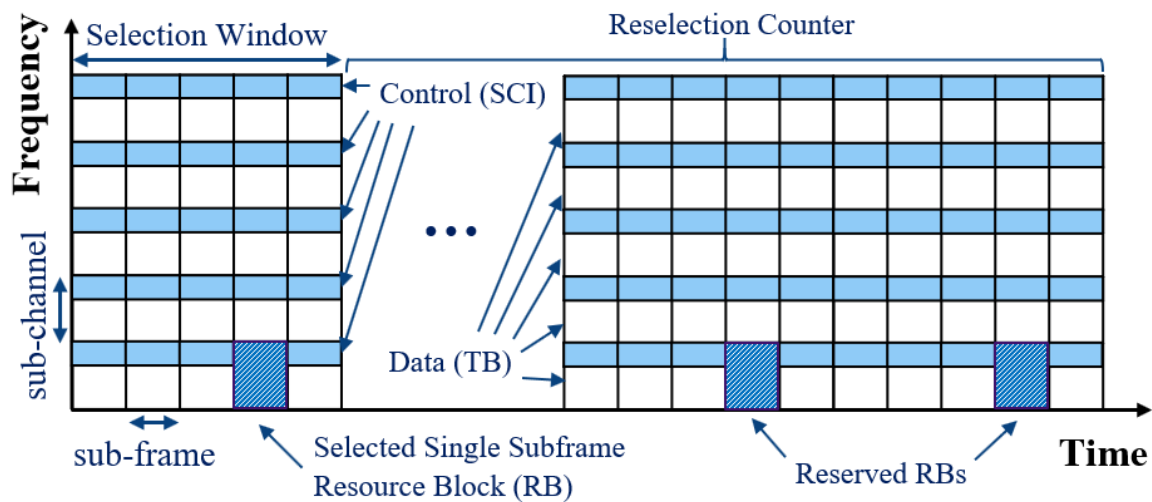


Fig. 15: C-V2X sidelink resource pool and its constituents.

2.2.4.3. LTE-V2X

C-V2X was first introduced in Rel. 14 [54], completed in 2017, based on the PC5 interface for sidelink communication specified in Rel. 12 [183] for Device-to-Device (D2D) communication. Rel. 15 [184], which was completed in 2018, introduced a wide range of enhancements to the Rel. 14 C-V2X technology. As both releases are based on LTE and LTE Advanced (better known as 4G), Rel. 14/15 C-V2X is commonly referred to as LTE-V2X. It features two direct communication modes: (i) mode 3 or network-controlled mode, and (ii) mode 4 or autonomous mode [185]. While LTE-V2X mode 3 only supports in-coverage, and with further constraints, partial network coverage scenarios, LTE-V2X mode 4 is also available in out-of-coverage scenarios. Being able to operate even without

cellular network coverage is a stringent requirement of all safety and traffic efficiency supporting services introduced in Subsection 2.2.2, making the autonomous scheduling mode's availability indispensable for such services operated based on cellular access technologies.

LTE-V2X uses Resource Pool (RP) similar to the RPs of D2D communication introduced in Rel. 12 [185]. An LTE-V2X RP is composed of sub-channels in the frequency domain and of sub-frames in the time domain, built of Resource Blocks (RB) [186], as shown in Fig. 15. Their configuration can be obtained from the network (mode 3), given that the User Equipment (UE) is connected to a base-station, or pre-configured in advance in the UE (mode 4) [185]. The configuration information specifies among others RP period and number of sub-frames in the time domain, sub-channel bandwidth and number of consecutive sub-channels in the frequency domain, and the lowest RB-index for synchronization of the channel access by different UEs. In LTE-V2X mode 4 the connected stations autonomously select and reserve their radio resources for transmission based on the Semi-Persistent Scheduling (SPS) sensing mechanism (cf. [A4]), which tries to exploit the quasi-periodic nature of V2X traffic [185]. SPS allows to reserve periodic resources for a defined number of consecutive packet transmissions, i.e., defined by a reselection counter. Reservation periods, also referred to as packet transmission intervals, e.g., of 100 subframes (i.e., 10 packets per seconds) or multiples of 100 subframes are allowed [187]. The reselection counter and the packet transmission interval are included in the Sidelink Control Information (SCI) to allow other ITS-Ss to identify free resources for their own transmissions. A correct reception and decoding of the SCI are required for the successful reception of the user data contained in Transport Blocks (TB). To reduce the collision probability and avoid transmitting on resources being used by other UEs in the vicinity, a sensing mechanism is used. It consists of continuously monitoring the received information on each subframe and measuring the received energy level on the resource blocks belonging to the resource pool. The reservation is performed based on the past Received Signal Strength Indicator (RSSI) measurements and the reservations by other stations (cf. [188] for details). The latency introduced by SPS depends on the size of the selection window, which is given by the packet periodicity. Messages such as CAM or CPM will suffer from up to 100 ms additional MAC latency due to their periodicity of 10 Hz under relaxed channel conditions. With rising channel congestion, the periodicity falls reaching 1 Hz under saturated channel conditions, hence reaching MAC latencies of up to 1000 ms (cf. analytical model in [A4]).

On the PHY layer LTE-V2X uses Discrete Fourier Transform spread OFDM (DFT-s-OFDM) as carrier modulation technique and supports channel bandwidths such as 10 and

20 MHz. While the SCIs are transmitted using Quaternary Phase-Shift Keying (QPSK), the payload can be transmitted using higher order modulations reaching from QPSK up to 64-QAM. LTE-V2X uses turbo coding and a normal cyclic prefix for the OFDM symbols. Each user transmission lasts exactly one sub-frame (1 ms) and occupies a certain number of subchannels in the frequency domain depending on the size of the data to transmit, the modulation, and the coding rate used.

Overall, LTE-V2X with its SPS-based scheduling offers a less-suited MAC for vehicular applications in terms of latency as compared to IEEE 802.11p [A4]. It further requires strict time synchronization with the cellular network (LTE-V2X mode 3) or GNSS (LTE-V2X mode 4) for resource allocation, making it dependent on the coverage of these systems. From a facility layer perspective also the reduced time granularity of LTE-V2X is inferior to the one of both discussed Wi-Fi based access technologies. On the PHY LTE-V2X presents a more advanced channel coding and higher modulation schemes than IEEE 802.11p enabling higher data rates and ranges [175]. However, it is outperformed by IEEE 802.11bd in these aspects. Further, the OFDM symbol duration of LTE-V2X is an order of magnitude longer than the one of IEEE 802.11p, making it more susceptible to carrier frequency offsets, but improving robustness against multipath and inter-symbol interference [189]. C-V2X and IEEE 802.11p can coexist if placed on different channels, i.e., non-cochannel coexistence.

2.2.4.4. NR-V2X

3GPP Rel. 15 introduced C-V2X based on the 5G NR waveform, thus often referred to as 5G-V2X, NR-V2X or 5G NR-V2X, to differentiate it from LTE-V2X. However, the bulk of the specifications related to NR-V2X are contained in Rel-16 [190]/Rel-17 [191]. While LTE-V2X mainly focusses on basic safety use cases, NR-V2X also targets more advanced use cases such as platooning, extended sensors, advanced driving, and remote driving. Apart from broadcast, the only LTE-V2X supported communication cast type, NR-V2X includes unicast and groupcast. Rel-16 further introduced a Hybrid Automatic Repeat reQuest (HARQ) for unicast and groupcast communication, enabling re-transmissions based on the intended receivers' feedback. Moreover, the protocol stack is extended by the so-called Service Data Adaptation Protocol (SDAP) sub layer, which maps between a sidelink QoS flow and its corresponding sidelink data radio bearer (cf. [192]). As in LTE-V2X, NR-V2X features two resource allocation modes, a network-assisted mode (mode 1) and an autonomous mode (mode 2). NR-V2X mode 2 deviates from LTE-V2X mode 4 in that the former allows resources reserved by traffic of lower priority (specified in SCI) to still be selected for transmission, and in the newly added dynamic scheduling

enhancements for aperiodic traffic, i.e., via re-evaluation [193]. The latter selects resources after channel sensing, without further reservations for future transmissions as done in SPS-based scheduling. In view of the vast number of enhancements, the interested reader may refer to [194] for further details.

On the PHY layer, NR-V2X adopts most features from 5G NR uplink. In contrast to LTE-V2X it reintroduces OFDM in addition to DFT-s-OFDM to enable high throughput efficiency and high energy efficiency operations, respectively. Like IEEE 802.11bd it further supports mmWave communication in addition to the sub-6 GHz operation. For enhanced use case flexibility NR-V2X introduces different OFDM sub carrier spacings, referred to as numerologies, reaching from 15 to 60 kHz in the sub-6 GHz bands and from 60 to 120 kHz in the mmWave spectrum. For higher throughput and reliability, in NR-V2X the modulation schemes supported by LTE-V2X are extended by 256 QAM and turbo coding for TBs is replaced by LDPC coding, as will be utilized in IEEE 802.11bd. A subdivision of sub-frames and the option to use so-called mini-slots for transmission is intended to significantly reduce the transmission latency. Overall, NR-V2X is expected to present superior average data rates but also higher transmission latencies as compared to IEEE 802.11bd [175]. A more comprehensive treatment of the technology's PHY layer is offered in [195].

2.2.5. Management and Security Layer

The management and security layers are cross-layer entities (cf. Fig. 6) that provide services to all of the layers introduced above [196]. The management entity is responsible for the configuration of the ITS-S and the exchange of data between the layers of the ITS reference architecture (MAC: [197], NET & TRA: [198], FAC: [199], SEC: [200]). For this purpose, it administrates the so-called Management Information Base (MIB), containing all relevant cross-layer parameters [201]. Of special relevance for this thesis are the congestion control services offered by the management layer discussed in more detail in Section 2.3. These are responsible for the congestion mitigation of the communication channel, e.g., by dynamically reducing the amount of transmitted data.

The security cross-layer entity offers functionalities to ensure confidentiality, integrity, availability, accountability, and authenticity according to [202] and [203]. Supported security configurations include cryptographic protection by digital signatures, encryption, consistency checks, plausibility checks, and anonymous address configuration for the use of pseudonyms [204]. The confidentiality requirements of most of the V2X messages introduced in Subsection 2.2.2. are comparatively low since the messages are typically broadcasted to all connected stations. On the other hand, they have high integrity,

availability, accountability, and authenticity requirements and make use of the respective security configurations, causing a significant security-overhead of up to several hundred bytes. Similar to the management entity, the security entity is connected to all other layers of the protocol stack. For a comprehensive analysis of ITS security standards, threats, and cryptographic countermeasures the reader is encouraged to refer to [205].

2.3. Congestion Control Mechanisms

To counteract the channel load generated by the multiple V2X services competing for communication resources, various congestion control mechanisms have been introduced by the respective SDOs. These mechanisms act on different protocol layers and control the generation and transmission of V2X messages. In the following, congestion control is discussed on the example of the Decentralized Congestion Control (DCC) mechanisms, originally introduced by ETSI for ITS-G5. To prevent excessive channel congestion by single stations, ETSI stipulates that the DCC mechanisms must jointly comply with a maximum transmission duration of 4 ms, a maximum duty cycle of 3% and a channel load dependent minimum inter-message interval as defined in [206]. This section introduces the architecture proposed by ETSI for the DCC mechanisms on the various layers (see Fig. 16): DCC_FAC (Subsection 2.3.1), DCC_NET (Subsection 2.3.2), DCC_ACC (Subsection 2.3.3), and DCC_CROSS (Subsection 2.3.4). Subsection 2.3.5 then offers the reader an insight into the recently developed congestion control mechanisms of C-V2X. Where relevant, reference is made to the congestion control standards of SDOs in other regions of the world.

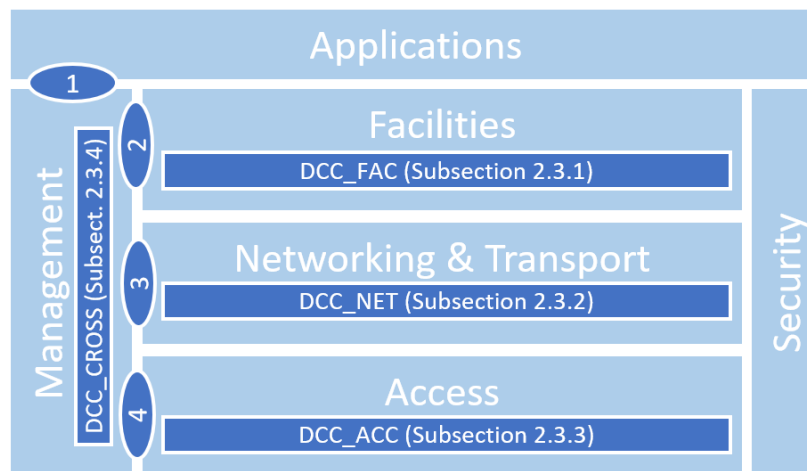


Fig. 16: DCC Architecture developed by ETSI for ITS-G5, adapted from [207].

2.3.1. Facility Layer DCC

The facility layer DCC entity was recently standardized by ETSI [208]. After being rejected during remote consensus, the final draft was reviewed in a series of comment resolution meetings, and finally approved and published in November 2021. The purpose of DCC_FAC is to provision the numerous V2X services with an estimation of the available resources they can consume to achieve a well-orchestrated resource allocation among services and stations. To this end, DCC_FAC monitors the resource consumption by the different services and the number of available resources as provided by the interface to DCC_CROSS on the management layer. The standard approach of DCC_FAC, also used in the scope of this work, is described in Annex A of [208].

DCC_FAC estimates the average message length \overline{L}_{ij} per service j and TC i based on the latest estimation \overline{L}_{ij}^* and the length of the last generate message $L_{on\ ij}$:

$$\overline{L}_{ij} = w \cdot L_{on\ ij} + (1 - w) \cdot \overline{L}_{ij}^* \quad (1)$$

L_{ij} can be obtained from the corresponding V2X service on facility layer, including an estimation of the protocol headers required for transmission. The parameter w corresponds to a weight coefficient. Similarly, the average inter-message interval can be computed as:

$$\overline{T_{off\ ij}} = w \cdot T_{off\ ij} + (1 - w) \cdot \overline{T_{off\ ij}}^* \quad (2)$$

Subsequently, the channel resources claimed by each service and TC are computed following the equation:

$$\overline{CRE}_{ij} = \frac{\overline{L}_{ij}}{\overline{L}_{ij} + R_{ij} \cdot \overline{T_{off\ ij}}} \quad (3)$$

where R_{ij} is the utilized MCS data rate provided by the DCC_CROSS interface. The total estimated claimed channel resources per TC can then be computed as:

$$\overline{CR}_i = \sum_j \overline{CRE}_{ij} \quad (4)$$

The available channel resources CR_a , also obtained from the DCC_CROSS interface, are then distributed among the services and TCs following:

$$ACR_i = \begin{cases} \max(CR_{0min}, CR_a) & \text{for } i = 0 \\ \max(CR_{0min}, ACR_{(i-1)} - \overline{CR}_{i-1}) & \text{for } i \geq 1 \end{cases} \quad (5)$$

where $CR_{0min} > 0$ is set to prevent service starvation. Once the available resources are assigned to TCs, a distribution among the V2X services of each TC can be performed:

$$ACR_{ij} = \frac{\overline{CRE_{ij}}}{\overline{CR_i}} \cdot ACR_i \quad (6)$$

Finally, the suggested inter-message interval can be computed for each service and provided to DCC_CROSS in the management plane, following the equation:

$$T_{off\ min\ ij} = \frac{\overline{L_{ij}}}{R_{ij}} \cdot \frac{1 - ACR_{ij}}{ACR_{ij}} \quad (7)$$

It should be mentioned that the implementation of DCC_FAC V2.1.1 is optional. However, it will most likely be conditional for the use of data-intensive Day 2+ V2X services such as Collective Perception and Maneuver Coordination. For this reason, the compatibility of DCC_FAC with C-V2X is essential. The latest modifications to the TS include an extended interface to DCC_CROSS, to allow the operation with C-V2X. However, in view of the current maturity of the technology several issues are still to be investigated and solved for deployment. Already during the review process of V2.1.1 ETSI TC ITS opened a new work item “MCO facilities layer congestion-control functionality”. The target of this new work item is to update the recently published congestion control requirements and mechanisms to support MCO while ensuring interoperability.

A range of alternative or additional congestion control mechanisms have been proposed for the facility layer. A selection of these is treated in more depth in Section 2.4.

2.3.2. Networking and Transport Layer DCC

The networking and transport layer DCC entity [166, 167] is optional and allows connected stations to share the perceived channel load with their one- and two-hop neighbors, making use of the so-called DCC_NET piggybacking scheme. It thus mainly serves as support for the DCC functions acting on the adjacent layers by making the piggybacked channel loads accessible over the DCC_CROSS interface. Sharing status information concerning the congestion of the communication channel perceived by neighboring connected stations is essential to mitigate fairness and oscillation issues [209, 210]. Fairness issues arise, e.g., when ITS-Ss trying to transmit identical messages with equal frequency converge to different equilibrium states, i.e., diverging numbers of allocated resources, despite measuring the same channel load. Oscillations in turn may arise if the resource allocation mechanisms include unstable states in their parameter space, leading to oscillating

numbers of assigned resources per ITS-S, strongly impairing the system's performance (cf. [A18]).

2.3.3. Access Layer DCC for IEEE 802.11p/bd

The DCC_ACC entity [211] controls the channel access behavior of a station by adjusting its communication parameters in dependence of the channel load. The most investigated mechanism is the so-called Transmit Rate Control (TRC) that regulates the time interval T_{off} between transmitted packets, operating as a gatekeeper between MAC and the upper layers. DCC_ACC specifies a reactive state-based approach (Subsection 2.3.3.1) and a linear adaptive approach (Subsection 2.3.3.2) to determine the packet transmission rate in dependence of the CBR. Subsection 2.3.3.3 then introduced Transmit Power Control (TPC) and Transmit Data-rate Control (TDC), allowing to reduce the transmit power and the data-rate, respectively, to mitigate the congestion of the V2X channel. Finally, in view of the extensive work dealing with comparable data-agnostic resource allocation mechanisms these are discussed in the dedicated Subsection 2.4.2.

2.3.3.1. Reactive Approach

The DCC_ACC defined for ITS-G5 consists of three processes as specified in [211]: (i) Prioritization. Each generated packet receives a priority level referred to as Traffic Class (TC). The DCC_ACC component associates each of the four specified TCs to a DCC Profile (DP), which is ultimately mapped to one of the EDCA ACs of ITS-G5 as introduced in Subsection 2.2.4. (ii) Queuing. Packets associated to each of these EDCA ACs are queued before their transmission. The queues have a maximum size, discarding any additional packets until the queue is sufficiently emptied to accept newly generated packets. In addition, packets that reach their maximum lifetime are discarded to make space for new entries. (iii) Flow control. Packets are de-queued and handed over to the lower layers for their transmission. The flow control preferences queues with higher priorities (i.e., lower ACs), possibly leading to starvation effects on the less relevant queues. Packets within the same queue are transmitted according to their generation time, favoring older packets. A more in-depth discussion is offered in [212].

The reactive DCC (R-DCC) approach defined in clause 5.3 in [211] introduces a state machine whose states are associated to channel load ranges. Table 1 exemplarily shows a five-state configuration for packets with durations of up to $T_{on} = 0.5$ ms, currently being the best-investigated configuration [213]. However, also three- and seven-state

configurations are possible. A table for higher packet durations as would be required for a significant fraction of CLMs and MCMs is provided in the Informative Annex A in [211].

Table 1: Parameters for the 5-state reactive approach of DCC_ACC ($T_{on} \leq 0.5$ ms)

State	CBR	T_{off}	Packet Rate
Relaxed	< 30%	50 ms	20 Hz
Active 1	[30-40%)	100 ms	10 Hz
Active 2	[40-50%)	200 ms	5 Hz
Active 3	[50-65%)	250 ms	4 Hz
Restrictive	> 65%	1000 ms	1 Hz

Generally, the lowest and highest state are referred to as *Relaxed State* and *Restrictive State*, respectively. Depending on the chosen configuration, one to five intermediate *Active States* are possible. Each of these states defines an idle time T_{off} between consecutive transmissions. Its inverse is the maximum packet rate allowed by each state, ranging from 1 to 20 Hz.

2.3.3.2. Adaptive Approach

The adaptive DCC (A-DCC) approach defined in clause 5.4 in [211] makes use of the same three processes as the reactive approach introduced in the previous subsection: prioritization, queuing, and flow control. It is based on the linear adaptive congestion control protocol LIMERIC [214, 215] that will be discussed in Subsection 2.4.1 and is aimed at maximizing the packet throughput for any given number of connected stations. ITS-S following the adaptive approach choose the inter-message time T_{off} such that the channel load tends towards a pre-defined $CBR_{tar} = 68\%$ on the control channel and roughly 10% higher on the service channels⁸:

$$T_{off} = \frac{T_{on}}{\delta} \quad (8)$$

with

$$25 \text{ ms} \leq T_{off} \leq 1000 \text{ ms} \quad (9)$$

⁸ Studies showed that the optimum channel throughput can be reached at approx. 78% channel load [317]. The target load of the control channel considers a buffer of 10% for safety critical messages

where the occupancy limit δ corresponds to the maximum fraction of time that the station is allowed to transmit. It is computed every 200 ms by subtracting a fraction α of its previous value δ_{prev} and adding an offset δ_{offset} :

$$\delta = (1 - \alpha) \cdot \delta_{prev} + \delta_{offset} \quad (10)$$

with δ_{offset} depending on the deviation from CBR_{tar} and a gain constant β :

$$\delta_{offset} = \beta \cdot (CBR_{tar} - CBR) \quad (11)$$

The CBR is calculated as a weighted average of the CBR sensed by the ITS-S and the CBRs of other connected ITS-Ss provided by DCC_NET. To ensure convergence towards a stable state δ_{offset} is restricted to:

$$-0.00025 \leq \delta_{offset} \leq 0.0005 \quad (12)$$

In addition, the algorithm parameters are set to:

$$\alpha = 0.016 \quad \text{and} \quad \beta = 0.0012 \quad (13)$$

where α and β correspond to the memory loss parameter or fairness parameter and the convergence leverage parameter, respectively. They are discussed in detail in Subsection 3.5.2.

Overall, the adaptive approach was found to generally outperform the reactive approach in terms of packet reception intervals, system stability, and CBR tracking accuracy [216].

2.3.3.3. Other Approaches

A disadvantage of TRC is the eventual dropping of packets regardless of their content. Thus, different alternative techniques have been specified and can be used by the DCC algorithm in any combination. The most relevant are TPC and TDC. TPC reduces the output power P_t at higher channel loads. A lower output power leads to a reduction of the communication range d_{com} relieving the communication channel. This relationship can be expressed, e.g., by a quadratic path loss according to the Friis-model [217] (for further pathloss models the interested reader may refer, e.g., to [218]):

$$d_{com}(P_t) = \sqrt{P_t} \cdot \frac{\lambda}{4\pi} \sqrt{\frac{G_t G_r}{LR_{th}}} \quad (14)$$

with the carrier wavelength λ , the transmitter and receiver gains G_t and G_r , the loss factor L and the reception threshold R_{th} . The main downside of TPC is a reduced Packet Delivery Ratio (PDR) for ITS-Ss that are further away from the transmitting station [219]:

$$PDR(d, m, d_{com}) = e^{-m \left(\frac{d}{d_{com}}\right)^2} \left[1 + m \left(\frac{d}{d_{com}}\right)^2 + \frac{m^2}{2} \left(\frac{d}{d_{com}}\right)^4 \right] \quad (15)$$

with Nakagami- m fading intensity, typically set to $m = 3$. However, it should be remarked that empirical studies have proved m to be scenario dependent [218]. Further it was shown that surrounding infrastructure and vegetation both have a major impact on signal fading [220, 221].

Finally, TDC increases the data rate by controlling the MCS to decrease the packet duration T_{on} . The main downside is a higher susceptibility to decoding errors at the receiver, which decreases the communication reliability and range. It is the less investigated of the three DCC_ACC techniques. Nevertheless, TDC has been found to outperform TPC [222]. Especially for safety critical messages a 6-state TDC (with data rates ranging from 3 Mbps to 24 Mbps) was reported to perform significantly better than a 10-state TPC (with transmit powers shifting from 24 dBm to -10 dBm with rising congestion) for various investigated traffic densities [223].

2.3.4. Cross-Layer DCC

The DCC functionalities introduced in the previous subsections are orchestrated by DCC_CROSS [207]. It administrates the relevant DCC parameters and makes them accessible to the DCC entities in the facilities, networking & transport, and access layers. The interface to DCC_FAC (interface 2 in Fig. 16) was recently subject to extensive amendments and will include parameters such as the access layer identifier (indicating the access layer technology), the channel number (indicating the radio channel for which the DCC parameters are retrieved), the used MCS, the available resources CR_a (formerly CBR_a), an application or service identifier, and the TC, among others (cf. Subsection 2.3.1). The interface to DCC_NET (interface 3 in Fig. 16) comprises parameters such as global CBR (defined as the maximum of local, 1-hop, and 2-hop CBR [167]), channel number, local CBR, available resources CR_a , last transmit time, idle time T_{off} , and transmit power

level limit for the selected radio channel, among others. Finally, the current specification of the interface to DCC_ACC (interface 4 in Fig. 16) includes channel number, local CBR, message length T_{on} , last transmit time, idle time T_{off} , and transmit power level limit. In view of the data required for DCC_FAC, this interface is expected to be adapted accordingly. Besides the various interfaces, DCC_CROSS features the so-called DCC parameter evaluation function. It is responsible for computing, e.g., the available resources CR_a from the measurements provided by DCC_ACC and DCC_NET.

2.3.5. Congestion Control in C-V2X

Congestion control for direct cellular vehicular communication was introduced in 3GPP Rel-14 [54]. To differentiate the technology from its Wi-Fi based competitor, 3GPP avoids the term DCC and uses the general term congestion control as it additionally offers a network-assisted mode.

The SPS-based LTE-V2X Mode 4 (cf. Subsection 2.2.4.3) has been proven to present fast decaying reliability as the channel load increases [188]. To mitigate such effects, 3GPP introduced two metrics to monitor the state of the wireless communication channel, the CBR and the Channel occupancy Ratio (CR) (see Subsection 23.14.1.1 in [185]). In LTE-V2X the CBR quantifies the ratio of occupied sub-channels, i.e., whose RSSI exceeds a pre-configured threshold, within the last 100 subframes (Subsection 5.1.30 in [224]). The CR in turn represents the resource share occupied by the evaluating station within a window of 1000 ms (Subsection 5.1.31 in [224]). Of these at least 500 ms must lie in the past, corresponding to actual transmissions (Subsection 14.1.1.4B in [225]). The remaining time corresponds to a reselection-counter-based forecast of reserved resources.

A novelty introduced with NR-V2X in this regard is the introduction of a more flexible time window, (pre-)configurable per RP [193]. It defines two options: (i) a static 100 slot time window, and (ii) a numerology-dependent, i.e., Subcarrier Spacing (SCS)-based (cf. Subsection 2.2.4.4) time window size for the computation of the CBR [226]. Further, the RSSI measurements benefit from the much-enhanced granularity of NR-V2X in the frequency and the time domains. Similar amendments as for the estimation of the CBR are introduced for the computation of the CR in NR-V2X. The standard stipulates the size of the evaluation window to likewise be defined in slots rather than in sub-frames. Additionally, it may analogously be either fix per RP, corresponding to 1000 slots, or take a SCS-dependent value. As for LTE-V2X, packet dropping shall not be assumed within the forecast range.

Based on the measured CBR and the computed CR values, each station then adapts its transmission access behavior. To this end, the standard defines a state machine comparable to the reactive approach defined for ITS-G5 (cf. Subsection 2.3.3.1). It consists of up to 16 CBR ranges linked to pre-configured upper CR limits in dependence of the TB's priority and the station's absolute speed threshold [187]. To comply with the specified maximum CR limit, 3GPP does not define a particular congestion control algorithm, but rather provides a series of possible mechanisms to reduce the channel load, such as adjusting (i) the MCS, (ii) the number of sub-channels, (iii) the number of transmissions and retransmissions, e.g., by dropping lower prioritized TBs, and (iv) the transmit power. In lack of detailed algorithms, studies have investigated the performance of congestion control based on the algorithms defined by ETSI [227, 228] (cf. Subsection 2.3.3), and SAE J2945/1 [229]. In LTE-V2X mode 3 and NR-V2X mode 1, eNB and gNB are responsible for the control of the channel load. To this end, both network-controlled modes require the connected stations to provide their local CBR measurements [230, 187].

2.4. Resource Allocation Optimization

In the previous section, the need for a channel load control that could be caused by dense vehicular networks featuring a plurality of V2X services was presented together with the most relevant standards in this field. Being able to allocate the scarce communication resources wisely is a key factor to maintain a high QoS within the network. To this end, awareness of the communication channel's state, further referred to as *congestion-awareness* or *load-awareness*, is a strict requirement. Besides monitoring the number of available resources, a network is often conceived to prioritize data according to its relevance. This attribute is referred to as *content-awareness* or *data-awareness*. Both congestion- and content-awareness, may be subdivided into a local *station-centric* or *local awareness* and a *network-extended* or *global awareness*, depending on whether a station is aware only of its own state or if also the states of connected stations are taken into account. An essential difference between congestion-aware and content-aware resource allocation mechanisms is their typical location in the V2X protocol stack. While the former require input from the lower communication layers, the message content is managed by the V2X applications and services located on top of the protocol stack.

The vast majority of research has focused on improving either the control mechanisms on the access layer employing congestion-aware resource allocation methods or the message generation rules of the V2X services based on content-awareness. With the standardization of DCC_FAC that allows V2X services to generate messages in a

congestion- and content-aware manner by providing them with an estimation of the resources at their disposal, a variety of such hybrid approaches have been emerging.

In the following, a selection of research advances in mainly congestion-aware (Subsection 2.4.1), mainly content-aware (Subsection 2.4.2), and integrated congestion- and content-aware (Subsection 2.4.3) resource allocation mechanisms is presented. Subsection 2.4.4 then draws conclusions on the existing state-of-the-art related to resource allocation mechanisms and details the research gap, previously only roughly identified in Section 1.1.

2.4.1. Congestion-aware Approaches

Despite effectively reducing the channel load generated by the V2X network, the standardized congestion control mechanisms discussed in the previous subsection were found to present some major drawbacks. Besides the issues mentioned in Subsection 2.3.3 related to unfairness and oscillations [209, 210, 231], DCC may lead to excessive throttling of messages, as demonstrated for platooning [232], Collective Perception [233], and Maneuver Coordination [A18], among others. Further, the authors of [234] report limited capability of the current standard regarding multi-service operation and several studies have pointed out the relevance of an accurate parametrization to achieve better performances, e.g., in terms of communication ranges and reliabilities [235, 232, 236]. These and other identified potentials for improvement have led to the development of numerous congestion-aware approaches.

Most proposed approaches focus on TRC. Probably the most prominent is LInear MESSage Rate Integrated Control (LIMERIC) [214, 215]. LIMERIC was proposed to overcome the limitations of the state-machine-based R-DCC, by gradually adjusting the maximum allowed transmission rate to converge to a predetermined channel load (cf. CBR_{tar} in Subsection 2.3.3.2). Its much-improved performance led to the extension of the DCC ACC standard by A-DCC introduced in Subsection 2.3.3.2, a reparametrized version of LIMERIC. Several extensions have been proposed for LIMERIC, such as the Error Model Based Adaptive Rate Control (EMBARC [237]) that makes resource allocation additionally dependent on the transmitting ITS-S dynamics, reducing the inter packet gap and increasing the environmental awareness of ITS-S with CAM- or BSM-like messages. EMBARC could thus additionally be viewed as partly content-aware with regard to the latter messages. However, for messages such as the CPM the dynamics of the transmitting ITS-S play a secondary role [A14], expectably limiting the applicability of EMBARC to ego-centric messages. As it is evidently not suited for RSUs and VRUs, the protocol's applicability is further restricted to dynamic transmitters. Another approach is taken by

Periodically Updated Load Sensitive Adaptive Rate control (PULSAR [238]), which introduces CBR piggybacking to increase fairness, by using the 2-hop CBR to control the message rate and converge towards the intended CBR_{tar} . Additional control mechanisms, such as cooperative LIMERIC (C-LIMERIC [239]) and Fair Adaptive Beaconing Rate for Inter-vehicular Communications (FABRIC [240]) have been introduced to further increase fairness in resource allocation. Gozalvez and Sepulcre introduce the OPportunistic-driven adaptive RAdio resource Management (OPRAM [241]) that additionally considers the environment of the connected stations to allocate resources. The authors extended OPRAM [242, 243, 244] and introduced a MINimum packet Transmission frequency (MINT) that sets the transmission frequency slightly above the packet reception frequency required by the supported application. The consideration of this safety margin was shown to present encouraging performance results.

To overcome LIMERIC's limitations when dealing with high ITS-S densities (cf. Subsection 3.5.3), Lorenzen introduced Self-Weighted Rate Control (SWeRC [245]). SWeRC makes use of the network's channel access behavior to adjust the convergence leverage factor β , obtaining substantial performance increases over LIMERIC in high-density scenarios. For more extensive reviews on resource allocation and congestion control mechanisms in vehicular networks, the interested reader is strongly encouraged to refer to [246] and [247], respectively.

2.4.2. Content-aware Approaches

A significant drawback of the congestion-aware mechanisms presented in the previous subsection is the random dropping of packets, regardless of the relevancy of their content [248]. Even though some of these mechanisms consider the ITS-S dynamics or their environment, a discrimination based on the actual information that is being transmitted is not taken into account, often leading to significant deviations from an optimal resource allocation [A18]. Similar findings have led to the development of a series of content-aware resource allocation mechanisms that prioritize data on facility layer.

A content-aware resource allocation may be static, prioritizing messages or stations generically. An example are the TCs mapped, among others, on DPs and ACs in ITS-G5 [167] and Proximity service Per-Packet Priority (PPPP) in C-V2X [168]. TCs are attributed to packets on facility layer and are often used to prioritize data on service level. The authors of [249] investigate the prioritization of CPMs (formerly Environmental Perception Message; EPM) relative to CAMs. In a similar way, messages may be prioritized depending on the type of transmitting station. Emergency vehicles or RSUs may

generically be allocated more communication resources, as they are expected to transmit more relevant data.

On the other side, a content-aware resource allocation may be dynamic, assessing the relevancy on message level or even on sub-message level. An example of the former are the current specifications of the DENM [142]. While high priority DENMs are attributed the highest TC, common DENMs are assigned the second and forwarded DENMS the fourth and last TC. The decision regarding the relevancy of the transmitted data is generally in the responsibility of the generating V2X service. For this reason, the corresponding generation rules are a popular research field. The result is that dynamic generation rules have gradually been displacing static, e.g., periodic, generation rules. Examples are CAMs and CPMs that are transmitted based on the dynamic states of the transmitting vehicle and the detected objects they describe, respectively.

With the CPM being the most relevant Day 2 V2X message, and in view of its ongoing standardization by ETSI, different approaches have intended to enhance its generation rules. A major drawback of CAM-based generation rules for the CPM (see Subsection 2.2.2.3) is the redundant information disseminated within the network, reaching over 70 updates per object per second [A14]. To tackle this problem a range of redundancy mitigation techniques have been introduced [250, 251, 252, 253]. They are intended to filter the number of objects included in a CPM based on the potential contribution to the network. Another proposed mechanism, referred to as look-ahead, was introduced to group objects within fewer messages, effectively reducing the required message overheads, and hence the generated channel load [254]. Overall, it was shown that the look-ahead extended CPM generation rules led to a more reliable connectivity due to the positive effects on the load of the communication channel. Even though most of current research is focusing on the CPM to support its ongoing standardization, first studies have shown that also for Day 2+ V2X messages, such as the MCM, dynamic generation rules are potentially superior to static ones [160].

A more generic content-aware approach is proposed in [255]. The authors introduce the notion of the Value of Information (VoI) for vehicular networks. They propose to allocate resources based on the VoI linked to the data to be transmitted. An example of a VoI-based resource allocation mechanism is given in [256]. The authors developed an algorithm to compute the VoI of detected objects for the network. CPMs are then generated and transmitted based on the determined VoIs of each candidate object. The authors in [257] investigated the VoI of optional fields within the CPM, concluding that data such as correlation terms in the covariance matrices may often be omitted without major impact

on the performance of the service. Similar VoI functions, despite often being referred to by other names, are discussed in Subsection 3.4.4.

Nevertheless, it has been shown for different services that purely content-aware approaches are too greedy in high-density scenarios (CPM: [A4, A7], MCM [A18], CLM: [A16]) and must rely on DCC to deal with excessive channel congestion. On the other side, congestion-agnostic approaches require designs that are too conservative in low-density scenarios, lacking the capability to exploit the full potential of the channel by wasting valuable resources (CPM: [A14] and [233], MCM [A18], CLM: [A16]).

2.4.3. Integrated Approaches

As discussed in the previous subsections, congestion-awareness and content-awareness bear significant potential to improve resource allocation within the network. Both present weaknesses when used individually. For this reason, first approaches coupling or integrating congestion-awareness and content-awareness have emerged lately.

The ETSI V2X protocol stack is a prominent example of a coupling between congestion- and content-aware mechanisms. The imminent introduction of DCC_FAC will lead to an integration of these mechanisms by providing the V2X services with the required information regarding the state of the communication channel. With this, the latter will then be able to request resources based on the managed data and the channel congestion, presenting a significant improvement compared to the blind message transmission attempts of the current coupled V2X protocol stack.

An interesting cross-layer coordination of multiple vehicular protocols (COMPASS [212]) has recently been introduced to orchestrate multiple independent or loosely coupled protocols. The benefits of COMPASS are demonstrated by coordinating MINT and A-DCC, achieving high application performances by complying with the defined channel congestion limits in most scenarios. The authors state that COMPASS is also capable of coordinating other protocol combinations, such as PULSAR with MINT.

An extension of LIMERIC [258] considers inhomogeneous VoI distribution within the network. Stations with higher average VoI are assigned more resources than their peers by introducing special weights. The tuning of these weights will allow the connected stations to converge towards different weight-dependent transmission rates. A drawback of this modified LIMERIC version is the systems quasi-static convergence behavior. While a firetruck may claim higher resource shares for long periods in time, an emergency-braking passenger car would instantaneously require an extended channel access. By the time the system has converged against the new resource shares, it may be too late.

Another approach that is worth pointing out is the one proposed in [64]. The authors introduce an innovative mechanism for multi-service orchestration based on a static service rank that could be the service's TC, a content-based usefulness, and an urgency determined by a service-set expiration time of the message. The message VoI, referred to as multi factor priority, is given by a weighted sum of these three factors. Resource allocation is performed based on the channel load and the determined VoI (cf. Subsection 3.4.4).

Finally, the authors in [A18] propose an approach to increase the VoI, referred to as Accessible Information Relevance (AIR), in maneuver coordinating vehicular networks. The AIR is defined based on the relative projected and announced trajectories of the cooperating traffic participants. The AIR is then maximized within the network by considering the channel load and the expected reception probabilities of the intended receivers. Despite being applicable only to Maneuver Coordination in its proposed form, the introduced resource allocation mechanism is likely to present the highest combined congestion- and content-awareness proposed to date.

2.4.4. Research Gap Refinement

After Section 1.1 briefly introduced V2X communication, elucidating the major societal, environmental, and technical challenges the technology is intended to address, Chapter 2 provided the reader the necessary information for the understanding of the remainder of this work. Based on this background and the literature review provided in the previous subsections, the research gap envisioned in Section 1.1 is refined in the following.

In view of the narrow bandwidth allocated for ITS safety applications and the associated scarcity of communication resources, a highly efficient resource management is essential. The distributed and highly dynamic nature of V2X networks sets additionally stringent requirements to the system conception and design. Significant development efforts have been conducted by research institutes, industry, and SDOs to introduce and enhance new technologies optimizing the value of information disseminated within V2X networks. Congestion-aware resource allocation mechanisms, such as DCC, have risen as an important instrument to optimize the radio communication performance. However, most of the mechanisms are content-agnostic, treating messages like “black-boxes” and thus disregarding the relevance of the carried data. This can lead to the dropping of safety critical messages in favor of less relevant ones, negatively impacting the performance of the underlying V2X services.

On the other side, numerous content-aware resource allocation mechanisms have been proposed to prioritize more relevant data. These mechanisms generally work best under very specific conditions, especially with regard to the channel load. Nevertheless, if the

system deviates from these optimal conditions the performance drops significantly. Examples are the various mechanisms designed for the generation of CPMs that are aimed at selecting the most relevant objects for transmission. For channel loads higher than the optimal range, too many objects will be included, potentially leading to a channel saturation, with detrimental effects on communication reliability, latency, and range. For channel loads below the optimum, too few objects are included, wasting valuable channel resources.

For this reason, late advances in research have pointed out the need for integrated congestion- and content-aware dissemination mechanisms that optimize the value of information shared within the network, accounting for the state of the radio communication channel and distributing the available resources based on the expected added value of the transmitted data [A18]. The resource allocation on sub-message level is especially interesting, as it allows to adapt the message size based on the relevancy of the available message segments.

Overall, to maximize the value (and thus the benefit) of information shared in vehicular networks, a decentralized content- and congestion-aware sub-message resource allocation is required. Despite recent advances in this field, there is still a vast research gap in this area, especially when it comes to a coordinated multi-service resource allocation. This gap, essential to an efficient large-scale deployment of the V2X technology, is addressed in the following chapter.

3. DECENTRALIZED VOI-MAXIMIZING RESOURCE ALLOCATION

In the concluding section of the previous chapter, the lack of a V2X resource allocation mechanism explicitly maximizing the VoI was identified. The present chapter aims at mitigating this lack. It is structured as follows: Section 3.1 introduces the underlying combinatorial optimization problem along with its constraints and points out the main peculiarities attributed to the V2X context. Section 3.2 presents the V2X-service independent core components of the decentralized VoI-maximizing resource allocation protocol VALINDRA developed in the scope of this work. In Section 3.3 an application example of VALINDRA is discussed. Section 3.4 then focusses on the computation of the VoI for three distinct V2X services: Collective Perception, Maneuver Coordination, and Collaborative Localization. Finally, Section 3.5 offers a preliminary theoretical examination of the proposed cross-layer VoI-aware resource allocation, treating the systems stability, compatibility with other approaches, and possible limitations.

3.1. Problem Formulation

Even if specific bands of the RF spectrum have been allocated for exclusive use by V2X safety applications in the various regions of the world (see Subsection 2.1.1), the increasing number of V2X services and the expected, rapidly growing traffic equipment with the necessary communication systems make a smart resource allocation necessary. The underlying resource allocation problem belongs to the field of combinatorial optimization and can be expressed as a complex dynamic variation of the 0-1 knapsack problem [259]. It searches to maximize the VoI disseminated within a network consisting of stations i featuring V2X services j transmitting messages k consisting of segments l ⁹. The system is further subject to the physical limitations of the communication channel. Two approaches are conceivable:

- (i) **Cross-service optimization:** The benefit of V2X communication can be maximized by assigning the available resources across stations, services, messages, and message segments:

⁹ For the sake of readability evident indices are omitted in the following.

$$\max \sum_i \sum_j \sum_{k|T} \sum_l x_{ijkl} \cdot \Omega_{ijkl} \quad (16)$$

$$\sum_i \sum_j \sum_{k|T} \sum_l x_{ijkl} \cdot T_{onijkl} \leq T \cdot CBR_{tar} \quad (17)$$

where T and CBR_{tar} correspond to a time period that accounts for the dynamics of the system and the target CBR, respectively. To average out the microscopic ripple a period $T \geq 200 \text{ ms}$ should generally be considered [208, 211]. Ω_{ijkl} and T_{onijkl} correspond to the message segment's VoI and its channel access time. T_{onijkl} can be estimated as the message segment length L_{ijkl} divided by the used MCS data rate R_{ijk} with which the packet is transmitted (cf. Subsection 2.3.1). It should be noted that a cross-service optimization requires the VoIs of different services to be comparable.

- (ii) **Service-specific optimization:** The service-specific resource allocation optimization presents somewhat less potential for optimization, but also significantly less complexity. It can be used in case a cross-service optimization should not be possible or wanted. For each service j the resource allocation optimization problem can be described by:

$$\max \sum_i \sum_{k|T} \sum_l x_{ijkl} \cdot \Omega_{ijkl} \quad (18)$$

$$\sum_i \sum_{k|T} \sum_l x_{ijkl} \cdot T_{onijkl} \leq T \cdot CBR_{j,tar} \quad (19)$$

For both resource allocation approaches the binary optimization parameter $x_{ijkl} \in \{0,1\}$ encodes a discarded and a transmitted segment, respectively. However, compared to the standard knapsack problem further difficulties arise:

- **Distributed optimization:** The distribution of the relevant information among the nodes of the network requires a decentralized optimization of the resource allocation. In particular, the lack of knowledge about the number of segments and the associated VoIs available to other connected stations poses a major difficulty to the system design.

- **Incomplete knowledge:** The lack of knowledge even extends to some of the segments transmitted by a station. This is the case for the headers of the protocols below the facility layer. While some may be estimated accurately, for others only expectancy values are available.
- **Additional constraints:** While some data segments are optional, others are not (cf. Fig. 8). These mandatory data segments \mathcal{M} must be included to every transmitted message. On the other side a message is only transmitted if segments of the relevant data class \mathcal{R} are available for transmission. The latter could be detected objects, motion trajectories, or satellite measurements, without which the corresponding CPM, MCM, or CLM would not be transmitted (see Subsection 2.2.2). Thus, the optimization problem is further subject to the condition:

$$x_{ijkl} = \begin{cases} 0 & \text{if } x_{ijkl} = 0 \quad \forall l \in \mathcal{R} \\ 1 & \text{else} \quad \forall l \in \mathcal{M} \end{cases} \quad (20)$$

Moreover, similar constraints may apply between segments of the relevant data class \mathcal{R} . As an example, the value of an additionally transmitted satellite measurement in the CLM or a trajectory in the MCM highly depends on the other satellite measurements and trajectories that are being transmitted. The interdependency of message segments with respect to their VoIs is one of the hardest but most essential requirements to maximize the overall VoI shared within the network.

- **System dynamics:** In contrast to the standard variations of the knapsack problem, the VoI-driven resource allocation is a dynamic system, and its solution must further guarantee stability on each quasi-static path through the parameter space.
- **Service starvation:** The situation when one or more services are excluded from the resource allocation is called service starvation. In the scope of the ETSI TS 103 141 drafting sessions it was decided in common agreement to avoid service starvation [208]. A resource allocation mechanism should thus guarantee each service access to channel resources if the available data justifies it.

In the following section, the cross-layer protocol VALINDRA, designed in the scope of this doctoral thesis to solve the stated decentralized combinatorial optimization problem, is introduced.

3.2. Introducing VALINDRA

A prerequisite for a system to prevail is the lowest possible complexity that does not impair its performance. This statement equally applies to the introduction of new V2X communication techniques. With special consideration of this observation the VoI-driven resource allocation mechanism developed within the scope of this thesis is presented systematically in the following. Particular attention is further paid to the differences between the two approaches identified in the previous section.

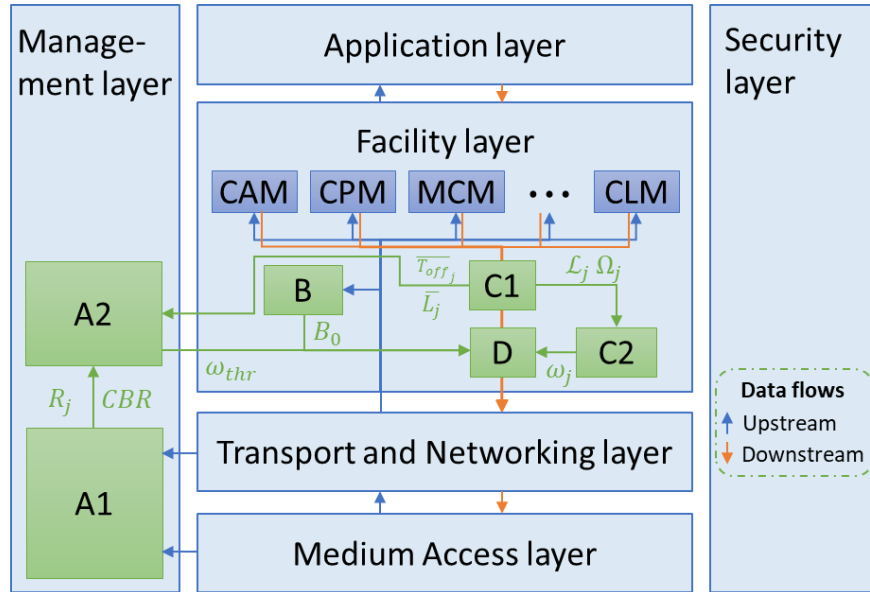


Fig. 17: Architecture and main data flows of VALINDRA.

As depicted in Fig. 17, VALINDRA is distributed among management and facility layer to maintain communication technology neutrality. It features the following steps:

A1: Channel load monitoring

The connected stations continuously monitor the load on the communication channel by assessing the moving average of measured CBR values conform to the standard in [211]:

$$CBR = 0.5 \cdot CBR_{prev} + 0.25 \cdot CBR_{meas} + 0.25 \cdot CBR_{meas,prev} \quad (21)$$

where CBR_{prev} and $CBR_{meas,prev}$ correspond to the last computed CBR- and last measured CBR_{meas} -values, respectively. On the other side CBR_{meas} is determined by the globally measured CBR obtained from the GeoNetworking header if [260] is supported and

otherwise by the locally measured CBR as provided by the MAC layer (e.g., by the DCC_ACC entity in ITS-G5 [208]).

A2: Determination of the information density threshold

Using the underlying control mechanism of ETSI's LIMERIC-based A-DCC approach (see Subsection 2.3.3.2), the information density threshold ω_{thr} for the multi-service VoI maximization is chosen so that the channel load jointly generated by all services accessing the same communication channel converges to a desired target value CBR_{tar} :

$$\omega_{thr} = (1 - \alpha) \cdot \omega_{thr} - \Delta\omega \quad (22)$$

where α is the system-specific memory loss constant and $\Delta\omega$ ¹⁰ represents the adaptation of the threshold value with the CBR:

$$\Delta\omega = \beta \cdot (CBR_{tar} - CBR) \quad (23)$$

As discussed previously, the parameter β controls the convergence speed and needs to be carefully selected to guarantee the system's convergence against a stable solution in steady state. CBR_{tar} can either be set constant, such as is the case in LIMERIC and A-DCC or be obtained implicitly by throughput optimization as demonstrated in [A15].

In the same way, for the service-specific VoI maximization, an individual information density threshold $\omega_{j,thr}$ is determined for each service j :

$$\omega_{j,thr} = (1 - \alpha_j) \cdot \omega_{j,thr} - \Delta\omega_j \quad (24)$$

where $\Delta\omega_j$ depends on the respective $CBR_{j,tar}$ defined for each service:

$$\Delta\omega_j = \beta_j \cdot (CBR_{j,tar} - \overline{CBR}_j) \quad (25)$$

The parameters α_j and β_j correspond to α and β in their function and can be set individually for each service j . \overline{CBR}_j is the channel load caused by each service j and is estimated as follows:

$$\overline{CBR}_j = \frac{\overline{CRE}_j}{CRE} \cdot CBR \quad (26)$$

¹⁰ Note the inverted sign with respect to Eq. 10, required to ensure stability (see demonstration in Section 3.5).

where \overline{CRE}_j corresponds to the average resources consumed by service j :

$$\overline{CRE}_j = \frac{\overline{L}_j}{\overline{L}_j + R_j \cdot \overline{T_{off}_j}} \quad (27)$$

with the average message length \overline{L}_j and the average message interval $\overline{T_{off}_j}$ of service j . R_j corresponds to the used data rate. All parameters can be obtained as described in the current TS of DCC_FAC [208]. The total number of resources consumed by all services can then be computed as:

$$CRE = \sum_j \overline{CRE}_j \quad (28)$$

B: Estimation of the number of mandatory bits per message

The total number of messages K and the number of messages K_j received per service in the time period T are updated along with \overline{CRE} and \overline{CRE}_j , respectively. They allow to compute the average number of mandatory bits per message:

$$B_0 = \sum_j \frac{K_j}{K} \cdot B_{j0} \quad (29)$$

where B_{j0} corresponds to the average number of mandatory bits required for each message of service j , including an estimation of lower layer protocol header sizes.

C1: Determination of the message segment Vols

Simultaneously to the determination of the information content threshold, each V2X service j provides a list \mathcal{L}_j of message segment alternative lists A_{jm} , consisting of one or more alternative candidate message segments S_{jml} . Each of these message segments S_{jml} is linked to an information value Ω_{jml} :

$$\mathcal{L}_j = \{A_{j1}, \dots, A_{jM}\} ; A_{jm} = \{S_{jm1}, \dots, S_{jml}\} \leftrightarrow \Omega_{jm} = \{\Omega_{jm1}, \dots, \Omega_{jml}\} \quad (30)$$

The message segment sizes can be determined freely by the V2X service, comprising from a single bit up to a set of objects, such as trajectories or satellite measurements for MCM and CLM, respectively. In the latter case, some message fields may be included in various

message segment alternatives. Ω_{jml} is non-negative and must generally not exceed a per bit value of 1. Larger values are justified particularly in the special case when the transmission of a segment must be guaranteed for the cross-service optimization:

$$\Omega_{prio} = B_0 + L_{j,prio} \quad (31)$$

and analogously for the service-specific optimization:

$$\Omega_{j,prio} = B_{j0} + L_{j,prio} \quad (32)$$

When considering the cross-service optimization mechanism, the main difficulty of this step is ensuring the comparability of the information values between the services. An interesting approach to determine the relative relevance of the data provided by different services is introduced in [64]. The calculation of this information relevancy Ω is discussed in detail in Section 3.4 using the examples of Collective Perception, Collaborative Localization, and Maneuver Coordination.

C2: Determination of the message segment information densities

In the next step, the information value densities of each segment S_{jml} are computed as:

$$\omega_{jml} = \frac{\Omega_{jml}}{L_{jml}} \quad (33)$$

where L_{jml} corresponds to the segment's length in bits. Due to the restrictions of the VoI, the information density is generally normed to the range $\omega_{jml} \in [0,1]$ and may take larger values only in special cases (compare priority-VoI computations in Eq. 31 and 32).

D: Selection of the message segments for transmission

The message segments whose information density does not exceed the CBR-dependent information density threshold value are then discarded, as their VoI density does not justify their transmission. Subsequently, per list of dependent segment alternatives only one segment is selected and brought together in a second list E_j . This is done by considering the overall message density. Cross-service VALINDRA estimates the VoI-density of the respective messages taking into account all message overheads:

$$\omega_j = \frac{\sum_m \sum_l \Omega_{jml} \cdot \Theta(\omega_{jml} - \omega_{thr})}{\tilde{B}_j} ; \Omega_{jml} = 0 \quad \forall l \neq l_{opt} \quad (34)$$

where Θ represents the Heaviside function and \tilde{B}_j represents the adjusted size of all message segments up to and including segment l contained in \mathcal{E}_j , and l_{opt} is the index of the VoI maximizing message segment alternative $S_{jml_{opt}} \in A_{jm}$. Its determination is presented below. \tilde{B}_j can be calculated as follows:

$$\tilde{B}_j = B_0 + \sum_m L_{jml_{opt}} \quad (35)$$

where B_0 represents the previously determined expectancy value of the number of mandatory bits across all messages transmitted during the period T . Analogously, the service-specific VALINDRA computes the message VoI-density as:

$$\omega_j = \frac{\sum_m \Omega_{jml_{opt}} \cdot \Theta(\omega_{jml_{opt}} - \omega_{j,thr})}{B_j} \quad (36)$$

with the combined size of all message segments in \mathcal{E}_j :

$$B_j = B_{j0} + \sum_m L_{jml_{opt}} \quad (37)$$

It is worth noticing that the consideration of equally distributed message overheads among messages from different services (Eq. 29 and Eq. 35) is the most effective mechanism to avoid service starvation in the cross-service optimization approach. Should, e.g., the expected minimum message size B_{j0} be used instead of the weighted average minimum size B_0 , then services with a lower ratio between fixed and optional data segments would have access to more resources than their peers carrying the same VoI, eventually leading to the latter's complete starvation. The implications of using the adjusted message size \tilde{B}_j instead of the accurate estimation B_j in terms of stability and impact on the channel load are discussed in Section 3.4.

The VoI maximization of the second list \mathcal{E}_i under the constraints $\omega_j > \omega_{thr}$ for the cross-service VALINDRA and $\omega_j > \omega_{j,thr}$ for the service-specific VALINDRA can be carried out with simple heuristics. For messages, such as the CPM, where the VoI of an object does not essentially depend on the other objects selected for transmission, each segment alternative list may contain only one alternative. Thus, for the cross-service VoI-maximization the list \mathcal{E}_j can be computed as:

$$\mathcal{E}_j = \left\{ S_{jml_{opt}} \mid S_{jml_{opt}} \in A_{jm}; A_{jm} \in \mathcal{L}_j \wedge \omega_{jml_{opt}} > \omega_{thr} \right\} \subseteq \mathcal{L}_j \quad (38)$$

In the same way, for the service-specific VoI-maximization the lists are built based on the individual information density thresholds $\omega_{j,thr}$:

$$\mathcal{E}_j = \left\{ S_{jml_{opt}} \mid S_{jml_{opt}} \in A_{jm}; A_{jm} \in \mathcal{L}_j \wedge \omega_{jml_{opt}} > \omega_{j,thr} \right\} \subseteq \mathcal{L}_j \quad (39)$$

Once the list \mathcal{E}_j of objects $S_{jml_{opt}}$ whose information value justifies their transmission has been computed, VALINDRA performs a final check to determine whether the overall VoI-density is sufficient for the generation of the corresponding message in the given point in time. To this end, the average VoI-density $\bar{\omega}_{jk}$ of the message k is again compared to the VoI-density threshold ω_{thr} for the cross-service VALINDRA or $\omega_{j,thr}$ for the service-specific VALINDRA computed in step 1. Finally, the list \mathcal{E}_j is updated as follows:

$$\mathcal{E}_j = \underbrace{\begin{cases} \mathcal{E}_j & \text{if } \bar{\omega}_{jk} > \omega_{thr} \\ \emptyset & \text{else} \end{cases}}_{\text{Cross service VALINDRA}} \quad \underbrace{\begin{cases} \mathcal{E}_j & \text{if } \bar{\omega}_{jk} > \omega_{j,thr} \\ \emptyset & \text{else} \end{cases}}_{\text{Service specific VALINDRA}} \quad (40)$$

Cross service VALINDRA

Service specific VALINDRA

The update of \mathcal{E}_j guarantees that a potentially generated message exceeds the required VoI-density even after accounting for the mandatory message segments. This is equivalent with setting $x_{ijkl} = 1$ in Eq. 16-19 for all segments $S_{jml_{opt}} \in \mathcal{E}_j$ and $x_{ijkl} = 0$ otherwise. An example of a heuristic applicable to services where the VoI of a segment depends on the combination of selected sub-segments, such as trajectories for the Maneuver Coordination Service or satellite measurements for the Collaborative Localization Service is given in Subsection 4.2.4.

3.3. A Service-specific Example

An exemplary illustration of VALINDRA's working principle is offered in Fig. 18 on the example of Collaborative Localization (cf. Subsection 2.2.2.4). Three connected vehicles, namely Car L (left), Car E (ego vehicle), and Car R (right), intend to enhance their positioning performance by exchanging raw GNSS and local range measurements. While E is only able to obtain 6 satellite measurements of poor quality due to obstructing buildings,

L and R obtain 9 and 11 higher quality measurements, respectively¹¹. To facilitate a better understanding the provided example considers each satellite measurement as a separate message segment. Hence, the inclusions of all segments are independent from each other. Thus, each message alternative consists of a single message segment (cf. Section 4.2).

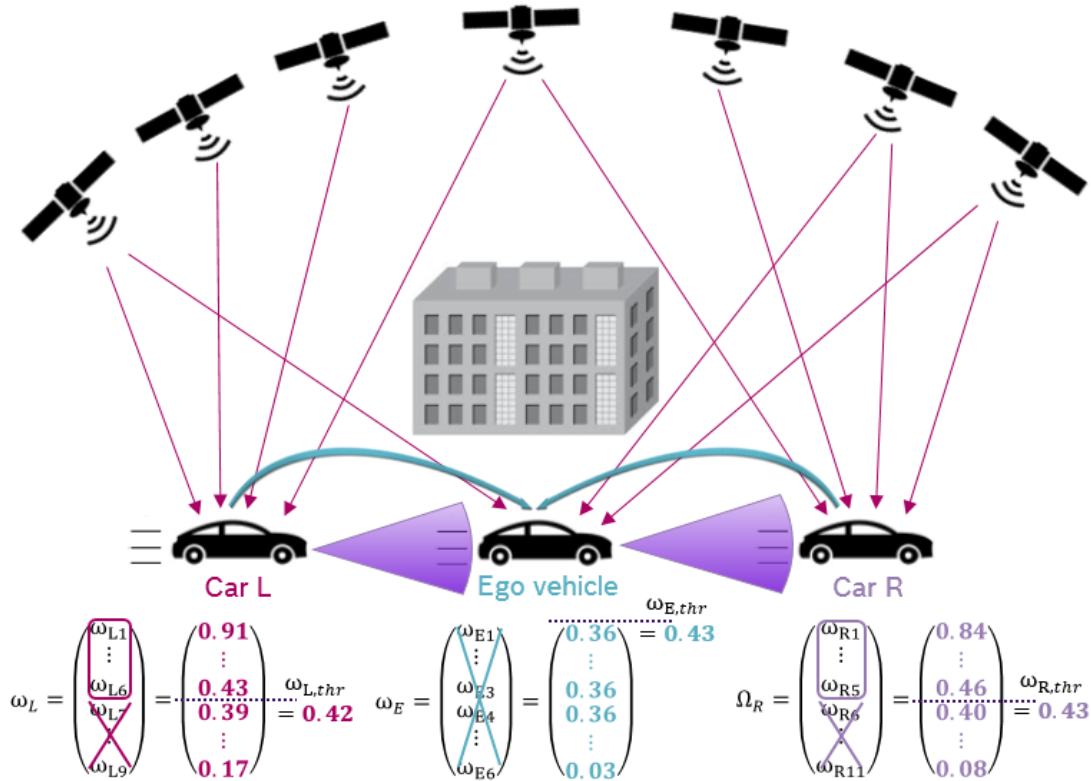


Fig. 18: Working principle of VALINDRA on the example of the Collaborative Localization Service.

In Step A1 and A2, all three vehicles independently compute the CBR and the resulting VoI-density threshold. Due to small heterogeneities, L senses a slightly less congested channel than E and R and thus computes a VoI-density threshold of 0.42, while E and R obtain values equal to 0.43. Apart from spatial heterogeneities of the channel load, the CBR computed by the MAC layer, and (if active) by the NT layer by making use of the piggy packing mechanism introduced in Subsection 2.2.3.2, can be subject to statistical and systematic measurement errors. However, these minor variations in the perception of

¹¹ Fig. 18 is intended for visualization purposes only. It does not provide a quantitative representation of the satellite measurements obtained by each vehicle.

the CBR are regulated to up to 3% in Europe by clause 4.2.10 in [206]. Simultaneously, in Step B each vehicle estimates the number of mandatory bits per CLM. In the example this estimation is carried out following the service-specific version of VALINDRA. The vehicles further compute the VoIs with their corresponding VoI-densities of each satellite measurement as described in Step C1 and C2, respectively. Due to the poor quality of E's satellite measurements the corresponding VoI-densities lie well below those of L and R. A peculiarity of Collaborative Localization is that even though the VoI may be computed per satellite measurement the four satellite measurements with the highest VoI are assigned the same VoI-density, since they only bring a benefit if at least four satellites are shared (cf. Section 4.2).

Subsequently, in Step D each vehicle selects the satellite measurements whose VoI-density exceed the previously determined threshold, discarding the remaining ones. Finally, the message is assembled on FAC layer, and a final check is performed to determine whether the overall message information density still exceeds the required threshold after consideration of the expectancy values of the lower-layer message headers. The computation of the CBR-dependent threshold guarantees an optimal resource allocation by the respective service, converging towards the target CBR and maximizing the VoI shared among the CVs. In the example R obtained a larger number of satellite measurements as compared to L, however, of inferior VoI, e.g., due to lower measurement qualities and satellite geometries (see Subsection 3.4.3). As a result of the maximization of the VoI within the VANET, R will thus only be allowed to transmit 5 out of its 11 measurements, while L can include 6 out of 9. On the other side, E would not transmit CLMs, leaving the channel resources to other vehicles transmitting information that is more valuable.

3.4. The Value of Information

A central part of VALINDRA is the determination of the message segment VoIs (Step C1) and the associated information densities (Step C2). The following subsections introduce the most relevant VoI dependencies for three of the V2X services introduced in Subsection 2.2.2, focusing on the main object class carried by each of them, namely detected objects in the CPM (Subsection 3.4.1), trajectories in the MCM (Subsection 3.4.2), and satellite measurements in the CLM (Subsection 3.4.3). These services are especially interesting as they are currently under standardization and present very distinct channel usage behaviors. For readability the indices are replaced by the object type: Ω_o (VoI of CPM object), Ω_t (VoI of MCM trajectory), and Ω_s (VoI of CLM satellite measurement). Subsection 3.4.4 finally gives introduces some implicit VoI definitions present in the current state-of-the-art.

3.4.1. Collective Perception

An ITS-S's environment model maintains a list of objects detected by its on-board sensors. VALINDRA computes the transmission relevancy of each of these detected objects in terms of its expected VoI contribution to the VANET. The VoI assignment needs to be carefully optimized and can be based, amongst others, on the following parameters:

- **Existence confidence:** Object tracking sensors compute existence likelihoods ψ for tracked objects. Typically, they make use of thresholds to determine the existence of an object. The higher the existence likelihood, the higher the VoI of the object (cf. [261]):

$$\Omega_o \mid \frac{\partial \Omega_o(\psi)}{\partial \psi} \geq 0 \quad (41)$$

- **Measurement precision:** Detected objects with high measurement precision should generally have a higher VoI if all other parameters are equal. Thus, the VoI Ω_o of the detected object should obey:

$$\Omega_o \mid \frac{\partial \Omega_o(|\Sigma|)}{\partial |\Sigma|} \leq 0 \quad (42)$$

where $|\Sigma|$ corresponds to the determinant of the measurement's covariance. It can represent either unfused data Σ_{meas} or fused data Σ_{LEM} as specified by [146]. As the covariance matrix is the inverse of the so-called concentration or precision matrix, a decreasing determinant implies an increasing precision and a higher VoI. Of particular interest are precision-thresholds. The VoI may also depend on individual components of the covariance matrix (e.g., position, speed, or acceleration errors).

- **Precision contribution to the GEM:** As the object's relevance has to be estimated from the perspective of the VANET, it is sensible to investigate the object's contribution to the GEM. A simple way could be by estimating the average precision available to the VANET by comparing the precisions of LEM and GEM. From the Kalman filter we know:

$$\Sigma_{GEM} = \Sigma_{LEM} \Sigma_{V2X} (\Sigma_{LEM} + \Sigma_{V2X})^{-1} \quad (43)$$

where Σ_{V2X} corresponds to the covariance contribution of the object's state by the VANET. Further, it can be assumed that similar information is also available to the connected stations within the VANET:

$$\Sigma_{VANET} \approx \Sigma_{V2X} = \Sigma_{LEM} \Sigma_{GEM} (\Sigma_{LEM} - \Sigma_{GEM})^{-1} \quad (44)$$

The lower the precision (higher covariance) of the object's state shared by the network, the higher the expected contribution and thus the VoI of the object:

$$\Omega_o \mid \frac{\partial \Omega_o(|\Sigma_{VANET}|)}{\partial |\Sigma_{VANET}|} \geq 0 \quad (45)$$

- **Absolute dynamic state:** The relevance of an object o is typically coupled to its dynamic state $\vec{S}_o = (\vec{r}_o, \dot{\vec{r}}_o, \ddot{\vec{r}}_o, \dots, \vec{\theta}_o, \dot{\vec{\theta}}_o, \ddot{\vec{\theta}}_o, \dots, \dots)^T$, where \vec{r}_o and $\vec{\theta}_o$ correspond to its position and heading, respectively. In contrast to the course (direction of movement), the heading (pointing direction) of an object cannot be implied from its velocity and is thus a principal component of the state vector. A higher absolute value of each linear strict subset $\vec{s}_o \subset \vec{S}_o$ of the first or higher order derivatives in the state vector \vec{S}_o may thus have a positive impact on the object's VoI:

$$\Omega_o \mid \frac{\partial \Omega_o(|\vec{s}|)}{\partial |\vec{s}|} \geq 0 \quad (46)$$

Examples justifying higher VoIs are a higher object speed, acceleration, or yaw rate.

- **Relative dynamic state:** Another relevant parameter describes the relative dynamics $\Delta \vec{S}_{o,t} = \vec{S}_o - \vec{S}_t$ of the measured object o with respect to other traffic participants t . Typically, these will be part of the network and are the main intended receivers of the measurement. However, not only the relative dynamics to connected stations have an impact on the VoI, but also those to not V2X-enabled stations may play a role, e.g., if the main addressee is the object itself. The differential distance and its time derivatives have a considerable effect on the safety of the system and can be determined by:

$$\begin{aligned}
d_{o,t} &= \frac{(\vec{r}_o - \vec{r}_t)}{\sqrt{(\vec{r}_o - \vec{r}_t) \cdot (\vec{r}_o - \vec{r}_t)}} \cdot (\vec{r}_o - \vec{r}_t) = \hat{r}_{o,t} \cdot \vec{r}_{o,t} \\
\dot{d}_{o,t} &= \frac{(\vec{r}_o - \vec{r}_t)}{\sqrt{(\vec{r}_o - \vec{r}_t) \cdot (\vec{r}_o - \vec{r}_t)}} \cdot (\dot{\vec{r}}_o - \dot{\vec{r}}_t) = \hat{r}_{o,t} \cdot \dot{\vec{r}}_{o,t} \\
\ddot{d}_{o,t} &= \frac{(\vec{r}_o - \vec{r}_t)}{\sqrt{(\vec{r}_o - \vec{r}_t) \cdot (\vec{r}_o - \vec{r}_t)}} \cdot (\ddot{\vec{r}}_o - \ddot{\vec{r}}_t) = \hat{r}_{o,t} \cdot \ddot{\vec{r}}_{o,t} \\
&\quad \vdots
\end{aligned} \tag{47}$$

While $d_{o,t}$ generally takes positive values, the corresponding scalar products involving $\dot{d}_{o,t}$ and $\ddot{d}_{o,t}$ also allow for negative values. The VoI negatively depends on these quantities:

$$\Omega_o \mid \frac{\partial \Omega_o(d_{o,t})}{\partial d_{o,t}} \leq 0 \wedge \frac{\partial \Omega_o(\dot{d}_{o,t})}{\partial \dot{d}_{o,t}} \leq 0 \wedge \frac{\partial \Omega_o(\ddot{d}_{o,t})}{\partial \ddot{d}_{o,t}} \leq 0 \wedge \dots \tag{48}$$

The differential heading and other state variables may also play a role in the VoI computation. However, in contrast to the VoI dependency of the absolute object's state, its interpretation is not as simple and its effect generally not as strong.

- **Environment:** Further, apart from the mere physical state, the object's trajectory within the scenario has an impact on the VoI. Should the object be outside a certain relevance area defined by the scenario the knowledge about its state may not be relevant for certain or even all connected stations. An example would be a vehicle driving on another road without collision possibilities.
- **Object type:** If classifiable, the object type may also have an effect on the object's VoI. In common agreement VRUs (such as pedestrians and cyclist) have stricter safety requirements than other road users (such as cars and trucks). An exception are special vehicles (such as ambulances, police cars, and fire trucks) whose behavior may differ from the road traffic regulations, requiring for higher update rates to counteract the elevated trajectory prediction uncertainty.
- **Last transmission and reception:** The times t_{tx} and t_{rx} since the last transmission and reception, respectively, of the detected object's state within a CPM may have a positive impact on its VoI, as longer times imply lower update rates about this object within the VANET:

$$\Omega_o \mid \frac{\partial \Omega_o(\Delta t_{tx})}{\partial \Delta t_{tx}} \geq 0 \wedge \frac{\partial \Omega_o(\Delta t_{rx})}{\partial \Delta t_{rx}} \geq 0 \quad (49)$$

- **Number of independent V2X sources:** The reliability of a measurement is strongly dependent on the number of independent measurement sources. In the V2X context, independent sources η correspond to different connected ITS-Ss reporting about the same tracked object. Thus, if an object is being reported by only a small number of sources its transmission by an additional station yields a higher increase in the VANETs VoI than when a large number of sources are reporting:

$$\Omega_o \mid \frac{\partial \Omega_o(\eta)}{\partial \eta} \leq 0 \quad (50)$$

3.4.2. Maneuver Coordination

The maneuver planner of an MCM-enabled CV (cf. Subsection 2.1.4) supplies the Maneuver Coordination Service with different possible trajectories to be driven by the vehicle with their associated costs (see Subsection 2.2.2.6). The VoI Ω_t of each trajectory t can depend, among others, on the following parameters:

- **The execution cost C_t :** The maneuver planner provides estimated costs C_t associated to every trajectory passed to the Maneuver Coordination Service (see Subsection 2.2.2.6). The lower the costs, the higher the benefit and thus the VoI of the trajectory:

$$\Omega_t \mid \frac{\partial \Omega_t(C_t)}{\partial C_t} \leq 0 \quad (51)$$

In other words, the trajectory's VoI function is chosen such that *ceteris paribus* (i.e., all other parameters being equal) its value decreases (does not increase) with increasing trajectory costs.

- **The trajectory type:** In case different types of trajectories are supported, the VoI of each trajectory may depend on its type. For the Maneuver Coordination Service approach introduced in Subsection 2.2.2.6 reference trajectories always must be transmitted; hence they are attributed the highest VoI $\Omega_t(ref) = 1$. For request

and alternative trajectories, the VoI function should be chosen in a way that yields the intended equilibrium between the numbers of both depending on the equilibrium constant ε_{eq} :

$$\Omega_t \mid \Omega_t(ref) = 1 > \begin{cases} \Omega_t(alt) \geq \Omega_t(req) & \frac{n_{req}}{n_{alt}} \geq \varepsilon_{eq} \\ \Omega_t(req) > \Omega_t(alt) & \frac{n_{req}}{n_{alt}} < \varepsilon_{eq} \end{cases} \quad (52)$$

Thus, the trajectory's VoI function is further chosen such that *ceteris paribus* reference trajectories have a higher priority than request and alternative trajectories. Alternative trajectories have a higher priority than request trajectories if their relative number lies below a certain equilibrium constant and vice-versa.

- **The level of detail:** The higher the level of detail at which the trajectory is described, the higher the amount of data needed for its description and hence the caused channel load. An increasing level of detail thus generally leads to a decreasing VoI density. While the amount of data needed for the trajectory's description is accounted for by Step C1 of VALINDRA, the level of detail D_t of trajectory t has a positive effect on its VoI:

$$\Omega_t \mid \frac{\partial \Omega_t(D_t)}{\partial D_t} \geq 0 \quad (53)$$

Thus, the trajectory's VoI will further increase or remain constant with increasing level of detail of the described trajectory if all remaining parameters are kept constant.

- **The time Δt since the last transmission:** The longer the neighboring connected stations have not been informed about a relevant trajectory, the higher its VoI should be:

$$\Omega_t \mid \frac{\partial \Omega_t(\Delta t)}{\partial \Delta t} \geq 0 \quad (54)$$

The trajectory's VoI will increase *ceteris paribus* with increasing time since its last transmission.

- **The trajectory's relative dynamics to other ITS-S's trajectories:** If the trajectory does not collide with those of other vehicles (as it should be the case for the reference trajectory), its transmission relevancy depends on the connected stations' states relative to the trajectory. Trajectories that pass at a lower distance $d_{min}(t)$ to other traffic participants are attributed higher VoIs and thus transmission priorities. $d_{min}(t)$ is, e.g., defined as the minimal distance between the future positions of objects in the vehicle environmental model and the positions of the considered trajectory for each time instant within the relevant future. Further, the higher-order derivatives of this minimal distance (relative speed \dot{d}_{min} , relative acceleration \ddot{d}_{min} , etc. defined in analogy to $d_{min}(t)$), which define the collision risk of the transmitting vehicle with other objects, can also be considered:

$$\Omega_t \mid \frac{\partial \Omega_t(d_{min}(t))}{\partial d_{min}} \leq 0 \wedge \frac{\partial \Omega_t(\dot{d}_{min}(t))}{\partial \dot{d}_{min}} \leq 0 \wedge \frac{\partial \Omega_t(\ddot{d}_{min}(t))}{\partial \ddot{d}_{min}} \leq 0 \wedge \dots \quad (55)$$

In other words, the trajectory's VoI will increase *ceteris paribus* the lower the (expected) lowest future distance between the ego-vehicle on that trajectory and of any other traffic participant. Further the trajectory's priority is chosen such that it decreases (does not increase) with higher maximal relative speed and momenta of higher order, all other trajectory attributes being equal.

- **The TTC with trajectories of other ITS-S:** If the trajectory collides with at least one trajectory of another vehicle (as it would most commonly be the case for request trajectories) the time available for harmonizing the maneuvers has an important impact on the relevancy of the trajectory. The lower the minimum time-to-collision (TTC) of the trajectory with all other colliding trajectories, the higher the trajectory's VoI:

$$\Omega_t \mid \frac{\partial \Omega_t(TTC)}{\partial TTC} \leq 0 \quad (56)$$

- **Number and type of colliding trajectories of other ITS-S:** Not only is the type of the evaluated trajectory itself of relevance. Its VoI may also depend on the number and type of the colliding trajectories. Should the evaluated trajectory, e.g., be colliding with $\times_{ref}=1$ reference-, $\times_{req}=2$ request-, and $\times_{alt}=1$ alternative trajectories (\times representing the number of colliding trajectories), then the latter has a

higher transmission priority than it would when colliding only with $x_{alt} = 1$ alternative trajectory. Generally, collisions with reference trajectories have a higher (or at least the same) impact on the VoI than collisions with request or alternative trajectories. Further, the higher the number of collisions with a type of trajectory, the higher the trajectory's VoI:

$$\Omega_t \mid \frac{\partial \Omega_t(x_{ref})}{\partial x_{ref}} \geq \left\{ \begin{array}{c} \frac{\partial \Omega_t(x_{req})}{\partial x_{req}} \\ \frac{\partial \Omega_t(x_{alt})}{\partial x_{alt}} \end{array} \right\} \geq 0 \quad (57)$$

- **The maneuver class described by the trajectory:** The maneuvers itself may be assigned to different classes with different maneuver priorities p_m . The trajectory's VoI increases with increasing maneuver priority class.

$$\Omega_t \mid \frac{\partial \Omega_t(p_m)}{\partial p_m} \geq 0 \quad (58)$$

The priorities p_m may further be scenario dependent. For example, a lane change maneuver may have a higher transmission priority than a takeover maneuver on a highway. However, on a narrow country road the takeover maneuver is much more relevant than lane changes.

- **The distinctiveness with more relevant candidate trajectories:** Transmitting a trajectory describing nearly the same future states, as already done by other trajectories with higher VoI densities generally makes less sense in terms of cooperation possibilities than transmitting a very distinct one. Thus, the difference to all other trajectories should be calculated, always reducing the priority of the trajectory ranked lower considering the combination of all other metrics. The VoI should correlate with the minimal difference Δ_{min} to any trajectory ranked higher based on the other criteria.

$$\Omega_t \mid \frac{\partial \Omega_t(\Delta_{min})}{\partial \Delta_{min}} \geq 0 \quad (59)$$

The minimal difference Δ_{min} could be obtained, e.g., by the RMS of the state-vectors interpolated for certain times in the future.

3.4.3. Collaborative Localization

The ITS-S's GNSS measurement engine periodically provides the Collaborative Localization Service with raw GNSS measurements. VALINDRA then computes the respective VoIs needed for the generation of the CLM. The VoI Ω_s of each satellite measurement s can depend, among others, on the following parameters:

- **The signal quality:** A GNSS receiver measures both the pseudorange measurements and the corresponding Code-to-Noise Ratio (CNR) or the equivalent Signal-to-Noise Ratio (SNR). The CNR (or SNR) is a measure for the signal quality. The higher the signal quality, the higher the probability to obtain a good positioning result (e.g., the signal quality is usually very poor in urban canyon and area with shaded skies or other forms of blockage).

Satellite measurements with a larger CNR (or SNR) are thus attributed a higher or equal VoI:

$$\Omega_s \mid \frac{\partial \Omega_s(\text{CNR})}{\partial \text{CNR}} \geq 0 \quad (60)$$

- **The measurement errors:** In the same way, a lower RMS σ_ρ of a measured pseudorange ρ is an estimator of the measurement's quality. The measurement's VoI function is further determined such that measurements with lower RMS have *centeris paribus* a higher or equal VoI:

$$\Omega_s \mid \frac{\partial \Omega_s(\sigma_\rho)}{\partial \sigma_\rho} \leq 0 \quad (61)$$

Pseudorange error and CNR are correlated and can be related with a variety of models such as the stochastic SIGMA-D model [9] or the following empirically determined CNR-dependent model:

$$\sigma_\rho = 293 \times 0.1 \times \sqrt{0.5} \times 10^{-(\text{CNR} - 2 \times |\text{CNR} - 53.99|)/20} \quad (62)$$

where the CNR is the above introduced measure for the signal quality. It is an observable and typically outputted by the station's GNSS receiver.

- **The geometric contribution:** The Dilution of Precision (DOP), also referred to as Geometric DOP (GDOP) is used to specify the error propagation as a mathematical

effect of the navigation satellite's geometry on positional measurement precision. The DOP can be determined from the system's covariance matrix H as [A1]:

$$\text{DOP} = \sqrt{h_x^2 + h_y^2 + h_z^2 + h_t^2} \quad (63)$$

where the covariance matrix H can be obtained from the geometry matrix G:

$$G = \begin{pmatrix} \frac{x_1 - x^1}{\rho_1^1} & \frac{y_1 - y^1}{\rho_1^1} & \frac{z_1 - z^1}{\rho_1^1} & 1 \\ \frac{x_1 - x^2}{\rho_1^2} & \frac{y_1 - y^2}{\rho_1^2} & \frac{z_1 - z^2}{\rho_1^2} & 1 \\ \vdots & \vdots & \vdots & \vdots \\ \frac{x_1 - x^n}{\rho_1^n} & \frac{y_1 - y^n}{\rho_1^n} & \frac{z_1 - z^n}{\rho_1^n} & 1 \end{pmatrix} \quad (64)$$

by computing the system's least-squares normal matrix:

$$H = (G^T G)^{-1} = \begin{pmatrix} h_x^2 & h_{xy} & h_{xz} & h_{xt} \\ h_{xy} & h_y^2 & h_{yz} & h_{yt} \\ h_{xz} & h_{yz} & h_z^2 & h_{zt} \\ h_{xt} & h_{yt} & h_{zt} & h_t^2 \end{pmatrix} \quad (65)$$

Collaborative Positioning has its analogue in the Collaborative DOP (CDOP). A smaller DOP or CDOP generally implies a higher positioning precision. It is thus possible to estimate the transmission priority of a satellite measurement by its effect on DOP and CDOP for different combinations of satellite measurements. Their VoIs must obey:

$$\Omega_s \mid \frac{\partial \Omega_s(\text{DOP})}{\partial \text{DOP}} \leq 0 \quad (66)$$

However, the computation complexity increases exponentially with the number of transmission-candidate satellite measurements. Thus, simplifications of the coupled problem may be used to determine the VoI and the associated transmission

priority. An example to reduce the complexity of the VoI determination could be as follows:

- 1) Determine the combination of four satellites (minimum required for a GNSS fix) with the lowest DOP and set their contribution $\Delta\text{DOP} = \text{DOP}_4$ (DOP achieved by these four satellites).
- 2) Compute the contribution of an additional measurement S_i to the DOP (analogously for CDOP):

$$\Delta\text{DOP} = -\text{trace}\left(\frac{H^i S_i^T S_i H^i}{1 + S_i H^i S_i^T}\right) \quad (67)$$

- 3) Find the measurement S_i with the largest ΔDOP or ΔCDOP , hence having the greatest contribution to DOP (or CDOP).
- 4) Repeat from Step 2) until ΔDOP has been computed for all satellite measurements.

This simplification allows to lower the computation complexity from $\mathcal{O}(n_{sat}^2)$ to $\mathcal{O}(n_{sat})$. The VoI must then obey:

$$\Omega_S \mid \frac{\partial \Omega_S(\Delta\text{DOP})}{\partial \Delta\text{DOP}} \geq 0 \quad (68)$$

- **The signal path:** In the optimal case, the satellite measurement is perceived in Single-Path Line-Of-Sight (SPLOS). Nevertheless, reflections are a common issue in satellite navigation [A1]. In some cases, the LOS path is still perceived, but one or more reflection paths are present in the measurement. This scenario is usually referred to as Multi-Path (MP) propagation. The measurements may still be used; however, the quality may suffer from MP. Nevertheless, most critical is the scenario where only reflecting rays reach the receiver. This scenario is referred to as Non-Line-Of-Sight (NLOS) and the measurements are generally much harder, if at all, to interpret. A fourth, for obvious reasons in the scope of the Collaborative Localization Service not relevant scenario, is shadowing, where a satellite is completely screened, remaining unperceived by the receiver. A more detailed descrip-

tion of the four signal propagation modes is given in Subsection 4.2.2 and the corresponding Fig. 26a. Different methods to determine the propagation paths of a measurement have been proposed [A11]. The measurement's VoI function must be chosen such that ceteris paribus it yields the highest value for SPLOS measurement, followed by MP and finally NLOS measurements:

$$\Omega_S \mid \Omega_S(SPLOS) \geq \Omega_S(MP) \geq \Omega_S(NLOS) \quad (69)$$

- **The elevation angle:** The effect of a satellite's elevation angle α on its transmission priority is much more complex. On one hand the CNR (or SNR) is positively correlated to the satellite's elevation angle, making it thus an indirect measure of the measurement quality. On the other hand, lower elevation angles generally increase DOP, CDOP, and WDOP (for the latter see Subsection 3.4.4) and thus lead to a better positioning precision. Hence, the effect of the elevation angle on the positioning precision is at least two-fold and the transmission priority of the corresponding satellite measurement may depend on it in several ways, depending on the scenario, the other measurements, etc. Finally, satellites perceived at low elevation angles have a higher probability to be occluded by shading objects and thus be lost from line-of-sight. As the positioning is considerably worsened by this effect, low elevation angles again imply a lower transmission priority according to this latter effect.
- **Multi-constellation:** Multi-constellation operation makes use of measurements from, e.g., GPS, GLONASS, Beidou, Galileo, and others. The theoretically achievable positioning accuracy increases the more data is available. However, different constellations have different time systems. Their synchronization may cause unwanted noise. This is just one of the examples how the consideration of multi-constellation satellite measurements may affect the positioning. Accordingly, the transmission priority may depend on the satellite system it belongs to.
- **Multi-frequency:** Depending on the carrier frequency, multipath reception produces different observables, such as pseudorange, SNR [262], and correlator output [263], which is why multi-frequency transmission is interesting for minimization of positioning errors in urban canyons (see [264] for a review). Many positioning methods are based on the different linear combination types of data from different bands, which, among others, allows to eliminate ionosphere errors through their ionosphere free linear combination [A11].

- **Receiver and antenna characteristics:** Measurements of an ITS-S with superior receiver and/or antenna characteristics should also be prioritized (or at least not have a lower priority).
- **Carrier phase measurements:** The carrier phase measurements may be used to achieve a much higher localization accuracy with modern positioning techniques. Its inclusion into the CLM may be considered if allowed by the communication channel.
- **SBAS system:** Multiple Satellite Based Augmentation Systems (SBAS) have been deployed such as the Wide Area Augmentation System (WAAS) in North America and the European Geostationary Navigation Overlay Service (EGNOS) in Europe. These systems provide corrections for satellite position errors, satellite clock errors and troposphere and ionosphere errors. Therefore, measurements of ITS-Ss may have a higher priority when access to SBAS data is enabled.
- **ITS-S network topology:** The network topology, determined by the traffic constellation, has been found to have a significant impact on the positioning performance provided by Collaborative Positioning [A16]. ITS-Ss further apart will generally increase the positioning accuracy more effectively than those in the direct proximity [A8]. Thus, the VoI may also depend on the specific traffic constellation.
- Many **other parameters** and parameter sets could be used to determine the transmission priority of a measurement. An overview of the most relevant observation data (p. 54ff) and navigation data (p. 68ff) is given, e.g., in [265].

3.4.4. VoI Functions in the Literature

After having introduced the main dependencies of the message-segment-specific VoI functions, we now proceed to discuss selected VoI-related functions present in the literature. These VoI functions are generally described only implicitly and typically combine several of the dependencies introduced in the previous subsections. Further, the mechanisms making use of them present different levels of awareness: (i) congestion or load awareness, referring to mechanisms sensitive to the load on the communication channel (cf. Subsection 2.4.1), and (ii) content or data awareness, referring to mechanisms that consider the data shared within the network (cf. Subsection 2.4.2). They may further be classified into

analytical, heuristic, and AI-based functions (cf. [255]). In the following, some of these VoI functions are presented and clustered according to the service they belong to:

- **Collective Perception – ETSI TR generation rules:** The ETSI TR for Collective Perception [146] prioritizes the detected objects according to the generation rules described in Subsection 2.2.2.3. The generation rules assess the relevancy of an object based on many of the parameters introduced in Subsection 3.4.1. In view of the number of rules and for the sake of readability a mathematical description is dispensed in favor of a written one. A first filter sets the objects VoI to zero if the *existence confidence* is below a not yet specified threshold. The second filter sets the VoI to zero if the traffic *environment* makes a collision unlikely, e.g., if the object is not on the transmitting station’s driving lane or any of the adjacent lanes. The next filter is given by the redundancy mitigation techniques. As they are optional, they are discussed separately. The *object type* determines the additionally applied filters. These may set the VoI to zero if the *object’s absolute state* has not changed more than a defined threshold since the object’s last transmission, or if the *time since the last transmission* is not larger than another threshold. Finally, all objects that have not yet been assigned a VoI equal to zero are sorted in dependence of their *absolute dynamic state* and the *existence confidence* and the objects with the highest ranking are assigned a positive VoI that guarantees their inclusion into the CPM until the MTU is reached. All further candidate objects are again assigned a VoI of zero. Apart from the mentioned complexity of this binary VoI determination, it lacks congestion-awareness and global content-awareness. To mitigate this lack, some level of the latter is introduced by the redundancy mitigation techniques described below.
- **Collective Perception – ETSI TR redundancy mitigation techniques:** The redundancy mitigation techniques introduced in [146] and investigated, e.g., in [256, 251, 250] add an additional network-data-aware filter to determine whether the information value of a detected object is sufficient to claim communication resources. The introduction of network-data awareness allows to estimate the knowledge-gain from the VANETs perspective. However, the proposed techniques lack network-load awareness. Four mechanisms are mentioned in the TR: (i) frequency-based redundancy mitigation techniques, setting the VoI to zero if the average *time between receptions* of CPMs containing the object falls below a not further specified threshold, (ii) dynamics-based redundancy mitigation techniques, setting the VoI

to zero if the change of the object's *absolute dynamic state* during the *time since its last reception* lies below a certain threshold, (iii) confidence-based redundancy mitigation techniques, setting the VoI to zero if the expected *precision contribution* to the network is lower than another threshold, and (iv) entropy-based redundancy mitigation techniques, setting the VoI to zero if all neighboring stations are predicted to have received the object (compare information-entropy-based VoI estimation below). Despite the paucity of research investigating redundancy mitigation techniques, which is certainly attributed to their novelty, they are a promising extension of the CAM-based CPM generation rules proposed in ETSI's TR as they allow stations to bi-directionally interact with the network. This is a standard prerequisite for the performance optimization of a distributed system.

- **Collective Perception – Information entropy:** The informative value of a transmitted object can further be determined by the relative entropy between the object's state as known to the VANET and the measured one. As fusion algorithms, such as the Kalman filter, typically assume normal distributions of the data, the relative entropy can be computed from the respective distributions:

$$N_{LEM}(\vec{r}_{LEM}, \Sigma_{LEM}) = (2\pi)^{-\frac{k}{2}} |\Sigma_{LEM}|^{-\frac{1}{2}} e^{-\frac{1}{2}(\vec{r} - \vec{r}_{LEM})^T \Sigma_{LEM}^{-1} (\vec{r} - \vec{r}_{LEM})} \quad (70)$$

$$N_{VANET}(\vec{r}_{VANET}, \Sigma_{VANET}) = (2\pi)^{-\frac{k}{2}} |\Sigma_{VANET}|^{-\frac{1}{2}} e^{-\frac{1}{2}(\vec{r} - \vec{r}_{VANET})^T \Sigma_{VANET}^{-1} (\vec{r} - \vec{r}_{VANET})} \quad (71)$$

where Σ_{VANET} is computed according to Eq. 44 and $\vec{r}_{LEM}, \vec{r}_{VANET} \in \mathbb{R}^k$. The relative entropy can now be obtained from the Kullback-Leibler divergence:

$$D_{KL}(N_{LEM} \parallel N_{VANET}) = \int_{\mathbb{R}^k} N_{LEM} \log \frac{N_{LEM}}{N_{VANET}} d\vec{r} \geq 0 \quad (72)$$

Combining Eq. 70-72 and performing some algebraic calculations yields the computationally less expensive representation:

$$D_{KL} = \frac{1}{2} \left\{ \text{tr}(\Sigma_{VANET}^{-1} \Sigma_{LEM}) + (\vec{r}_{VANET} - \vec{r}_{LEM})^T \Sigma_{VANET}^{-1} (\vec{r}_{VANET} - \vec{r}_{LEM}) - k + \ln \frac{|\Sigma_{VANET}|}{|\Sigma_{LEM}|} \right\} \geq 0 \quad (73)$$

The relative entropy is measured in Napierian digits. A division by $\ln 2$ thus yields the divergence in bits. Therefore, $D_{KL}/\ln 2$ can be interpreted as the expected number of additional bits that have to be transmitted by the station to complete the network's knowledge about N_{meas} given N_{VANET} . According to Gibbs' inequality the relative entropy is always non-negative $D_{KL} \geq 0$, with the equality holding only if $N_{LEM} = N_{VANET}$ almost anywhere. If instead unfused data is to be transmitted, the relative entropy can be obtained by substituting N_{LEM} by N_{meas} and computing $D_{KL}(N_{meas} \parallel N_{VANET})$.

The relative information entropy is a network-data-aware VoI, as it not only considers local knowledge such as the object's *absolute dynamic state* and *measurement precision*, but also global knowledge such as the estimated *precision contribution to the network* based on received V2X data.

An interesting approach using the relative information entropy to estimate the VoI of measured objects is provided in [256]. The authors propose to assess the potential relative entropy gain by each connected station if the object's state estimation is received. If any station is expected to increase its knowledge by more than a certain threshold, the measurement is included into the next CPM. This entropy-based VoI assignment was found to considerably reduce the 90th-percentile tracking error from over 10 *m* to around 6 *m* in a heavily congested V2V network with a careful optimization of the relative-entropy threshold. It is worth noting that the authors conclude their work by pointing out the importance of considering additional factors, such as the *objects' type* and *appearance*. It is further to be expected that the dynamic adaption of the VoI threshold based on the state of the communication channel, such as proposed in the scope of this thesis, will allow to generalize the VoI maximization to other scenarios. However, it should be mentioned that for adoption of the relative-entropy-based VoI estimation a normalization is needed (cf., e.g., Subsection 4.2.4).

- **Collective Perception – Time to collision and perceived risk:** Another measure for an object's relevance is its time to collision (TTC) with objects in its environment. The TTC can be computed based on the *relative dynamic states* of the objects. The VoI of an object decreases with increasing TTC. In [A14] a metric to assess the risk of a situation for a traffic participant based on the instantaneous approaching time t_i is proposed. The latter is closely related to the TTC and can be obtained from:

$$d_{t_0} + \dot{d}_{t_0} t_i + \frac{(\ddot{d}_{t_0} + \ddot{d}_{max}) \cdot t_i^2}{2} = 0 \quad (74)$$

where d_{t_0} , \dot{d}_{t_0} , and \ddot{d}_{t_0} are the distance, relative velocity, and acceleration of the detected object at the time t_0 , respectively. The parameter \ddot{d}_{max} is an estimator of the maximum expectable change in the object's relative dynamics, depending on its current velocity and the maximum acceleration, deceleration, and steering angle of the object. The collision risk emanating from the detected object can be determined in analogy to the perceived environmental risk awareness \widetilde{ERA}_p proposed in [A14]. It evaluates the extent to which a station is able to assess the risk associated to its current environment. The risk perceived by the detecting station can be computed from the instantaneous approaching time computed in Eq. 74, additionally accounting for the corresponding uncertainties for each dimension of the state vector¹²:

$$\widetilde{ERA}_p = \sum_{i; t_i > 0} \frac{\mu_i}{t_i + \tilde{u}(t_i)} \quad (75)$$

where the collision factor μ_i represents the severity of a potential collision between the *road user type* of the detected object and every other object i with which a collision is possible in the given *environment*. Contrary to the evaluation in [A14], the true relative dynamic states of the objects are not available and have to be approximated from the measurements of the detecting station. Further, $\tilde{u}(t)$ corresponds to the uncertainty of the approaching time and can be obtained from:

$$\tilde{u}(t_i) = \sqrt{\vec{\nabla} t_i^T \cdot \Delta \Sigma_i \cdot \vec{\nabla} t_i} \quad (76)$$

with $\Delta \Sigma_i$ being the difference between the covariance matrices (determined by the *measurement precisions*) of the states of the detected object and any other object i . The choice of the reference frame implies that Eq. 76 must not only consider the uncertainties of the object's position, velocity, and acceleration among others, but also those of the ego vehicle's state.

¹² Tildes are used in Eq. 75 and 76 to differentiate the parameters estimated during the message generation process from those used for offline performance evaluation in Eq. 113-116.

Finally, the VoI can be computed as the expected contribution to the networks environmental risk awareness. Thus, the \widetilde{ERA}_p -based VoI presents a high-degree of network-data awareness.

- **Maneuver Coordination – Cooperative Awareness based:** Correa et al [160] investigate the generation of MCMs when the *time since the last transmission* or the *displacement* of the transmitting station exceeds a certain threshold. The VoI of the whole MCM is thus binary and lacks network-data awareness. Similar CAM-like rules are applied in [266, 267]. The VoI function is neither load- nor data-aware.
- **Maneuver Coordination – Perceived Awareness over Time Horizon:** A more sophisticated function to quantify the relevancy of a transmission-candidate trajectory was introduced in [A15]. The Perceived Awareness over Time Horizon (PATH) denotes the risk of collision with other vehicles within the given time horizon and is based on the perceived environmental risk awareness ERA_p introduced above (see Eq. 75). The risk of a traffic situation perceived by a station depends on the *relative dynamics* of the surrounding stations, the *tracking accuracies*, and the *object types*. PATH computes the ERA_p for all pairs of future positions between the transmitting station's trajectory and those of other connected stations. PATH is then defined as the highest expected value that ERA_p takes the trajectory. The higher the PATH of their trajectory, the more communication resources are claimed by each connected station, making use of a facility layer rate control mechanism. Overall, the PATH-based VoI estimation is both network-load and network-data aware.
- **Collaborative Localization – Weighted dilution of precision:** The Weighted Dilution of Precision (WDOP) is used to describe an ITS-S's positioning precision. It considers both the *pseudorange error* and the *satellite geometry* and may be computed as:

$$WDOP = \text{trace}(H) \quad (77)$$

with

$$H = (G^T W G)^{-1} \quad (78)$$

where G represents the geometry matrix and can be calculated following Eq. 64. W on the other side corresponds to the matrix:

$$W = \begin{bmatrix} \sigma_{\rho 1}^{-2} & \cdots & 0 \\ \vdots & \ddots & \vdots \\ 0 & \cdots & \sigma_{\rho n}^{-2} \end{bmatrix} \quad (79)$$

The RMS σ_ρ of the pseudorange ρ can be obtained, e.g., following Eq. 62.

As a higher WDOP implies a poorer positioning accuracy of the cooperating stations, satellite measurements diminishing the WDOP the most will have the highest transmission priority. The effect of a measurement S_i on the WDOP may be computed as:

$$\Delta\text{WDOP} = \text{trace} \left(\frac{H^i S_i^T \sigma_i^{-2} S_i H^i}{1 + S_i H^i S_i^T} \right) \quad (80)$$

In the same way it is possible to determine the value of each combination of satellites to be transmitted. In [A17] the satellite measurements are sorted according to their contribution ΔWDOP to determine their transmission in dependence of the channel load. The proposed approach is both load- and content-aware. In the future a computation of the contributed relative information entropy could replace the computation of ΔWDOP aligning the VoI function with that proposed for the CPM in Eq. 70-73.

- **Collaborative Localization – Propagation mode based:** Ollander et al. [A11] introduce a reception mode R_n (*signal path* dependent) and a priority score B_n for the characterization and prioritization of the GNSS measurements. Both are derived from the *measured pseudoranges* and *SNRs* of each satellite. A variation of these parameters is used in [A17] to determine the VoI and the associated inclusion priority of each satellite measurement into the next CLM. The presented propagation mode based VALINDRA-like protocol is both load- and content-aware. An extension is presented in Section 4.2.
- **Cross-Service:** Khan et al. [64] propose a multi-service resource allocation orchestrator located at the facility layer of the V2X protocol stack. The authors argue that DCC_FAC (introduced in Subsection 2.3.1) is a promising option to increase the reduced QoS configuration spectrum of the access layer. However, they point out

the severe restrictions dealing from the absolute prioritization among TCs [268]. To overcome these constraints, a packet prioritization based on three properties is proposed: (i) the rank, based on a static value, e.g., matching the 4 EDCA ACs (see Subsection 2.2.4.1); (ii) the usefulness, assessing how relevant the specific data of the message is for potential receivers in the current traffic situation; and (iii) the urgency, reflecting the remaining time until the deadline set by the V2X service generating the message is reached. Finally, these parameters are fused into the so-called multi factor priority, which is a weighted sum of the parameters. Simulations with periodically generated DEMNs, CAMs, and CPMs, mapped to different ranks in descending priority order, proved a smoother resource usage over time. The approach is both content- and congestion-aware and thus a promising option for future resource allocation. However, the computation of the usefulness is not further specified and further research in this direction is needed to offer real content-awareness.

3.5. Analytical Evaluation

Before the performance of VALINDRA is investigated for different services through simulation in Chapter 4, this section offers an analytical evaluation of the protocol with regard to several relevant aspects. Subsection 3.5.1 discusses the fulfillment of the requirements established in Section 3.1. Subsection 3.5.2 then investigates the system's stability and the convergence properties to steady state. Subsection 3.5.3 compares the determined performance parameters of VALINDRA with those of state-of-the-art protocols. Finally, Subsection 3.5.4 reviews further relevant aspects of VALINDRA including interoperability with existing protocols and possible future enhancements.

3.5.1. Requirement Fulfillment

Together with the problem formulation a series of additional requirements were defined in Section 3.1. The extent to which VALINDRA copes with them is discussed below:

- **VoI-maximization:** The aim of VALINDRA is to maximize the VoI of the disseminated data under given channel constraints. The problem was formulated as a complex dynamic variation of the knapsack problem with two implementation alternatives: (i) a multi-service operation, and (ii) a service-specific operation. The design of the protocol allows for a fast system convergence towards steady state (see Subsection 3.5.2), determining VoI-thresholds that fulfill the equations of the

combinatorial resource allocation problem (Eq. 16-20), and ensuring that the channel capacity is utilized most effectively with regard to the disseminated information.

- **Distributed optimization:** The distributed coordination of the system is reached by the utilization of a LIMERIC-based VoI-threshold determination per connected station. The dependence of the threshold and hence of the disseminated data on the channel state and the data provided by the network makes VALINDRA both congestion- and content-aware.
- **Incomplete knowledge:** Instead of neglecting message segments whose size is unknown as is done in several cases, VALINDRA uses expectancy values to increase its stability and performance. While in low-density networks, where such approximations may lead to larger deviations, channel effects are negligible, in high-density networks the law of large numbers leads to the convergence of the system towards these expectancy values, justifying their use.
- **Message segment classes:** VALINDRA differentiates between mandatory and optional message segments. This differentiation is a relevant requirement for the VoI-maximizing resource allocation since it allows to realistically assess the channel load caused by each transmitted message.
- **System dynamics:** To deal with the system's dynamics the underlying knapsack problem had to be modified. VALINDRA's parametrization (see Subsection 3.5.2) allows to carefully adjust the system's memory loss and convergence speed to the network requirements.
- **Service starvation:** Special care was taken to avoid service starvation. In particular, a distribution of the message overheads was necessary to make sure services could always claim resources if the VoI of the candidate message segments required it. This requirement is in concordance with a common agreement by ETSI TC ITS WG1 during the work on DCC_FAC [208]. However, while [208] always assigns a minimum of resources to each service regardless of the actual information relevance, VALINDRA leaves it to the station and its services to decide whether resources are required, allowing to distribute the resources more efficiently.

3.5.2. System Stability

An essential requirement for dynamic systems is the convergence to equilibrium in steady state conditions. In the following, the stability of VALINDRA is analyzed on the example of the cross-service optimization, as the service-specific optimization may be considered as a special case of the former. The system is defined by the following equation resulting from merging Eq. 24 and 25:

$$\omega_j^{thr}(t) = (1 - \alpha) \cdot \omega_j^{thr}(t - 1) - \beta \cdot (CBR_{tar} - CBR) \quad (81)$$

The channel busy ratio can be expressed as ¹³:

$$CBR = \sum_i \sum_j \sum_{k|T} \sum_l \frac{E(T_{ijkl}^{on})}{T} \approx \frac{\overline{T_{req}^{on}} \cdot I + \sum_j (1 - \omega_j^{thr}(t - 1)) \cdot \overline{T_{opt}^{on}}}{T} \quad (82)$$

The time-discrete system equation can be rewritten by inserting Eq. 81 into Eq. 82 and using the dimensionless parameter $\hat{\beta}$:

$$\vec{\omega}_{thr}(t) = \mathbf{A}_{|x|} \cdot \vec{\omega}_{thr}(t - 1) - \beta \cdot \vec{b} \quad (83)$$

with

$$\hat{\beta} = \beta \cdot \frac{\overline{T_{opt}^{on}}}{T} \quad (84)$$

the transition matrix

$$\mathbf{A}_{|x|} = \begin{bmatrix} 1 - \alpha - \hat{\beta} & -\hat{\beta} & \dots & -\hat{\beta} \\ -\hat{\beta} & 1 - \alpha - \hat{\beta} & \dots & -\hat{\beta} \\ \vdots & \vdots & \ddots & -\hat{\beta} \\ -\hat{\beta} & -\hat{\beta} & -\hat{\beta} & 1 - \alpha - \hat{\beta} \end{bmatrix} \quad (85)$$

and the offset

¹³ With the assumption of equally distributed Vol probabilities among stations and segments and making use of a simplification by disregarding the omission of elements when summing over rows of Pascal's triangle.

$$\vec{b} = \left(CBR_{tar} - \frac{\overline{T}_{req} + \overline{T}_{opt}}{T} \cdot I \right) \cdot \mathbb{1}_{I \times 1} \quad (86)$$

where $\mathbb{1}_{I \times 1}$ corresponds to the all-ones matrix. The eigenvectors v_n and the corresponding eigenvalues λ_n can be computed from the system equation (Eq. 83). Applying the Leibniz formula yields a homogeneous, i.e., fair solution:

$$v_1 = \begin{pmatrix} 1 \\ 1 \\ \vdots \\ 1 \end{pmatrix} \quad \lambda_1 = 1 - \alpha - I \cdot \hat{\beta} \quad (87)$$

and I-1 degenerate solutions:

$$v_{2,3,\dots,I} = \left\{ \begin{pmatrix} 1 \\ -1 \\ 0 \\ 0 \\ \vdots \end{pmatrix}, \begin{pmatrix} 0 \\ 1 \\ -1 \\ 0 \\ \vdots \end{pmatrix}, \dots \right\} \quad \lambda_{2,3,\dots,I} = 1 - \alpha \quad (88)$$

A discrete time system is called stable if the absolute value of all its eigenvalues does not exceed 1. For the degenerate eigenvalues, the fulfillment of the condition is trivial. Also, the condition $\lambda_1 \leq 1$ is fulfilled by the definition of the system with $\alpha, \hat{\beta} \geq 0$. On the other hand, for the last condition $\lambda_1 \geq -1$:

$$\lambda_1 = 1 - \alpha - I \cdot \hat{\beta} \geq -1 \quad (89)$$

$$\Rightarrow \hat{\beta} \leq \frac{2 - \alpha}{I} \quad (90)$$

Thus, to ensure the stability of the system the value of β must always fulfill:

$$\beta = \hat{\beta} \cdot \frac{T}{\overline{T}_{opt}} \leq \frac{2 - \alpha}{I} \cdot \frac{T}{\overline{T}_{opt}} \quad (91)$$

Having determined the asymptotic stability of the discrete-time system, the equilibrium state can be found using $\vec{\omega}_{eq}(t) = \vec{\omega}_{eq}(t-1) = \vec{\omega}_{eq}$:

$$\vec{\omega}_{eq}(t) = \mathbf{A}_{k \times k} \cdot \vec{\omega}_{eq}(t-1) - \beta \cdot \vec{b} = \lambda_1 \cdot \vec{\omega}_{eq}(t) - \beta \cdot \vec{b} \quad (92)$$

Solving for $\vec{\omega}_{eq}$ and inserting Eq. 86 and Eq. 87 then yields the single convergence point:

$$\vec{\omega}_{eq} = -\beta \cdot \frac{\vec{b}}{1 - \lambda_1} = \beta \cdot \frac{(CBR_{max} - CBR_{tar})}{\alpha + I \cdot \hat{\beta}} \cdot \mathbb{1}_{I \times 1} \quad (93)$$

with the highest possible channel load arising from the transmission of all optional message segments:

$$CBR_{max} = \frac{\overline{T_{req}^{on}} + \overline{T_{opt}^{on}}}{T} \cdot I \quad (94)$$

All ω_i^{eq} converge towards the same value ω_{eq} , as could be expected from the LIMERIC-based $\bar{\omega}_{thr}(t)$ determination. Nevertheless, it should be noted that while LIMERIC controls the transmission rates of connected stations, VALINDRA dynamically adapts the VoI-threshold to the state of the communication channel. As opposed to the symmetrical resource allocation for all connected stations regardless of the relevance of their data, VALINDRA allows to introduce a disparity accounting for the heterogeneous distribution of the relevant data within the network. Having determined the equilibrium VoI-threshold, it is now possible to proceed computing the corresponding equilibrium channel load:

$$\begin{aligned} CBR_{eq} &= \frac{\overline{T_{req}^{on}} \cdot I + \sum_j (1 - \omega_{j,eq}) \cdot \overline{T_{opt}^{on}}}{T} = \frac{\overline{T_{req}^{on}} + (1 - \omega_{eq}) \cdot \overline{T_{opt}^{on}}}{T} \cdot I \\ &= CBR_{max} - \frac{\overline{T_{opt}^{on}} I \omega_{eq}}{T} = \frac{CBR_{tar} + \frac{\alpha}{I \cdot \hat{\beta}} CBR_{max}}{1 + \frac{\alpha}{I \cdot \hat{\beta}}} \end{aligned} \quad (95)$$

Analyzing Eq. 95 it becomes evident that for $\frac{\alpha}{I \cdot \hat{\beta}} \rightarrow 0$ the equilibrium state tends to the defined target channel utilization $CBR_{eq} \sim CBR_{tar}$. On the other side, it can easily be shown that $CBR_{eq} < CBR_{tar}$ is always fulfilled, never endangering the targeted QoS of the wireless communication channel (see Fig. 21a).

Similar to LIMERIC, the convergence speed to fairness of the system is defined by the degenerate eigenvalues (Eq. 87 and 89). In the presence of perturbations, e.g., caused by two stations m and n starting from a condition of unfairness with different VoI thresholds (e.g., due to entering each other's communication range), the convergence speed can be determined in analogy to [269] using Eq. 83:

$$\begin{aligned} \omega_m^{thr}(t) - \omega_n^{thr}(t) &= (1 - \alpha) \cdot [\omega_m^{thr}(t-1) - \omega_n^{thr}(t-1)] \\ &= (1 - \alpha)^t \cdot [\omega_m^{thr}(0) - \omega_n^{thr}(0)] \end{aligned} \quad (96)$$

with the perturbation happening at $t = 0$. The convergence speed towards a stable solution is $(1 - \alpha)^t$, thus depending only on α . Hence, the higher α , the faster the convergence.

On the other side, the convergence speed of the whole system is governed by the non-degenerate eigenvalue in a similar way:

$$\omega_{thr}(t) - \omega_{eq} = (1 - \alpha - I\hat{\beta})^t \cdot [\omega_{thr}(0) - \omega_{eq}] \quad (97)$$

The three determined characteristic relations of the defined dynamic system can be summarized as:

- **Stability condition:** $\alpha + I\hat{\beta} \leq 2$ (98)

- **Deviation from target CBR:** $\min_{\alpha, \hat{\beta}}(CBR_{eq} - CBR_{tar}) \Rightarrow \alpha/I\hat{\beta} \rightarrow 0$ (99)

- **Convergence speed:** $\max_{\alpha, \hat{\beta}}(1 - (1 - \alpha - I\hat{\beta})^t) \Rightarrow \alpha, \hat{\beta} \rightarrow 1$ (100)

Fig. 19 shows the stability regions of VALINDRA in the $\alpha - I\hat{\beta}$ parameter space, resulting from Eq. 98. It further shows CBR_{eq} in terms of CBR_{tar} in dependence of the parameter choice in the stable (blue) region. The tracking accuracy of CBR_{tar} hence depends proportionally on $I\hat{\beta}$ and inversely proportional on α as determined by Eq. 99, yielding the highest values in the upper left corner of the stable region.

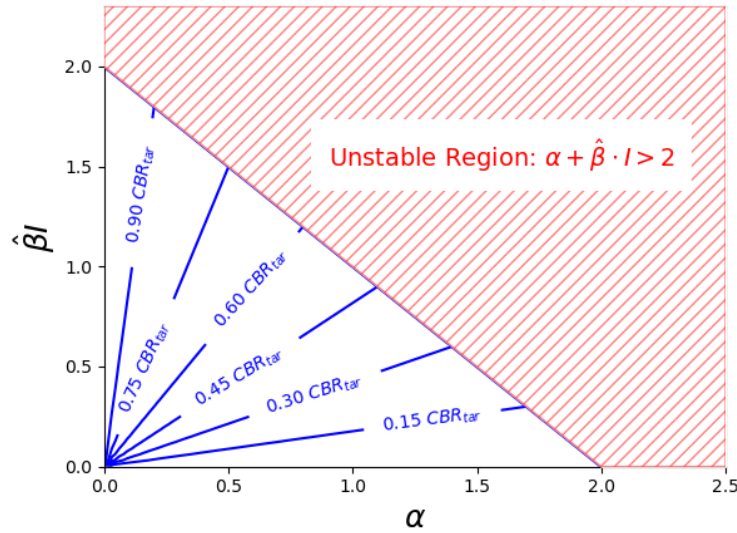


Fig. 19: Dynamic state space of VALINDRA in the $\alpha - I\hat{\beta}$ domain, showing the unstable region (red) and the equilibrium CBR as a fraction of the target CBR in the stable region (blue).

The dependence of CBR_{eq} on I with constant $\hat{\beta}(= 0.0012)$ is shown in Fig. 20a for different α cross-sections. As can be seen at low densities of connected stations fewer channel resources are consumed than intended. This tracking error falls asymptotically with an increasing number of connected stations. The positive effect of smaller α -values on the error is also clearly visible.

The opposite behavior can be observed with the convergence speed (see Fig. 20b). At time $t = 0$, the system is exposed to a significant disturbance with $\omega_m^{thr}(0) = 3\omega_n^{thr}(0)$. As already proved with Eq. 100, the system converges towards the equilibrium ω_{eq} if the stability condition of Eq. 98 is fulfilled. It is easy to see that higher α -values lead to faster convergence of the system towards fairness. The upper x-axis in Fig. 20b shows the convergence time under the assumption that each connected station experiences 20 generation events per second (e.g., two of the services presented in Subsection 2.2.2, each with 10 Hz)¹⁴.

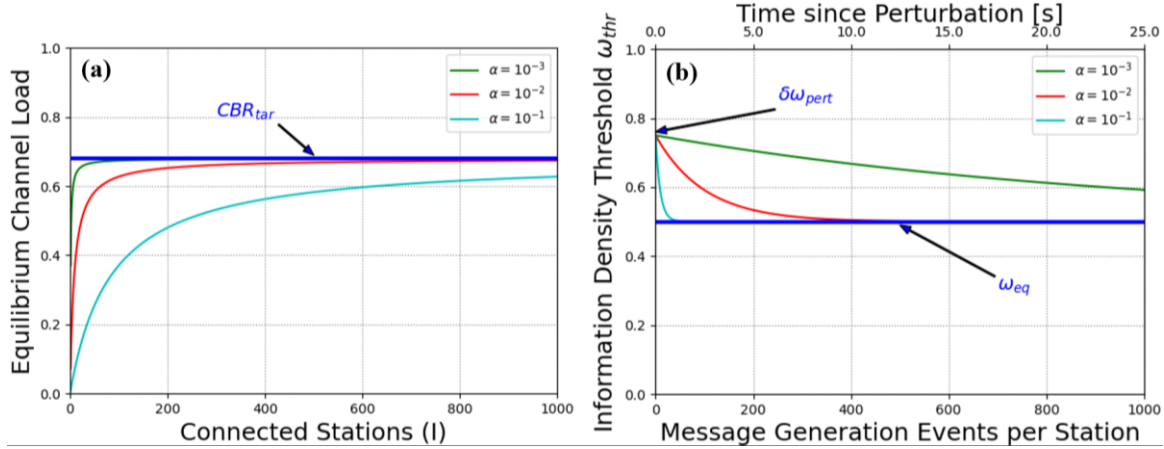


Fig. 20: System behavior of VALINDRA regarding (a) equilibrium channel load and (b) convergence to equilibrium after the occurrence of a system perturbation.

A suitable measure for the convergence speed towards fairness is the half-time $\tau_{1/2}$. It is defined by the required time to half the deviation of the system from the equilibrium state and can be calculated based on the following relationship:

$$(1 - \alpha)^{\tau_{1/2} f_{gen}} = \frac{1}{2} \quad (101)$$

¹⁴ It should be mentioned that for stations featuring a service-specific implementation of VALINDRA each service must independently converge to its corresponding equilibrium state.

where f_{gen} corresponds to the overall message generation frequency of the station. A rearranging of the equation above yields:

$$\tau_{1/2} = \frac{\ln\left(\frac{1}{2}\right)}{\ln(1 - \alpha) f_{gen}} \quad (102)$$

Table 2 summarizes the half-time $\tau_{1/2}$ of the system for the stability parameters investigated in Fig. 20a and Fig. 20b.

Table 2: Performance of VALINDRA for different parameter choices of α .

<i>Stability Parameter</i>	$\alpha = 0.1$	$\alpha = 0.01$	$\alpha = 0.001$
Half-time [iterations]	6.6	69.0	692.8
Half-time $\tau_{1/2}$ [s]	0.2	1.7	17.3

In view of the trade-off between convergence speed and CBR_{eq} tracking accuracy regarding the parameter choice, a compromise is required. Thus, the defining system parameters memory loss α and adjusted convergence leverage $\hat{\beta}$ were respectively set to:

$$\alpha = 0.01 \quad \text{and} \quad \hat{\beta} = 0.001 \quad (103)$$

With this parameter choice, using Eq. 98 it can be shown that the system's stability is ensured for up to a number of connected stations equal to:

$$I_{max} = \frac{2 - \alpha}{\hat{\beta}} = 1990 \quad (104)$$

representing an extremely high station density. Further, in scenarios where the channel utilization starts to become relevant $\frac{\alpha}{I \cdot \hat{\beta}} < 10\%$. Thus, CBR_{eq} approaches CBR_{tar} according to Eq. 99. Finally, the overall system convergence half-time amounts to 5.9 iterations for $I = 100$ and 0.15 iterations for $I = 1000$, respectively.

3.5.3. Comparison to other Protocols

In this subsection VALINDRA is analytically compared to the state-of-the-art LIMERIC and A-DCC protocols in terms of the investigated system properties. Fig. 21a shows the dependence of the generation frequency and the resulting CBR_{eq} on the number of connected stations for the three protocols on the example of CPM-like messages.

As can be seen the message frequency of stations employing LIMERIC or A-DCC gradually decreases. While LIMERIC is located at the FAC layer and thus reduces the message generation frequency, A-DCC acts as a gatekeeper between NT and MAC layer, discarding the previously generated messages (see Table 3). VALINDRA on the other side does not intervene the message generation frequency but only reduces the VoI-threshold to maintain the channel load.

It can further be seen that after an initial ramp up, the equilibrium channel load of all three protocols tends towards the target channel load. This ramp up is caused by the low number of connected stations, which limits the fraction of consumed resources. It is somewhat steeper for VALINDRA as compared to LIMERIC and A-DCC, since VALINDRA allows to increase the amount of transmitted data per message if sufficient resources are available. A better tracking of CBR_{tar} is the result. With higher numbers of connected stations CBR_{eq} is reached asymptotically and the system is governed by Eq. 99. In this region VALINDRA presents a slightly better tracking performance than A-DCC and LIMERIC. The corresponding values for a moderate and a high network density are presented in Table 3.

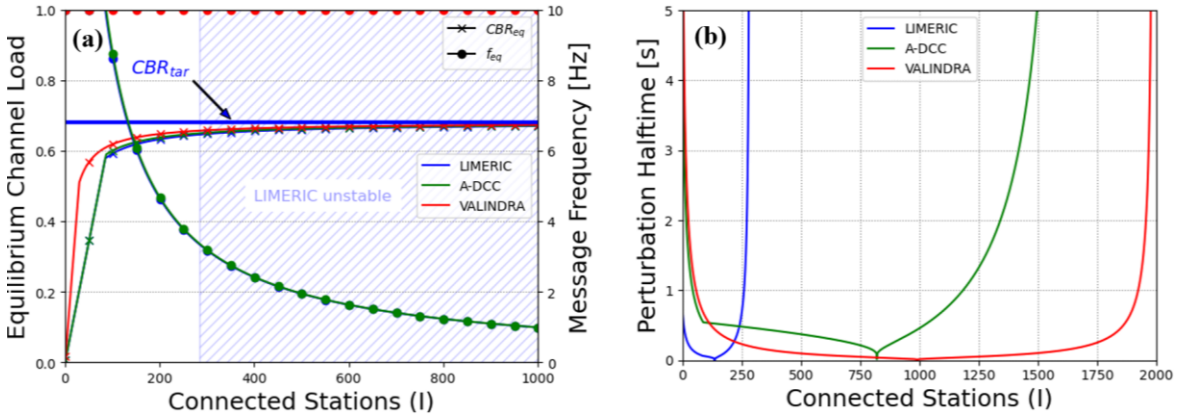


Fig. 21: Network-size-dependent protocol performances in terms of (a) equilibrium CBR and average message frequency, and (b) convergence speed.

Furthermore, while VALINDRA and A-DCC converge towards equilibrium in stable state in this region, LIMERIC becomes unstable for $I > 285$. This effect can be investigated with more detail in Fig. 21b. It shows the convergence half-time of the system on the example of the previously mentioned CPM-like messages. As can be observed, for low numbers of connected stations ($I < 200$) LIMERIC presents the fastest convergence. However, above $I_{max}^{Limeric} = 285$ LIMERIC becomes unstable, which is expressed by the asymptotically increasing convergence half-time. For higher network densities ($I > 200$)

VALINDRA significantly outperforms both LIMERIC and A-DCC, presenting convergence half-times of less than 100 ms over most of the depicted range. Thus, the deviation of the channel load from CBR_{eq} will roughly be halved every generation event of the CPM-like message. A-DCC on the other hand presents a much-extended stability range as compared to LIMERIC, however somewhat lower than that of VALINDRA. It can only slightly outperform VALINDRA in a very narrow range. This can be traced back to the reduction of the message frequency by A-DCC, which leads to fewer iterations as compared to the constant frequency used by VALINDRA (compare Fig. 21b). As shown in Table 3 the difference in the number of iterations needed for a halving of the deviation from CBR_{eq} is still significant (0.45 and 0.15 iterations for A-DCC and VALINDRA, respectively with $I = 1000$ connected stations), however less pronounced than the difference in convergence half-time.

Table 3: Performance comparison between VALINDRA and the two state-of-the-art V2X protocols LIMERIC and A-DCC.

<i>Protocol</i>	<i>LIMERIC</i>	<i>A-DCC</i>	<i>VALINDRA</i>
<i>Stability bound I_{max}</i>	285	1653	1990
<i>CBR_{eq}/CBR_{tar} ($I=100$)</i>	0.87	0.88	0.91
<i>CBR_{eq}/CBR_{tar} ($I=1000$)</i>	unstable	0.99	0.99
<i>Event half-time ($I = 100$)</i>	0.48	5.74	5.95
<i>Event half-time ($I = 1000$)</i>	unstable	0.45	0.15
<i>Data loss ($I = 100$)</i>	0%	12%	0%
<i>Data loss ($I = 1000$)</i>	unstable	90%	0%

Finally, it is worth noting that the exemplary comparison based on a network featuring only one V2X service may be misleading without mentioning the effect of a multi-service operation, especially in view of the high likelihood that such systems will be employed in the future. An increased number of services competing for a common resource pool leads to a further reduction of the message frequency for LIMERIC and A-DCC, and a reduced message size in VALINDRA. For low network densities, the effects of the throttled message generation in the former protocols and the increased number of iterations cancel each other out. However, at higher network densities the potential reaching of the lower limit of the message generation frequency further reduces the performance of LIMERIC and A-DCC, preventing compliance with the defined CBR_{tar} and shrinking the protocols' application windows even further. Previous work thus proposed to deactivate DCC for ad hoc communication [A13].

3.5.4. Further Aspects

In the previous subsections it was shown that VALINDRA solves the combinatorial optimization problem stated in Section 3.1 and fulfils the additionally identified requirements of the highly dynamic V2X environment. Apart from that, several other general observations are possible:

- **Simplicity and optimizability:** VALINDRA makes use of a single function to compute the VoI of each data-segment. On one side, this offers a high flexibility when combining the multiple system parameters constituting the VoI. On the other, it reduces the complexity of the system, offering the possibility to determine the impact of each parameter. Altogether, this allows for a more straightforward optimization of the VoI function, e.g., with the help of deep neural networks.
- **Multi-service orchestration:** VALINDRA intrinsically solves the so far largely disregarded problem of the multi-service orchestration [270], offering two operation modes: (i) assigning fix resource contingents to each service, and (ii) enabling a cross-service resource allocation based on the dynamic state of environment and network. VALINDRA may further help to overcome the integration challenges of DCC_FAC with heterogeneous V2X services identified, e.g., in [234].
- **Functional safety:** a basic safety requirement is the network knowledge related to the completeness of the disseminated information [271]. VALINDRA-based vehicular networks can estimate the amount of information discarded due to channel limitations making use of the homogeneity of the VoI density thresholds (see Subsection 3.5.2 on the convergence of the system to fairness). Further, instead of using TRC (see Subsection 2.3.3.3), VALINDRA regulates the amount of data transmitted. This allows to maintain a high QoS for safety critical information, while only lowering the rate of less relevant data.
- **Integration into ITS protocol stack:** VALINDRA was designed to fit the ITS protocol stack (cf. Fig. 6 and Fig. 17). It can be regarded as an access layer independent alternative to DCC_FAC, offering not a recommendation on the optimal message generation frequency, but additionally on the data-segments included in each generation event. However, VALINDRA requires the extension of existing interfaces. Promising discussions in this direction are carried out in the scope of the standardization activities led by the specialist task force 585 established for the

development of MCO functionalities. In case VALINDRA's advice should become mandatory for the V2X services, the access layer congestion control techniques could be switched off without risking channel congestion beyond the specified limits (cf. Subsection 3.5.2). This would help mitigating the negative performance effects of these techniques observed by numerous research studies [272, 273, 216, 248, 274]. It should further be mentioned that the channel usage limitations specified in [206] could be significantly relaxed if VALINDRA is mandated, as it ensures an optimal usage of the available resources.

- **Transmit Power Control (TPC):** VALINDRA can easily be combined with TPC, e.g., using metrics such as the introduced PATH (cf. Subsection 3.4.4 or [A15]) to assess the relevance of the information in a certain region and using either the VoI to set the transmit power or defining a similar distance-based metric to tune the TPC. An optimization of the system over the provided QoS within the area of relevance can be carried out in analogy to [A9, A18]. An interesting approach for integrating TPC with TRC is given in [212].
- **Transmit Datarate Control (TDC):** The use of TDC with VALINDRA is straight forward. The MCS (see Subsection 2.2.4) may be adjusted depending on the VoI carried by a message. Less relevant messages may be transmitted with a higher MCS, reducing their airtime T_{on} . The positive effect on the load of the communication channel comes at the cost of a compromised transmission reliability. On the other side, for information of higher relevancy, a correspondingly robust MCS may be used. The dynamic adaption of the MCS to deal with data where a low transmission reliability presents a safety-critical fault mode is a convenient mechanism in terms of functional safety (compare ISO-26262-5 [275] and IEC 61508-2 [276]).
- **Multi-Channel Operation (MCO):** VALINDRA is readily usable for a multi-channel operation, using the determined VoIs as decision basis for the channel selection. The required QoS of an already assembled message can be determined based on the VoIs of its segments. A monitoring of the QoS of different channels thus allows to transmit each message according to its individual needs (see, e.g., [A13]). Further, different target CBRs may be specified for the available channels to guarantee specific QoS-levels, as is currently the case for control channel and service channels.

4. PERFORMANCE EVALUATION

After having introduced VALINDRA in Chapter 3 and analytically investigating the behavior of the dynamic system in terms of stability, convergence speed, target channel load tracking accuracy and others, Chapter 4 evaluates the performance of the system in simulation. In view of the complexity of the V2X environment and the associated large number of system parameters the evaluation focusses on two examples: Collective Perception and Collaborative Localization. These V2X services present very distinct characteristics in terms of their interaction with the communication channel.

Chapter 4 first introduces the simulation environment TEPLITS in Section 4.1. TEPLITS is then used to investigate the performance of VALINDRA applied to Collaborative Localization (Section 4.2) and Collective Perception (Section 4.3).

4.1. Simulation Environment

To ensure traffic safety, newly introduced systems and technologies must meet high industry-wide quality standards as defined, e.g., by ISO 26262 for Functional Safety (FuSa) or ISO 21448 for Safety Of The Intended Functionality (SOTIF). However, especially when large numbers of vehicles are required (as is the case when channel congestion effects are to be accounted for), their integration into and testing with real test vehicles is costly and time consuming. For this reason, while the final validation still has to be carried out with real test vehicles, the earlier stages may be investigated with analytical models to gain an impression of the relevant factors before a more extensive investigation is carried out by means of virtual test drives. These test drives allow to quickly adjust the parameters and running the tests at high rates maintaining the expenses comparably low. Systems may be tested a priori in complex scenarios, with hundreds of vehicles for all kinds of constellations. However, the realistic replication of the relevant aspects of the simulated vehicles in their environment is critical.

Subsection 4.1.1 discussed the requirements for a suitable development and testing platform for ITS systems and scrutinizes existing simulators with regard to their fulfillment. Subsequently, a new platform and its main components are introduced in Subsection 4.1.2. Finally, Subsection 4.1.3 presents the system architecture of the developed simulation framework.

4.1.1. Requirements and State-of-the-Art

To investigate the performance of new ITS technologies, such as Collective Perception or Collaborative Localization, a virtual test platform should be capable of realistically modeling the following three components [A5]:

- **Vehicle dynamics and sensors:** traffic safety sensitively depends on a realistic reproduction of the vehicle dynamics. In the same way, the inclusion of detected objects into a CPM is triggered by the object's dynamics, highlighting the importance of their accurate modelling. High fidelity dedicated vehicle dynamics simulators are CarMaker [277] and Virtual Test Drive (VTD [278]) developed by IPG Automotive and VIRES of the MSC Software Group, respectively. Besides these proprietary simulators open-source solutions such as CARLA [279] have been introduced by the research community. Dedicated vehicle dynamics simulators generally further allow a detailed modelling of the vehicles' on-board sensors, such as cameras, radars, odometers, and GNSS receivers.
- **Traffic and environment:** besides the precise motion modelling of the traffic participants an accurate traffic simulation is required to obtain a representative set of testing scenarios. Widely used dedicated traffic simulators are SUMo [280], developed by the German Aerospace Center (ger. *Deutsches Zentrum für Luft- und Raumfahrt*; DLR) and Vissim [281] developed by PTV. Both SUMo and Vissim are microscopic traffic simulators supporting the individual adjustment of vehicle trajectories and properties. They include basic vehicle dynamics models, however much less comprehensive than the vehicle dynamics simulators introduced above.
- **Inter-vehicle communication:** the investigation of connected systems and technologies, such as the V2X-based Collective Perception, require a network simulation that allows modelling communication parameters such as communication latency and reliability. Well-known dedicated network simulators such as Network Simulator 2 and 3 (ns-2 [282] / ns-3 [283]) and the Objective Modular Network Tested in C++ (OMNeT++ [284]) are often used to simulate the communication network. An advantage of the above-mentioned publicly available discrete event-based simulators is the possibility to add self-coded extension modules to introduce new communication protocols, such as those belonging to the ITS protocol stack (see Sections 2.2 and 2.3).

Multiple approaches exist to couple dedicated simulators belonging to these three groups, such as the Vehicle in Network Simulation (VEINS [285]) framework combining SUMO

and OMNeT++, its Platooning Extension (PLEXE [286]), the Traffic and Network Simulation Environment (TraNS [287]) project launched to couple SUMO with ns-2, the iTetris framework [288], combining SUMO and ns-3, the more generic V2X Simulation Runtime Infrastructure (VSimRTI [289]) multi-directional framework, and a simulator joining Vis-sim with ns-3 and a MatLab-based traffic management applications [290] [291]. However, the integration potential is generally limited, and time synchronization of the various modules remains a major challenge [A5]. For these reasons, besides dedicated and coupled simulators, a third group of simulators have been proposed, aimed at intrinsically solving synchronization issues: Highly integrated simulation frameworks. Examples are GrooveNet [292] and the Motor Vehicle Emission Simulator (MoVES) [293]. However, the high integration comes at the cost of a lower level of detail as compared to dedicated simulators in their respective domains [282, 289]. A more comprehensive review of the different simulation frameworks was carried out in the scope of this doctoral work [A5] based on pre-studies of the publicly funded project IMAGinE [294], concluding that none of the alternatives satisfies the requirements of the three categories thoroughly. For this reason, the Test Platform for Intelligent Transportation Systems (TEPLITS) was developed. It is introduced below.

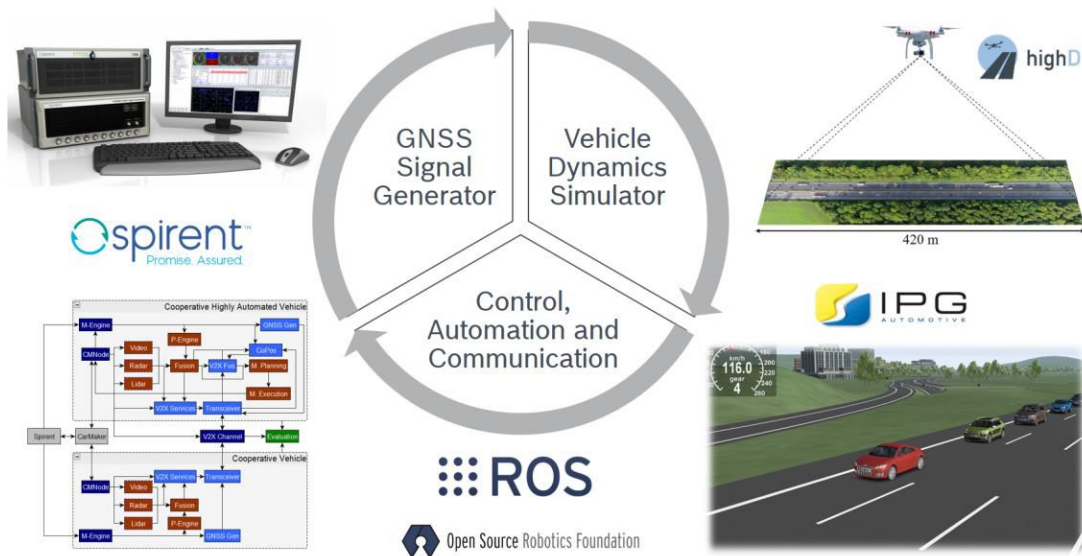


Fig. 22: Components and functionalities of the ITS development and testing platform TEPLITS [A14].

4.1.2. Introducing TEPLITS

Due to the lack of a suitable development and testing environment determined in the previous subsection a new platform was designed to meet the identified requirements. Its core is built by the open-source robotics middleware Robot Operating System (ROS) that orchestrates the interplay of all integrated components schematically depicted in Fig. 22. Besides covering the minimal test platform requirements, TEPLITS includes multiple additional features and functionalities. These not only include environmental perception systems such as object-tracking sensors and a highly accurate GNSS signal generator, but also, among others, vehicle controllers such as platoon-controllers and a cooperative highway merging assistant that was fully developed and tested with the help of TEPLITS [A5]. The main components are presented in the following.

4.1.2.1. Traffic and Vehicle Dynamics

The accurate modeling of the traffic both on a microscopic and a macroscopic level is essential for analyzing intelligent transportation systems. TEPLITS offers five distinct options for the generation of traffic trajectories: (i) the online evaluation with real test vehicles [295], (ii) inputting prerecorded object tracks, e.g., from the open-source highD [296] and KoPER datasets [297], (iii) real-track-based data extended, e.g., by Bayesian networks [A2], (iv) vehicle tracks generated by the vehicle dynamics simulator CarMaker developed by IPG-Automotive, and (v) artificially generated tracks, such as the spider web scenario [146]. Each of the options has its advantages and disadvantages compared to the others. For this reason, a different option, or a combination of these may be chosen depending on the respective investigation needs. For instance, if a more theoretical analysis is targeted, an artificial scenario with precise speeds and routes may be chosen. For a realistic, large-scale scenario investigation, recorded vehicle tracks are preferable. In case rarely occurring, critical situations are of interest, the tracks may be generated using, e.g., Bayesian networks to artificially augment these situations. For tests where the bidirectional interaction with traffic participants is required, they may be controlled by CarMaker, which was extended by a ROS interface in the scope of the public funded project IMAGinE [294]. Further, a combination of real or Bayesian-network-generated vehicle tracks with CarMaker is also possible. Should the systems be ready for testing in real test vehicles, a fast transfer of the modules is made possible due to the common interface of CarMaker and the vehicles.

4.1.2.2. *Vehicle Sensors and Communication*

Traffic participants in TEPLITS can be equipped with several sensors. These can be divided into three classes:

- **Positioning sensors:** The main technologies to estimate the ego-position of a traffic participant are satellite navigation, odometry, IMUs, and SLAM. While IMUs and odometry are implemented in a simple way in TEPLITS, GNSS is modeled in detail due to its high importance for V2X systems for being the state-of-the-art absolute positioning sensor. For this purpose, the GNSS signal generator SPIRENT GSS7000 developed by Spirent Communications is used. It allows to control a wide range of parameters, such as tropospheric and ionospheric errors, satellite clock and ephemeris errors, obscuration and multipath, receiver antenna characteristics, and RF interference for any given point in time and space. It further allows multi-constellation and multi-frequency operation, including GPS, GLONASS, Beidou, and Galileo signals. Besides this proprietary solution, TEPLITS can be used with an open-source ray-tracing module as introduced in [298], also featuring multi-constellation and multi-frequency operation. SLAM has not yet been implemented in TEPLITS.
- **Object tracking sensors:** Object tracking sensors, such as radars, LIDARs, and cameras are implemented in CarMaker and the data is outputted over the integrated ROS interfaces. For partially automated vehicles, the human driver must also be considered as an additional or even the primary sensor, releasing driving functions, such as the merging onto a highway. For this reason, the human driver can also be modeled as a sensor in CarMaker [A5]. However, it must be noted that the data is processed separately, and not merged into the vehicle's environmental model. All these object-tracking sensors have also been implemented in ROS based on the Bosch product lines for the CarMaker-independent operation of TEPLITS.
- **V2X communication:** TEPLITS offers two different ways to model the V2X communication: (i) a full stack implementation, and (ii) the application of analytical models developed by the Universidad Miguel Hernandez in Elche, Spain. Generally, the latter is preferable if the focus does not lie on an in-depth analysis of the communication performance, as the full stack software implementation, combined with all the other simulation components, tends to considerably slow down the simulation. The analytical models for 802.11p [299] and C-V2X autonomous mode

[188] have been validated with state-of-the-art network simulators and are suitable for most applications.

4.1.2.3. Vehicle Perception and Control

The information gathered by the vehicle sensors is subsequently processed with the open-source robotics middleware platform ROS. The objects are extracted from the measurements, associated, and fused into the LEM (cf. Subsection 2.1.4). The track manager entity is responsible for updating existing tracks, creating new, and deleting outdated ones. A situation analysis assesses the current traffic situation based on the sensor data and possible further information, e.g., from map services. V2X messages are generated based on these two modules and handed over to the communication control unit for transmission. Received V2X messages are processed and utilized for the generation of the GEM and the V2X-enhanced situation analysis. Further, V2X services such as Collaborative Localization have also been implemented in TEPLITS and support the generation of a precise decision basis for the maneuver planning of the vehicle, as it is the GEM and the situation analysis. The functions implemented range from an intersection assistant to platooning and from a C-ACC to a highway on-ramping assistant, depending on the vehicle's level of automation (cf. Subsection 2.1.5). Finally, if CarMaker or a real test vehicle is connected, the maneuver can be executed according to the control commands generated in the maneuver execution module.

4.1.3. System Architecture

As the understanding of the connected vehicle's system architecture is a prerequisite for the following investigation of Collective Perception and Collaborative Localization this subsection sheds light on its implementation within TEPLITS. In particular, the vehicle control architecture of TEPLITS is aligned to that introduced in Subsection 2.1.4. As mentioned before, TEPLITS is based on ROS, and so is the vehicle control. ROS is a widely used automation framework that allows a highly modular development of modules within so-called ROS nodes. These nodes may subscribe to or request data from sensors or other ROS nodes, to process it and make it available by publishing it or directly hand it over to other nodes and actuators.

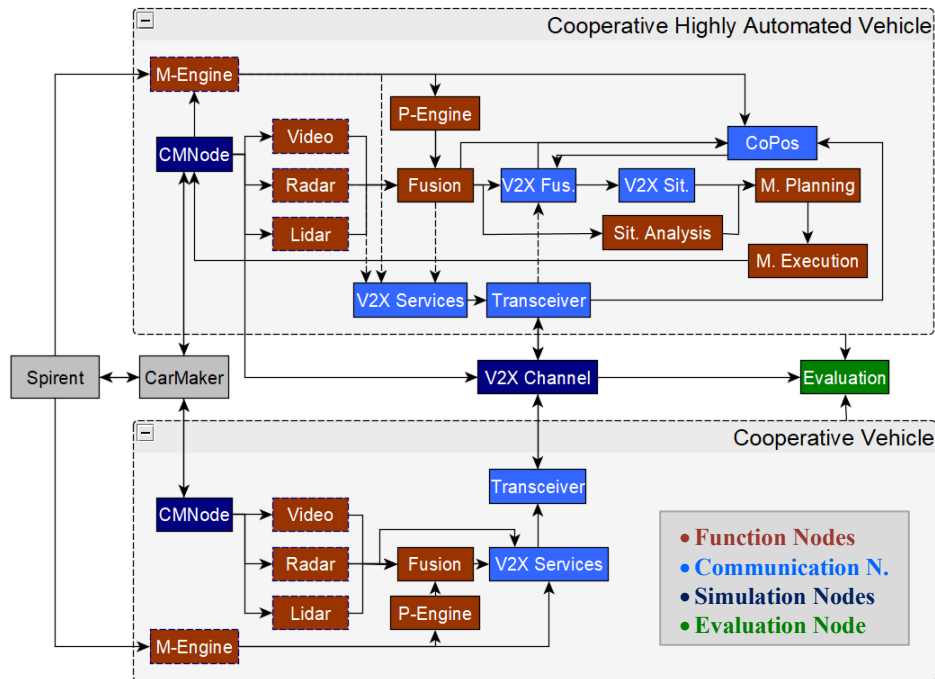


Fig. 23: Simplified overview of the vehicle system architecture in TEPLITS with the ROS-based modules depicted in colors according to functional groups and the coupled CarMaker and Spirent GNSS applications depicted in gray.

Fig. 23 shows a simplified architecture of a connected (lower box) and a connected and automated vehicle (upper box). Non-connected non-automated vehicles can be handled with a single vehicle state node in TEPLITS and are thus not depicted individually. The blocks represent ROS nodes or ROS node clusters. They are again grouped in function- (brown), V2X- (light blue), system monitoring (green), and simulation-relevant nodes (deep blue). For the sake of readability, the arrows in Fig. 23 depict only the main data-streams between the modules. Further, intersecting arrows are represented with dashed lines for differentiation purposes. A short description of the modules belonging to each of these groups is offered in the following:

Function nodes are the minimal set of nodes necessary for function implementation. These are grouped in:

- Measurement Engine: ROS interface to the GNSS measurement engine in the vehicle or the GNSS signal generator Spirent in simulation. For the latter, a synchronization of Spirent with CarMaker through a common simulated ROS time is required to enable

Spirent to provide the raw GNSS signals detectable at the positions of each traffic participant as provided by CarMaker. The measurement engine node processes the obtained or simulated GNSS signals and outputs the result in a RINEX-like format.

- **Positioning Engine:** processes the data provided by the measurement engine node and computes the Position, Velocity, and Time (PVT) solution to estimate the receiver's absolute position.
- **Sensor Nodes:** nodes processing the data coming from each of the vehicle's environment-tracking sensors (e.g., radar, LIDAR, or video). The dashed blue line surrounding them is intended to show that these nodes are dependent on the specifications of the used sensors' interfaces when used in real test vehicles and are based on sensor models in simulation.
- **Sensor Fusion:** this module subscribes to data published by the sensor nodes and fuses it to obtain the LEM containing all objects directly detected by the vehicle, including other vehicles and pedestrians, but also lane markings and traffic signs among others. Its main component is the track manager entity creating new, updating existing, and deleting outdated tracks.
- **Situation Analysis:** the situation analysis uses the information managed by the LEM to assess the situation the vehicle is facing. As an example, the situation analysis could determine that the ego vehicle just crossed an intersection, that it is approaching a slight turn to the right, that it is situated on the rightmost lane of the street, and that there are no further vehicles in its direct vicinity (see [A5] for more details on the described scenario). Additionally, it could infer the speed limit of the road segment from previously detected traffic signs or from the street type and its environment. The situation analysis may further incorporate data from local maps.
- **Maneuver Planning:** the maneuver planning module builds on the information provided by the situation analysis and the sensor fusion and (if available) their V2X-enhanced analogues described below. A possible maneuver planning could look as follows: the maneuver planner of the vehicle in the example introduced above receives the information from the situation analysis and determines that the vehicle is on an empty street with 100 km/h speed limit approaching a moderate right turn. It will thus probably choose to maintain or slightly reduce its speed. Should the V2X-enhanced situation analysis further provide the information that the vehicle is approaching a freeway with moderate traffic, then it could compute possible gaps at the approximate merging time from the V2X-extended sensor fusion and choose the most suitable one.

- **Maneuver Execution:** the maneuver execution module is responsible for the correct implementation of the planned maneuver. Following the example, it would determine the required acceleration profile to reach the target gap on the freeway, adjust its speed when reaching the acceleration lane and finally merging onto the freeway. The determined acceleration profile is then passed to the CarMaker node or the real test vehicle's CAN bus for its final execution.

V2X nodes are responsible for all V2X functionalities of the ITS stations. These nodes are grouped in:

- **V2X Services:** each V2X service has its own generation rules. These include the aggregation of the data to be transmitted and the message frequency, among others. As an example, a cooperative vehicle on the freeway (lower box in Fig. 3) may be transmitting CAMs, CPMs, and CLMs. CAMs are generated based on the transmitting vehicle's state obtained from the CarMaker node (introduced below) in the simulation or from the vehicle's CAN bus in real vehicles. The generation frequency depends on the transmitting vehicle's dynamics reaching from 1 to 10 Hz [146]. Collective Perception, Collaborative Localization, and other V2X services may further include raw data from the vehicle's on-board sensors, the GNSS measurement engine or the already aggregated data from the local environmental model provided by the sensor fusion. It should be mentioned that data from the GEM provided by the later described V2X-enhanced sensor fusion should generally not be retransmitted, to avoid back coupling within the vehicular networks.
- **Message Transceiver:** once a V2X message has been generated, it is handed over to the message transceiver. This module then implements the lower layers of the V2X protocol stack and decides over which technology the message should be transmitted. TEPLITS currently features both standard V2X-enabling communication technologies: IEEE 802.11p and C-V2X Mode 4. The module further receives messages transmitted by vehicles within the communication range and hands them over to the respective modules. Additionally, the node is responsible for all components of DCC as specified by ETSI to limit the channel load in high-density scenarios, including DCC_FAC (see Subsection 2.3.1).
- **V2X-extended Sensor Fusion:** while the sensor fusion node introduced above is responsible for the management of the LEM generated from the information locally available to the vehicle, the V2X-enhanced sensor fusion considers V2X as an additional sensor. The internally and externally gathered data is then fused altogether constituting the

GEM. It should be remarked that the latter does not represent a substitute for the LEM, since it may be corrupted by inaccurate or manipulated data. Thus, the LEM should always be available as a fallback possibility [A5].

- V2X-extended Situation Analysis: the consideration of information additionally received by means of V2X communication may improve the situation analysis. An example is the already mentioned approach of a vehicle towards a freeway and hence the upcoming merge into it, which would typically be known to the vehicle's V2X situation analysis long before the information reaches the local situation analysis, only relying on the vehicle's local perception systems.

Simulation nodes are only needed offline for simulation and evaluation purposes:

- CarMaker Node: constitutes the interface to the vehicle dynamic simulator CarMaker. It offers the simulation time for synchronization, the dynamic state of the ego-vehicle, sensor measurements and ground truth values for all traffic participants and infrastructure, among others.
- V2X Channel: transmitted V2X messages are subject to different forms of fading and shadowing effects. In virtual test drives, these effects must be simulated.

The *Evaluation ode* is used to monitor the system and evaluate the performance of newly developed modules or technologies. It may subscribe and process any relevant data streams of the system.

4.2. Collaborative Localization

Having introduced the simulation environment in the previous section, this section proceeds to investigate the application of VALINDRA to Collaborative Localization. Collaborative Localization, also known as Collaborative Positioning, is a recently introduced technology receiving rising interest from research institutes and industry [A17]. As opposed to Collective Perception, discussed in Section 4.3, which has been subject of standardization since 2015, no Collaborative Localization related work item has been set up by ETSI TC ITS WG1 to date. For this reason, Subsection 4.2.1 is aimed at introducing the first set of comprehensive specifications for Collaborative Localization. The investigated scenarios and parameter settings are subject of Subsection 4.2.2. The core of the analysis is conducted in Subsections 4.2.3, 4.2.4 and 4.2.5, investigating the performance of the service in terms of channel utilization, different VoI definitions, and the positioning performance enhancement enabled by VALINDRA, respectively. Finally, Subsection 4.2.6 concludes the investigation of Collaborative Localization.

4.2.1. Service Definition

Despite the extensive research on the underlying positioning technology, so far, no comprehensive V2X service has been defined to support it. Most studies are either of theoretical nature [A10], neglecting the effects of error-prone sensors and packet losses [300, 301], or demonstrate the technology with only few receivers at a short range [A08], again making packet losses negligible. In the scope of this doctoral work, extensive research on Collaborative Localization was carried out, however, only individual aspects of the service and the enabling technology have been made public. For this reason, this subsection summarizes the key concepts necessary for the understanding of the subsequent performance analysis of VALINDRA-based Collaborative Localization.

4.2.1.1. Positioning Algorithms

As with Cooperative Awareness and Collective Perception, Collaborative Localization belongs to the services whose main purpose is the generation and enhancement of the GEM. It allows connected stations to share their raw GNSS measurements to obtain a more robust and precise positioning. Further, a station making use of the service cannot only substantially enhance its own absolute localization, but also its knowledge about the states of connected stations, leading to a significant improvement of its GEM's accuracy. A series of positioning algorithms come into question for Collaborative Positioning. Some of the most prominent are: (i) the Extended Kalman Filter (EKF), (ii) Weighted-Least-Squares (WLS), (iii) the Gauss-Newton (GN) solver, and (iv) alternative algorithms such as the recently introduced Cognitive Particle Filter (CPF). The EKF is the algorithm that has received most attention as enabling technology for Collaborative Positioning. It is a non-linear version of the Kalman filter and makes use of a transition model, thus sensitively depending on the initial conditions. WLS and the GN solver are independent of such a-priori knowledge. However, the downside of not relying on a transition model is the stringent need for sufficient measurements to obtain a positioning solution. While the computation complexity of WLS is comparably low, the GN solver performs several linearization steps for each GNSS epoch, thus showing a much faster convergence than EKF and WLS. A comparison of the EKF with WLS is provided in [302]. [A11] offers a comparison of the performance of an EKF with the GN solver. A thorough discussion of the CPF's performance is provided in [148].

All algorithms compute the state vectors in the Earth-Centered-Earth-Fixed coordinate system, making a transformation into, e.g., the East-North-Up (ENU) coordinate system

necessary. The latter represents the positions on a local tangent plane and is thus generally preferred for ground ITS-Ss.

4.2.1.2. Message Generation

The message format briefly introduced in Subsection 2.2.2.4 consists of six data containers (cf. Fig. 8). While ITS-PDU header and management container carry generic data, GNSS information container, GNSS measurement container, local range container, and in the future the additional positioning container include the central information for the functioning of the Collaborative Localization Service. The GNSS information container carries the specifications of the station's GNSS receiver and a list of satellite PRNs whose positions are known to the transmitting station. The input data for the positioning algorithms introduced above is contained in the local range container and the GNSS measurement container. The former includes a list of connected stations taking part in Collaborative Localization. Each station is characterized by its ID, if available taken from the station's last received V2X message, and an estimated local range computed with data from the LEM. The latter carries the measurement objects and optionally the satellite ephemeris. An example of such a measurement object is provided in Fig. 24, containing all relevant information for Collaborative Localization (see [A10, A11, A12] for in depth deductions of the corresponding algorithms).

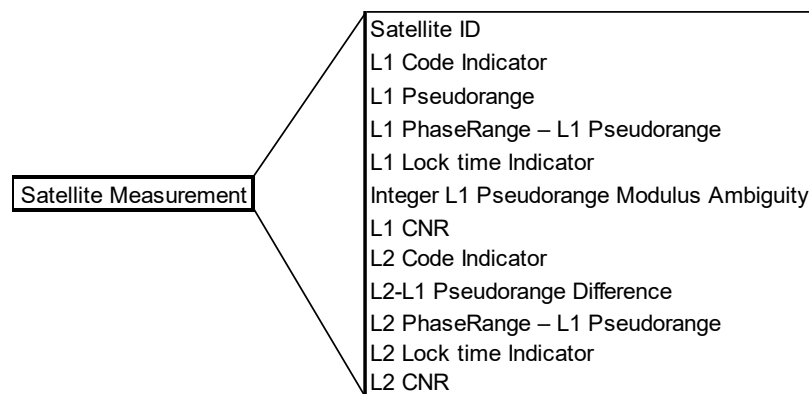


Fig. 24: Proposed content of a satellite measurement object as included in the satellite measurement container of the Collaborative Localization Message (CLM).

A peculiarity of the Collaborative Localization Service is the almost perfectly synchronous reception of GNSS measurements by all connected stations every GPS second. The synchronization error is typically well below $1 \mu s$ (comparable to a positioning error of as much as 300 m considering the speed of light $c = 3 \cdot 10^8 m/s$). Further, while the

message generation period is much lower than for state-of-the-art messages, such as CAM and CPM, the message size is comparably large, amounting to between 400 and 2000 bytes. The difficulty of these large, synchronously generated messages is the formation of sharp channel load peaks, leading to a considerable drop of the PDR. To mitigate this effect, a dynamic generation jitter is introduced at the FAC layer. It strongly depends on the number of available resources for the Collaborative Localization Service and the number of connected stations. Further parameters, such as the topology of the vehicular network may also play a role. The CLM generation jitter is investigated in more detail in Subsection 4.2.3.



Fig. 25: CarMaker view of the investigated city square in Frankfurt (Main). Trees and other obstructions are omitted in the figure to allow a clear view on the cooperating traffic participants.

4.2.2. Parameter Settings

In the scope of this doctoral work, Collaborative Localization was analyzed in open-skies scenarios such as highways [A1, A8, A10] and in urban canyons with poor satellite-receiver link qualities [A11, A12, A17]. The results showed that Collaborative Localization can significantly increase the positioning performance in all scenarios. However, the poor stand-alone positioning performance in scenarios with reduced satellite visibility brings along a higher need for improvements. For this reason, the following investigation focuses on these more challenging scenarios. To this end, an urban square in the city of Frankfurt was recreated in TEPLITS. Fig. 25 shows a close-up of CarMaker's video interface. As CarMaker is only responsible for the accurate modelling of the vehicle dynamics, leaving communication and satellite signal propagation to the other components in TEPLITS, the scenario was simplified for the sake of comprehensibility. In particular, the vegetation and parts of the infrastructure are omitted to avoid screening the vehicles.

Further, the building heights do not correspond to the ones used by the ray-tracing software (cf. Fig. 26b).

A city square is a specially interesting scenario, as it presents considerable challenges to the satellite navigation, while still allowing vehicles to communicate and share data in different topologies (in contrast to state-of-the-art urban canyons where a 2D topology is only possible at intersections). The importance of the vehicle topology for Collaborative Localization was proved in earlier work [A8].

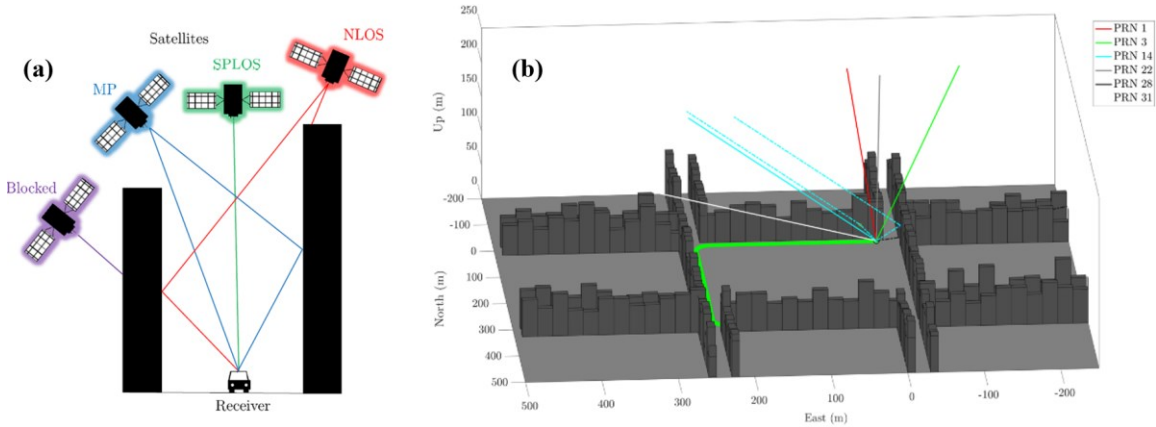


Fig. 26: Propagation modes of the GNSS signals in (a) a schematic representation and (b) the investigated Frankfurt city square [A11].

Table 4: Simulation parameters for a city square in Frankfurt.

Scenario Parameters	Values
Square dimensions [m ²]	250 x 300
Building heights [m]	~ 30
Number of vehicles	1-25
Average speed [km/h]	30
Total driving time per run [s]	1250

The buildings surrounding the city square vary in height, empirically following a Rice distribution with non-centrality parameter and spread of 35 m and 5 m, respectively [A11]. Their average width is set to 17 m. Fig. 26a shows an illustration of the signal propagation modes occurring in this scenario. Consumer grade GNSS receivers generally require a Single Path Line-of-Sight (SPLOS) for an accurate positioning. Non-Line-of-Sight (NLOS) and Multipath (MP) propagations generally lead to significant errors in the localization. Finally, satellites whose signals are fully blocked cannot be used for positioning and are

thus useless to the receiver. Fig. 26b shows the city square in the ray-tracing module from [298]. The light green line represents a vehicle trajectory around the square and the colored straight lines are propagation paths of selected satellites, showing the different propagation modes. Table 4 brings together some of the main simulation parameters regarding the scenario.

A total of 31 GPS and 24 Galileo satellites were used throughout the simulation. Apart from multi-constellation navigation, also multi-frequency reception, a technology newly introduced into the mass-market, was considered. As of 2020, only two out of the three frequency bands of GPS are available: L1 and L2. For this reason, the dual-frequency multipath detection of [263] was implemented based on $f_1 = 1.5754$ GHz (GPS L1 or Galileo E1) and $f_2 = 1.2276$ GHz (GPS L2 or Galileo E5b). Multipath detection techniques are used to categorize the GNSS signal propagation modes (shown in Fig. 26). The implemented detection technique makes use of the different physical behavior of signals belonging to both bands when propagating and reflecting, expressing itself in observables such as SNR, correlator output, Doppler-shift, and pseudorange. It further relies on the transmit power difference between both frequencies of $f_1 - f_2 = 3$ dB. For a detailed mathematical deduction of the used multi-constellation dual-frequency multipath detection technique the reader is kindly forwarded to [A11]. Finally, a GN solver was used to find the positioning solution, as it was found to be more suitable for such highly dynamical systems as VANETS (see previous subsection). The tolerance of the GN solver was set to 10^{-6} and with a maximum number of iterations $I = 100$ after which the solver stops if the quality of the measurements is not sufficient for a reliable localization and the system falls back to the last computed position.

As messages are transmitted only every GNSS second, congestion control mechanisms such as ITS-G5's DCC_ACC never come into action (cf. Subsection 2.3.3). Further relevant GNSS-, sensor-, and communication parameters are summarized in Table 5.

Table 5: GNSS-, sensor-, and communication parameters.

Sensors Parameters	Values	GNSS Parameters	Values
Number of cameras	6	Number of GPS satellites	31
Maximal system range [m]	> 150	GPS L1-band [MHz]	1575.42
		GPS L2-band [MHz]	1227.60
		Power difference L1-L2 [dB]	3
		Number of Galileo satellites	24
		Galileo E1-band [MHz]	1575.42
		Galileo E5b-band [MHz]	1227.60
		Power difference E1-E5b [dB]	3
V2X Parameters	Values		
Transmit power [dBm]	23		
Receiver sensitivity [dBm]	-90.5		
Carrier frequency [GHz]	5.9		
Channel bandwidth [MHz]	10		

4.2.3. Channel Sensitivity

The vast majority of research on Collaborative Positioning is still driven by the GNSS community, leading to an insufficient consideration of the communication channel. The present subsection aims at closing this gap by investigating the service's sensitivity to channel effects.

As stated earlier, one of the main challenges for Collaborative Localization is the simultaneous reception of GNSS signals by all connected stations, forcedly leading to sharp channel load peaks if the messages are generated immediately after the measurement. A potential solution is the introduction of a generation jitter on FAC layer. However, a careful tuning of this jitter is required to address the tradeoff between peak sharpness and age of information. The latter is not to be underestimated either, as the stations must have received all measurements before triggering the positioning algorithms. Data received after the computation started cannot be used and is thus worthless. Further, allowing for the maximum generation jitter to be equal to the generation cycle, corresponding to 1000 ms, would introduce an unbearable latency for such a dynamic system. Therefore, a good coordination among the stations is essential.

Fig. 27 shows the average positioning accuracy of a connected station in the investigated scenario in dependence of the maximum allowed generation jitter. Each station randomly selects a generation delay smaller than the respective maximum allowed generation jitter. The CLMs are generated and handed over to the lower layers for transmission by considering this individual delay. After transmission the stations wait for a time equivalent to the maximum generation jitter while receiving the CLMs disseminated by the other vehicles. The stations then carry out their positioning. As can be seen, in the given scenario the positioning accuracy reaches an optimum for a maximum generation jitter of 40 ms. Smaller generation jitters lead to higher packet losses due to more pronounced CBR peaks. Larger generation jitters on the other side lead to worse state predictions due to higher latencies. As can be seen, both effects have devastating consequences for the positioning accuracy. It should be noted that this generation jitter maximizes the performance of Collaborative Localization only for this particular scenario. In general, the jitter should be computed dynamically in dependence of parameters such as the number of connected stations, the number of available resources, the VANET's topology, and the message sizes.

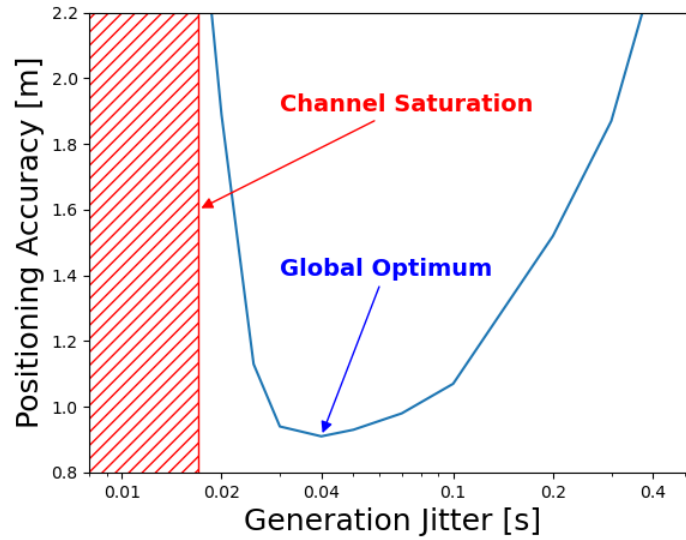


Fig. 27: Positioning accuracy as a function of the generation jitter induced at FAC layer.

Having found a suitable generation jitter to avoid excessively pronounced channel peaks, the service can now be analyzed with regard to its sensitivity to variations in the channel load. To this end, Collaborative Localization was first tested in the described Frankfurt city square scenario by applying different background channel loads. The generation jitter is kept constant for the remainder of the investigation to ease comparability of the results. Fig. 28 shows the dependence of the number of received CLMs and the average inter-packet interval on the background channel congestion as could be caused by other V2X messages on the same communication channel. The PDF and CDF of the number of connected stations from which CLMs are received every timestamp are depicted in Fig. 28a. As can be seen, on an almost idle channel (CBR = 0, grey bars), the communication quality is high enough to have an average of almost 22.6 collaboration partners per GNSS epoch, corresponding to a packet loss of less than 6%. With rising channel load, the number of dropped packets increases to 11% (CBR = 0.3, green bars), 23% (CBR = 0.6, blue bars) and reaching up to 40% under saturated channel conditions (CBR = 0.9, yellow bars). This translates into an average of 21.3, 18.5 and 14.4, received CLMs per transmission cycle, respectively. The update periods per station are shown in Fig. 28b. As can be seen, the communication with most stations is quite stable, receiving messages every GPS second. Only in some rare cases up to 4 consecutive CLMs are lost in the low channel load scenario. With rising channel congestion, the connection to some stations is lost for up to 18 seconds, showing that the channel load affects the connected stations with different intensities. This

extremely high instability of the communication is the reason for preferring the GN solver over the standard EKF for the computation of the navigation solution.

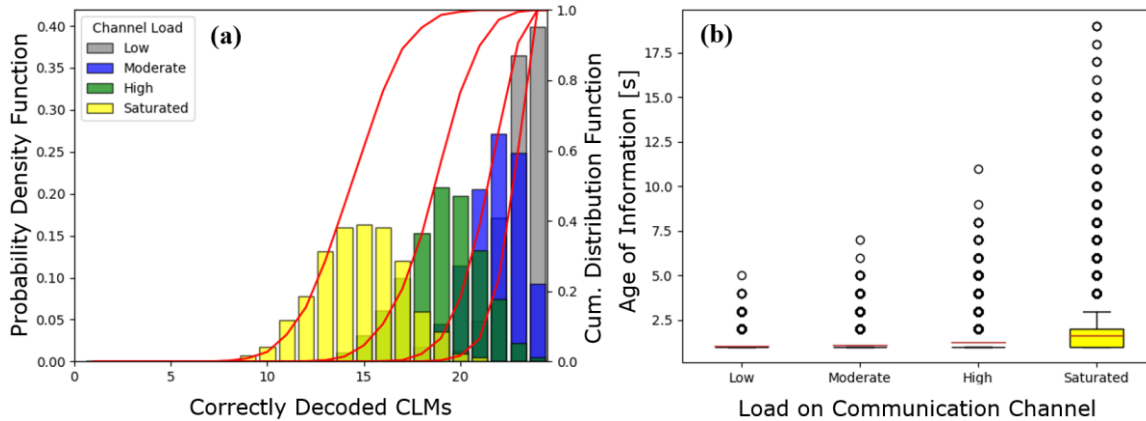


Fig. 28: (a) Probability density functions (coloured bars) and corresponding cumulative distribution functions (red lines) of the number of received messages for different channel loads, and (b) effect of the channel load on the age of information of the received CLMs.

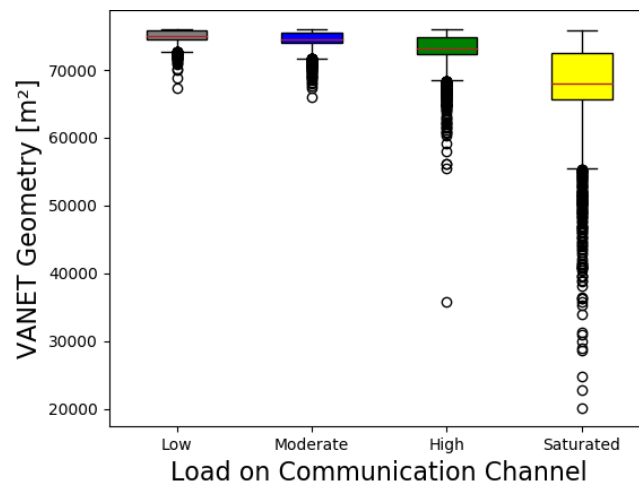


Fig. 29: Effect of the channel load on the area spanned by the vehicles of which CLMs are received [A17].

Having investigated the dependence of communication parameters such as the PDR and the update rate, we now have a closer look at the topology of the connected stations, as it is to be expected that the reliability of the communication suffers proportionally to the distance between the stations. This is verified by Fig. 29, showing the area spanned by the VANET in dependence of the channel load. Previous studies in the scope of this doctoral

work have shown that the positioning performance of Collaborative Localization is strongly influenced by the VANET's topology. In particular, the reduction of the positioning error is most pronounced into the directions of the connected stations. Further, its magnitude is determined by the distance of the collaboration partners into each direction. Thus, the area spanned by the VANET is a strong indicator of the positioning accuracy the VANET can reach.

While the VANET covers approximately the full area of the city square for low background channel loads, the median spatial coverage (orange line) falls by over 10% under saturated channel conditions. The effect of the background load is even worse when considering the outliers. Since the GN solver does not consider a transition model, as the EKF does, it is much more sensitive to the sudden appearance of large errors. As can be seen, the worst-case spatial coverage is a decrease of around 12%, 15%, 52%, and 73% for the low, moderate, high, and saturated channel congestion scenarios.

In conclusion, the investigation of background channel load effects shows that the service is highly sensitive to the number of available resources. The drop in communication reliability not only reduces the average number of collaboration partners per GNSS cycle, but more importantly, the most beneficial collaborators are the most affected, receiving their CLMs only very sporadically. However, analogously to DOR, AOI, and EAR discussed for Collective Perception in Subsection 4.3.3, the number of received CLMs, update period, and area coverage are only indicators for the positioning performance of Collaborative Localization.

4.2.4. VoI Definition

Having analyzed the channel-sensitivity of relevant performance indicators for Collaborative Localization, we now investigate the performance in terms of positioning accuracy. While the message content does not play a role in terms of communication reliability, it is the defining factor for the positioning performance. For this reason, and having in mind the findings from the previous subsection suggesting the necessity of a careful selection of the transmitted data, the value of the candidate data for transmission needs to be assessed. A simple strategy to define a VoI compliant with Eq. 30-37 and 60-69 could consist of the following three steps:

- **Identification of relevant VoI-parameters:** Section 3.4 introduced some of the most relevant parameters on the example of V2X services currently standardized in the different regions of the world. Depending on the wished level-of-detail in which the VoI is to be assessed a selection of these parameters needs to be done.

Example: for Collaborative Localization the most relevant parameters are the signal quality and the geometrical contribution of single measurements. The former could be assessed for each satellite measurement i by a signal-quality score S_i , e.g., based on the reception-mode B_i defined in [A11] (cf. Subsection 3.4.3):

$$S_i = \begin{cases} 2/3 & B_i = SPLOS \\ 1/3 & B_i = MP \\ 0/3 & B_i = NLOS \end{cases} \quad (105)$$

The geometric-contribution score G_n can be defined for a set n of satellites with cardinality $|n| \geq 4$, e.g., by the differential entropy of the navigation solution:

$$G_n = - \int_{\mathbb{R}} \int_{\mathbb{R}} \int_{\mathbb{R}} \int_{\mathbb{R}} \mathcal{N}_4(r, \Sigma_{GNSS}) \ln[\mathcal{N}_4(r, \Sigma_{GNSS})] dr = \frac{1}{2} \ln(|2\pi e \Sigma_{GNSS}|) \quad (106)$$

with the state vector r , the corresponding covariance matrix $\Sigma_{GNSS} = (G^T W G)^{-1}$, and the 4-variate normal distribution \mathcal{N}_4 (see also Eq. 77 and 79 in Subsection 3.4.3). $|\Sigma| \equiv \det \Sigma$ represents the determinant of Σ .

- **Determination of parameter ranges:** once the parameters are identified, their existence space needs to be determined.

Example: following up on the introduced example, the parameter spaces of signal-quality score and geometric-contribution score can be determined as follows:

$$S_i \in \left\{0, \frac{1}{3}, \frac{2}{3}\right\} \quad G_n \in \mathbb{R}_0^+ \quad (107)$$

- **Design of suitable VoI function:** finally, the VoI function Ω_n can be specified, complying with Eq. 60-69. To be suitable for its use with VALINDRA the function must further comply with the requirements listed for the VoI-determination step in Section 3.2.

Example: with the chosen set of dependencies, Ω_n fulfills the vast majority of the constraints given by Eq. 60-69. Only Eq. 60, 61, 66, and 69 are not intrinsically satisfied. Reparametrizing these equations for S_i and G_n yields (with $i \in n$):

$$\Omega_n \mid \frac{\partial \Omega_n(S_i)}{\partial S_i} \geq 0 \quad \forall \quad \frac{\partial \Omega_n(G_n)}{\partial G_n} \leq 0 \quad (108)$$

An example of a fitting VoI function meeting the constraints of Eq. 108 empirically determined based on the studies in [A11, A17] is:

$$\Omega_n = \begin{cases} \widehat{\Omega}_n & \text{if } \widehat{\Omega}_n = \max_{|m|=|n|} \{\widehat{\Omega}_m\} \\ 0 & \text{else} \end{cases} \quad (109)$$

where:

$$\widehat{\Omega}_n = b \left(\min_{i \in n} S_i + a e^{-G_n} \right) \quad (110)$$

Taking into account the parameter ranges identified in Eq. 107 and adhering to the requirements of the corresponding step in Section 3.2 the constants can be computed as:

$$a = \frac{1}{3} \quad b = B_0 + 4B_n \quad (111)$$

Including Eq. 106 and Eq. 111 into Eq. 109 and 110 yields:

$$\widehat{\Omega}_n = (B_0 + 4B_n) \left(\min_{i \in n} S_i + \frac{1}{3\sqrt{|2\pi e \Sigma_{GNSS}|}} \right) \quad (112)$$

This parameter choice ensures that the total message VoI density remains within the required range $\omega_{thr} \in [0, 1]$ for any set of satellites n , achieving the highest value only with combinations of $n = 4$ SPLOS satellites and very high precisions. Further, sets of satellites containing disadvantageous signal propagation modes are penalized. Finally, due to the dependencies between the satellite measurements, all satellite combinations with $\Omega_n > 0$ are wrapped together in one message segment alternative list (see Section 3.2 steps C1, C2 and D). Only the set of measurements which jointly achieve the highest VoI for a given channel load is selected for transmission in VALINDRA. All other combinations are discarded.

In order to gain a deeper understanding of the impact the definition of the VoI has on the performance of the Collaborative Localization Service, the number of includable satellites per CLM is set the same for all stations and used as system parameter. Additionally, the number of Collaborative Localization enabled vehicles is considered to be an environment parameter. Fig. 30 exemplarily shows the average horizontal positioning error for different numbers of connected stations and transmitted satellites using the above-defined VoI

function as satellite selection criterion. The first observation that catches the eye is the rising positioning accuracy with increasing number of connected stations and transmitted satellites. At second sight, an optimum for the number of included satellite measurements can be noted. This optimum depends on the number of connected stations. While the latter is an environment parameter and cannot be influenced, the number of transmittable satellite measurements is a tunable system parameter and could thus be adjusted in dependence of it.

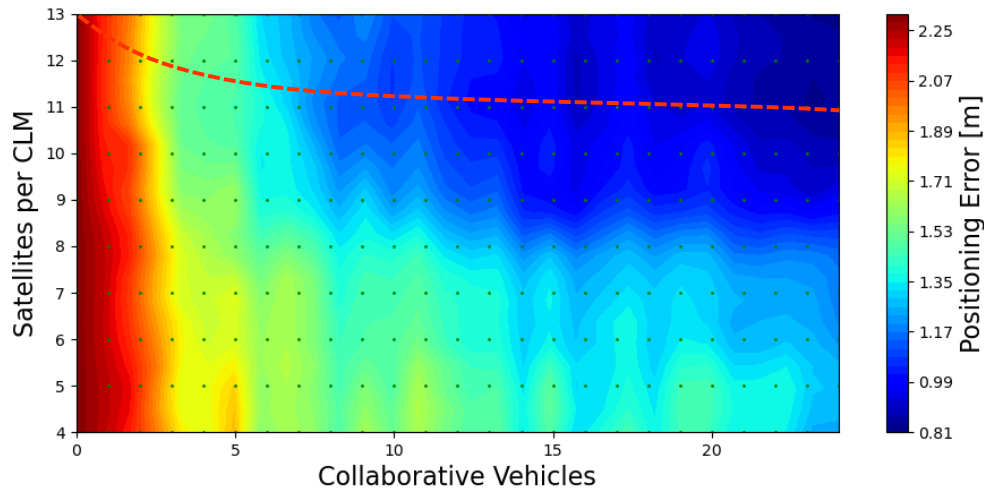


Fig. 30: Performance of Collaborative Localization in dependence of the number of connected stations and the number of shared satellite measurements per CLM [A17].

The figure further shows the tremendous potential of Collaborative Localization, reducing the positioning error from more than 230 cm (with 200 cm standard deviation) to below 80 cm (with 60 cm standard deviation). However, despite this noticeable performance increase a merely local VoI-based resource allocation that is a data-aware dissemination, does not reach the positioning threshold of lane accuracy, which is a strict requirement for future autonomous vehicles.

In the same way, the best achievable positioning accuracy was obtained for alternative VoI definitions based on the previously defined signal-quality score S_i and extended by (i) a random selection serving as benchmark, e.g., mimicking a DCC_ACC like message content agnostic dissemination method, (ii) a prioritization based on the satellite measurements SNR, and (iii) a selection based on the satellites' elevation angles (see Subsection 3.4.3).

Fig. 31 shows a comparison of the local optima achievable with the investigated VoI definitions when all stations are assigned an equal share of the available resources. The

lines can be obtained performing similar analyses to the one above. E.g., the locally optimized positioning accuracy of the entropy-based resource allocation investigated above is depicted by the red line in Fig. 30 corresponds to the blue line with triangle-shaped markers in Fig. 31.

The figure further shows the required urban 3D localization accuracy limit that ensures the compliance with a 10^{-8} failure probability per hour of operation as derived in [303]. For comparability the mean acceptable positioning error is computed from the offered 95% confidence accuracy ranges.

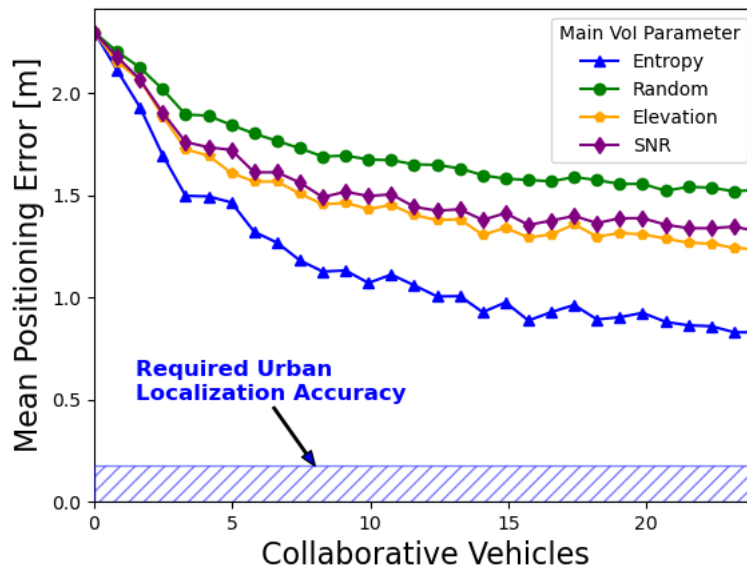


Fig. 31: Local optimum of the average horizontal positioning accuracy as a function of the number of connected stations for different VoI definitions given an equal resource allocation among the stations.

As can be seen, the entropy-based VoI definition largely outperforms the other methods for all VANET sizes and is hence our choice for the computation of the VoI in the following section. Already with around 3-5 collaboration partners the entropy-based approach achieves the performance of a random, elevation-based, or SNR-based VoI assignment with all 25 connected stations. When used with the 24 collaboration partners the performance increases by roughly 100% as compared to the random satellite selection and by 60% as compared to the SNR-based and the elevation angle-based satellite selection. Despite providing significant improvements to the positioning performance, Collaborative Localization relying on entropy-based generation rules exceed the strict urban localization accuracy limit by a factor of 5.

It is worth noting that a similar dependence of the positioning error on the number of connected stations was observed, e.g., in [304]. The considerably higher positioning errors, even though GNSS signal propagation errors are not considered, can be explained by the lack of data prioritization, the single-constellation (GPS), and the single-frequency operation, as well as the good performance of the multipath detection algorithms [A11] used in this work.

4.2.5. VALINDRA-based Resource Allocation

The previous subsection introduced a method to define the VoI for different message segments. Subsequently, the impact of a suitable VoI definition was investigated on the example of Collaborative Localization and the enabled positioning accuracy. While the investigation already used a VoI-based message generation, each station was still assigned the same number of communication resources. This subsection lifts that constraint and investigates the performance increase achievable with the VALINDRA-based distributed VoI maximization.

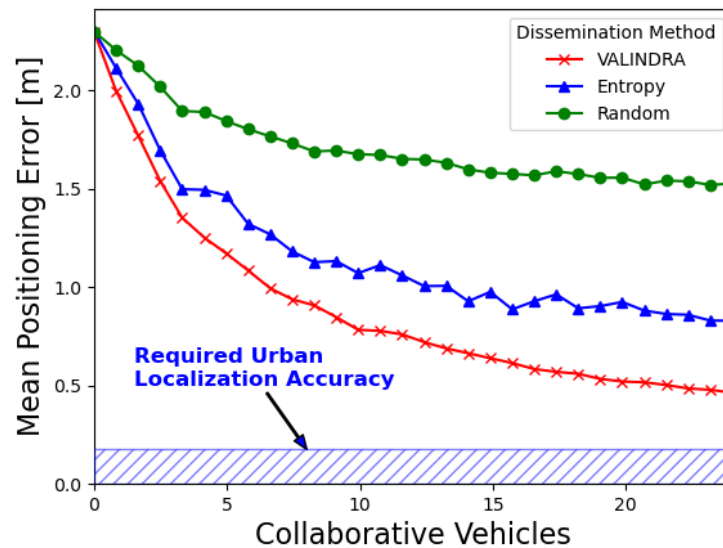


Fig. 32: Global optimum of the average horizontal positioning accuracy as a function of the number of connected stations employing VALINDRA.

Fig. 32 shows the mean achievable horizontal positioning accuracy of a Collaborative Localization enabled network using VALINDRA for the CLM dissemination. The random and the entropy-based message dissemination introduced in the previous subsection serve

as benchmarks. As can be seen, even though VALINDRA relies on the same VoI function as the entropy-based dissemination approach, it shows a significantly better performance, almost doubling the positioning accuracy of the entropy-based approach. Even though also VALINDRA is not able to reach the required localization accuracy limit derived in [303], this observation proves the enormous potential of a VoI-based resource allocation if compared to an equal resource distribution among the stations regardless of the data they can contribute to the network.

Finally, it should be noted that the benefit of VALINDRA compared to a static, equal resource allocation increases with the knowledge-heterogeneity of the network. The investigated city square in Frankfurt (Main) for example is one of these more heterogeneous scenarios, since vehicles at the corners of the square present much poorer satellite visibility than those on the edges of the square. On a highway, in turn, the knowledge contribution of the connected stations is distributed quite homogeneously [A08, A12]. Heterogeneities may however still arise, e.g., through the equipped GNSS receivers and their operation modes (multi-constellation, multi-frequency, etc.).

4.2.6. Conclusion

In Section 4.2 VALINDRA was demonstrated on the example of the newly introduced Collaborative Localization service. After an initial definition of the service and the description of the challenging GNSS scenario (achievable stand-alone positioning accuracy ~ 2.4 m) used for the later performance investigation, the sensitivity of the service regarding the state of the communication channel was analyzed. It was found that especially two effects make the performance of the channel highly congestion-dependent: (i) the large message sizes, and (ii) the extremely synchronized channel access of all Collaborative Localization Service enabled stations every GNSS epoch. The positioning performance could be optimized with the introduction of a scenario-dependent message generation time jitter for a fixed number of connected stations. The high impact of an efficient resource allocation was further motivation for the use of VALINDRA. In a first step the service's performance was optimized by varying the message sizes following different VoI-based message segment prioritizations. It could be shown that the localization accuracy increased significantly when adapting the message size on a per-vehicle basis, reaching submeter accuracy. In a second step an information entropy based VALINDRA was tested against the previously derived benchmarks. The distributed optimization of the communication channel resource allocation enabled positioning accuracies of around 0.49 m, thus representing an enormous advance towards the 0.21 m required for automated driving in such scenarios. Further research to improve the

Collaborative Localization Service is strongly encouraged for its introduction as a V2X Day 3+ service.

4.3. Collective Perception

In the previous chapter the working principle of VALINDRA was investigated based on the Collaborative Localization Service. While the latter is currently in an early stage of development, Collective Perception has already received considerable attention by the V2X community during the past years. Thus, a large variety of dissemination mechanisms and performance metrics have been proposed in the literature. In the scope of this doctoral work Collective Perception was investigated extensively, both analytically [A3, A4, A7] as well as in simulation [A5, A14, A16, A19]. A review of the most used metrics for determining the added value of Collective Perception is offered in [A14] and constitutes the basis of the investigation in this section. With only few exceptions, these are network and perception metrics, each of which assesses a specific aspect of the service. To the best of the author's knowledge, higher-level metrics that could be used to compare, e.g., different generation rules or redundancy mitigation techniques in a more generic way have not been proposed to date. For this reason, two new metrics have been introduced, the aim of which is to quantify the safety provided by the service. The present section focusses on comparing the performance of state-of-the-art dissemination mechanisms with that achieved by VALINDRA.

To investigate the impact of VALINDRA on Collective Perception, a highway scenario was chosen for mainly three reasons: (i) the high vehicle dynamics make precise environmental models indispensable, (ii) the high variability of the channel congestion, and (iii) the availability of publicly available high-quality real-world datasets. Subsection 4.3.1 describes the investigated scenarios and simulation parameters before evaluating VALINDRA in terms of the generated channel load (Subsection 4.3.2), the enabled environmental perception (Subsection 4.3.3), and the provided safety (Subsection 4.3.4). Subsection 4.3.5 then draws conclusions on the VALINDRA-based CPM dissemination.

4.3.1. Parameter Settings

Previous analytical studies have shown that the performance of Collective Perception strongly depends on traffic density, average speed and the number of lanes [A3, A4, A7]. For this reason, two highway segments that differ notoriously in their traffic densities were selected for this investigation. The vehicle traces were obtained from the HighD dataset in the region of Cologne (see Figure 5 in [296]).

To smoothen the results, up to 10 runs of the approx. 15-minute recordings were carried out for the intermediate V2X equipment rates ¹⁵. An overall characterization of both scenarios is given in Table 6. The corresponding vehicle densities and speeds are shown in more detail in Fig. 33, differentiating between trucks and cars. In total over 1,000 h of total driving time where simulated.

Table 6: Investigated highway scenarios with low (A) and high (B) traffic density.

Scenario	A	B
Speed limit [km/h]	-	120
Total distance driven [m]	342235	1120346
Total time driven [s]	10298	80676
Number of vehicles (trucks)	856 (168)	2850 (389)
Number of lanes	3↓↑3	3↓↑3

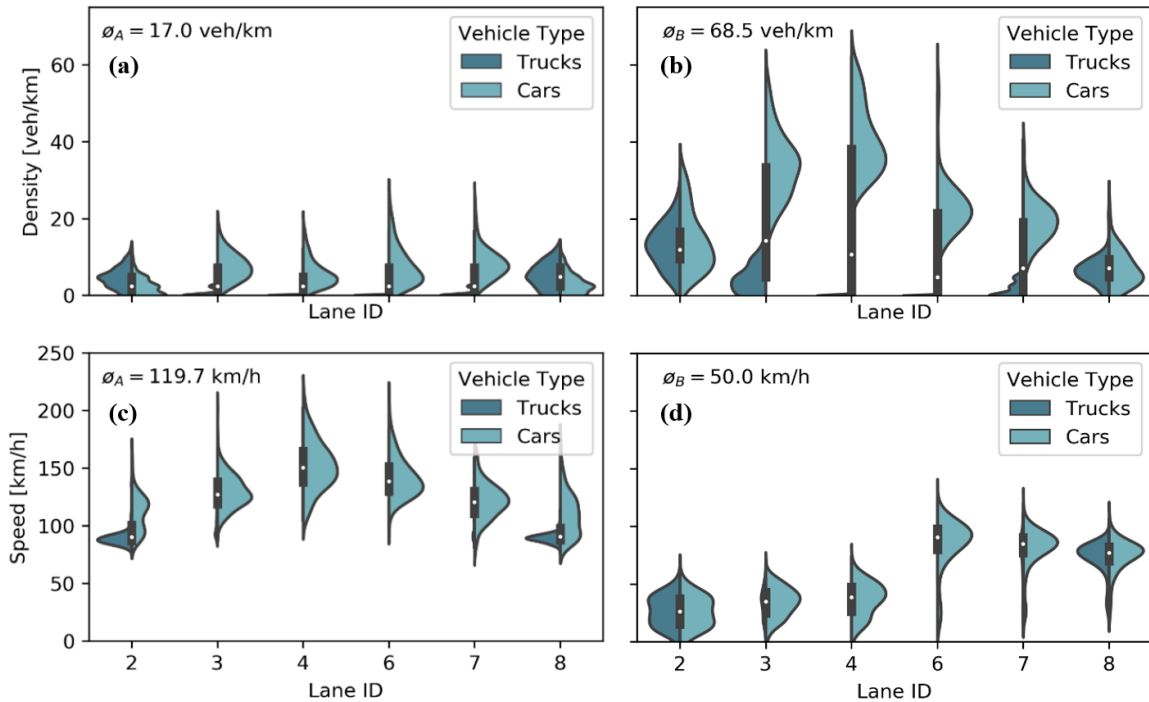


Fig. 33: Traffic characterization in terms of: **(a,b)** vehicle density and **(c,d)** speed distribution for **(a,c)** the low and **(b,d)** the high traffic density scenario. Traffic speed and density have a high impact on the performance of Collective Perception.

¹⁵ In this thesis the terms *V2X market penetration*, *V2X market share*, and *V2X equipment rate* are used as synonyms.

The high quality of the HighD dataset allows to use real vehicle traces and dimensions, with an accuracy of < 10 cm (see Fig. 34a). For simplicity, the vehicles are all equally equipped with multiple cameras as depicted in Fig. 34b. The camera system has an effective 360° field-of-view and a tracking range of 85 m (shaded green area). Both detection probability and detection accuracy are inversely proportional to the distance of the tracked object and directly proportional to the fraction of its visible cross section. The ego-vehicle's sensor measurements are illustrated in pink. It is clearly visible how the pink bounding boxes grow with increasing distance from the ego-vehicle and some vehicles are not even detected due to the obstructed line-of-sight. It can further be seen that the GEM (brown boxes) reaches far beyond the field-of-view of the ego-vehicle's sensor system, includes the shadowed vehicles, and has a higher precision than the stand-alone measurements, clearly demonstrating the benefit of Collective Perception with the exemplarily depicted 25% V2X market penetration.

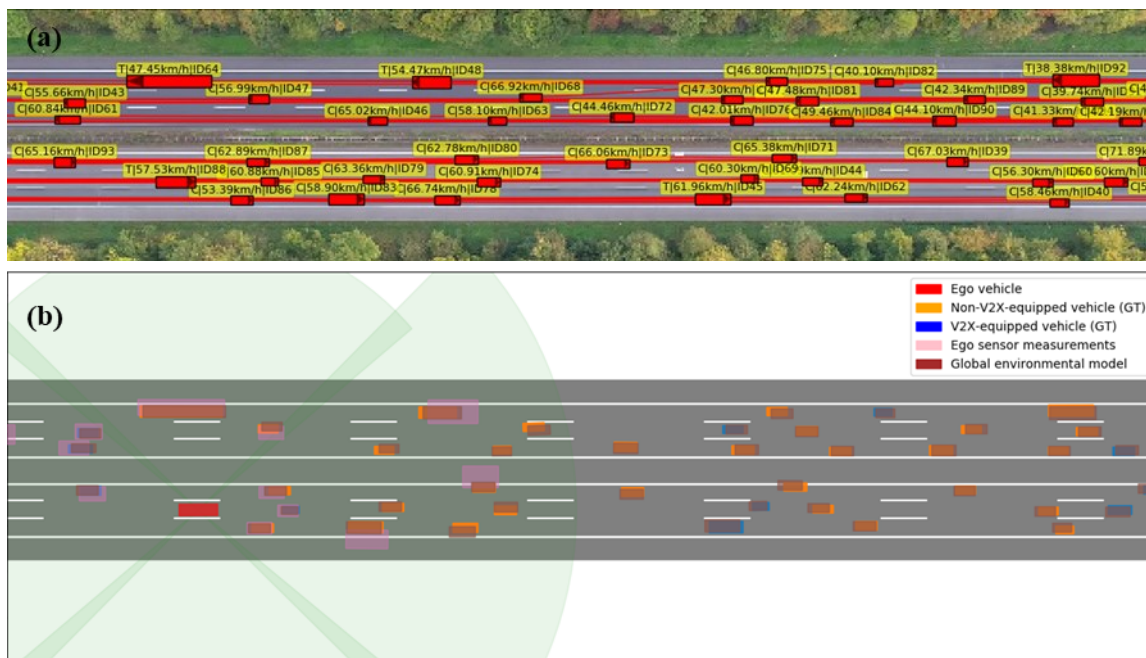


Fig. 34: High-density highway segment of scenario B: (a) Ground truth positions of the vehicles as contained in the highD dataset; (b) Visualization of the environmental perception of a vehicle (red box), showing the sensor measurements (pink boxes) and the fused global environment model (brown boxes) for a V2X market penetration of 25%. They superposed over the ground truth states' bounding boxes of the surrounding traffic, differentiating between V2X-equipped (orange boxes) and non-V2X-equipped vehicles (blue boxes).

For the evaluation, IEEE 802.11p is used with a QPSK modulation and a coding rate of 0.7. Antenna and average environmental heights, sensing power threshold, background noise and the transmission power were adopted from [A4, A7]. The transmitted CPMs correspond to the latest state of standardization at the ETSI [146], following the specified dynamic object inclusion rules. According to practical experience [295] and to foster reproducibility, all optional data fields of the detected object container are filled, while the freespace addendum is omitted (see CPM message format in Subsection 2.2.2.3). For the purposes of this evaluation a single dedicated channel for Collective Perception is considered to isolate the relevant effects and allow their investigation. Five distinct dissemination modes were selected for comparison:

- **ETSI-CPM (E-CPM):** standard CAM-based CPM rules as defined by the current draft of the ETSI standard. To serve as benchmark DCC is turned off in ECPM mode.
- **Reactive CPM (R-CPM):** resembles E-CPM but is extended by the 5-state reactive approach of DCC_ACC (see Subsection 2.3.3.1).
- **Adaptive CPM (A-CPM):** resembles E-CPM but is extended by the full DCC protocol stack including the current version of DCC_FAC (see Subsection 2.3.1), and the LIMERIC-based adaptive approach of DCC_ACC (see Subsection 2.3.3.2).
- **Priority-based CPM (P-CPM):** CPMs of equal size as generated in E-CPM mode, however making use of a VALINDRA-like VoI function to determine the included objects. The VoI function uses the relative information entropy as derived in Eq. 70-72 to select the objects.
- **VoI-based CPM (V-CPM):** generates CPMs following VALINDRA for VoI-maximization. The underlying VoI-function is again determined by the relative information entropy as used for P-CPM, however the threshold is not set by the current CPM generation rules but by the channel load (see Eq. 22 and 23).

4.3.2. Channel Demand

This subsection analyses the effect of the proposed VoI-maximizing resource allocation on Collective Perception and compares it to the other four dissemination modes defined in

the previous subsection. The upper part of Fig. 35 shows a section of scenario A (low density) with seven connected vehicles. The messages generated on the facility layer by these vehicles within 1000 ms are displayed below. Besides CPMs, also CAMs and DENMs (see V2X services in Subsection 2.2.2) are displayed for comparison purposes.

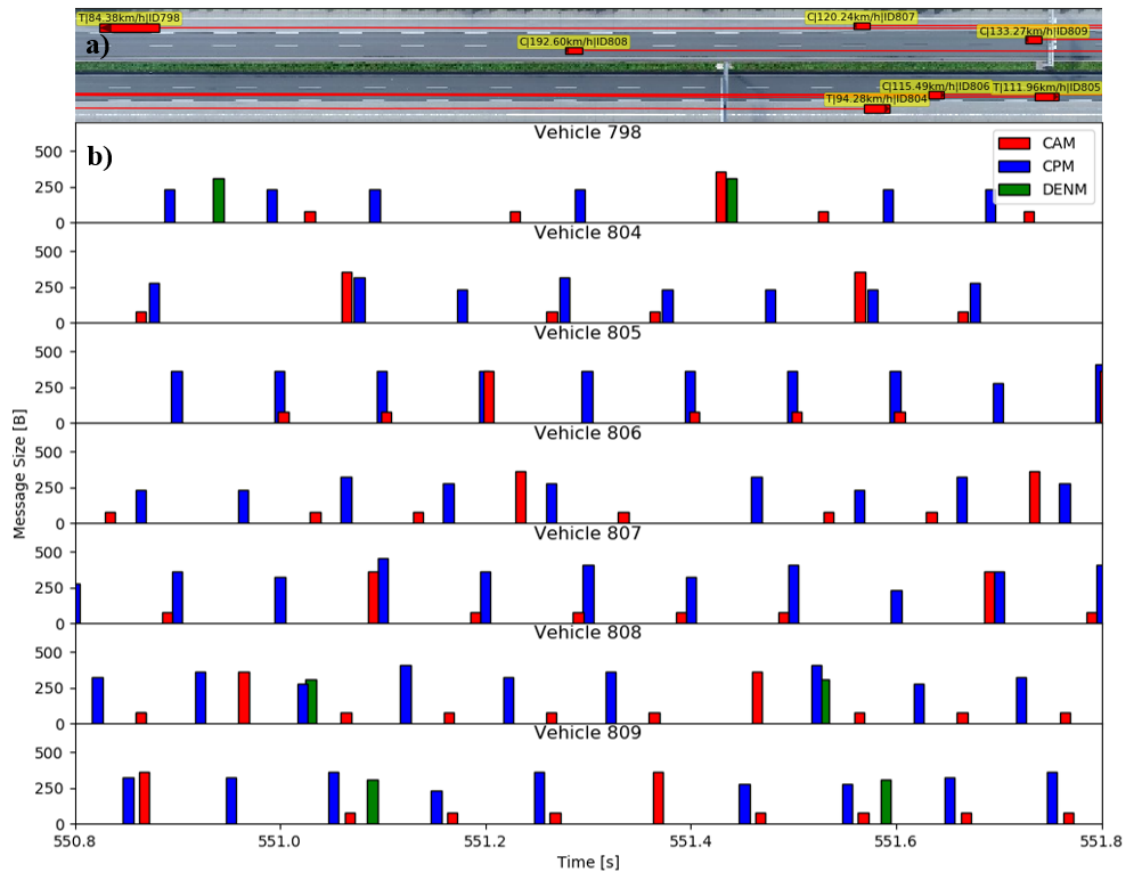


Fig. 35: Message generation of the ETSI stack for the low-density scenario: (a) Vehicles on a highway section; (b) corresponding generated messages over time. The temporal extension of the messages is only for visualization purposes.

The CAM is of interest for the analysis of the CPM due to the related generation rules. On a highway, the dissemination of the CAM is mainly governed by the vehicle speed [A14]. Vehicles driving at higher speeds will generate CAMs more frequently. Truck 798 for instance, driving at a speed of 84 km/h, moves the required 4 m every 171 ms, thus generating CAMs at roughly a rate of 5 Hz. Vehicle 808 on the other side, driving at 193 km/h, takes 75 ms for the triggering displacement of 4 m, which translates into the maximum CAM generation frequency of 10 Hz. As can be seen, the CAMs are generally

very light-weight messages with sizes <100 B. These high-frequency CAMs are extended every 500 ms by a low frequency container with supplementary information, leading to a significant increase in size.

In addition to the CAMs, DENMs are also sent in the selected time period. Truck 798, for instance, detects a potentially hazardous situation and transmits a DENM to warn the surrounding vehicles. The DENM is received and immediately retransmitted by vehicle 808. The relayed DENM is then received by vehicles 807 and 809, but only retransmitted by the latter, as this vehicle is located further away from the last transmitter (vehicle 808). The DENM dissemination rules (see Subsection 2.2.2.2) allow for the transmission of further DENMs later in time to warn about the persistence of the event causing them. In this case the DENM is retransmitted by the service-initiating truck after 500 ms. The event-triggered nature of the DENM makes a direct comparison of the average caused channel load more complex. An estimation of the C2C-CC estimates that the channel load caused by DENMs and other less frequent messages, such as SPaTs and Maps (see Subsection 2.2.1.1), amounts to less than 10% of the load caused by CAMs [305].

While CAMs are generated based on the transmitting vehicle's state, the CPM includes detected objects depending on their estimated states. Since a CPM is generated whenever at least one detected object has been selected for transmission, vehicles generally disseminate more CPMs than CAMs even at such low traffic densities as in scenario A. In analogy to the low-frequency container of the CAM, a sensor container is added to the CPM every 1000 ms. Overall, it is evident that the CPM demands significantly more resources compared to CAMs or DENMs. This dominance is even more pronounced at higher vehicle densities, increasing the relevance of channel-aware generation rules.

Furthermore, the CPM is much less predictable than the CAM in both size and periodicity, posing not yet solved problems for the semi-persistent scheduling (see Subsection 2.2.4.3) of C-V2X mode 4 [176]. The high variability of the CPM size in the high-density scenario is represented in more detail in Fig. 36 in terms of the included objects. A comparison with the message sizes of CPMs generated with low traffic densities is offered in [A14]. While the message sizes resulting from the generation and transmission modes E-CPM, P-CPM, A-CPM, and R-CPM converge towards the CBR-independent distribution shown in Fig. 36a, those obtained operating in V-CPM mode depend on the channel load. For unrestricted generation states, i.e., channel loads lower than CBR_{tar} , the shape of the message size distribution takes the form of Fig. 36b. The blue bars correspond to the probability distribution of the number of objects included in a CPM. The red lines represent the cumulative distribution function. CPMs not transmitted in lack of included objects are depicted by the green bars. As was to be expected, the average number of

objects included in V-CPMs is higher than that corresponding to other modes, leading to a rough doubling from ~ 7 to ~ 14 objects. However, the standard deviations, which have a significant impact on the performance of the periodicity-requiring autonomous-mode C-V2X, are approximately equal. It should be noted that the high variability of the CPM sizes is further increased by the occasional appending of sensor information containers (see Subsection 2.2.2.3) and security headers (see Subsection 2.2.5), both generating additional peaks of lower magnitude at higher message sizes. Less expected is the right-skewness of the V-CPM-based message size distribution, which can be traced back to the vehicle density distribution. The reason is the resource availability based on the low V2X equipment rate, which also allows less relevant objects to be transmitted in order to maximize the network's VoI. These findings are in good agreement with the analytical evaluation in [A3], especially as scenario B is already close to the critical traffic density (20–40 Veh/km/lane depending on the sensor system's range) where occlusion effects by the dense traffic become dominant and the probability of a high number of objects detected at the same time is disproportionately reduced. However, scenario A shows similar, albeit less skewed distributions since it is far from the critical traffic density.

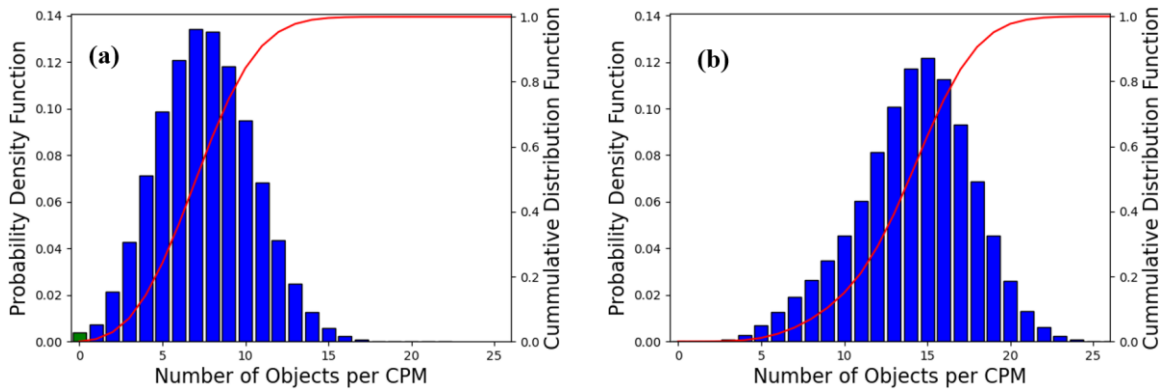


Fig. 36: Probability Density Function (PDF; blue bars) and Cumulative Distribution Function (CDF; red line) of the number of objects per CPM for the high traffic-density scenario for (a) E-CPM, R-CPM, A-CPM or P-CPM and (b) V-CPM. Not transmitted CPMs are depicted by green bars.

After the number of included objects, which is a decisive parameter for the message size, has been examined under relaxed channel conditions, the total message size is now to be investigated for higher channel loads. Fig. 37a shows the size of the CPMs generated in E-CPM (green line) and V-CPM mode (blue line) in dependence of the V2X equipment rate. The shaded areas correspond to the respective 1 standard deviation confidence intervals. As for the number of objects per CPM in Fig. 36, the modes P-CPM, A-CPM

and R-CPM are omitted as their message sizes correspond to the ones generated by the E-CPM. In addition, as stated earlier the message sizes of the four last mentioned modes are not dependent on the channel load, which is confirmed by the figure. The situation is different with the V-CPM mode where the message size, as discussed, is significantly larger than that of the other modes in relaxed channel conditions. At an equipment rate of around 33.8% the channel load reaches the equilibrium state during first sporadic periods of time, which leads to a minor increase of the VoI-threshold according to Eq. 81. As a result, the first objects with lowest VoI are excluded from the CPMs, which leads to a reduction in the message size. As the fraction of connected stations increases further, the VoI must be raised accordingly in order not to exceed the target CBR. Eventually, the message size even drops below that of the E-CPMs. This indicates that the E-CPM has exceeded CBR_{tar} , which can be confirmed by looking at the CBRs in Fig. 38. The almost perfectly overlapping confidence ranges with a 100% equipment rate are the result of a random combination of parameters and would diverge, e.g., with a slightly different traffic density. In the low-density scenario, the average message sizes are 255 and 364 bytes for E-CPM and V-CPM, respectively. As CBR_{tar} is never reached, the message sizes are constant regardless of the equipment rates.

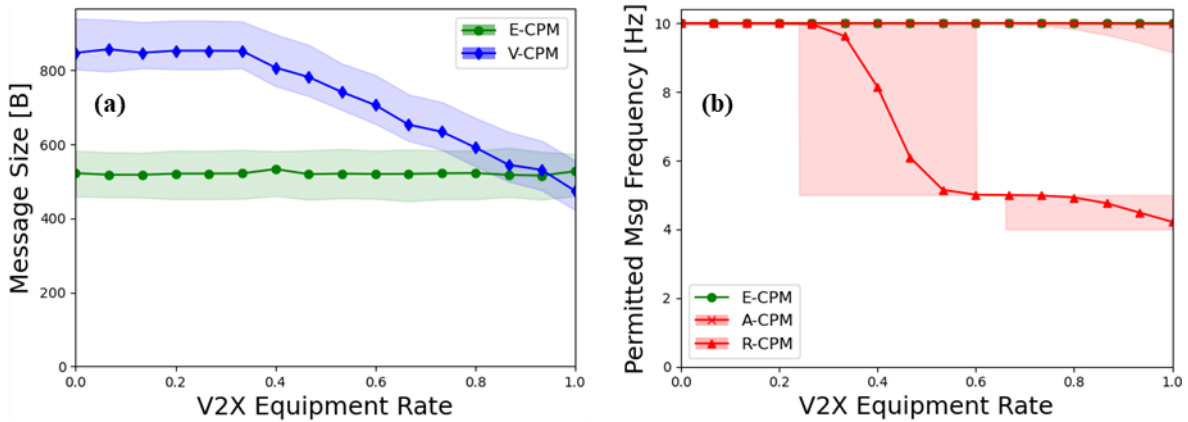


Fig. 37: Equipment rate dependence of (a) message size and (b) maximum permitted message frequency for the high-density scenario, showing means (solid lines) and (a) 1σ and (b) 3σ confidence intervals (shaded regions).

In addition to the message size, the maximum allowed message frequency is also an important description parameter for the channel usage of a service. The maximum allowed message frequency is in turn determined by the minimum inter-message time T_{off} (see Subsection 2.3.3). It is worth noticing that it is not equal to the actual message frequency,

as it does not consider the fraction of messages dropped on facility layer in lack of objects passing the object selection filters in case of E-CPM, R-CPM, A-CPM, and P-CPM and exceeding the VoI threshold in case of the V-CPM. Fig. 37b shows the reciprocal of T_{off} for E-CPM, A-CPM, and R-CPM in the high-density scenario. P-CPM and V-CPM are omitted as their inter-message time corresponds to the one of E-CPM and remains constant at 100 ms. R-CPM and especially A-CPM, on the other hand, present the same constant $T_{off} = 100$ ms at low equipment rates, but then increase with rising equipment rates. Since the deviation for A-CPM is very small in the examined scenario, the 3σ confidence intervals are displayed for A-CPM and R-CPM in Fig. 37b.

The transition of the 5-state reactive DCC state machine from the relaxed to the first and then to the second active state are clearly visible, increasing T_{off} to 200 ms and then to 250 ms. The course of the mean inverse inter-message period shown in the graphic should not hide the fact that the frequencies of the connected vehicles are quantized and can only assume values of 10, 5 and 4 Hz. This fact is made clear by the shaded 3σ confidence interval, which comprises the respective adjacent quantized frequencies. In these regions, the CBR is kept stable by gradually increasing the fraction of vehicles operating in the next higher DCC state with rising V2X equipment rate. The quantization of the frequency therefore leads to instabilities in T_{off} that are not coordinated with the facility layer of the vehicles in these regions. States with stable T_{off} are intercalated with these regions. Within the regions all connected vehicles assume the same minimum message intervals. However, in particular the range between 0.60 and 0.66 V2X equipment rate, which corresponds to $1 / T_{off} = 5$ Hz, appears to be relatively limited in Fig. 37b. This is caused by a blurring due to the varying traffic densities investigated for each equipment rate. The stable inter-message interval regions are somewhat more extensive if they are viewed as a function of the number of connected stations instead of the V2X equipment rate.

The effects of higher equipment rates on the T_{off} caused by A-CPM are significantly smaller. The maximum permissible message rate $1/T_{off}$ is only reduced in isolated traffic situations if the proportion of connected vehicles is over 70% (see shaded 3σ confidence interval). On average, however, the maximum permissible message rate remains close to 10 Hz. The fact that no reductions occur at all is because the equilibrium CBR would otherwise be exceeded in some situations. The system reacts by increasing T_{off} to remain in the stable state.

In scenario A, the channel load generated is even too small to cause an increase above $T_{off} = 100$ ms for either A-CPM or R-CPM (compare Fig. 9a in [A14]). Even though R-

CPM reaches active state 1 in $\sim 0.25\%$ of the time, for the scenario's small packet sizes this does not further limit the maximum generation frequency (cf. Table 1 in Subsection 2.3.3.1). Thus, the maximum message transmission rates of all five generation and transmission modes remain constant at 10 Hz.

The combined impact of number of connected stations, message size, and message rate of the different modes on the communication channel is shown in Fig. 38a. It shows the development of the CBR with increasing V2X equipment rate for the high-density scenario. Since the maximum message transmission frequency is constant in the low-density scenario and the message size is only increased by a constant offset in V-CPM mode, the interested reader is kindly referred to [A14] for more details.

Fig. 38a shows the dependence of the CBR caused by the five investigated CPM modes with their respective 1σ confidence intervals. The probability distribution function of the CBR for a complete V2X market penetration is shown in Fig. 38b, which corresponds to the cross section at $V2X = 1.0$ of Fig. 38a.

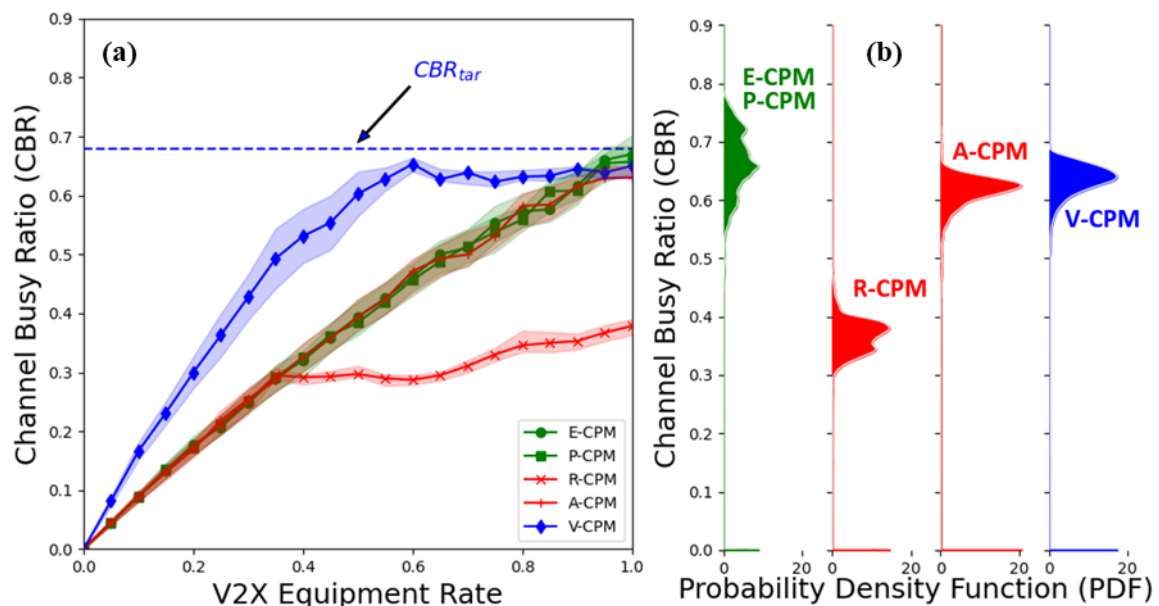


Fig. 38: CBR resulting from the five CPM generation and dissemination modes for scenario B: (a) for varying V2X equipment rates and (b) as PDF for full V2X equipment.

Taking E-CPM as benchmark, it is noticeable that P-CPM presents identical characteristics in terms of its impact on the channel, while the behavior of A-CPM differs slightly and R-CPM and V-CPM present strong deviations from the E-CPM channel demand. The correspondence between E-CPM and P-CPM is easy to explain by the

identical message sizes and rates established by the definition of P-CPM. The agreement of the A-CPM up to high equipment rates was also to be expected, since CBR_{eq} is only then achieved. From this point on, the minimum inter-message period is increased, as previously discussed, so as not to exceed the defined CBR_{tar} (indicated by the blue-dashed line). As can be seen, the latter is constant and presents an upper limit for the latter. CBR_{eq} , however, depends on the number of connected stations and the choice of the system parameters according to Eq. 95. Also the V-CPM depends on CBR_{tar} . As shown in Chapter 3, this VALINDRA-based dissemination mode maximizes the VoI in the network for a given CBR_{tar} . With low V2X equipment rates, this means that detected objects with a low associated VoI contribution are also included in CPMs, which leads to a significantly higher CBR compared to E-CPM. Once the equilibrium is reached, the VoI threshold is gradually raised, whereby the less relevant objects are discarded and, as a result, the channel load does not exceed CBR_{tar} . The threshold is raised for the first time in isolated traffic situations with an equipment rate of 33.2% (compare message size in Fig. 37a). Interestingly, the distribution also narrows because the different traffic situations converge towards similar stable states. This is also the case for A-CPM, as can be seen better in Fig. 38b. R-CPM shows the most discontinuous behavior, which is attributed to the underlying 5-state state machine. From a V2X equipment rate of 24.3%, the R-DCC gatekeeper in R-CPM begins to reduce the maximum message rate of isolated vehicles (cf. Fig. 37b). This has an impact on the mean CBR, but not on the 1σ confidence range. Only at higher equipment rates do traffic situations within the 1σ confidence range begin to be affected by the message rate throttling. The CBR converges towards the transition threshold between the DCC states and the distribution narrows, as already observed with A-CPM and V-CPM. The stable CBR region that follows corresponds to the unstable minimum message interval region in Fig. 37b (note different confidence ranges!). The connected vehicles keep the CBR constant in this region by switching between 10 and 5 Hz maximum message rates. As the V2X equipment rate continues to rise, the proportion of the time in which vehicles transmit at a maximum of 5 Hz also increases. With an equipment rate of almost 0.60, connected vehicles transmit at a constant 5 Hz in the first traffic situations. It is no longer possible to counteract the increase in the channel load by further lowering the transmission rate probability of 10 Hz in favor of that of 5 Hz. As a result, a new region is reached in which the CBR increases again in isolated traffic situations, but the mean message rate still fluctuates in many other situations. Only with a further increase in the V2X equipment rate will a point be reached at which road users in all situations have switched to active state 1 of R-DCC and the message rate becomes stable. It should be mentioned that this is only the case because of the overall relatively homogeneous traffic

density. Otherwise, a stronger scattering of the unstable states would occur, whereby the stable states would at some point completely disappear in this representation. Conversely, the stable states are more extensive under consideration of smaller periods of time, as already discussed. The CBR then continues to rise, with the vehicles remaining in active state 1 for most of the time. With a total V2X equipment, the mean CBR and the corresponding 1σ confidence interval are still below the transition threshold to active state 2, but as Fig. 38b shows, it is still reached and even exceeded in several times. The distribution of the CBRs caused by R-CPM in Fig. 38b also clearly shows how a peak is formed at the transition CBR. A further compression of the traffic would merge the second peak on the left into the main peak.

In summary, P-CPM and E-CPM claim the channel at high equipment rates beyond the maximum CBR_{tar} threshold since they lack channel load awareness. A-CPM shows a similar behavior but controls the channel load to satisfy CBR_{tar} . R-CPM regulates the channel load even further, so that it only reaches half of the target value despite the high density of connected vehicles. The VALINDRA-based V-CPM demands the channel significantly more than the other modes at low equipment rates but does not exceed the target values either and thus has the lowest RMS in terms of CBR_{tar} -tracking accuracy.

4.3.3. Environmental Perception

Having compared the extent to which the different dissemination modes strain the communication channel, we now investigate their benefit in terms of enhanced environmental perception. Several metrics have been suggested in the literature to quantify the increased perception of road users equipped with Collective Perception. They are usually used in connection with communication metrics, as they were examined in the previous subsection. However, they may as well be employed in a stand-alone fashion, e.g., to optimize the service with given channel constraints (single vs. multi-channel, dedicated vs. shared channel, etc.). In the following, VALINDRA is examined using three state-of-the-art perception metrics and compared with the other CPM dissemination modes. Since the modes show strongly overlapping performances for many parameter combinations, from now on only characteristic equipment rates are examined to enhance readability.

4.3.3.1. Environmental Awareness Ratio

The benefit of Collective Perception is most often described by the fraction of perceived elements in the environment of the connected road user. Several different metrics are in

use, which are collectively referred to as Environmental Awareness Ratio (EAR) [A14]. The Object Awareness Ratio (OAR), which describes the proportion of perceived (mostly moving) objects within a relevance area at a given point in time, enjoys the greatest popularity. It is used in [249, 250, 252, 306, 274, 251, 307, 308, 309, 310] and [A7], among others. Opposite this is the spatial awareness ratio (SAR), which shows the proportion of the area within the region of interest whose occupancy status is known at the given time. A typical use case is to find a proper traffic-gap, e.g., during lane-change maneuvers. SAR-like metrics are used in [311, 312] and [A5]. In addition to the distinction between OAR and SAR, there are also differences in the definition of the relevance area and time. The relevance area is usually defined by a safety radius around the road user. In individual cases, however, an area on the future path of the traffic participant can also be selected which does not yet contain him at this point in time. Application examples are intersection assistants or motorway merge-in assistants, for which the crossing and merging areas are of interest. The same applies to the relevance time in these examples. While OAR and SAR are usually estimated for the present, maneuvers that look further into the future require an estimation at the relevant point in time (e.g., reaching the intersection or the threading moment, respectively). An example of SAS and OAS being applied to a highway on-ramping maneuver is given in [A5]. For the purposes of this investigation, we stick to the OAR-based definition of the EAR.

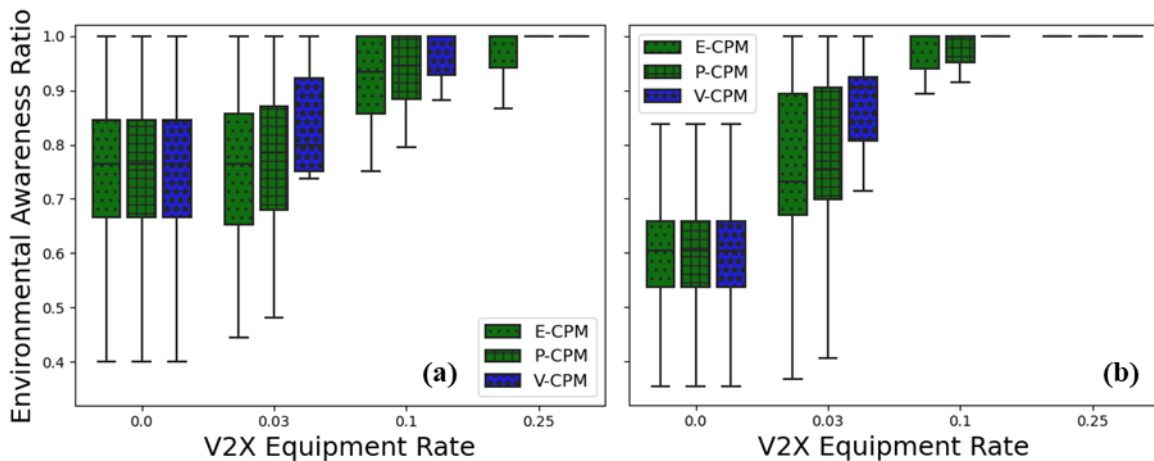


Fig. 39: Environmental Awareness Ratio obtained with the five investigated dissemination modes in dependence of the V2X equipment rate for (a) the low-density scenario and (b) the high-density scenario for a 250m-diameter area around the vehicles.

Fig. 39 shows the EARs achieved by the five examined CPM dissemination modes depending on the V2X equipment rate for a) the low-density and b) the high-density

scenario. As expected, in both scenarios a higher equipment rate leads to a significant increase in environmental perception by connected road users. The effect is all the more pronounced with high traffic densities, since the field-of-view of the object tracking sensors is significantly more restricted by occlusions in such scenarios. This effect was also modeled and verified analytically in [A3]. With high traffic densities a noticeable increase in environmental perception through Collective Perception occurs even with very low V2X equipment rates. This is due to the absolute number of connected road users within the communication range. While with, e.g., an equipment rate of 3% in scenario A there is barely one connected road user on average sharing information, in scenario B there are already around four. For further general observations on the benefits of Collective Perception in the two scenarios examined, the interested reader is kindly referred to [A14].

While traffic density and especially V2X equipment rate are the most determining parameters for the performance of Collective Perception, the influence of the dissemination modes is significantly less pronounced, principally with regard to the EAR. However, in contrast to traffic density and V2X equipment rate, which are both determined by the environment and therefore cannot be directly influenced, the dissemination mode is a system parameter and can be optimized accordingly. Since newly detected objects are usually included directly into the next generated CPM regardless of the dissemination mode, the EAR of different modes differs only in particular cases (in contrast to other metrics examined later). These include: (i) with E-CPM (and due to the identical underlying generation rules also with R-CPM and A-CPM), newly detected objects are immediately determined to be candidates for the next CPM without having to pass the numerous filters. However, if the length of the CPM exceeds a certain threshold referred to as maximum transmission unit (MTU) the message may be segmented transmitting only those objects that present the highest message utility function as defined by ETSI [145]. The transmission candidate objects are sorted according to this utility function and the CPM is then filled with the objects whose previously determined value is the highest until the MTU is reached (see Subsection 2.2.2.3). Since newly detected objects generally have a significantly lower confidence [261], an important component of the utility function, the risk of a delay or even rejection of newly detected objects is particularly high. With V-CPM and P-CPM, however, the VoI is used again as selection criterion to comply with the MTU. Since the VoI of newly detected objects is correspondingly high, the risk of rejection due to uncoordinated filters connected in series is intrinsically avoided by this consistent relevancy assessment of the candidate objects. (ii) With A-CPM and especially with R-CPM, there is a risk that the CPM carrying the newly detected object will be queued by the DCC gatekeeper and potentially even discarded, as DCC_ACC described in Subsection

2.3.3 has no access to the message contents. The parameter combinations in which the respective DCC_ACC comes into force have been investigated in Subsection 4.3.2 (iii). Last but not least, the object update rate described below also has a relevant influence on the EAR. Objects newly detected by connected stations can be lost on the way to the receiver due to packet losses (see Subsection 2.2.4). In this case, the time until the object is sent again in a CPM by one of the notifying stations determines the performance of the system. While P-CPM has the same object update rate as E-CPM, A-CPM and R-CPM have a negative influence on the object update rate by throttling the message frequency. The opposite is true for V-CPM. By maximizing the VoI, objects are sent more frequently under given channel restrictions and minimizing the time span until objects of a lost CPM are retransmitted. This effect is dominant with low V2X equipment rates. CPMs of a connected station that is newly entering the communication range generally contain a high degree of EAR-relevant information, since the probability of receiving the latter through another connected station is comparatively low. Due to the distance, packet losses caused by fading effects occur comparatively frequently. The higher packet collision probability caused by the higher resource demand of V-CPM, on the other hand, is negligible in view of the low equipment rate.

The discussed effects can clearly be identified in Fig. 39. With low equipment rates, E-CPM, A-CPM and R-CPM perform identically apart from statistical deviations. P-CPM shows a noticeable improvement for all non-zero V2X equipment rates in both scenarios, since every road user preferably transmits the objects to which he can make a larger VoI contribution. This leads connected stations to increase the inclusion frequency of objects that are not known to potential recipients at the expense of objects that are well-known to the VANET (compare Kullback-Leibler divergence in Eq. 73 used for P-CPM and V-CPM). As discussed, increasing the frequency reduces the time until the first reception of previously unknown objects and therefore has a positive effect on the EAR. V-CPM brings an even more pronounced improvement (up to 17% in the median) with low equipment rates, since this mode does not sort out any objects with channel loads under CBR_{tar} and thus has a correspondingly high update rate. Interestingly, by comparing it to P-CPM, it can be seen that the majority of the EAR surge is due to a smart choice of the transmitted objects. This can be explained by the fact that the additionally transmitted objects all have a lower VoI and therefore do not have such a strong influence on the performance of the system.

With a high V2X equipment rate, the average object update rates of all objects with A-CPM, V-CPM, and R-CPM decrease slightly compared to E-CPM and P-CPM in the first two cases and strongly in the latter case. On the other side, the average object update rates

of relevant objects increase in comparison to P-CPM and V-CPM. However, both effects are negligible compared to the high number of informing stations, which leads to such low object update periods that all transmission modes present have almost perfect EARs.

Before the several-times-mentioned object update rate is discussed in more detail below, it should be reminded that the results presented in this subsection are heavily dependent on the track manager of the environment model (see Subsection 4.1.3). It tracks objects for a certain time after their last detection by predicting their new states, until the accuracy threshold is reached. The result is a more robust environmental perception to packet losses as, e.g., compared to [A3] by mitigating sudden EAR drops.

4.3.3.2. Detected Object Redundancy and Update Period

In addition to the ratio of detected relevant objects in the environmental model of a road user, the redundancy with which these objects are perceived is a key performance indicator for Collective Perception. A higher DOR implies a lower update period (inverse of the update rate) and thus reduces the Age of Information (AOI). The AOI includes all occurring latencies and thus, in addition to the update period, especially sensor, communication and processing latencies. For a more in-depth study of the AOI on the example of C-V2X mode 4, the interested reader is referred to [A4]. Also dependent on the DOR is the distance covered by a tracked object between updates, which indicates how much the current state of the GEM can deviate from reality. A somewhat more distant but still closely related metric is the number of independent information sources for each relevant object, which leads to a higher integrity of the data managed in the GEM. The choice of the metric used depends on the objective of the study. DOR [250, 251, 306, 311] and [A3, A4], update rate or update period [252, 306, 307, 310] and [A4, A7], distance covered by the object between updates [307] and [A4, A7], AOI [A4, A7], and number of independent sources [A14] have been used extensively in the literature, making it the second most relevant measure of the benefit of Collective Perception to date. It should however be pointed out that some of the cited works making use of the DOR also use it to prove unnecessary resource allocation in case it exceeds certain not yet well-defined thresholds. These studies are also the motivation for the possible extension of the Collective Perception Service by redundancy mitigation techniques as mentioned in ETSI's TR analyzing the service [146].

The DORs achieved by the five examined transmission modes are shown separately in Fig. 40 for both scenarios. To enable an in-depth analysis, the average updates per second for an object in the relevance area are displayed against the number of independent information sources. Source zero represents the ego vehicle. The other sources are sorted

in descending order of the contributed DOR. The solid lines represent the means and the shaded areas the standard deviation for the different investigated CPM transmission modes and V2X equipment rates as denoted in the figure. As can be seen, the on-board sensors yield a total average of 14 and 12 updates per second in scenario A and B respectively. Considering the sensor update rate of 25 Hz, this corresponds to around 50%. The difference is caused by the physical limitation of the FOV of the sensor system (see parameter settings in Subsection 4.3.1) and the obstruction of the line-of-sight by other road users. The graphs clearly show the benefits of Collective Perception. Due to the high number of combinations of equipment rates and CPM transmission modes, only the most characteristic pairs are shown. The E-CPM (green lines) is used again as a benchmark. As can be seen, the most reliably informing connected vehicle provides an additional 2-5 updates per second depending on the V2X equipment rate and the scenario. Further informing V2X sources contribute fewer updates mainly for three reasons: (i) they are further away from the target object and do not detect it continuously, (ii) they are further away from the receiving vehicle and the communication becomes less reliable, and (iii) the object is included at lower rates for various reasons, such as diverging state estimations. Overall, the bulk of the updates is provided by 10 and 20 V2X sources in scenario A and B, respectively, in the E-CPM transmission mode. The remaining sources contribute only sporadic updates, totaling around 21 and 43 information sources for scenario A and B, respectively, with a complete V2X equipment. For a comprehensive analysis of the DOR in E-CPM mode, the reader is kindly referred to [A14].

While the DOR achieved by P-CPM is identical to that of E-CPM in all scenarios, A-CPM and R-CPM deviate with parameter combinations where the corresponding access layer DCCs come into play. As found in Subsection 4.3.2 this is the case for high equipment rates in the high-density scenario. For this reason, the DORs achieved by both these modes with a full V2X traffic equipment of scenario B are shown in Fig. 40b (red curve). As expected, the increase of the minimum inter-message duration T_{off} leads to a reduction of the update rate for both modes. Especially R-CPM is strongly affected, reducing the average update rate from around 75 updates per second (E-CPM) to around 41. The fact that the number of updates is still over 50% despite the almost 60% reduction in transmission frequency is due to the significantly less congested communications channel and the associated higher PDR. As expected, the effect is much less pronounced for A-CPM (cf. channel state Fig. 38). For both modes the number of independent V2X sources is reduced only marginally, since the only received CPM from them may have been dropped by the gatekeepers of the corresponding underlying DCC mechanisms.

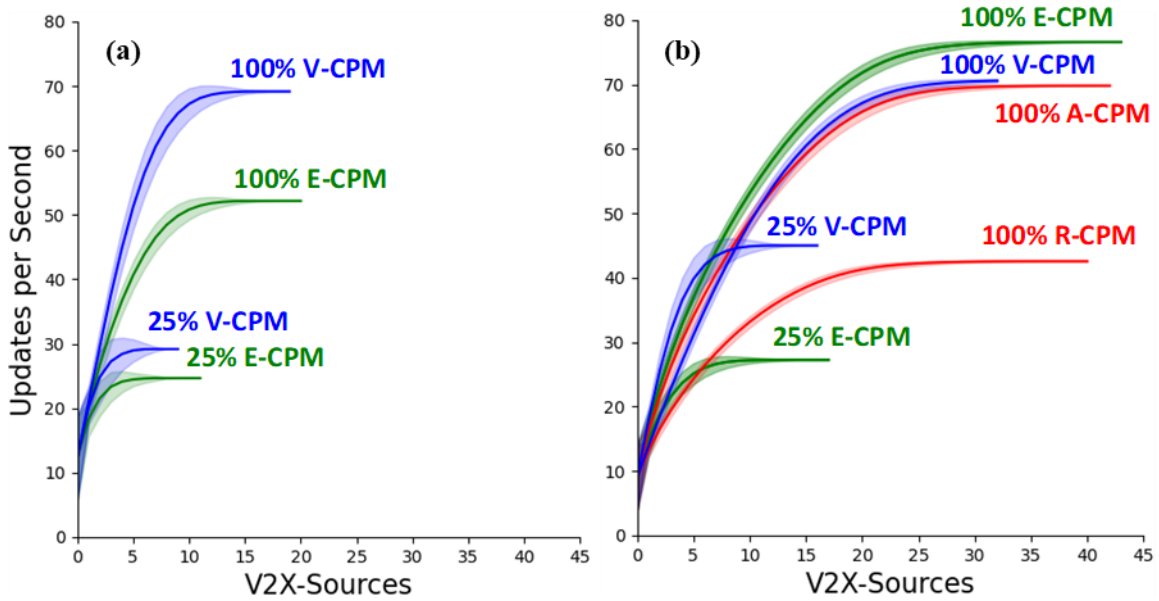


Fig. 40: Updates per second for (a) the low-density scenario and (b) the high-density scenario, displaying the contribution of each connected station for a selection of V2X equipment rates and CPM dissemination modes.

V-CPM on the other side increases the update rate in scenarios where E-CPM does not reach the target CBR. The increase is larger for the high-density scenario, as there are more detected candidate objects to include that were discarded by the E-CPM inclusion filters. Contrary to both DCC-based methods, the change in DOR is caused not by a change in the message frequency, but by a change in the number of objects carried per message. Once the target CBR is reached and eventually exceeded, less relevant objects are excluded from the CPMs to keep the system within the defined CBR levels. This causes a stagnation of the average number of received updates per relevant object in the GEM. As can be seen, the update rate at 100% V2X equipment rate even drops below that of E-CPM. This is in good accordance with the findings of the previous subsection, showing that the number of included objects in V-CPMs falls below that of E-CPM while the transmission rates remain equal. Further, the number of objects of V-CPM is very close to the one of A-CPM, proving a similar performance of both modes in terms of DOR with approximately the same resource demand. Another interesting finding is that the number of independent sources drops by around 24% in V-CPM mode under congested channel conditions as compared to the other modes. This can be explained by the fact that the VoI-contribution of less reliable V2X sources is generally considerably lower than that of more reliable sources.

The underlying mechanisms of V-CPM lead the system to allocate more resources to sources that can contribute more VoI to the VANET.

The analysis showed that A-CPM, R-CPM and V-CPM lead to a more constant DOR regardless of the traffic density and V2X equipment rate compared to E-CPM and P-CPM. However, while the DCC-based dissemination modes only limit the DOR, V-CPM also increases it in low-DOR scenarios, allowing for a more constant performance. Nevertheless, while the disadvantages due to the higher resource demand associated to a higher DOR have already been examined in Subsection 4.3.2 one of the main questions remains: What is the impact of the DOR on the vehicle's perception? This question is investigated in the following subsection dealing with the tracking accuracy of perceived objects.

4.3.3.3. Object Tracking Accuracy

The environmental perception of a road user can be described not only by the fraction of perceived relevant objects and the number of sources for each of these objects but also by the accuracy with which the states of the objects are perceived. The corresponding metric is known as Object Tracking Accuracy (OTA). The OTA can be evaluated for certain measurements (e.g., horizontal positioning error or speed uncertainty) but also for their combinations (e.g., multi-dimensional covariance matrix or general information entropy). In contrast to EAR and DOR, however, their calculation is significantly more complex. Measurements of different objects must be associated, fused, filtered, and the current state of the tracked object must be predicted (for details see [A14] and [A15]). An association is also necessary for the DOR but can take place in post-processing within the scope of the evaluation, which significantly simplifies the process. This is also the reason why OTA-based metrics to date were only rarely used as performance indicators for Collective Perception. Examples in the literature are [256, 257] and [A14]. The CPM study carried out by the C2C-CC on behalf of ETSI deserves special mention. It aims at investigating the optimal representation of the measurement inaccuracies within a CPM, using various OTA-like target metrics [261].

In this subsection, the OTA is expressed in terms of the horizontal positioning accuracy. Although it is one of many relevant measured variables, this choice makes it much easier to interpret the observations due to the application-related meaning of the metric. It should also be mentioned that a completely decoupled evaluation of the inaccuracies of different measured variables is neither possible nor useful. Due to the entanglement of the system through the sensor fusion measurement errors, e.g., in speed and acceleration, as well as latencies (cf. AOI in the DOR subsections) have an influence on the positioning error that

cannot be neglected. An explicit joint consideration of all relevant occurring measurement inaccuracies is offered in Subsection 4.3.4.

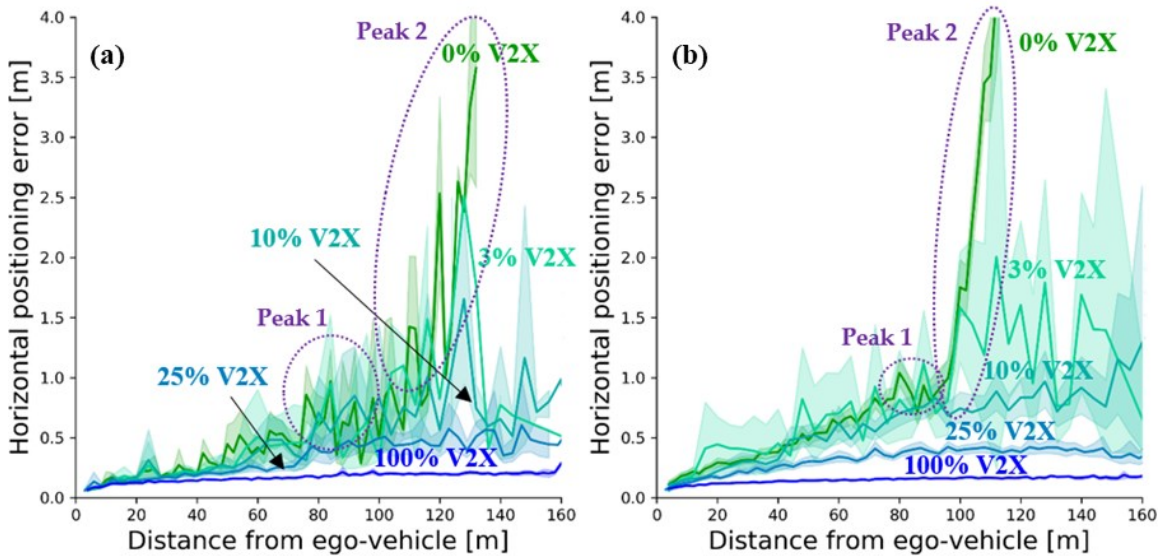


Fig. 41: Object Tracking Accuracies and their standard deviations for (a) the low traffic scenario and (b) the high traffic scenario in dependence of the V2X equipment rate and the distance to the ego vehicle [A14].

Fig. 41 shows the horizontal positioning error as a function of the distance of the tracked object for both examined scenarios. The same V2X equipment rates previously identified as characteristic are displayed again taking the benchmark E-CPM as an example. The decrease in the positioning accuracy of objects in the LEM (0% V2X) increases significantly with increasing distance. On closer inspection, two peaks are apparent. Since Peak 1 in particular is difficult to see due to the nature of the data, the peaks for both scenarios are specially highlighted in Fig. 41. In order to understand their meaning, it makes sense to understand the temporal course of an object in an environmental model. If an unknown object enters the FOV of a station's object-tracking sensor-system, it will only be detected after a certain time, depending on the sensor system's update rate and traffic density. Until its eventual detection, the object penetrates a certain relative-speed-dependent distance into the FOV. The positioning accuracy of the object is still comparatively poor after the first detection. For this reason, if the distance is slightly reduced compared to the sensor range, a first peak (see Peak 1 in Fig. 41) occurs. Due to the positive relative speed, the detected object approaches the ego vehicle in the further course of time. In the course of this approximation, further measurements can be obtained,

whereby the Kalman filter starts to converge, and the positioning accuracy increases. After the minimum distance between the ego vehicle and the object is finally reached, the distance begins to grow again. At the same distance, however, the objects moving-away have a smaller positioning error compared to the approaching objects due to the already converged Kalman filter. If the object finally reaches the edge of the FOV and thus the region around Peak 1, the positioning inaccuracy is still comparatively high, and the object's state can still be predicted for a certain period of time after the object has eventually left the FOV. The greater distance and in particular the lack of further measurements causes the positioning error to increase exponentially in this region causing a second peak (see Peak 2 in Fig. 41). The spread between Peak 1 and Peak 2 is mainly determined by the speed of the objects. It can be clearly seen that the significantly higher speeds in scenario A leads to a more pronounced hysteresis than in scenario B. The different magnitudes of Peak 1 and Peak 2 are owed to the fact that Peak 1 does not only contain newly detected objects approaching the ego vehicle, but also objects with a negative relative speed and thus already converged positioning accuracy.

The examination of the OTA shows new aspects of the benefits of Collective Perception. In addition to a significant expansion of the perception range, there is a noticeable improvement in tracking errors. Only with low equipment rates does the opposite seem counterintuitively to be the case. With equipment rates of 3% and 10%, the OTA is just above that of the LEM. This interesting observation can be explained by the increase in the EAR. The OTA of objects already contained in the LEM is, as actually expected, improved by Collective Perception. In addition, there are other objects that are only perceived via V2X. Since these objects in the LEM have no (or an infinite) positioning error, they are not considered in the OTA of the LEM. Compared to objects also contained in the LEM, however, these objects perceived only by V2X have a significantly poorer positioning accuracy. The connected stations have comparable sensor systems and thus detection accuracies, but data transmitted through V2X communication are subject to additional error sources. The most relevant is the absolute positioning of both sender and recipient [A1]. Objects are perceived in the local reference frame of the sensor system and must be transformed into absolute coordinates by the transmitter. Its GNSS positioning accuracy is crucial for the transformation. Once a message is successfully received, the receiving station then must transform the objects back into its local reference frame, whereby again GNSS errors are induced through error propagation. This effect is dominant at low equipment rates. The averaging of the only slightly improving OTAs in the LEM due to the low equipment rate with the significantly poorer OTAs of objects only detected via Collective Perception thus leads to a decrease in the average OTA at low equipment rates. The higher

the equipment rate, the more the average DOR increases compared to the EAR. The additional measurements lead to an improved OTA of exclusively V2X perceived objects, so that it ultimately surpasses that of the LEM despite the additionally induced GNSS errors. With 100% V2X equipment, an almost constant low positioning error can ultimately be achieved. For a deeper investigation of the distance dependency of the OTA, the interested reader is referred to [A14].

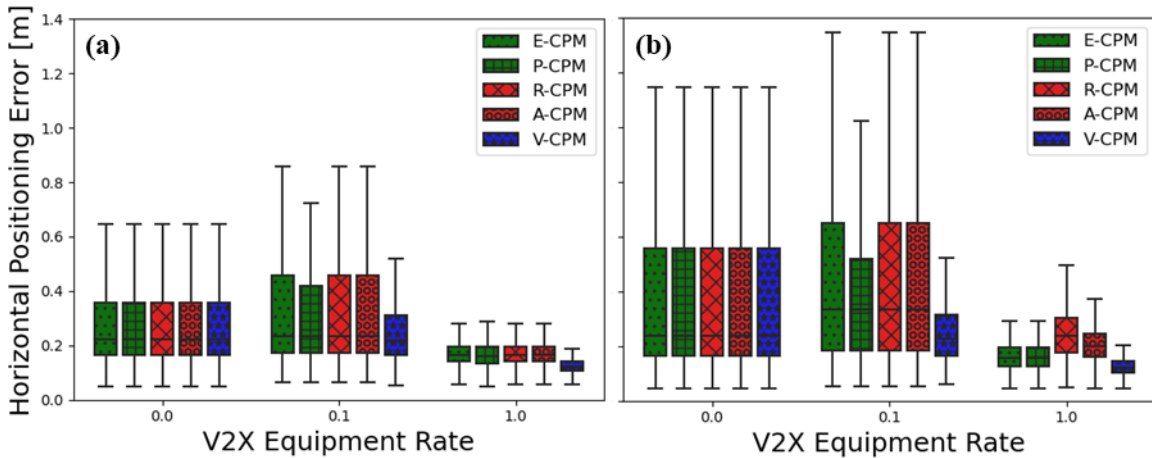


Fig. 42: Object Tracking Accuracy of distinct CPM dissemination modes for (a) the low traffic scenario and (b) the high traffic scenario in dependence of the V2X equipment rate aggregated for the objects within the security range.

After the general effects of Collective Perception on the OTA of road users have been discussed, the OTAs achieved by the different transmission modes are examined next. Fig. 42 shows the OTAs of the various dissemination approaches in aggregated form. First, the drop in OTA that has already been examined is noticeable at low equipment rates. Interestingly, however, this effect does not seem to occur with V-CPM. The reason for this is the significantly increased DOR in both variants examined previously: (i) the higher object update rate and (ii) the higher expectancy value of the number of independent information sources. Another effect occurs with low P-CPM equipment rates. The intelligent resource allocation for objects with a higher VoI-contribution cause P-CPM to achieve a noticeable improvement in the information entropy and thus the accuracy of the GEM compared to E-CPM with an overall identical resource demand. As expected, the DCC-based A-CPM and R-CPM, on the other hand, show only statistical OTA deviations compared to E-CPM with low equipment rates. Another interesting effect occurs with higher equipment rates. While V-CPM further outperforms E-CPM due to the more

intelligent resource allocation, the resource demand of A-CPM, R-CPM and V-CPM decreases compared to the latter. Due to the same underlying object inclusion rules of E-CPM, A-CPM and R-CPM, the in this order decreasing demand of channel resources leads to a corresponding deterioration in the OTA. The situation is different with V-CPM. Despite the lower resource demand, V-CPM presents a better OTA than E-CPM, which suggests that the decentralized global VoI-maximizing resource allocation may outweigh the effect of a lower number of available resources. On the other hand, V-CPM performs slightly worse than P-CPM in the high-load scenarios. This is a clear indication that the optimal target CBR is above that defined by A-DCC. This observation was also confirmed in [A18]. The authors were able to show that the optimal CBR_{tar} for a VoI-driven dissemination of MCMs is $CBR_{tar} \sim 86\%$. However, an optimization of the CBR_{tar} is out of the scope of this thesis and interested readers are referred to the cited work.

4.3.4. Risk Awareness and Safety

The investigation of the simple perception metrics EAR, DOR and OTA carried out in the previous subsection showed that none of them can thoroughly describe the benefits of Collective Perception. Rather, each of these performance indicators considers a specific aspect of the perception capabilities of equipped road users. In the absence of known metrics to quantify the improvement of driving safety, efficiency, and comfort, two candidates were introduced as part of this doctoral thesis [A14]: (i) the newly developed Environmental Risk Awareness (ERA), and the Comprehensive Safety Metric (CSM) adapted from an existing metric to suit the needs of Collective Perception. Based on these metrics, the examined transmission modes are then compared regarding the enhanced risk awareness and traffic safety they provide.

4.3.4.1. Environmental Risk Awareness

As part of the drafting sessions for the Collective Perception Service led by ETSI TC ITS WG1, the lack of a target metric for comparing different CPM generation approaches was identified. The most important two requirements were a comprehensive consideration of all relevant influencing factors with the highest adequate computation simplicity. To mitigate this lack, the ERA was introduced in [A14]. It evaluates how aware a station is of the risk the current traffic situation bears for it. The ERA represents the quotient between perceived risk ERA_p and real risk ERA_0 . The real risk of a traffic situation can be approximated by:

$$ERA_0 = \sum_{i; t_i > 0} \frac{\mu_i}{t_i} \quad (113)$$

The collision factor μ_i represents the severity of a potential collision between the road user classes of ego vehicle and object i . The dynamic state is described by the instantaneous approaching time t_i of object i whose defining motion equation is stated in Eq. 74. Further, only objects with which a collision is possible are considered in the summation in Eq. 113.

The risk perceived by the ego vehicle can be computed in a similar way, additionally accounting for the corresponding uncertainties of each dimension of the state vector:

$$ERA_p = \sum_{i; t_i > 0} \frac{\mu_i}{t_i + u(t_i)} \quad (114)$$

where $u(t)$ corresponds to the uncertainty of the approaching time and can be obtained from:

$$u(t_i) = \sqrt{\vec{v}t_i^T \cdot \Sigma_i \cdot \vec{v}t_i} \quad (115)$$

with Σ_i being the covariance matrix for the state of object i in the ego vehicle's reference frame. The choice of the reference frame implies that Eq. 115 must not only consider the uncertainties of the object's position, velocity, and acceleration among others, but also those of the ego vehicle's state. In the evaluation below, a 95% confidence interval is used, as specified in ETSI's TR for Collective Perception [146]. However, as stated in [A14] also higher order protection levels (e.g., 99.99%) may be used depending on the requirements.

The environmental risk awareness ranges from 0 (no perceived risk, leading to poor risk awareness) to 1 (perceived risk equal to real risk, resulting in a perfect risk awareness). It can simply be computed as:

$$ERA = \frac{ERA_p}{ERA_0} \quad (116)$$

The main strength of the ERA is that it can aggregate all relevant components of the environmental model into one physically meaningful metric. Furthermore, unlike the metrics investigated in the previous subsection, it weighs objects according to their relevance for the analyzed station, making it a very integer metric.

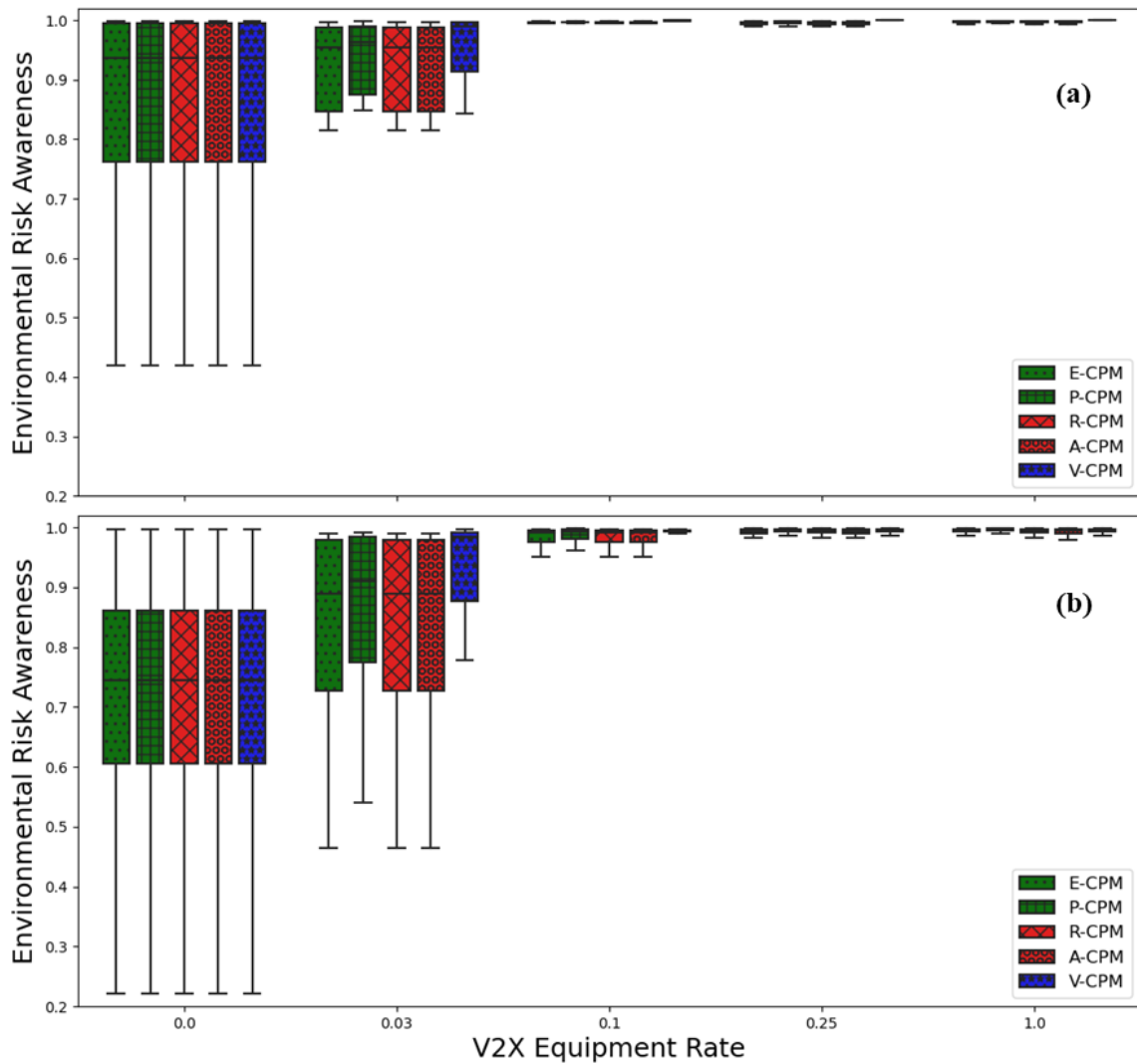


Fig. 43: Environmental Risk Awareness for (a) the low-density scenario and (b) the high-density scenario obtained with the investigated CPM dissemination modes.

The ERA achieved by the different CPM modes is shown in Fig. 43 for a) the low-density and b) the high-density scenario. In contrast to the OTA, undetected objects are also considered, which makes the metric much more meaningful and the results easier to interpret. In 95% of the cases vehicles not participating in Collective Perception estimate the median risk up to 7% (scenario A) and 25% (scenario B) lower than it is. Even if the risk in scenario A is correspondingly high due to the higher vehicle dynamics, the risk perception in this scenario seems to be more robust than in the dense traffic of scenario B due to the better visibility conditions. As expected, the improved environmental awareness

through Collective Perception leads to a significant increase in ERA in both scenarios and all CPM transmission modes. As the V2X equipment rate increases, so does the ERA. With an equipment rate of 100%, the ERA can even be assessed almost completely correctly in 95% of cases.

Compared to the E-CPM, both A-CPM and R-CPM present losses of less than 1% in DCC-active parameter combinations. The losses are therefore reasonably limited for a 95% confidence interval. Expectably, the negative influence of both DCC-based modes is much more devastating in the remaining 5% of the cases. With identical channel access behavior as E-CPM, P-CPM can achieve better EARs for all equipment rates. The ERA increase is strongest at low equipment rates, since even small shifts in the update rates between the transmitted objects have a major impact due to the overall comparatively high update periods. The situation is similar with V-CPM. This mode enables by far the best risk perception of the connected road users with low to medium channel loads. V-CPM can only be outperformed by one of the other transmission modes, namely P-CPM, in the high-density scenario with a full V2X equipment rate. As already discussed, this is due to the higher number of communication resources claimed by P-CPM, which indicates that the CBR_{tar} defined in [211] for Collective Perception is below the optimum (compare findings in [A18]).

Overall, these results strongly encourage the deployment of Collective Perception in future autonomous vehicles, as a highly accurate risk assessment is a strict requirement for their market introduction [A14]. It is worth reminding that for the approval of autonomous vehicles in public transport, however, an almost perfect ERA must be guaranteed even with significantly higher protection levels. The channel load dependent VoI maximization developed within the scope of this work can clearly make an important contribution in this direction.

4.3.4.2. *Comprehensive Safety Metric*

The ERA examined above convinces due to its easy interpretability at the application level and its simple, purely physical definition. However, the probability with which critical situations are recognized is not a direct measure of the safety of the V2X-equipped road users guaranteed by the system. For example, a road user can correctly assess the risk emanating from a certain traffic situation, but under the given circumstances, a reaction is no longer possible. For this reason, a safety metric known from the literature [313] was adapted in [A14] for its applicability to the V2X context. The metric is based on well-known detection and safety models [314, 315], as well as on the accident categories defined by the Ministry of the Interior of the state North Rhine-Westphalia [316]. Just like

the ERA, the Comprehensive Safety Metric (CSM)¹⁶ considers object relevance, detection delays and the potential consequences of the accident based on the classes and relative dynamics of the traffic participant.

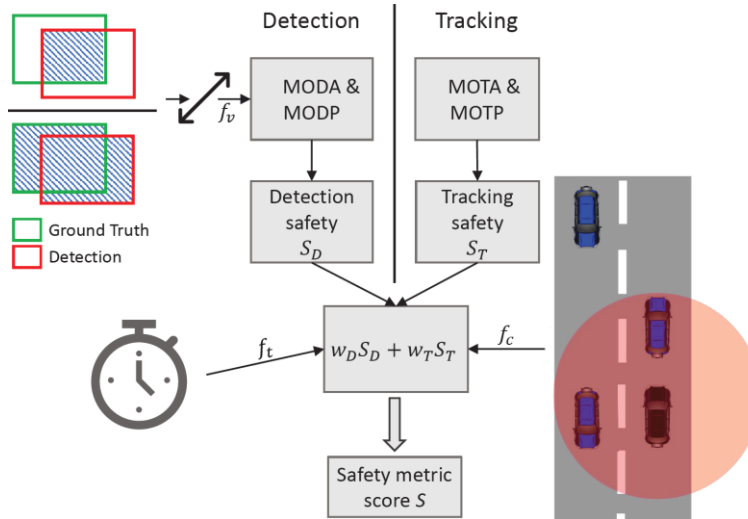


Fig. 44: Schematic visualizing the computation of the Comprehensive Safety Metric. Adopted from [313].

Fig. 44 gives a schematic overview for determining the CSM. It is based on the CLEAR metrics Multiple Object Detection Accuracy (MODA), Multiple Object Detection Precision (MODP), Multiple Object Tracking Precision (MOTP), and Multiple Object Tracking Accuracy (MOTA) [315]. For the computation of the CSM, the detection and tracking accuracies are considered separately. Volk et. al. [313] expanded the metrics to include a verification factor f_v that affects the Intersection over Union (IoU). It ensures that closer and therefore more safety-critical objects are given more importance. In addition, according to [A14], for non-detected objects $\text{IoU} = 0$ is assumed to determine MODP in order to make the metric suitable for sensor networks such as VANETS. As shown in Fig. 44, the separate consideration of detection and tracking evaluation leads to the corresponding interim results for detection safety S_D and tracking safety S_T . The CSM safety score S is then obtained as the weighted sum of both interim results multiplied by a collision factor f_c and a detected time factor f_t . The collision factor f_c is computed based on the severity of a potential collision with objects within the minimal longitudinal and

¹⁶ The word "safety" is generally assigned a variety of meanings, such as "functional safety", "safety of the intended functionality", and "traffic safety". The CSM is based on the context of the latter.

lateral safety distances as defined by the Responsibility-Sensitive Safety (RSS) model [314]. The detected time factor f_t is determined by the elapsed time until an object is detected after entering the safety region. As its name suggests the CSM is a very comprehensive safety metric and the safety levels defined in [313] allow for a straightforward interpretation of the results. However, considering so many relevant factors comes at a price: the high complexity of the CSMs computation. As a thorough description would go beyond the scope of this subsection, the interested reader is kindly referred to [313], and [A14].

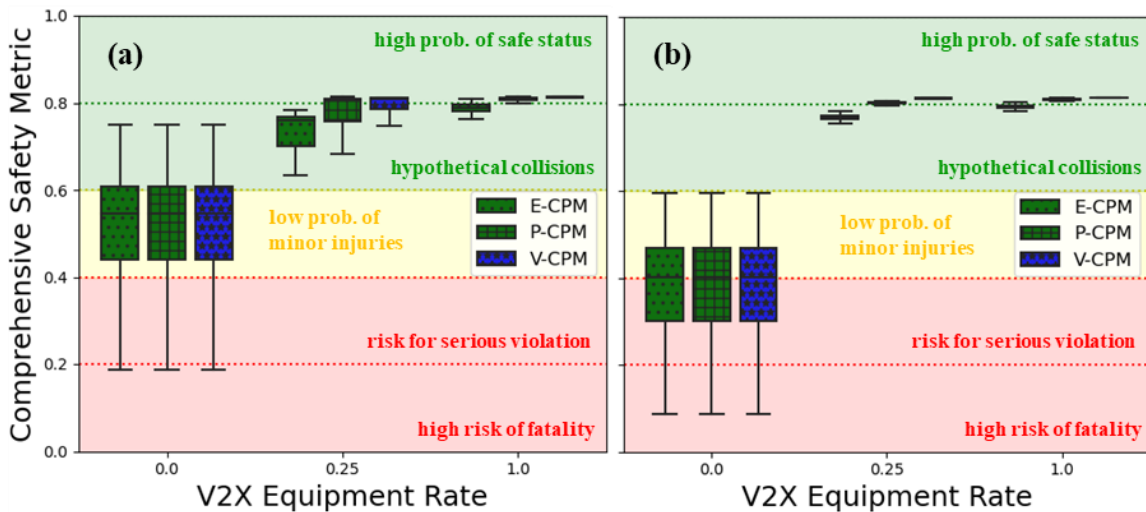


Fig. 45: Comprehensive Safety Metric for (a) the low-density scenario and (b) the high-density scenario obtained with the investigated CPM dissemination modes showing the corresponding safety levels as stated in [313].

Fig. 45 shows the safety score achieved by each CPM mode for both scenarios examined in dependence of characteristic V2X equipment rates. In addition to the safety scores, the figure further depicts the safety levels as defined in [313]. The latter range from high risk of fatality (CSM level I: “insufficient”) to high probability of safe status (CSM level V: “excellent”). A vehicle that only relies on its own on-board sensor system presents an existing risk of serious violation (CSM level II: “bad”) in almost 25% of the driving time with low traffic densities, a low probability of minor injuries (CSM-level III: “good”) in another 50%, and a remaining hypothetical risk of collisions without minor injuries (CSM-level IV: “very good”) only in the remaining 25%. As the analysis of the ERA already suggested, high traffic densities are even more critical. In scenario B, the reduction of the perception range dominates together with the lower inter-vehicle distance compared to the

lower traffic dynamics. These effects cause the 360 ° sensor system to just offer bad or even insufficient safety over half of the driving time. The investigation of both scenarios shows that a vehicle equipped only with a non-redundant 360 ° environment model cannot guarantee sufficient safety for a highly or even fully autonomous operation.

The main purpose of the introduction of Collective Perception is to enhance traffic safety. As can be seen this is achieved as all examined CPM dissemination modes lead to a noticeable improvement in vehicle safety. While the DCC-active modes A-CPM and R-CPM again lead to a performance drop with increased channel loads, P-CPM and especially V-CPM perform significantly better than the benchmark E-CPM. In particular the VoI-based CPM transmission modes can ensure the highest safety level specified by [313] over the entire driving time in both scenarios when the traffic is fully V2X equipped. The fact that P-CPM, which only optimizes the VoI locally, shows slightly better results than V-CPM, which optimizes the VoI globally, is due to the higher number of communications resources consumed. It is therefore to be expected that further safety gains can be achieved through the V-CPM with a corresponding increase in the CBR_{tar} . These findings that the currently defined CBR_{tar} does not fully exploit the potential of the wireless communication channel, were also confirmed by [A18]. In conclusion, it can be observed that while an equipment rate of 25% leads to a very good safety of connected vehicles in all dissemination modes in both low and high traffic density, equipping all road users with P-CPM and even more so with V-CPM at a higher CBR levels can lead to excellent safety. In view of the simplicity of the sensor systems used by the traffic participants, these results are remarkable. In addition, they shed new light on the usefulness of higher V2X equipment rates (> 30%), which could be questioned considering only simple performance metrics such as EAR and DOR examined in Subsection 4.3.3.1 and 4.3.3.2, respectively.

4.3.5. Conclusion

After the application of VALINDRA was discussed step by step in Section 4.2 on the example of Collaborative Localization, Section 4.3 dealt with the comparison of VALINDRA with state-of-the-art resource allocation mechanisms for Collective Perception. The congestion-awareness of VALINDRA proved to optimally exploit the available communication resources achieving a much improved CBR_{tar} tracking accuracy as compared to the investigated benchmarks. It could further be shown that selecting objects for transmission based on the relative information entropy they are expected to contribute to the vehicular network can greatly enhance the performance of the system. This integrated channel-congestion and message-content awareness led to an increase of

up to 10% in environmental awareness. In addition, the negative consequences of too little or too high data redundancies, as encountered with other resource allocation mechanisms, could be prevented. Too little data redundancy generally leads to low update rates, tracking accuracies, and trust in the received data. Excessively high data redundancies, on the other hand, fill the channel unnecessarily and can lead to unacceptable processing latencies and packet losses [A15]. VALINDRA, however, made it possible to keep the data redundancy of tracked objects stable within appropriate limits. The information-entropy-optimized data dissemination also led to significantly increased object tracking accuracies within the CVs' environmental models. For these reasons, the risk awareness of CVs, and thus the overall traffic safety, saw major benefits when CPMs were disseminated based on VALINDRA. Overall, VALINDRA enabled the traffic safety level "excellent" with full penetration rates, while conventional dissemination methods reached "very good" at best, strongly encouraging the future adoption of higher levels of content and congestion awareness in the corresponding communication standards.

5. CONCLUSION AND OUTLOOK

Modern transportation systems are continuously becoming more connected and automated. In view of these developments, connectivity is increasingly emerging as key enabler of future mobility. A multitude of applications have been developed in the past few years, all posing their specific requirements to the enabling communication technologies. Some of the major requirements of traffic safety and efficiency applications are extremely low latencies coupled with sufficiently high reliabilities, which as of today can only be met by direct V2X communication between connected stations. However, as the level of automation of connected stations is rapidly rising, the amount of information needed for their decisions also increases. In order to meet this demand, a fast-growing number of V2X services, such as Cooperative Awareness, Collective Perception, and Maneuver Coordination, have been introduced in recent years. However, the communication resources dedicated to ITS applications are very limited. To maintain high QoS levels an efficient distributed multi-service resource allocation is required to orchestrate the channel access of different C-ITS and the V2X services they feature.

In this context, the main contributions of this doctoral work are four-fold: (i) the development and performance analysis of the value of information aware distributed resource allocation protocol VALINDRA, (ii) the introduction of a new ROS-based simulation and testing environment for ITS technologies TEPLITS, (iii) the introduction of a new V2X service for high-precision localization even in challenging GNSS scenarios, and (iv) the extension and investigation of Collective Perception in view of the progressed standardization at ETSI.

To address the problem of an efficient decentralized resource allocation among different traffic participants and V2X services the value of information aware distributed resource allocation protocol **VALINDRA** was designed. It allows vehicular networks to converge towards a specified optimal channel occupancy while maximizing the value of the shared information. After an initial analytical problem formulation and the subsequent conception of an optimal solution, VALINDRA was investigated theoretically in terms of system stability, convergence speed towards equilibrium in steady state conditions, and tracking accuracy of the targeted channel load. The analytically derived limitations of VALINDRA and its performance in dependence of the environmental conditions were compared to those of state-of-the-art protocols. It could be shown that VALINDRA outperforms the latter under nearly all conditions. Finally, a series of topics were addressed, such as areas of application and compatibility with other ITS protocols.

The analysis of newly designed ITS technologies such as VALINDRA is complex and requires appropriate testing facilities. As testing in real field tests is costly and time consuming, especially with large numbers of C-ITS, virtual test drives have risen as promising alternatives. In lack of sufficiently comprehensive frameworks, the ROS-based test platform for ITS **TEPLITS** was introduced in the scope of this doctoral work. It allows to design and test a large variety of ITS applications and technologies, ensuring a rapid transfer of developed modules into test vehicles. To the best of the authors knowledge, it is the first platform comprising an accurate simulation of road traffic, vehicle dynamics, communication network, and GNSS signal propagation while maintaining the highest possible level of real-world transferability.

Subsequently, based on the findings of field tests carried out in different GNSS coverage scenarios highlighting the need for more advanced positioning technologies, a new V2X service for positioning was introduced and named **Collaborative Localization**. The initial design of the service presented very promising results in terms of improved positioning accuracy and availability. However, the high-precision GNSS time synchronization of the connected stations when accessing the communication channel made an extensive customization of the channel access behavior necessary. Different mechanisms, such as the introduction of a multi-frequency, multi-constellation multipath detection, a FAC layer message generation jitter, and a dynamic message-content- and channel-congestion-aware variation of the message size allowed to improve the positioning accuracy of connected stations to meter-level accuracy in a scenario where standalone positioning evidenced average positioning errors of 2.4 m. The decentralized coordination of the channel access behavior by means of VALINDRA was able to further increase the positioning performance, finally reaching a cooperative positioning accuracy in the order of 0.5 m despite the complexity of the investigated urban environment. Such an enhanced positioning performance is especially relevant for all types of connected distributed systems, as transformations between coordinate frames sensitively depend on the respective absolute positioning accuracies.

Finally, **Collective Perception**, the V2X service that is without doubt currently receiving the most attention of the C-ITS community in view of its advanced state of standardization, was investigated. Among the various utilized performance indicators were channel related metrics, such as the CBR, perception related metrics, such as the environmental awareness ratio, the detected object redundancy, and the object tracking accuracy, as well as the risk awareness and traffic safety metrics introduced in the scope of this doctoral work. In a first step the generation rules of the Collective Perception Service were considerably simplified by introducing a VALINDRA-like VoI for all

transmission-candidate objects, improving their consistency. Despite these simplifications, the new generation rules proved to outperform the current draft of the service's technical specifications in all investigated metrics. The main identified reason for this improvement were the prioritization of objects based on the expected contribution to the network's information entropy. In a second step, the generation rules were extended by VALINDRA. The possibility of allocating resources in a distributed fashion among connected stations based on the value of the information they could contribute yielded another significant increase in the performance of the service. Overall, the previously determined analytical predictions that VALINDRA-based message generation rules would present a much-enhanced tracking accuracy of the targeted channel load could be confirmed using TEPLITS with drone-recorded data from German highways. Finally, it could be shown that Collective Perception based on VALINDRA could improve traffic safety from "very good" to "excellent" with full market penetration as compared to the current generation rules. These results are remarkable when considering that no additional hardware is required.

Despite the very encouraging outcomes it would be presumptuous to equate these with a straightforward market launch. In the following, it is therefore intended to explicitly point out some of the open research topics that should be addressed before an eventual deployment.

The need for a content- and congestion-aware resource allocation is increasingly perceived by the C-ITS community. VALINDRA is a very promising approach, though extensive testing and enhancement is required to reach acceptable maturity levels. At first sight VALINDRA seems to offer a good basis for extensions such as MCO, TPC, and TDC among others, however, the corresponding amendment efforts should not be underestimated.

Collaborative Localization, also just having been introduced, offers high potential for further developments of the technology. Enhanced dissemination mechanisms, more robust multipath detection algorithms, the inclusion of communication signal based local range measurements, the adoption of cutting-edge carrier-phase enhanced algorithms, and the consideration of infrastructure as fixed anchor-points are only a few of the most promising future research directions.

The performance of Collective Perception was shown to directly depend on the additional knowledge each station can contribute to the network. Approaches like the information entropy based VALINDRA thus yield promising results. However, the role of functional safety, the impact of heterogeneously distributed network knowledge, e.g., including vehicles and infrastructure equipped with sensor systems of strongly deviating

characteristics, and the performance in more complex urban scenarios must still be investigated.

The future of road traffic is undoubtedly connected and automated. It is up to us to make it happen!

PUBLICATIONS

- [A1] F. A. Schiegg, T. Frye and F. Wildschütte, "Analysis of the GNSS Error Distribution for the Generation of a Cooperative Environmental Model for Advanced Driver Assistance Systems," in *4th International Conference on Vehicle Technology and Intelligent Transport Systems (VEHITS2018)*, Funchal, Madeira - Portugal, 2018.
- [A2] S. Jesenski, J. E. Stellet, F. A. Schiegg and J. M. Zöllner, "Generation of scenes in intersections for the validation of HAD-functions" in *2019 30th IEEE Intelligent Vehicles Symposium (IV'19)*, Paris, France, 2019.
- [A3] F. A. Schiegg, I. Llatser and T. Michalke, "Object Detection Probability for Highly Automated Vehicles: An Analytical Sensor Model" in *5th International Conference on Vehicle Technology and Intelligent Transport Systems (VEHITS2019)*, Heraklion, Crete - Greece, 2019.
- [A4] F. A. Schiegg, N. Brahmi and I. Llatser, "Analytical Performance Evaluation of the Collective Perception Service in C-V2X Mode 4 Networks" in *2019 IEEE 22nd Intelligent Transportation Systems Conference (ITSC'19)*, Auckland, New Zealand, 2019.
- [A5] F. A. Schiegg, J. Krost, S. Jesenski and J. Frye, "A novel Simulation-Framework for the Design and Testing of Advanced Driver Assistance Systems" in *2019 IEEE 90th Vehicular Technology Conference (VTC2019-Fall)*, Honolulu, Hawaii - USA, 2019.
- [A6] D. Bischoff, F. A. Schiegg, T. Meuser, D. Schuller and R. Steinmetz, "What Cooperation Costs: Communication Quality and Cooperation Cost for Cooperative Vehicular Maneuvering in Large-Scale Scenarios" in *6th International Conference on Vehicle Technology and Intelligent Transport Systems (VEHITS2020)*, Prague, Czech Republic (online), 2020.
- [A7] F. A. Schiegg, D. Bischoff, J. Krost and I. Llatser, "Analytical Performance Evaluation of the Collective Perception Service in IEEE 802.11p Networks" in *2020 IEEE Wireless Communications and Networking Conference (WCNC'20)*, Seoul, South Korea (online), 2020.
- [A8] F. A. Schiegg, S. Li and N. Mikhaylov, "TEPLITS: A comprehensive Test Platform for Intelligent Transportation Systems" in *2020 IEEE 91st Vehicular Technology Conference (VTC2020-Spring)*, Antwerp, Belgium (online), 2020.
- [A9] D. Bischoff, F. A. Schiegg, T. Meuser and R. Steinmetz, "Impact of Imperfect Communication on Cooperative Vehicular Maneuvering at Intersections" in *2020*

- IEEE 91st Vehicular Technology Conference (VTC2020-Spring)*, Antwerp, Belgium (online), 2020.
- [A10] S. Li, N. Mikhaylov and F. A. Schiegg, "Performance analysis of collaborative positioning method in automated car driving", in *2020 International Conference on Localization and GNSS (ICL-GNSS)*, Tampere, Finland (online), 2020.
- [A11] S. Ollander, F. A. Schiegg, F-W. Bode and M. Baum, „Dual-frequency Collaborative Positioning for Minimization of GNSS Errors in Urban Canyons”, in *23rd International Conference on Information Fusion (FUSION)*, Sun City, South Africa (online), 2020.
- [A12] N. Mikhaylov, F. A. Schiegg, S. Li, Y. Jiang, and Y. Liu, "Collaborative positioning in automated car driving: accounting for communication channel and multipath" in *33rd International Technical Meeting of the Satellite Division of The Institute of Navigation (ION GNSS+ 2020)*, St. Louis, Missouri – USA (online), 2020.
- [A13] D. Bischoff, F. A. Schiegg, T. Meuser, D. Schuller, and R. Steinmetz, "Adaptive Heterogeneous V2X Communication for Cooperative Vehicular Maneuvering" in *Klein C., Helfert M., Berns K., Gusikhin O. (eds) Smart Cities, Green Technologies, and Intelligent Transport Systems. SMARTGREENS 2020, VEHITS 2020. Communications in Computer and Information Science, vol 1475. Springer, Cham, 2021.*
- [A14] F. A. Schiegg, I. Llatser, D. Bischoff, and G. Volk, "Collective Perception: A Safety Perspective" in *Sensors*, 21(1), 159, 2021.
- [A15] G. Volk, Q. Delooz, F. A. Schiegg, A. von Bernuth, A. Festag, O. Bringmann, "Towards Realistic Evaluation of Collective Perception for Connected and Automated Driving " in *2021 IEEE 22nd Intelligent Transportation Systems Conference (ITSC'21)*, Indianapolis, Indiana - United States, 2021.
- [A16] F. A. Schiegg, S. Ollander, S. Li, D. Pototzky, I. Llatser, "Collaborative Localization: A new promising V2X Service", in *27th ITS World Congress and Exhibition*, Hamburg, Germany, 2021.
- [A17] F. A. Schiegg, F. Hofmann, F. Wildschütte, I. Llatser, H. Tchouankem, "Removing Blind Spots: Infrastructure-assisted Collective Perception" in *International VDI-Congress Electronics in Vehicles (ELIV'21)*, Bonn, Germany, 2021.
- [A18] D. Bischoff, F.A. Schiegg, T. Meuser, D. Schuller, J. Lemke, and R. Steinmetz, "Prioritizing Relevant Information: Decentralized V2X Resource Allocation for Cooperative Driving", in *IEEE Access*, 9, 135630-135656, 2021.
- [A19] Johan Thunberg, D. Bischoff, F.A. Schiegg, T. Meuser, and Alexey Vinel, "Unreliable V2X Communication in Cooperative Driving: Safety Times for Emergency Braking", in *IEEE Access*, 9, 148024 - 148036, 2021.

REFERENCES

- [1] T. Skutnabb-Kangas and D. Harmon, "Biological Diversity and Language Diversity," in *The Routledge Handbook of Ecolinguistics*, New York, Routledge, 2017, pp. 11-25.
- [2] H. Zhang and R. Mace, "Cultural extinction in evolutionary perspective," *Evolutionary Human Sciences*, vol. 3, no. E30, 2021.
- [3] R. Nuwer, "Languages: Why we must save dying tongues," BBC Future, 6 June 2014. [Online]. Available: <https://www.bbc.com/future/article/20140606-why-we-must-save-dying-languages>. [Accessed 2020 09 27].
- [4] C. Moseley, *The UNESCO atlas of the world's languages in danger: Context and process.*, Cambridge, UK: World Oral Literature Project, 2012.
- [5] G. Ceballos, P. R. Ehrlich, A. D. Barnosky, A. García, R. M. Pringle and T. M. Palmer, "Accelerated modern human-induced species losses: Entering the sixth mass extinction," *Science Advances*, vol. 1, no. 5, 2015.
- [6] J. M. de Vos, L. N. Joppa, J. L. Gittleman, P. R. Stephens and S. L. Pimm, "Estimating the normal background rate of species extinction," *Conservation Biology*, vol. 29, no. 2, p. 452–62, 2015.
- [7] T. Kaneda, C. Greenbaum and K. Kline, "2020 World Population Data Sheet," Population Reference Bureau, Washington DC, 2020.
- [8] United Nations, Department of Economic and Social Affairs, "World Population Prospects: The 2019 Revision," United Nations, New York, USA, 2019.
- [9] T. Kaneda and C. Haub, "How Many People Have Ever Lived on Earth?," Population Reference Bureau, 18 May 2021. [Online]. Available: <https://www.prb.org/articles/how-many-people-have-ever-lived-on-earth/>. [Accessed 27 September 2021].
- [10] S. C. Davis, S. E. Williams and R. G. Boundy, *Transportation Energy Data Book: Edition 36.2*, Oak Ridge, TN - USA: Oak Ridge National Laboratory, 2018.
- [11] S. C. Davis, S. W. Diegel and R. G. Boundy, *Transportation Energy Data Book: Edition 30*, Oak Ridge, TN - USA: Oak Ridge National Laboratory, 2011.
- [12] S. C. Davis and R. G. Boundy, *Transportation Energy Data Book: Edition 38.2*, Oak Ridge, TN - USA: Oak Ridge National Laboratory, 2020.
- [13] World Health Organization (WHO), "Global status report on road safety 2018," World Health Organization, Geneva, Switzerland, 2018.

- [14] World Health Organization (WHO), "WHO methods and data sources for global causes of death 2000-2019. Global Health Estimates Technical Paper WHO/DDI/DNA/GHE/2020.2.," World Health Organization, Geneva, 2020.
- [15] United Nations, Department of Economic and Social Affairs, Population Dynamics Division, "World Population Prospects 2019," United Nations, New York, 2019 .
- [16] World Health Organization (WHO), "Global Health Estimates 2019: Deaths by Cause, Age, Sex, by Country and by Region, 2000-2019," World Health Organization, Geneva, 2020.
- [17] World Health Organization (WHO), "Road traffic injuries," World Health Organization, 21 June 2021. [Online]. Available: <https://www.who.int/news-room/fact-sheets/detail/road-traffic-injuries>. [Accessed 9 October 2021].
- [18] S. Chen, M. Kuhn, K. Prettner and D. E. Bloom, "The global macroeconomic burden of road injuries: estimates and projections for 166 countries," *The Lancet Planetary Health*, vol. 3, no. 9, pp. e390-e398, 2019.
- [19] World Bank, "The World Bank database, gross savings (% of GDP)," [Online]. Available: <https://data.worldbank.org/indicator/NY.GNS.ICTR.ZS>. [Accessed 9 October 2021].
- [20] World Bank, "The World Bank Database, Global Economic Prospects," 30 September 2021. [Online]. Available: <https://datacatalog.worldbank.org/search/dataset/0037888>. [Accessed 9 October 2021].
- [21] S. L. James, D. Abate, K. H. Abate, S. M. Abay, C. Abbafati, N. Abbasi and A. M. Briggs, "Global, regional, and national incidence, prevalence, and years lived with disability for 354 diseases and injuries for 195 countries and territories, 1990–2017: a systematic analysis for the Global Burden of Disease Study 2017," *The Lancet*, vol. 392, no. 10159, pp. 1789-1858, 2018.
- [22] Texas A&M Transportation Institute; INRIX, Inc., "2015 Urban Mobility Scorecard," August 2015. [Online]. Available: <https://trid.trb.org/view/1367337>. [Accessed 9 October 2021].
- [23] European Commission, "Hours spent in road congestion annually | Mobility and Transport," [Online]. Available: https://ec.europa.eu/transport/facts-fundings/scoreboard/compare/energy-union-innovation/road-congestion_en#2017. [Accessed 9 October 2021].
- [24] INRIX Location Analytics, "Berlin ist Deutschlands Stauhauptstadt - INRIX," [Online]. Available: <https://inrix.com/press-releases/scorecard-2018-de/>. [Accessed 9 October 2021].
- [25] University of Leeds, "One-fifth Of Fossil-fuel Emissions Absorbed By Threatened Forests," *ScienceDaily*, 19 February 2009.

- [26] Centre for Economics and Business Research (Cebr), "50% Rise in Gridlock Costs by 2030," CEBR, 14 October 2014. [Online]. Available: <https://cebr.com/reports/the-future-economic-and-environmental-costs-of-gridlock/>. [Accessed 14 October 2021].
- [27] C. Benz, "Patent DRP 37435 - Vehicle with gas engine operation (German; Fahrzeug mit Gasmotorenbetrieb)," German Imperial Patent Office, Berlin, Germany, January 1886.
- [28] J. Bähr and P. Erker, *Bosch: Geschichte eines Weltunternehmens*, CH Beck, 2013.
- [29] K. Rabe, *Aller Laster Anfang. Technik, Geschichte und Geschichten*, Braunschweig: Westermann, 1985.
- [30] D. Patrascu, "Braking Systems History," *Autoevolution*, 20 May 2009. [Online]. Available: <https://www.autoevolution.com/news/braking-systems-history-6933.html>. [Accessed 23 October 2021].
- [31] S. Moyer, "Mr. 'Trafficlight'," *Motor News. Automobile Club of Michigan*, no. 27, pp. 14-15, March 1947.
- [32] Daimler AG, "Patent No. DBP 854 157, life-saver of thousands," Daimler AG, 23 January 2009. [Online]. Available: <https://media.daimler.com/marsMediaSite/en/instance/ko.xhtml?oid=9913733>. [Accessed 23 October 2021].
- [33] N. I. Bohlin, "A Statistical Analysis of 28,000 Accidents with Emphasis on Occupant Restraint Value," SAE Technical Paper 670925, 1967.
- [34] S. O. Grady, "The man who saved a million lives: Nils Bohlin - inventor of the seatbelt," *The Independent*, 23 October 2011. [Online]. Available: <https://www.independent.co.uk/life-style/motoring/features/man-who-saved-million-lives-nils-bohlin-inventor-seatbelt-1773844.html>. [Accessed 23 October 2021].
- [35] N. Ravop, "Allen K. Breed, 72, a Developer of Air Bag Technology for Cars," *The New York Times*, 14 January 2000.
- [36] Daimler AG, "März 1981: Airbag und Gurtstrammer feiern Weltpremiere," Daimler AG, 7 February 2011. [Online]. Available: <https://media.daimler.com/marsMediaSite/de/instance/ko/Maerz-1981-Airbag-und-Gurtstrammer-feiern-Weltpremiere.xhtml?oid=9915294>. [Accessed 7 October 2021].
- [37] Daimler AG, "Mercedes-Benz and the invention of the anti-lock braking system: ABS, ready for production in 1978," Daimler AG, 1 July 2008. [Online]. Available: <https://media.daimler.com/marsMediaSite/en/instance/ko.xhtml?oid=9913502>. [Accessed 7 October 2021].

- [38] Toyota Motor Corporation, "75 Years of Toyota: Technical Development - Electronics Parts," Toyota Motor Corporation, [Online]. Available: http://www.toyota-global.com/company/history_of_toyota/75years/data/automotive_business/products_technology/technology_development/electronics_parts/index.html. [Accessed 14 August 2021].
- [39] Daimler AG, "Mercedes-Benz S-Class, W 220 series (1998 to 2005)," Daimler AG, 11 May 2009. [Online]. Available: <https://media.daimler.com/marsMediaSite/en/instance/ko.xhtml?oid=9273052>. [Accessed 23 October 2021].
- [40] Daimler AG, "Technical highlights of the CL-Class and its predecessor series," Daimler AG, 1 July 2010. [Online]. Available: <https://media.daimler.com/marsMediaSite/en/instance/ko/Technical-highlights-of-the-CL-Class-and-its-predecessor-series.xhtml?oid=9271770>. [Accessed 23 October 2021].
- [41] Proto Corporation, "Subaru Legacy Lancaster - Lancaster ADA Specification," Proto Corporation, [Online]. Available: https://www.goo-net-exchange.com/catalog/SUBARU__LEGACY_LANCASTER/4501945/. [Accessed 23 October 2021].
- [42] H. Winner, S. Hakuli and G. Wolf, Handbuch Fahrerassistenzsysteme, Wiesbaden, Deutschland: Vieweg+Teubner - GWV Fachverlage GmbH, 2009.
- [43] Honda Motor Co., Ltd., "Honda Announces a Full Model Change for the Inspire," Honda Motor Co., Ltd., 18 June 2003. [Online]. Available: <https://global.honda/newsroom/news/2003/4030618-inspire-eng.html>. [Accessed 23 October 2021].
- [44] IEEE 802.11p-2010, "IEEE Standard for Information technology - Local and metropolitan area networks - Specific requirements - Part 11: Wireless LAN Medium Access Control (MAC) and Physical Layer (PHY) Specifications Amendment 6: Wireless Access in Vehicular Environments," IEEE, 2010.
- [45] ETSI EN 302 663 V1.2.0 (2012-11), "Intelligent Transport Systems (ITS); Access layer specification for Intelligent Transport Systems operating in the 5 GHz frequency band," European Telecommunications Standards Institute (ETSI), 2012.
- [46] SAE J2735_200612, "V2X Communications Message Set Dictionary," SAE International, 2006.
- [47] ARIB STD-T109 Version 1.0, "Association of Radio Industries and Businesses. 700 MHz Band Intelligent Transport Systems," ARIB Standard, 2012.
- [48] SAE International, "SAE International Releases Updated Visual Chart for Its "Levels of Driving Automation" Standard for Self-Driving Vehicles," SAE International, 11 December 2018. [Online]. Available: <https://www.sae.org/news/press-room/2018/12/sae-international-releases-updated-visual-chart-for-its-%E2%80%9D-Clevels-of-driving-automation%E2%80%9D-standard-for-self-driving-vehicles>. [Accessed 24 April 2020].

- [49] S. Abuelsamid, "Toyota Has Big Plans To Get Cars Talking To Each Other And Infrastructure In The U.S.," *Forbes*, 16 April 2018. [Online]. Available: <https://www.forbes.com/sites/samabuelsamid/2018/04/16/toyota-launches-aggressive-v2x-communications-roll-out-from-2021/?sh=51496eb0146c>. [Accessed 23 October 2021].
- [50] MarkLines, "Toyota ITS Connect: New system equipped in Prius and other models - Real-time road information transmitted to improve safety of autonomous vehicles," *Automotive Industry Portal - MarkLines*, 30 May 2016. [Online]. Available: https://www.marklines.com/en/report_all/rep1487_201604. [Accessed 23 October 2021].
- [51] Audi MediaCenter, "Der neue Audi A8 – hochautomatisiertes Fahren auf Level 3," Audi AG, 11 September 2017. [Online]. Available: <https://www.audi-mediacyber.com/de/per-autopilot-richtung-zukunft-die-audi-vision-vom-autonomen-fahren-9305/der-neue-audi-a8-hochautomatisiertes-fahren-auf-level-3-9307>. [Accessed 23 October 2021].
- [52] L. P. Vellequette, "Audi A8's semi-autonomous features face legal hurdles," *Automotive News*, 12 July 2017. [Online]. Available: <https://www.autoweek.com/news/technology/a1825671/audis-semi-autonomous-a8-faces-legal-hurdles/>. [Accessed 23 October 2021].
- [53] B. Conrad, "Audi stoppt Pläne für teilautonomen A8," *Motor Presse Stuttgart GmbH & Co. KG*, 30 Apr 2020. [Online]. Available: <https://www.auto-motor-und-sport.de/tech-zukunft/audi-a8-autonom-level-3-gesetz-grundlage/>. [Accessed 23 October 2021].
- [54] 3GPP TR 21.914 V14.0.0 (2018-05), "Release 14 Description; Summary of Rel-14 Work Items (Release 14)," 3rd Generation Partnership Project (3GPP), 2018.
- [55] BMVI - Mobilität, Digitales, "Gesetz zum autonomen Fahren tritt in Kraft," Bundesministerium für Verkehr und digitale Infrastruktur, 27 Juli 2021. [Online]. Available: <https://www.bmvi.de/SharedDocs/DE/Artikel/DG/gesetz-zum-autonomen-fahren.html>. [Accessed 23 October 2021].
- [56] M. Culver, "More Than 11.2 Million Vehicles Will Be Equipped with V2X Communications in 2024, IHS Markit Says," *IHS Markit*, 16 May 2019. [Online]. Available: https://news.ihsmarkit.com/prviewer/release_only/slug/automotive-more-112-million-vehicles-will-be-equipped-v2x-communications-2024-ihs-mark. [Accessed 23 October 2021].
- [57] A. Turley, "Euro NCAP and German Automobile Club ADAC Confirm Life-Saving Potential of V2X," *NXP Semiconductors*, 25 March 2020. [Online]. Available: <https://www.nxp.com/company/blog/euro-ncap-and-german-automobile-club>

adac-confirm-life-saving-potential-of-v2x:BL-NCAP-ADAC-CONFIRM-POTENTIAL-OF-V2X. [Accessed 23 October 2021].

- [58] Euro NCAP, "Volkswagen Safety Technology Rewarded by Euro NCAP," Euro NCAP, 18 March 2020. [Online]. Available: <https://www.euroncap.com/en/press-media/press-releases/volkswagen-safety-technology-rewarded-by-euro-ncap/>. [Accessed 23 October 2021].
- [59] W. Rudschies, "C2X im VW Golf 8: Erster ADAC Test," Allgemeine Deutsche Automobil-Club e. V., 14 July 2020. [Online]. Available: <https://www.adac.de/rundums-fahrzeug/tests/assistentensysteme/c2x-im-vw-golf-8/?redirectId=quer.c2x>. [Accessed 23 October 2021].
- [60] J. Harding, G. Powell, R. Yoon, J. Fikentscher, C. Doyle, D. Sade, ... and J. Wang, "Vehicle-to-vehicle communications: readiness of V2V technology for application (No. DOT HS 812 014)," National Highway Traffic Safety Administration (NHTSA), United States, 2014.
- [61] NHTSA, "2020 Fatality Data Show Increased Traffic Fatalities During Pandemic," National Highway Traffic Safety Administration (NHTSA), 3 June 2021. [Online]. Available: <https://www.nhtsa.gov/press-releases/2020-fatality-data-show-increased-traffic-fatalities-during-pandemic>. [Accessed 23 October 2021].
- [62] NHTSA, "Traffic Safety Facts Annual Report, May 2021," May 2021. [Online]. Available: <https://cdan.nhtsa.gov/tsftables/National%20Statistics.pdf>. [Accessed 23 October 2021].
- [63] Texas A&M Transportation Institute; INRIX, Inc., "2021 Urban Mobility Report and Appendices," June 2021. [Online]. Available: <https://mobility.tamu.edu/umr/report/>. [Accessed 23 October 2021].
- [64] M. I. Khan, S. Sesia and J. Harri, "In Vehicle Resource Orchestration for Multi-V2X Services," in *2019 IEEE 90th Vehicular Technology Conference (VTC2019-Fall)*, Honolulu, HI - USA , 2019.
- [65] M. Bijelic, T. Ritter and W. Gruber, "Benchmarking Image Sensors Under Adverse Weather Conditions for Autonomous Driving," in *IEEE Intelligent Vehicles Symposium (IV)*, Changshu, 2018.
- [66] A. J. Hawkins, "Waymo's autonomous vehicles keep getting stuck in a dead-end street in San Francisco," The Verge, 14 October 2021. [Online]. Available: <https://www.theverge.com/2021/10/14/22726534/waymo-autonomous-vehicles-stuck-san-francisco-dead-end>. [Accessed 23 October 2021].
- [67] A. J. Hawkins, "The investigation into Tesla Autopilot's emergency vehicle problem is getting bigger," The Verge, 14 September 2021. [Online]. Available:

- <https://www.theverge.com/2021/9/14/22673497/tesla-nhtsa-autopilot-investigation-data-ford-gm-vw-toyota>. [Accessed 23 October 2021].
- [68] F. d. P. Müller, E. M. Diaz and I. Rashdan, "Cooperative positioning and radar sensor fusion for relative localization of vehicles," in *IEEE Intelligent Vehicles Symposium (IV)*, Gothenburg, 2016.
- [69] A. Festag, "Standards for Vehicular Communication - from IEEE 802.11p to 5G," in *e & i Elektrotechnik und Informationstechnik* 132.7, 2015.
- [70] FCC 99-305, "Amendment of Parts 2 and 90 of the Commission's Rules to Allocate the 5.850-5.925 GHz Band to the Mo-bile Service for Dedicated Short Range Communications of Intelligent Transportation Services - ET Docket No. 98-95, RM-9096," Federal Communications Commission (FCC), Washington DC, United States, October 1999.
- [71] US Department of Transportation, "5.9 GHz Transportation Safety Band Testing," 6 April 2021. [Online]. Available: <https://www.transportation.gov/research-and-technology/59-ghz-transportation-safety-band-testing>. [Accessed 23 October 2021].
- [72] NYC Connected Vehicle Project, "Connected Vehicle technology is coming to the streets of New York City! This technology holds the potential to make our streets safer and smarter," New York City Department of Transportation, [Online]. Available: <https://www.cvp.nyc/>. [Accessed 23 October 2021].
- [73] U.S. Department of Transportation, "New York City (NYC) DOT Pilot," [Online]. Available: https://www.its.dot.gov/pilots/pilots_nycdot.htm. [Accessed 23 October 2021].
- [74] U.S. Department of Transportation, "Wyoming (WY) DOT Pilot," [Online]. Available: https://www.its.dot.gov/pilots/pilots_wydot.htm. [Accessed 23 October 2021].
- [75] Wyoming Department of Transportation, "WYOMING DOT Connected Vehicle Pilot - Improving safety and travel reliability on I-80 in Wyoming," [Online]. Available: <https://wydotcvp.wyoroad.info/>. [Accessed 23 October 2021].
- [76] U.S. Department of Transportation, "Ann Arbor Connected Vehicle Test Environment (AACVTE)," [Online]. Available: https://www.its.dot.gov/research_archives/safety/aacvte.htm. [Accessed 23 October 2021].
- [77] University of Michigan Transportation Research Institute (UMTRI), "Ann Arbor Connected Vehicle Test Environment (AACVTE)," [Online]. Available: <https://aacvte.umtri.umich.edu/>. [Accessed 23 October 2021].
- [78] Virginia Tech Transportation Institute (VTTI), "Virginia Connected Corridors," [Online]. Available: <https://www.vtti.vt.edu/vcc/>. [Accessed 23 October 2021].

- [79] Virginia Transportation Research Council, "Virginia Connected Corridors Next," [Online]. Available: <http://vtrc.virginiadot.org/ProjDetails.aspx?Id=647>. [Accessed 23 October 2021].
- [80] Harding, J.; Powell, G., R.; Yoon, R.; Fikentscher, J.; Doyle, C.; Sade, D.; Lukuc, M.; Simons, J.; Wang, J., "Vehicle-to-Vehicle Communications: Readiness of V2V Technology for Application (Report No. DOT HS 812 014)," U.S. Department of Transportation - National Highway Traffic Safety Administration (NHTSA), Washington DC, United States, August 2014.
- [81] National Highway Traffic Safety Administration (NHTSA), Department of Transportation (DOT)., "Federal Motor Vehicle Safety Standards: Vehicle-to-Vehicle (V2V) Communications - A Proposed Rule by the National Highway Traffic Safety Administration on 08/20/2014 (ANPRM 79 FR 49270)," Federal Register, United States, 2014.
- [82] FCC-CIRC1912-YY, "FACT SHEET: Use of the 5.850-5.925 GHz Band Notice of Proposed Rulemaking – ET Docket No. 19-138," Federal Communications Commission (FCC), United States, 2019.
- [83] IEEE 802.11ac-2013, "IEEE Standard for Information technology--Telecommunications and information exchange between systems--Local and metropolitan area networks--Specific requirements--Part 11: Wireless LAN Medium Access Control (MAC) and Physical Layer (PHY) Specifications--A," IEEE, 2013.
- [84] IEEE 802.11ax-2021, "IEEE Standard for Information Technology--Telecommunications and Information Exchange between Systems Local and Metropolitan Area Networks--Specific Requirements Part 11: Wireless LAN Medium Access Control (MAC) and Physical Layer (PHY) Specifications Ame," IEEE, 2021.
- [85] Federal Communications Commission (FCC), "Use of the 5.850–5.925 GHz Band - 47 CFR Parts 2, 15, 90 and 95 [ET Docket No. 19–138; FCC 20–164; FR ID 17510]," Federal Register, United States, 2021.
- [86] USDOT Spectrum Team, "Concerns with Draft FCC NPRM: Use of the 5.850-5.925 GHz Band [ET Docket No. 19-138]," U.S. Department of Transportation (USDOT), United States, 2019.
- [87] Commission of the European Communities, "Commission Decision 2008/671/EC: On the harmonised use of radio spectrum in the 5875-5905 MHz frequency band for safety-related applications of Intelligent Transport Systems (ITS)," Official Journal of the European Union, Brussels, Belgium, 2008.
- [88] ETSI EN 302 571 V1.1.1 (2008-09), "Harmonized European Standard (Telecom. series): Intelligent Transport Systems (ITS); Radiocommunications equipment operating in the 5 855 MHz to 5 925 MHz frequency band; Harmonized EN covering

the essential requirements of article 3.2 of the R&TTE Directive," European Telecommunications Standards Institute (ETSI), Sophia Antipolis Cedex, France, 2008.

- [89] European Parliament, Council of the European Union , "Directive 2010/40/EU of the European Parliament and of the Council of 7 July 2010 on the framework for the deployment of Intelligent Transport Systems in the field of road transport and for interfaces with other modes of transport Text with EEA relevance," Official Journal of the European Union, Brussels, European Union, 2010.
- [90] ECC Recommendation (08)01, "Use of the band 5855-5875 MHz for Intelligent Transport Systems (ITS)," CEPT/ECC, Copenhagen, Denmark, 2020.
- [91] ECC Decision (08)01, "The harmonised use of Safety-Related Intelligent Transport Systems (ITS) in the 5875-5935 MHz frequency band," CEPT/ECC, Copenhagen, Denmark, 2020.
- [92] Europe Daily Bulletin No. 12291, "EU Council confirms objection to delegated act on deployment of cooperative intelligent transport systems," Agence Europe, July 2019.
- [93] C-Roads, "C-Roads - The Platform of harmonised C-its deployment in europe," AustriaTech – Gesellschaft des Bundes für technologiepolitische Maßnahmen GmbH, [Online]. Available: <https://www.c-roads.eu/platform.html>. [Accessed 23 October 2021].
- [94] Atelier VorSicht, "Cooperative ITS Corridor Joint deployment," Bundesministerium für Verkehr und digitale Infrastruktur (BMVI), Wiesbaden, Germany, 2015.
- [95] TRIMIS, "SCOOP@F Part 2," Transport Research and Innovation Monitoring and Information System, [Online]. Available: <https://trimis.ec.europa.eu/project/scoopf-part-2>. [Accessed 23 October 2021].
- [96] G. Hanson, "The UK Corridor –A2/M2 Connected Vehicle Corridor," British Department for Transport, [Online]. Available: <https://amsterdamgroup.mett.nl/downloads/handlerdownloadfiles.ashx?idnv=486686>. [Accessed 23 October 2021].
- [97] Nordic Way GmbH, "Your companion on the northern road," [Online]. Available: <https://www.nordic-way.eu/en/>. [Accessed 23 October 2021].
- [98] InterCor, "Interoperable Corridors Deploying Cooperative Intelligent Transport Systems," [Online]. Available: <https://intercor-project.eu/>. [Accessed 23 October 2021].
- [99] European Commission, "COMMISSION IMPLEMENTING DECISION (EU) 2020/1426 of 7 October 2020 on the harmonised use of radio spectrum in the 5 875-5 935 MHz frequency band for safety-related applications of intelligent transport systems (ITS)

- and repealing Decision 2008/671/EC," Official Journal of the European Union, Brussels, Belgium, October 2020.
- [100] 5GAA Automotive Association, "Deployment band configuration for C-V2X at 5.9 GHz in Europe," Position Paper, Munich, Germany, 2021.
- [101] International Telecommunication Union, Radiocommunication Sector, "M.1453: Intelligent transport systems - Dedicated short range communications at 5.8 GHz," ITU-R, Recommendation M.1453-2 (06/2005), June 2005.
- [102] J. Choi, V. Marojevic, C. B. Dietrich, J. H. Reed and S. Ahn, "Survey of Spectrum Regulation for Intelligent Transportation Systems," *IEEE Access*, vol. 8, pp. 140145 - 140160, 2020.
- [103] ACMA, "Radiocommunications (Intelligent Transport Systems) Class Licence 2017," Australian Communications and Media Authority (ACMA), 2017.
- [104] IMDA, "Decision issued by the IMDA: Regulatory Framework and Standards for Intelligent Transport Systems ("ITS") in the 5.9 GHz (5.875 - 5.925 GHz) Frequency Band," Info-Communications Media Development Authority, Mapletree Business City, Singapore, 2017.
- [105] MarketsandMarkets, "Connected Car Market by Service (OTA Update, Navigation, Cybersecurity, Multimedia Streaming, Social Media, e-Call, Autopilot, Home Integration & Other), Form, End Market (OE, Aftermarket), Network, Transponder, Hardware & Region - Global Forecast to 2025," MarketsandMarkets Research Private. Ltd., Pune, India, 2020.
- [106] M. Cäsar, R. Mehl, S. Tschödrich, M. Pauli, B. Ruther, R. Wendt, D. Blöchl, A. Stotz, M. Völko, W. Song and W. Dupont, "Connected Vehicle Trend Radar - The drive to add value: lessons from China," Capgemini Invent, Paris, France, 2019.
- [107] MarketsAndMarkets, "Automotive V2X Market by Connectivity (DSRC, and Cellular), Communication (V2V, V2I, V2P, V2G, V2C, and V2D), Vehicle (Passenger Car, and Commercial Vehicle), Propulsion (ICE and EV), Unit, Offering, Technology, and Region - Global Forecast to 2028," MarketsandMarkets Research Private Ltd., Pune, India, 2020.
- [108] MarketsandMarkets, "Automotive V2X Market worth \$12,859 million by 2028," MarketsandMarkets Research Private Ltd., Pune, India, 2020.
- [109] TechVisionGroup of Frost & Sullivan, "Vehicle-to-Everything Technologies for Connected Cars - DSRC and Cellular Technologies Drive Opportunities," Frost & Sullivan, New York, United States, 2017.
- [110] K. Serizawa, M. Mikami, K. Moto and H. Yoshino, "Field Trial Activities on 5G NR V2V Direct Communication Towards Application to Truck Platooning," in *2019 IEEE 90th Vehicular Technology Conference (VTC2019-Fall)*, Honolulu, HI, USA, 2019.

- [111] E. Verlinden, "The sense of virtual sensors," Siemens AG, 6 September 2018. [Online]. Available: <https://blogs.sw.siemens.com/simcenter/the-sense-of-virtual-sensors/>. [Accessed 23 October 2021].
- [112] Robert Bosch GmbH, "Road Signature - Enables reliable localization for automated vehicles at all times based on data from radar and video sensors," Robert Bosch GmbH, [Online]. Available: <https://www.bosch-mobility-solutions.com/en/solutions/automated-driving/road-signature/>. [Accessed 23 October 2021].
- [113] Y. Dobrev, M. Vossiek, M. Christmann, I. Bilous and P. Gulden, "Steady delivery: Wireless local positioning systems for tracking and autonomous navigation of transport vehicles and mobile robots," *IEEE Microwave Magazine*, vol. 6, no. 18, pp. 26-37, 2017.
- [114] W. Sakpere, M. Adeyeye-Oshin and N. B. Mlitwa, "A state-of-the-art survey of indoor positioning and navigation systems and technologies," *South African Computer Journal*, vol. 29, no. 3, pp. 145-197, 2017.
- [115] S. H. Rezatofghi, A. Milan, Z. Zhang, Q. Shi, A. Dick and I. & Reid, "Joint probabilistic data association revisited," in *IEEE International Conference on Computer Vision (ICCV)*, 2015.
- [116] R. E. Kalman, "A new approach to linear filtering and prediction problems," *Transaction of the ASME, Journal of Basic Engineering*, pp. 35-45, 1960.
- [117] P. Del Moral, "Non Linear Filtering: Interacting Particle Solution," *Markov Processes and Related Fields*, vol. 2, no. 4, p. 555-580, 1996.
- [118] F. R. Kschischang, B. J. Frey and H.-A. Loeliger, "Factor Graphs and the Sum-Product Algorithm," *IEEE Transactions on Information Theory*, vol. 47, no. 2, pp. 498-519, 2001.
- [119] Robert Bosch GmbH, "The Car as 3rd living space," Robert Bosch GmbH, [Online]. Available: <https://www.bosch.com/stories/the-car-as-3rd-living-space/>. [Accessed 23 October 2021].
- [120] ITU-T X.200, "Information technology – Open Systems Interconnection – Basic Reference Model: The basic model," ITU Telecommunication Standardization Sector (ITU-T), 1983.
- [121] ISO 35.100, "Open systems interconnection (OSI)," International Organization for Standardization (ISO), 1984.
- [122] ETSI TS 101 539-1 V1.1.1 (2013-08), "Intelligent Transport Systems (ITS);V2X Applications; Part 1: Road Hazard Signalling (RHS) application requirements specification," European Telecommunications Standards Institute (ETSI), 2013.

- [123] ETSI TS 101 539-2 V1.1.1 (2018-06), "Intelligent Transport Systems (ITS); V2X Applications; Part 2: Intersection Collision Risk Warning (ICRW) application requirements specification," European Telecommunications Standards Institute (ETSI), 2018.
- [124] ETSI TS 101 539-3 V1.1.1 (2013-11), "Intelligent Transport Systems (ITS); V2X Applications; Part 3: Longitudinal Collision Risk Warning (LCRW) application requirements specification," European Telecommunications Standards Institute (ETSI), 2013.
- [125] ISO 20901:2020, "Intelligent transport systems — Emergency electronic brake light systems (EEBL) — Performance requirements and test procedures," ISO/TC 204, 2020.
- [126] M. Mueck and . Karls, *Networking Vehicles to Everything: Evolving Automotive Solutions*, Berlin, Germany: Walter de Gruyter GmbH & Co KG, 2018.
- [127] C-Roads Germany, "Green light optimal speed advisory," ITS mobility GmbH , [Online]. Available: <https://www.c-roads-germany.de/english/c-its-services/glosa/>. [Accessed 23 October 2021].
- [128] C2C-CC, "Guidance for day 2 and beyond roadmapCAR 2 CAR Communication Consortium," Car 2 Car Communication Consortium, 2019.
- [129] M. Botte, L. Pariota, L. D'Acerno and G. N. Bifulco, "An overview of cooperative driving in the European Union: Policies and practices," *Electronics*, vol. 8, no. 6, p. 616, 2019.
- [130] ISO/TS 19091:2019, "Intelligent transport systems — Cooperative ITS — Using V2I and I2V communications for applications related to signalized intersections," ISO/TC 204, 2019.
- [131] ISO/TS 19321:2020, "Intelligent transport systems — Cooperative ITS — Dictionary of in-vehicle information (IVI) data structures," ISO/TC 204 , 2020.
- [132] Office of the Assistant Secretary for Research and Technology, "CV Pilot Deployment Program - Connected Vehicle Applications," U.S. Department of Transportation, [Online]. Available: https://www.its.dot.gov/pilots/cv_pilot_apps.htm. [Accessed 23 October 2021].
- [133] ETSI TR 101 607 V1.2.1 (2020-02), "Intelligent Transport Systems (ITS); Cooperative ITS (C-ITS); Release 1," European Telecommunications Standards Institute (ETSI), 2020.
- [134] 5GAA, "White Paper: A visionary roadmap for advanced driving use cases, connectivity technologies, and radio spectrum needs," 5G Automotive Association, 2020.

- [135] ETSI TR 102 638 V1.1.1 (2009-06), "Intelligent Transport Systems (ITS); Vehicular Communications; Basic Set of Applications; Definitions," European Telecommunications Standards Institute (ETSI), 2009.
- [136] SAE J2735_202007, "V2X Communications Message Set Dictionary," Society of Automotive Engineers (SAE) International, 2020.
- [137] Y. Shengbo, "ITU-T Meeting Report: Introduction of China C-V2X Industry and Standards," China Society of Automotive Engineers (C-SAE) & China Industry Innovation Alliance for the Intelligent and Connected Vehicles (CAICV), 2020.
- [138] Volkswagen AG, "Car2X: The new era of intelligent vehicle networking," Volkswagen AG, [Online]. Available: <https://www.volkswagenag.com/en/news/stories/2018/10/car2x-networked-driving-comes-to-real-life.html>. [Accessed 23 October 2021].
- [139] ETSI EN 302 637-2 V1.3.2 (2014-11), "Intelligent Transport Systems (ITS); Vehicular Communications; Basic Set of Applications; Part 2: Specification of Cooperative Awareness Basic Service," European Telecommunications Standards Institute (ETSI), 2014.
- [140] ETSI TS 103 300-2 V2.1.1 (2020-05), "Intelligent Transport System (ITS); Vulnerable Road Users (VRU) awareness; Part 2: Functional Architecture and Requirements definition; Release 2," European Telecommunications Standards Institute (ETSI), 2020.
- [141] SAE J2945/9_201703, "Vulnerable Road User Safety Message Minimum Performance Requirements," Society of Automotive Engineers (SAE) International, 2017.
- [142] ETSI EN 302 637-3 V1.2.1 (2014-09), "Intelligent Transport Systems (ITS); Vehicular Communications; Basic Set of Applications; Part 3: Specifications of Decentralized Environmental Notification Basic Service," European Telecommunications Standards Institute (ETSI), 2014.
- [143] ETSI TS 102 637-3 V1.1.1 (2010-09), "Intelligent Transport Systems (ITS); Vehicular Communications; Basic Set of Applications; Part 3: Specifications of Decentralized Environmental Notification Basic Service," European Telecommunications Standards Institute (ETSI), 2010.
- [144] SAE J2945/4 (WIP), "Road Safety Applications," Society of Automotive Engineers (SAE) International, 2016.
- [145] ETSI TS 103 324 V0.0.22 (2021-05), "Intelligent Transport Systems (ITS); Vehicular Communications; Basic Set of Applications; Specification of the Cooperative Perception Service," European Telecommunications Standards Institute (ETSI), 2021.
- [146] ETSI TR 103 562 V2.1.1 (2019-12), "Intelligent Transport System (ITS); Vehicular Communications; Basic Set of Applications; Analysis of the Collective Perception Service (CPS)," European Telecommunications Standards Institute (ETSI), 2019.

- [147] SAE J3224 (WIP), "V2X Sensor-Sharing for Cooperative & Automated Driving," Society of Automotive Engineers (SAE) International, 2019.
- [148] A. Minetto, A. Gurrieri and F. Dovis, "A Cognitive Particle Filter for Collaborative DGNSS Positioning," *IEEE Access*, vol. 8, no. 194765-194779, 2020.
- [149] B. Huang, Z. Yao, X. Cui and M. Lu, "Dilution of precision analysis for GNSS collaborative positioning," *IEEE Transactions on Vehicular Technology*, vol. 65, no. 5, pp. 3401-3415, 2015.
- [150] G. Zhang, B. Xu, H. F. Ng and L. T. Hsu, "GNSS RUMS: GNSS Realistic Urban Multiagent Simulator for Collaborative Positioning Research," *Remote Sensing*, vol. 13, no. 4, p. 544, 2021.
- [151] ENSEMBLE Project, "ENSEMBLE - Platooning Together," Nederlandse Organisatie voor toegepast-natuurwetenschappelijk onderzoek, [Online]. Available: <https://platooningensemble.eu/>. [Accessed 23 October 2021].
- [152] B. Atanassow and K. Sjöberg, "Platooning protocol definition and Communication strategy," D2.8of H2020 project ENSEMBLE, 2018.
- [153] A. Vinel, L. Lan and N. Lyamin, "Vehicle-to-vehicle communication in C-ACC/platooning scenarios," *IEEE Communications Magazine*, vol. 53, no. 8, pp. 192-197, 2015.
- [154] A. Böhm, M. Jonsson and E. Uhlemann, "Performance comparison of a platooning application using the IEEE 802.11p MAC on the control channel and a centralized MAC on a service channel," in *2013 IEEE 9th International Conference on Wireless and Mobile Computing, Networking and Communications (WiMob)*, Lyon, France, 2013.
- [155] T. Bijlsma and T. Hendriks, "A fail-operational truck platooning architecture," in *2017 IEEE Intelligent Vehicles Symposium (IV)*, Los Angeles, CA - USA , 2017.
- [156] ETSI TR 103 298 V0.0.4 (2019-01), "Intelligent Transport Systems (ITS); Platooning; Pre-standardization study," European Telecommunications Standards Institute (ETSI), 2019.
- [157] TransAID Project, "TransAID - Transition Areas for Infrastructure-Assisted Driving," [Online]. Available: <https://www.transaid.eu/>. [Accessed 23 October 2021].
- [158] PAC V2X Project, "PAC-V2X - Perception Augmentée par Coopération V2X," [Online]. Available: <http://www.pacv2x.fr/>. [Accessed 23 October 2021].
- [159] IMAGinE Project, "IMAGinE – Solutions for Cooperative Driving," Verbundprojekt IMAGinE (Intelligente Manöver Automatisierung - kooperative Gefahrenvermeidung in Echtzeit), [Online]. Available: <https://www.imagine-online.de/en/home>. [Accessed 23 October 2021].

- [160] A. Correa, R. Alms, J. Gozalvez, M. Sepulcre, M. Rondinone, R. Blokpoel, L. Lücken and G. Thandavarayan, "Infrastructure support for cooperative maneuvers in connected and automated driving," in *2019 IEEE Intelligent Vehicles Symposium (IV)*, Paris, France, 2019.
- [161] ETSI TR 103 578 V0.0.6 (2021-10), "Intelligent Transport System (ITS); Vehicular Communications; Vehicular Communications; Informative report for the Maneuver Coordination Service," European Telecommunications Standards Institute (ETSI), 2021.
- [162] ETSI TS 103 561 V0.0.1 (2018-01), "Intelligent Transport Systems (ITS); Vehicular Communications; Basic Set of Applications; Maneuver Coordination Service," European Telecommunications Standards Institute (ETSI), 2018.
- [163] SAE J3186 (WIP), "Application Protocol and Requirements for Maneuver Sharing and Coordinating Service," Society of Automotive Engineers (SAE) International, 2018.
- [164] ETSI EN 302 636-5-1 V2.1.0 (2017-05), "Intelligent Transport Systems (ITS); Vehicular Communications; GeoNetworking; Part 5: Transport Protocols; Sub-part 1: Basic Transport Protocol," European Telecommunications Standards Institute (ETSI), 2017.
- [165] ETSI TS 103 248 V1.2.1 (2018-08), "Intelligent Transport Systems (ITS); GeoNetworking; Port Numbers for the Basic Transport Protocol (BTP)," European Telecommunications Standards Institute (ETSI), 2018.
- [166] ETSI EN 302 636-4-1 V1.3.1 (2017-08), "Intelligent Transport Systems (ITS); Vehicular Communications; GeoNetworking; Part 4: Geographical addressing and forwarding for point-to-point and point-to-multipoint communications; Sub-part 1: Media-Independent Functionality," European Telecommunications Standards Institute (ETSI), 2017.
- [167] ETSI TS 102 636-4-2 V1.2.1 (2020-04), "Intelligent Transport Systems (ITS); Vehicular Communications; GeoNetworking; Part 4: Geographical addressing and forwarding for point-to-point and point-to-multipoint communications; Sub-part 2: Media-dependent functionalities for ITS-G5," European Telecommunications Standards Institute (ETSI), 2020.
- [168] ETSI TS 103 613 V1.1.1 (2018-11), "Intelligent Transport Systems (ITS); Access layer specification for Intelligent Transport Systems using LTE Vehicle to everything communication in the 5,9 GHz frequency band," European Telecommunications Standards Institute (ETSI), 2018.
- [169] J. Wannstrom, "LTE-Advanced," 3rd Generation Partnership Project (3GPP), June 2013. [Online]. Available: <https://www.3gpp.org/technologies/keywords-acronyms/97-lte-advanced>. [Accessed 23 October 2021].

- [170] 3GPP TR 21.915 V0.5.0 (2018-12), "Release 15 Description; Summary of Rel-15 Work Items," 3rd Generation Partnership Project (3GPP), 2018.
- [171] IEEE 802.11a-1999, "IEEE Standard for Telecommunications and Information Exchange Between Systems - LAN/MAN Specific Requirements - Part 11: Wireless Medium Access Control (MAC) and physical layer (PHY) specifications: High Speed Physical Layer in the 5 G," IEEE, 1999.
- [172] IEEE 802.11p-2010, "IEEE Standard for Information technology-- Local and metropolitan area networks-- Specific requirements-- Part 11: Wireless LAN Medium Access Control (MAC) and Physical Layer (PHY) Specifications Amendment 6: Wireless Access in Vehicular Environments," IEEE, 2010.
- [173] IEEE 802.11e-2005, "IEEE Standard for Information technology--Local and metropolitan area networks--Specific requirements--Part 11: Wireless LAN Medium Access Control (MAC) and Physical Layer (PHY) Specifications - Amendment 8: Medium Access Control (MAC) Quality of Service," IEEE, 2005.
- [174] C. F. Mecklenbrauker, A. F. Molisch, J. Karedal, F. Tufvesson, A. Paier, L. Bernado, T. Zemen, O. Klemp and N. Czink, "Vehicular channel characterization and its implications for wireless system design and performance.," *Proceedings of the IEEE*, vol. 99, no. 7, pp. 1189-1212, 2011.
- [175] W. Anwar, S. Dev, A. Kumar, N. Franchi and G. Fettweis, "PHY Abstraction Techniques for V2X Enabling Technologies: Modeling and Analysis," *IEEE Transactions on Vehicular Technology*, vol. 70, no. 2, pp. 1501-1517, 2021.
- [176] R. Molina-Masegosa, J. Gozalvez and M. Sepulcre, "Comparison of IEEE 802.11p and LTE-V2X: An Evaluation With Periodic and Aperiodic Messages of Constant and Variable Size," *IEEE Access*, vol. 8, pp. 121526-121548, 2020.
- [177] T. Shimizu, H. Lu, J. B. Kenney and S. Nakamura, "Comparison of DSRC and LTE-V2X PC5 Mode 4 Performance in High Vehicle Density Scenarios," in *ITS World Congress 2019*, Singapore, 2019.
- [178] G. Naik, B. Choudhury and J.-M. Park, "IEEE 802.11bd & 5G NR V2X: Evolution of Radio Access Technologies for V2X Communications," *IEEE Access*, vol. 7, pp. 70169-70184, 2019.
- [179] IEEE P802.11bd (NGV), "IEEE P802.11-TASK GROUP BD (NGV) MEETING UPDATE - Status of Project IEEE P802.11bd," IEEE, [Online]. Available: https://www.ieee802.org/11/Reports/tgbd_update.htm. [Accessed 23 October 2021].
- [180] H. Sun and H. Zhang, "802.11 NGV proposed PAR," IEEE 802.11-18/086lr8, 2018.

- [181] B. Y. Yacheur, T. Ahmed and M. Mosbah, "Analysis and Comparison of IEEE 802.11p and IEEE 802.11bd," in *Communication Technologies for Vehicles: 15th International Workshop, Nets4Cars/Nets4Trains/Nets4Aircraft 2020*, Bordeaux, France, 2020.
- [182] H. Gu and K. Moerman, "Choosing the right V2X technology - Straight talk on DSRC and 5G," NXP Semiconductors, 2020.
- [183] 3GPP TR 36.843 V12.0.1 (2014-03), "Study on LTE Device to Device Proximity Services; Radio Aspects (Release 12)," 3rd Generation Partnership Project (3GPP), 2014.
- [184] 3GPP TR 21.915 V15.0.0 (2019-09), "Release 15 Description; Summary of Rel-15 Work Items (Release 15)," 3rd Generation Partnership Project, 2019.
- [185] 3GPP TS 36.300 V16.6.0 (2021-06), "Evolved Universal Terrestrial Radio Access (E-UTRA) and Evolved Universal Terrestrial Radio Access Network (E-UTRAN); Overall description; Stage 2 (Release 16)," 3rd Generation Partnership Project (3GPP), 2021.
- [186] 3GPP TR 37.985 V16.0.0 (2020-06), "Overall description of Radio Access Network (RAN) aspects for Vehicle-to-everything (V2X) based on LTE and NR (Release 16)," 3rd Generation Partnership Project (3GPP), 2020.
- [187] 3GPP TS 36.331 V16.6.0 (2021-09), "Evolved Universal Terrestrial Radio Access (E-UTRA); Radio Resource Control (RRC); Protocol specification (Release 16)," 3rd Generation Partnership Project (3GPP), 2021.
- [188] M. Gonzales-Martín, M. Sepulcre, R. Molina-Masegosa and J. Gozalvez, "Analytical Models of the Performance of C-V2X Mode 4 Vehicular Communications," *IEEE Transactions on Vehicular Technology*, vol. 68, no. 2, pp. 1155-1166, Feb. 2019.
- [189] W. Anwar, N. Franchi and G. Fettweis, "Physical Layer Evaluation of V2X Communications Technologies: 5G NR-V2X, LTE-V2X, IEEE 802.11bd, and IEEE 802.11p," in *2019 IEEE 90th Vehicular Technology Conference (VTC2019-Fall)*, Honolulu, HI, USA, 2019.
- [190] 3GPP TR 21.916 V16.0.1 (2021-09), "Release 16 Description; Summary of Rel-16 Work Items (Release 16)," 3rd Generation Partnership Project (3GPP), 2021.
- [191] 3GPP, "Release 17," 3rd Generation Partnership Project (3GPP), 12 December 2020. [Online]. Available: <https://www.3gpp.org/release-17>. [Accessed 23 October 2021].
- [192] 3GPP TS 37.324 V16.3.0 (2021-06), "E-UTRA and NR; Service Data Adaptation Protocol (SDAP) specification (Release 16)," 3rd Generation Partnership Project (3GPP), 2021.
- [193] 3GPP TS 38.214 V16.7.0 (2021-09), "NR; Physical layer procedures for data (Release 16)," 3rd Generation Partnership Project (3GPP), 2021.

- [194] M. Harounabadi, D. M. Soleymani, S. Bhadauria, M. Leyh and E. Roth-Mandutz, "V2X in 3GPP Standardization: NR Sidelink in Release-16 and Beyond," *IEEE Communications Standards Magazine*, vol. 5, no. 1, pp. 12-21, 2021.
- [195] M. H. C. Garcia, A. Molina-Galan, M. Boban, J. Gozálvez, B. Coll-Perales, T. Şahin and A. Kousaridas, "A Tutorial on 5G NR V2X Communications," *IEEE Communications Surveys & Tutorials*, vol. 23, no. 3, pp. 1972-2026, 2021.
- [196] ETSI TS 102 723-1 V1.1.1 (2012-11), "Intelligent Transport Systems (ITS);OSI cross-layer topics; Part 1: Architecture and addressing schemes," European Telecommunications Standards Institute (ETSI), 2012.
- [197] ETSI TS 102 723-3 V1.1.1 (2012-11), "Intelligent Transport Systems (ITS); OSI cross-layer topics; Part 3: Interface between management entity and access layer," European Telecommunications Standards Institute (ETSI), 2012.
- [198] ETSI TS 102 723-4 V1.1.1 (2012-11), "Intelligent Transport Systems (ITS); OSI cross-layer topics; Part 4: Interface between management entity and networking & transport layer," European Telecommunications Standards Institute (ETSI), 2012.
- [199] ETSI TS 102 723-5 V1.1.1 (2012-11), "Intelligent Transport Systems (ITS); OSI cross-layer topics; Part 5: Interface between management entity and facilities layer," European Telecommunications Standards Institute (ETSI), 2012.
- [200] ETSI TS 102 723-6 V1.1.1 (2012-11), "Intelligent Transport Systems; OSI cross-layer topics; Part 6: Interface between management entity and security entity," European Telecommunications Standards Institute (ETSI), 2012.
- [201] ETSI TS 102 723-2 V1.1.1 (2012-11), "Intelligent Transport Systems (ITS);OSI cross-layer topics; Part 2: Management information base," European Telecommunications Standards Institute (ETSI), 2012.
- [202] ETSI TS 102 731 V1.1.1 (2010-09), "Intelligent Transport Systems (ITS);Security;Security Services and Architecture," European Telecommunications Standards Institute (ETSI), 2010.
- [203] ETSI TS 102 940 V1.3.1 (2018-04), "Intelligent Transport Systems (ITS);Security; ITS communications security architecture and security management," European Telecommunications Standards Institute (ETSI), 2018.
- [204] ETSI TS 103 097 V1.3.1 (2017-10), "Intelligent Transport Systems (ITS); Security; Security header and certificate formats," European Telecommunications Standards Institute (ETSI), 2017.
- [205] E. B. Hamida, H. Noura and W. Znaidi, "Security of Cooperative Intelligent Transport Systems: Standards, Threats Analysis and Cryptographic Countermeasures," *Electronics*, vol. 4, no. 3, pp. 380-423, 2015.

- [206] ETSI EN 302 571 V2.1.1 (2017-02), "Harmonized European Standard: Intelligent Transport Systems (ITS); Radiocommunications equipment operating in the 5 855 MHz to 5 925 MHz frequency band; Harmonised Standard covering the essential requirements of article 3.2 of Directive 2014/53/EU," European Telecommunications Standards Institute (ETSI), 2017.
- [207] ETSI TS 103 175 V1.1.1 (2015-06), "Intelligent Transport Systems (ITS); Cross Layer DCC Management Entity for operation in the ITS G5A and ITS G5B medium," European Telecommunications Standards Institute (ETSI), 2015.
- [208] ETSI TS 103 141 V2.1.1 (2021-11), "Intelligent Transport Systems; Facilities layer; Communication congestion control; Release 2," European Telecommunications Standards Institute (ETSI), 2021.
- [209] S. Kuk and H. Kim, "Preventing Unfairness in the ETSI Distributed Congestion Control," *IEEE Communications Letters*, vol. 18, no. 7, pp. 1222 - 1225, 2014.
- [210] A. Autolitano, M. Reineri, R. M. Scopigno, C. Campolo and A. Molinaro, "Understanding the channel busy ratio metrics for decentralized congestion control in VANETs," in *2014 International Conference on Connected Vehicles and Expo (ICCVE)*, Vienna, Austria, 2014.
- [211] ETSI TS 102 687 V1.2.1 (2018-04), "Intelligent Transport Systems (ITS); Decentralized Congestion Control Mechanisms for Intelligent Transport Systems operating in the 5 GHz range; Access layer part," European Telecommunications Standards Institute (ETSI), 2018.
- [212] M. Sepulcre and J. Gozalvez, "Coordination of Congestion and Awareness Control in Vehicular Networks," *Electronics*, vol. 7, no. 11, p. 335, 2018.
- [213] G. Thandavarayan, M. Sepulcre and J. Gozalvez, "Cooperative Perception for Connected and Automated Vehicles: Evaluation and Impact of Congestion Control," *IEEE Access*, vol. 8, pp. 197665 - 197683, 2020.
- [214] G. Bansal, J. Kenney and C. Rohrs, "LIMERIC: A Linear Adaptive Message Rate Algorithm for DSRC Congestion Control," *IEEE Transactions on Vehicular Technology*, vol. 62, pp. 4182-4197, 2013.
- [215] G. Bansal and J. Kenney, "Controlling Congestion in Safety-Message Transmissions: A Philosophy for Vehicular DSRC Systems," *IEEE Vehicular Technology Magazine*, vol. 8, pp. 20-26, 2013.
- [216] A. Rostami, B. Cheng, G. Bansal, K. Sjöberg, M. Gruteser and J. B. Kenney, "Stability Challenges and Enhancements for Vehicular Channel Congestion Control Approaches," *IEEE Transactions on Intelligent Transportation Systems*, vol. 17, no. 10, pp. 2935 - 2948, Oct. 2016.

- [217] H. Friis, "A Note on a Simple Transmission Formula," *IEEE Proceedings of the IRE*, vol. 34, no. 5, pp. 254-256, 1946.
- [218] H. Schumacher and T. H. Narcisse, "Highway Propagation Modeling in VANETs and Its Impact on Performance Evaluation," in *2013 10th Annual IEEE/IFIP Conference on Wireless On-Demand Network Systems and Services (WONS 2013)*, Banff, AB, Canada, 2013.
- [219] M. Killat and H. Hartenstein, "An empirical model for probability of packet reception in vehicular ad hoc networks," *EURASIP Journal on Wireless Communications and Networking*, pp. 1-12, 2009.
- [220] H. Tchouankem, T. Zinchenko and H. Schumacher, "Impact of buildings on vehicle-to-vehicle communication at urban intersections," in *2015 12th Annual IEEE Consumer Communications and Networking Conference (CCNC)*, Las Vegas, NV, USA, 2015.
- [221] H. Tchouankem, T. Zinchenko, H. Schumacher and L. Wolf, "Effects of vegetation on vehicle-to-vehicle communication performance at intersections," in *2013 IEEE 78th Vehicular Technology Conference (VTC Fall)*, Las Vegas, NV, USA, 2013.
- [222] A. Patil, M. Deeksha, N. Shekar, V. Shet and M. Kulkarni, "Transmit Data Rate Control Based Decentralized Congestion Control Mechanism for VANETs," in *2019 International Conference on Data Science and Communication (IconDSC)*, Bangalore, India, 2019.
- [223] C. B. Math, A. Ozgur, S. H. de Groot and H. Li, "Data rate based congestion control in v2v communication for traffic safety applications," *2015 IEEE Symposium on Communications and Vehicular Technology in the Benelux (SCVT)*, pp. 1-6, 2015.
- [224] 3GPP TS 36.214 V16.2.0 (2021-03), "Evolved Universal Terrestrial Radio Access (E-UTRA); Physical layer; Measurements (Release 16)," 3rd Generation Partnership Project (3GPP), 2021.
- [225] 3GPP TS 36.213 V16.7.1 (2021-10), "Evolved Universal Terrestrial Radio Access (E-UTRA); Physical layer procedures (Release 16)," 3rd Generation Partnership Project (3GPP), 2021.
- [226] 3GPP TS 38.215 V16.4.0 (2020-12), "NR; Physical layer measurements (Release 16)," 3rd Generation Partnership Project (3GPP), 2020.
- [227] A. Mansouri, V. Martinez and J. Härri, "A First Investigation of Congestion Control for LTE-V2X Mode 4," in *2019 15th Annual Conference on Wireless On-demand Network Systems and Services (WONS)*, Wengen, Switzerland , 2019.
- [228] ETSI TS 103 574 V1.1.1 (2018-11), "Intelligent Transport Systems (ITS); Congestion Control Mechanisms for the C-V2X PC5 interface;Access layer part," European Telecommunications Standards Institute (ETSI), 2018.

- [229] B. Toghi, M. Saifuddin, Y. P. Fallah and M. O. Mughal, "Analysis of Distributed Congestion Control in Cellular Vehicle-to-everything Networks," in *2019 IEEE 90th Vehicular Technology Conference (VTC2019-Fall)*, Honolulu, HI, USA , 2019.
- [230] 3GPP TR 38.885 V16.0.0 (2019-03), "NR; Study on NR Vehicle-to-Everything (V2X) (Release 16)," 3rd Generation Partnership Project (3GPP), 2019.
- [231] E. Cinque, "An adaptive strategy to mitigate instability in the ETSI DCC: Experimental validation," in *2017 15th International Conference on ITS Telecommunications (ITST)*, Warsaw, Poland , 2017.
- [232] N. Lyamin, A. Vinel, D. Smely and B. Bellalta, "ETSI DCC: Decentralized Congestion Control in C-ITS," *IEEE Communications Magazine*, vol. 56, no. 12, pp. 112-118, December 2018.
- [233] Q. Delooz, A. Festag and A. Vinel, "Revisiting Message Generation Strategies for Collective Perception in Connected and Automated Driving," in *VEHICULAR - The Ninth International Conference on Advances in Vehicular Systems, Technologies and Applications*, (online), 2020.
- [234] I. Khan and J. Härrri, "Integration Challenges of Facilities-Layer DCC for Heterogeneous V2X Services," in *2018 IEEE Intelligent Vehicles Symposium (IV)*, Changshu, China , 2018.
- [235] S. Kuk, S. Yang, Y. Park and H. Kim, "On the connectivity problem of ETSI DCC algorithm," 15 March 2017. [Online]. Available: <http://arxiv.org/abs/1703.05174>.
- [236] S. Yang and H. Kim, "Configuring ETSI DCC parameters for better performance and stability," *Electronics Letters*, vol. 52, no. 8, pp. 667-669, 2016.
- [237] G. Bansal, H. Lu, J. Kenney and C. Poellabauer, "EMBARC: Error Model Based Adaptive Rate Control for Vehicle-to-Vehicle Communications," *ACM Press*, p. 41, 25 June 2013.
- [238] T. Tielert, D. Jiang, Q. Chen, L. Delgrossi and H. Hartenstein, "Design methodology and evaluation of rate adaptation based congestion control for Vehicle Safety Communications," in *2011 IEEE Vehicular Networking Conference (VNC)*, Amsterdam, Netherlands, 2011.
- [239] T. Lorenzen and M. Garrosi, "Achieving Global Fairness at Urban Intersections Using Cooperative DSRC Congestion Control," *ACM Press*, p. 52–59, 2016.
- [240] E. Egea-Lopez and P. Pavon-Mariño, "Distributed and Fair Beaconing Rate Adaptation for Congestion Control in Vehicular Networks," *IEEE Transactions on Mobile Computing* , vol. 15, no. 12, pp. 3028-3041, 2016.

- [241] J. Gozalvez and M. Sepulcre, "Opportunistic-Driven Adaptive Radio Resource Management Technique for Efficient Wireless Vehicular Communications," in *2007 IEEE 66th Vehicular Technology Conference*, Baltimore, MD, USA, 2007.
- [242] J. Gozalvez and M. Sepulcre, "Channel efficiency of adaptive transmission techniques for wireless vehicular communications," in *Proceedings of the International World Congress on ITS*, New York, NY, USA, 2008.
- [243] M. Sepulcre, J. Gozalvez, J. Härri and H. Hartenstein, "Application-Based Congestion Control Policy for the Communication Channel in VANETs," *IEEE Communications Letters*, vol. 14, no. 10, pp. 951-953, 2010.
- [244] M. Sepulcre, J. Gozalvez, J. Härri and H. Hartenstein, "Contextual Communications Congestion Control for Cooperative Vehicular Networks," *Transactions on Wireless Communications*, vol. 10, no. 2, pp. 385-389, 2011.
- [245] T. Lorenzen, "SWeRC: self-weighted semi-cooperative DSRC congestion control based on LIMERIC, in," in *2017 IEEE 86th Vehicular Technology Conference (VTC-Fall)*, Toronto, Canada, 2017.
- [246] M. Noor-A-Rahim, Z. Liu, H. Lee, G. G. M. N. Ali, D. Pesch and P. Xiao, "A Survey on Resource Allocation in Vehicular Networks," *IEEE Transactions on Intelligent Transportation Systems*, pp. 1-21, 4 September 2020.
- [247] A. Balador, E. Cinque, M. Pratesi, F. Valentini, C. Bai, A. Alonso Gómez and M. Mohammadi, "Survey on decentralized congestion control methods for vehicular communication," *Vehicular Communications*, 5 August 2021.
- [248] M. Sepulcre, J. Mira, G. Thandavarayan and J. Gozalvez, "Is Packet Dropping a Suitable Congestion Control Mechanism for Vehicular Networks?," in *2020 IEEE 91st Vehicular Technology Conference (VTC2020-Spring)*, Antwerp, Belgium, 2020.
- [249] H. Günther, R. Riebl, L. Wolf and C. Facchi, "Collective perception and decentralized congestion control in vehicular ad-hoc networks," in *2016 IEEE Vehicular Networking Conference (VNC)*, Columbus, OH, 2016.
- [250] H. Huang, H. Li, C. Shao, T. Sun, W. Fang and S. Dang, "Data Redundancy Mitigation in V2X Based Collective Perceptions," *IEEE Access*, vol. 8, pp. 13405 - 13418, 2020.
- [251] G. Thandavarayan, M. Sepulcre and J. Gozalvez, "Redundancy Mitigation in Cooperative Perception for Connected and Automated Vehicles," in *2020 IEEE 91st Vehicular Technology Conference (VTC2020-Spring)*, Antwerp, Belgium, 2020.
- [252] K. Garlich, H.-J. Günther and L. C. Wolf, "Generation Rules for the Collective Perception Service," in *2019 IEEE Vehicular Networking Conference (VNC)*, Los Angeles, CA, USA, 2019.

- [253] A. Chtourou, P. Merdrignac and O. Shagdar, "Context-Aware Content Selection and Message Generation for Collective Perception Services," *Electronics*, 15 October 2021.
- [254] G. Thandavarayan, M. Sepulcre and J. Gozalvez, "Generation of Cooperative Perception Messages for Connected and Automated Vehicles," *IEEE Transactions on Vehicular Technology*, vol. 69, no. 12, pp. 16336 - 16341, 2020.
- [255] M. Giordani, A. Zanella, T. Higuchi, O. Altintas and M. Zorzi, "Investigating value of information in future vehicular communications," in *2019 IEEE 2nd Connected and Automated Vehicles Symposium (CAVS)*, Honolulu, HI - USA, 2019.
- [256] T. Higuchi, M. Giordani, A. Zanella, M. Zorzi and O. Altintas, "Value-Anticipating V2V Communications for Cooperative Perception," in *2019 IEEE Intelligent Vehicles Symposium (IV)*, Paris, France, 2019.
- [257] C. Allig and G. Wanielik, "Dynamic Dissemination Method for Collective Perception," in *2019 IEEE Intelligent Transportation Systems Conference (ITSC)*, Auckland, New Zealand, 2019.
- [258] G. Bansal and J. B. Kenney, "Achieving weighted-fairness in message rate-based congestion control for DSRC systems," in *2013 IEEE 5th International Symposium on Wireless Vehicular Communications (WiVeC)*, Dresden, Germany, 2013.
- [259] H. Kellerer, U. Pferschy and D. Pisinger, *Knapsack Problems*, Berlin : Springer, 2004.
- [260] ETSI TS 102 636-4-2 V1.2.1 (2020-04), "Intelligent Transport Systems (ITS); Vehicular Communications; GeoNetworking; Part 4: Geographical addressing and forwarding for point-to-point and point-to-multipoint communications; Sub-part 2: Media-dependent functionalities for ITS-G5," European Telecommunications Standards Institute (ETSI), 2020.
- [261] C2C-CC, "A 'cookbook' for data quality in CPM," Car 2 Car Communication Consortium, 2021.
- [262] P. R. Strode and P. D. Groves, "GNSS multipath detection using three-frequency signal-to-noise measurements," *GPS solutions*, vol. 20, no. 3, pp. 399-412, 2016.
- [263] S. Ollander, F.-W. Bode and M. Baum, "The dual-frequency post-correlation difference feature for detection of multipath and non-line-of-sight errors in satellite navigation," in *2019 22th International Conference on Information Fusion (FUSION)*, Ottawa, Canada, 2019.
- [264] S. Ollander, F.-W. Bode and M. Baum, "Multi-frequency GNSS signal fusion for minimization of multipath and non-line-of-sight errors: A survey," in *15th Workshop on Positioning, Navigation and Communications (WPNC)*, 2018.

- [265] International GNSS Service (IGS), "The Receiver Independent Exchange (RINEX) Format," [Online]. Available: <ftp://igs.org/pub/data/format/rinex303.pdf>. [Accessed 2020 Dec 8].
- [266] L. Eiermann, O. Sawade, S. Bunk, G. Breuel and I. Radusch, "Cooperative automated lane merge with role-based negotiation," in *2020 IEEE Intelligent Vehicles Symposium (IV)*, Las Vegas, NV - USA, 2020.
- [267] D. Heß, R. Lattarulo, J. Pérez, T. Hesse and F. Köster, "Negotiation of Cooperative Maneuvers for Automated Vehicles: Experimental Results," in *2019 IEEE Intelligent Transportation Systems Conference (ITSC)*, Auckland, New Zealand, 2019 .
- [268] I. Khan and J. Härrri, "Flexible Packet Generation Control for Multi-Application V2V Communication," 2018 IEEE 88th Vehicular Technology Conference (VTC-Fall), Chicago, IL, USA , 2018.
- [269] J. B. Kenney, G. Bansal and C. E. Rohrs, "LIMERIC: a linear message rate control algorithm for vehicular DSRC systems," in *VANET '11: Proceedings of the Eighth ACM international workshop on Vehicular inter-networking*, Las Vegas, NV - USA, 2011 .
- [270] M. I. Khan, S. Sesia and J. Harri, "In Vehicle Resource Orchestration for Multi-V2X Services," in *2019 IEEE 90th Vehicular Technology Conference (VTC2019-Fall)*, Honolulu, HI-USA, 2019.
- [271] ISO/IEC 25012:2008, cl. 5.3.1.2, "Software engineering - Software product Quality Requirements and Evaluation (SQuaRE) - Data quality model," International Organization for Standardization (ISO), International Electrotechnical Commission (IEC), Geneva, Switzerland, 2008.
- [272] A. Vesco, R. Scopigno, C. Casetti and C.-F. Chiasserini, "Investigating the Effectiveness of Decentralized Congestion Control in Vehicular Networks," in *2013 IEEE Globecom Workshops (GC Wkshps) - Vehicular Network Evolution*, Atlanta, GA - USA, 2013.
- [273] S. Kühlmorgen, A. Festag and G. Fettweis, "Impact of decentralized congestion control on contention-based forwarding in VANETs," in *2016 IEEE 17th International Symposium on A World of Wireless, Mobile and Multimedia Networks (WoWMoM)*, Coimbra, Portugal , 2016.
- [274] H. J. Günther, R. Riebl, L. Wolf and C. Facchi, "The Effect of Decentralized Congestion Control on Collective Perception in Dense Traffic Scenarios," *Computer Communications*, vol. 122, pp. 76-83, 2018.
- [275] ISO 26262-5:2018, "Road vehicles — Functional safety — Part 5: Product development at the hardware level," International Organization for Standardization (ISO), Geneva, Switzerland, 2018.
- [276] IEC 61508-2:2010, "Functional safety of electrical/electronic/programmable electronic safety-related systems - Part 2: Requirements for electrical/electronic

- /programmable electronic safety-related systems," International Electrotechnical Commission (IEC), Geneva, Switzerland, 2010.
- [277] IPG Automotive GmbH, "Everything about Virtual Test Driving," June 2019. [Online]. Available: <https://ipg-automotive.com/en/>.
- [278] VIRES Simulationstechnologie GmbH, "VTD - VIRES Virtual Test Drive," June 2019. [Online]. Available: <https://vires.com/vtd-vires-virtual-test-drive/>.
- [279] A. Dosovitskiy, G. Ros, F. Codevilla, A. Lopez and V. Koltun, "CARLA: An Open Urban Driving Simulator," in *Proceedings of the 1st Annual Conference on Robot Learning*, Mountain View, CA - USA, 2017.
- [280] German Aerospace Center, Institute of Transportation Systems, "SUMO - Simulation of Urban MObility," June 2019. [Online]. Available: <https://sumo.dlr.de/index.html>.
- [281] M. Fellendorf and P. Vortisch, "Microscopic traffic flow simulator VISSIM," in *Fundamentals of traffic simulation*, New York, Springer, 2010, pp. 63-93.
- [282] T. Issariyakul and E. Hossain, "Introduction to Network Simulator 2 (NS2) .," in *Introduction to network simulator NS2*, Boston, MA, Springer, 2009, pp. 1-18.
- [283] G. Carneiro, "NS-3: Network simulator 3," UTM Lab Meeting April Vol. 20, 2010.
- [284] A. Varga and R. Hornig, "An overview of the OMNeT++ simulation environment," in *Proceedings of the 1st international conference on Simulation tools and techniques for communications, networks and systems & workshops*, ICST (Institute for Computer Sciences, Social-Informatics and Telecommunications Engineering), 2008, p. 60.
- [285] C. Sommer, R. German and F. Dressler, "Bidirectionally Coupled Network and Road Traffic Simulation for Improved IVC Analysis," *IEEE Transactions on Mobile Computing*, vol. 10, no. 1, pp. 3-15, 2011.
- [286] M. Segata, S. Joerer, B. Bloessl, C. Sommer, F. Dressler and R. L. Cigno, "Plexe: A platooning extension for Veins," in *IEEE Vehicular Networking Conference (VNC)*, Paderborn, Germany, 2014.
- [287] M. Piorkowski, M. Raya, A. L. Lugo, P. Papadimitratos, M. Grossglauser and J. P. Hubaux, "TraNS: realistic joint traffic and network simulator for VANETs," *ACM SIGMOBILE mobile computing and communications review*, vol. 12, no. 1, pp. 31-33, 2008.
- [288] D. Krajzewicz, L. Bieker, J. Härri and R. Blokpoel, "Simulation of V2X applications with the iTETRIS system," *Procedia-Social and Behavioral Sciences*, vol. 48, pp. 1482-1492, 2012.

- [289] B. Schünemann, "V2X simulation runtime infrastructure VSimRTI: An assessment tool to design smart traffic management systems," *Computer Networks*, vol. 55, no. 14, pp. 3189-3198, 2011.
- [290] A. Choudhury, T. Maszczyk, C. B. L. H. Math and J. Dauwels, "An integrated simulation environment for testing V2X protocols and applications," *Procedia Computer Science*, vol. 80, pp. 2042-2052, 2016.
- [291] A. Ibrahim, C. B. Math, D. Goswami, T. Basten and H. Li, "Co-simulation framework for control, communication and traffic for vehicle platoons," *21st Euromicro Conference on Digital System Design (DSD)*, pp. 352-356, 2018.
- [292] R. Mangharam, D. Weller, R. Rajkumar, P. Mudalige and F. Bai, "Groovenet: A hybrid simulator for vehicle-to-vehicle networks," in *2006 Third Annual International Conference on Mobile and Ubiquitous Systems: Networking & Services*, San Jose, California, 2006.
- [293] L. Bononi, M. Di Felice, M. Bertini and E. Croci, "Parallel and distributed simulation of wireless vehicular ad hoc networks," in *Proceedings of the 9th ACM international symposium on Modeling analysis and simulation of wireless and mobile systems*, Terromolinos, Spain, 2006.
- [294] EICT GmbH, "IMAGinE (Intelligente Manöver Automatisierung - kooperative Gefahrenvermeidung in Echtzeit)," European Center for Information and Communication Technologies – EICT GmbH, [Online]. Available: <https://www.imagine-online.de/home>. [Accessed 17 02 2021].
- [295] I. Llatser, T. Michalke, M. Dolgov, F. Wildschütte and H. Fuchs, "Cooperative Automated Driving Use Cases for 5G V2X Communication," in *5G World Forum*, Dresden - Germany, 2019.
- [296] R. Krajewski, J. Bock, L. Kloeker and L. Eckstein, "The highD Dataset: A Drone Dataset of Naturalistic Vehicle Trajectories on German Highways for Validation of Highly Automated Driving Systems," in *2018 IEEE 21st International Conference on Intelligent Transportation Systems (ITSC)*, Maui, Hawaii - USA, 2018.
- [297] E. Strigel, D. Meissner, F. Seeliger, B. Wilking and K. Dietmayer, "The ko-per intersection laserscanner and video dataset," in *17th International IEEE Conference on Intelligent Transportation Systems (ITSC)*, Qingdao, China, 2014.
- [298] S. Ollander, F.-W. Bode and M. Baum, "Simulation-based analysis of multipath delay distributions in urban canyons," in *European Navigation Conference (ENC 2020)*, Dresden, Germany (online), 2020.
- [299] M. Gonzalez-Martín, M. Sepulcre, R. Molina-Masegosa and J. Gozalvez, "Analytical V2V Performance Model of IEEE 802.11p for Connected Vehicles," Technical Report, Universidad Miguel Hernandez, Feb. 2019.

- [300] A. Mahmoud, A. Noureldin and H. S. Hassanein, "VANETs positioning in urban environments: A novel cooperative approach," in *2015 IEEE 82nd Vehicular Technology Conference (VTC2015-Fall)* , Boston, MA, USA, 2015.
- [301] N. Alam and A. G. Dempster, "Cooperative positioning for vehicular networks: Facts and future," *IEEE Transactions on Intelligent Transportation Systems*, vol. 14, no. 4, pp. 1708-1717, 2013.
- [302] P. Pognet and M. Gautier, "Comparison of weighted least squares and extended kalman filtering methods for dynamic identification of robots," in *2000 IEEE International Conference on Robotics & Automation*, San Francisco, CA - USA, April 2000.
- [303] T. G. R. Reid, S. E. Houts, R. Cammarata, G. Mills, S. Agarwal, A. Vora and G. Pandey, "Localization Requirements for Autonomous Vehicles," 3 Jun 2019. [Online]. Available: arXiv preprint arXiv:1906.01061.
- [304] J. Yao, A. T. Balaei, N. Alam, M. Efatmaneshnik, A. G. Dempster and M. Hassan, "Characterizing cooperative positioning in VANET," *IEEE Wireless Communications and Networking*, pp. 28-31, March 2011.
- [305] C2C-CC, "Position Paper on ETSI ITS G5 Channel Usage," Car 2 Car Communication Consortium, 2014.
- [306] G. Thandavarayan, M. Sepulcre and J. Gozalvez, "Analysis of Message Generation Rules for Collective Perception in Connected and Automated Driving," in *2019 IEEE Intelligent Vehicles Symposium (IV)*, Paris, France, 2019.
- [307] Q. Delooz and A. Festag, "Network Load Adaptation for Collective Perception in V2X Communications," in *2019 IEEE International Conference on Connected Vehicles and Expo (ICCVE)*, Graz, Austria, 2019.
- [308] H.-J. Günther, O. Trauer and L. Wolf, "The potential of collective perception in vehicular ad-hoc networks," in *2015 14th International Conference on ITS Telecommunications (ITST)*, Copenhagen, Denmark, 2015.
- [309] S. Aoki, T. Higuchi and O. Altintas, "Cooperative Perception with Deep Reinforcement Learning for Connected Vehicles," in *2020 IEEE Intelligent Vehicles Symposium (IV 2020)*, Las Vegas, NV, United States, 2020.
- [310] K. Furukawa, M. Takai and S. Ishihara, "Controlling Sensor Data Dissemination Method for Collective Perception in VANET," in *2019 IEEE International Conference on Pervasive Computing and Communications Workshops (PerCom Workshops)*, Kyoto, Japan, Japan , 2019.
- [311] H. Huang, W. Fang and H. Li, "Performance Modelling of V2V based Collective Perceptions in Connected and Autonomous Vehicles," in *2019 IEEE 44th Conference on Local Computer Networks (LCN)*, Osnabrueck, Germany, 2019.

- [312] Y. Wang, G. d. Veciana, T. Shimizu and H. Lu, "Performance and Scaling of Collaborative Sensing and Networking for Automated Driving Applications," in *2018 IEEE International Conference on Communications Workshops (ICC Workshops)*, Kansas City, MO, USA, 2018.
- [313] G. Volk, J. Gamerding, A. v. Bernuth and O. Bringmann, "A Comprehensive Safety Metric to Evaluate Perception in Autonomous Systems," in *2020 IEEE Intelligent Transportation Systems Conference (ITSC)*, Rhodes, Greece, 2020.
- [314] S. Shalev-Shwartz, S. Shammah and A. Shashua, "On a Formal Model of Safe and Scalable Self-driving Cars," arXiv preprint arXiv:1708.06374, 2017.
- [315] R. Stiefelhagen, K. Bernardin, R. Bowers, J. Garofolo, D. Mostefa and P. Soundararajan, "The CLEAR 2006 Evaluation," in *International evaluation workshop on classification of events, activities and relationships*, 2006.
- [316] Ministry of the Interior of the state North Rhine-Westphalia, "Aufgaben der Polizei bei Straßenverkehrsunfällen, Anlage 2, Unfallgruppen und -kategorien," 2008. [Online]. Available: <https://recht.nrw.de/lmi/owa/brshowanlage?pid=2477>. [Accessed 31 12 2020].
- [317] D. Smely, S. Rührup, R. Schmidt, J. Kenney and K. Sjöberg, "Decentralized Congestion Control Techniques for VANETs," in *Campolo C., Molinaro A., Scopigno R. (eds) Vehicular ad hoc Networks*, Cham, Springer, 2015, pp. 165-191.

SCIENTIFIC CAREER

Name	Florian Alexander Schiegg
Birth date; place	12.05.1992; Berlin, Germany
Scientific Working Experience	
since 01/2021	Research Engineer at the Department Digital Mobile Communication and V2X Systems Robert Bosch GmbH, Hildesheim, Germany
07/2017-12/2020	PhD Candidate at the Department Advanced Engineering Connected Mobility Systems of Robert Bosch GmbH, Hildesheim, Germany
11/2013-04/2014	Student Assistant, Max Planck Institute for Physics (MPP) / Werner Heisenberg Institute, Munich, Germany <i>“Search for the Higgs-Boson: analysis of tau-tau and 4l decay for ATLAS, CERN”</i>
07/2012-09/2012	Student Assistant, Institute for Hadronic Structure and Fundamental Symmetries (E18), Technical University of Munich, Germany <i>“Production of GEM tracking detectors and investigation of aging effects for COMPASS, CERN”</i>
06/2011-08/2011	Student Assistant, Chair for Quantum Optics, Ludwig Maximillian’s University, Munich, Germany <i>“Equipping of circuit boards for the high precision control of laser shutters on an electromagnetically suspended table”</i>
Education	
since 07/2017	PhD Candidate in Electrical and Computer Engineering at the Institute of Communications Technology of the Leibniz University Hannover (LUH) and co-supervision of the Broadband Wireless Communication and Multimedia Laboratory of the Tongji University Shanghai <i>“On the Value of Information in Vehicular Networks”</i>
10/2014-06/2018	Master’s degree of Management: Marketing, Strategy, and Leadership, TUM School of Management (TUM) <i>“Stationary energy storage in Germany - A qualitative customer analysis”</i>

10/2014-12/2016	Master's degree of Condensed Matter Physics, Technical University of Munich (TUM) <i>"Synthesis and Characterization of a PBA-based Thin Film for Anode Application in Na-ion Batteries"</i>
04/2011-03/2014	Bachelor's degree of Nuclear-, Particle-, and Astrophysics, Technical University of Munich (TUM) <i>"Measuring the Masses of Stellar-Mass Black Holes in X-ray Binaries"</i>
03/2006-11/2010	PENTA UC and Advanced Placement, Pontificia Universidad Católica de Chile (PUC)

